UNIVERSITY OF BARI ALDO MORO

Department of Chemistry

PH.D. IN CHEMICAL AND MOLECULAR SCIENCES

CYCLE XXXVIII

Academic Discipline CHIM/03

ADVANCED PLASMA PROCESSING FOR AGRICULTURE APPLICATIONS

PhD student: Dr. Marianna Roggio

PIETRO
FAVIA
19.01.2026
13:20:46
GMT+00:00

Supervisor: Prof. Pietro Favia

Co-Supervisor: Dr. Fabio Palumbo

Coordinator: Prof. Pietro Favia

FINAL EXAM 2026

Funded by the European Union - Next Generation EU, Mission 4 Component 1 CUP H91I22000950007 Investment 4.1 Ministerial Decree no. 351 of 9 April 2022 - National Recovery and Resilience Plan. Project: "Title of the Project" (MANDATORY approved by the MUR and present on the cineca platform and approved by the Academic Board;)

UNIVERSITA' DEGLI STUDI DI BARI ALDO MORO

Dipartimento di Chimica

DOTTORATO DI RICERCA IN SCIENZE CHIMICHE E MOLECOLARI
CICLO XXXVIII
Settore Scientifico Disciplinare CHIM/03

ADVANCED PLASMA PROCESSING FOR AGRICULTURE APPLICATIONS

Dottoranda: Dott.ssa Marianna Roggio

Supervisore: Ch.mo Prof. Pietro Favia
Co-Supervisore: Dr. Fabio Palumbo

Coordinatore: Ch.mo Prof. Pietro Favia

ESAME FINALE 2026

Finanziato dall'Unione Europea - Next Generation EU, Missione 4 Componente 1 CUP H91I22000950007 Investimento 4.1 D.M. n. 351 del 9 Aprile 2022 – Piano Nazionale di Ripresa e Resilienza. Progetto:"Titolo del Progetto" (OBBLIGATORIO approvato dal MUR e presente sulla piattaforma cineca e approvato dal Collegio dei Docenti;)

UNIVERSITÀ DEGLI STUDI DI BARI ALDO MORO

Dipartimento di Chimica

DOTTORATO DI RICERCA IN SCIENZE CHIMICHE E MOLECOLARI

CICLO XXXVIII

Settore scientifico disciplinare: CHIM/03

ADVANCED PLASMA PROCESSING FOR AGRICULTURE APPLICATIONS

Dottorando: Dott. Marianna Roggio

Coordinatore: Ch.mo Prof. Pietro Favia

Supervisore (Tutor): Ch.mo Prof. Pietro Favia

Co-Supervisore (Co-Tutor): Dr. Fabio Palumbo

ESAME FINALE 2026

Table of Contents

Acknowledgements

I would like to express my deepest gratitude to my supervisors, Prof. Pietro Favia and Dr. Fabio Palumbo, for being constant mentors throughout the entire duration of this Ph.D. Their guidance, expertise, and unwavering support have shaped both my scientific and personal growth.

I would like to thank Prof. Antonella Milella for being an exceptional scientific mentor, providing invaluable academic guidance, and for training me in the use of the AFM instrument. I am sincerely grateful to Dr. Eloisa Sardella for the work shared on maize decontamination; it was a pleasure to assist her and contribute to her experimental activities. I thank Danilo Benedetti and Savino Cosmai for all the technical support they provided for the reactors I used.

I would like to acknowledge the PNRR program – NextGenerationEU for funding my PhD grant. I am also grateful to the projects PNRR PLASMA4SOIL, ONFOODS PNRR, and the Projects@CNR AGROPLASM, which supported and enabled a significant part of the research presented in this thesis. My sincere thanks go as well to COST ACTION 19111 for funding my participation in several important scientific events: the 2nd Training School “Cold plasmas to fight microorganisms, viruses & toxins for medical and agricultural applications” in Bari, the 4th PLAgri Workshop in Belgrade (Serbia), and the 3rd Workshop on Plasma Applications for Smart and Sustainable Agriculture in Gozd Martuljek (Slovenia). These experiences allowed me to broaden my scientific horizons and to engage with researchers from across Europe, enriching my professional development.

I am also thankful to Prof. Stefania Pollastro and Dr. Davide Cornacchia for their valuable evaluation of the zinc-containing films applied to wheat seeds. My gratitude extends to Dr. Michele Casiello for his support with the GC-MS analyses on the essential-oil-loaded zeolite samples coated with barrier films.

A significant part of this PhD was carried out at Ghent University, within the Research Unit Plasma Technology (RUPT), where I had the opportunity to work for seven months under the supervision of Prof. Nathalie De Geyter and Dr. Anton Nikiforov. The hospitality and the stimulating research environment they provided have been among the most enriching experiences of my academic path. I owe special thanks to Dr. Maryam Zabihzadeh

Khajavi, who trained in the laboratory with great professionalism and kindness, and supported me throughout my experimental activities.

I would also like to thank Prof. Frank Devlieghere and Prof. Peter Ragaert for welcoming me into their laboratory in the Department of Food Technology, Safety and Health – Research Unit Food Microbiology and Food Preservation at Ghent University. Working with them allowed me to deepen my understanding of food microbiology and to acquire essential new skills.

I would also like to express my sincere gratitude to my colleagues: Regina del Sole, Francesca Russo, Sara Lotito, Sara Covella, Angelica Maria Lanza, and Angela Pignatelli. Our office has been a place of professional growth and personal connection over these three years, where we shared challenges, achievements, and where strong friendships were formed.

In particular, I am deeply grateful to Dr. Regina del Sole and Dr. Francesca Russo, both of whom provided constant support throughout my doctoral journey through their scientific expertise, guidance, and valuable advice.

Dr. Regina del Sole is the colleague and friend one is always fortunate to have by one's side: someone with whom it is possible to speak openly about any topic, without fear of judgment. We often smile when recalling our first meeting. What began with mutual reserve gradually developed into a deep and meaningful friendship. Today, we remain in daily contact, openly sharing not only our academic experiences but also our personal lives, aspirations, and concerns. For me, she represents an example of freedom and perseverance, never giving up until one's dreams are achieved.

Dr. Francesca Russo has been a guiding and mentoring presence and has become a dear friend. She has offered thoughtful advice not only on academic matters but also on how to approach everyday life with balance and maturity. Through our conversations about work and daily routines, she has represented an important bridge between academic life and the value of family. For me, she is a true example of courage and of the willingness to continually challenge oneself, as well as a constant confidant.

I thank my partner Michele, who has been the guiding light of these three years. He supported and endured me with patience throughout this intense period of personal and professional growth. He has been a constant point of reference in every choice I made and stood by my side during moments when I doubted I could make it, through the

sleepless nights spent in front of the laptop. Simply to be close to me, he would remain silently by my side while I worked. I am deeply convinced that I would not have been able to undertake and complete any of my educational paths without him, who has been by my side and supported me for almost my entire life. I also thank my mother, my father, and my two brothers for their constant support throughout my life.

I thank my wonderful roommates: Flavia, for her support since my master's thesis, she is and will always be a constant presence in my life, Rosa, for her carefree spirit that she shares with me, Francesca, for her invaluable scientific and life advice and finally Angelica, for her constant smile.

Finally, I wish to express my sincere appreciation to all the people who, directly or indirectly, contributed to the realization of this thesis. Each of them has played an important role in shaping not only my research journey, but also the person I have become over these years.

Foreword

Plasma technologies have emerged as powerful and versatile tools for the development of innovative materials and processing. The use of plasma reduces the need for hazardous organic solvents, minimizes multistep procedures, and enables the fabrication of advanced materials through cleaner, faster, and more efficient processes. In recent years, agriculture has faced several challenges linked to global population growth, climate change, and the rapid spread of plant pathogens, including fungi, bacteria, and phytoparasites. Although chemical pesticides are efficient, they show critical limitations related to resistance development, environmental persistence, and toxicity toward non-target organisms. In this context, the search for innovative materials capable of reducing pesticide dosages while still ensuring effective crop protection has become a priority for the scientific community. Plasma deposition techniques provide promising tools in this direction, as they enable the formation of thin organic, inorganic, or hybrid coatings that can be designed with suitable properties to be active against pathogens.

In particular, Aerosol-Assisted Atmospheric Pressure Plasma (AA-APP) processes offer an alternative to traditional wet-chemistry approaches commonly used for surface engineering, coating deposition, and the incorporation of active compounds into functional matrices. The introduction of the precursors into the discharge allows for the encapsulation or controlled retention of plant-protection agents such as fungicides, essential oils, and biocontrol agents within plasma-polymerized organic matrices. These coatings can be applied in various ways, from vivo seed treatments to the functionalization of agricultural materials such as zeolites or mulching films.

The research presented in this Thesis was carried out at the Department of Chemistry of the University of Bari Aldo Moro, in collaboration with the CNR Institute of Nanotechnology (Bari). Part of the experimental activity was run at the Research Unit Plasma Technology (RUPT) and at the Research Unit Food Microbiology and Food Preservation of the Ghent University. Part of the microbiological experiments were conducted at the Department of Soil, Plant and Food Sciences of the University of Bari

Aldo Moro. This work investigates the potential of atmospheric-pressure plasma technologies for the development of coatings on both living and non-living agricultural materials, designed to address major challenges in modern agriculture. Through a multidisciplinary approach combining plasma engineering, materials science, agronomy, and microbiology, this research explores how plasma-made coatings can incorporate and release active substances effective against fungi, bacteria, and nematodes, in alignment with the sustainability principles of the European Green Deal and the Farm to Fork Strategy. In **Figure 1**, a graphical abstract of the work is presented. The main topic of this thesis revolves around the surface engineering of materials via AA-APP for agricultural applications.

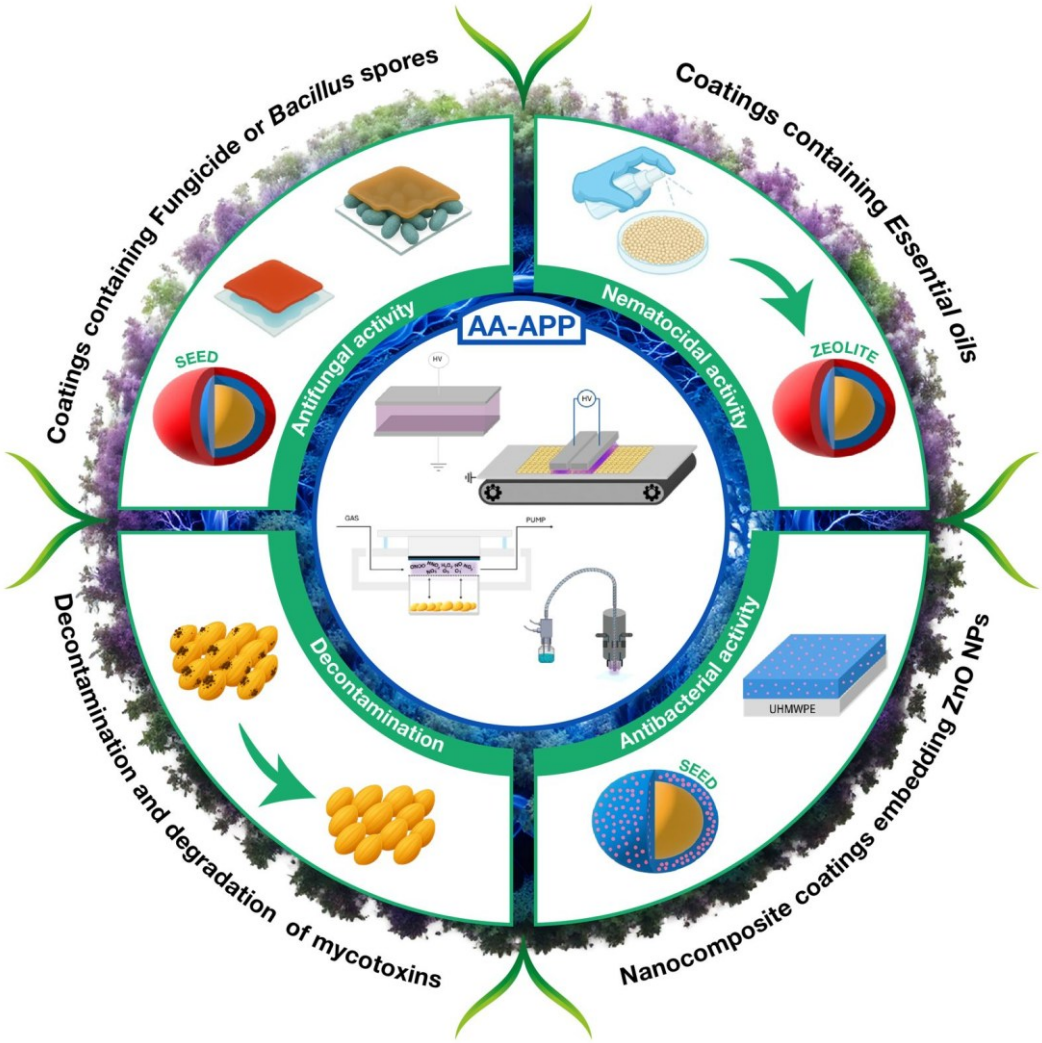

Figure 1. Graphical abstract of the topic covered in this thesis.

Chapter 1 introduces the general context of the doctoral project, focusing on the current

challenges faced by agriculture, with particular attention to crop yield losses caused by phytopathogens and conventional crop management. The European regulatory framework promoting reduced use of pesticides and fertilizers and the adoption of alternative crop protection strategies is also described.

The chapter concludes by introducing advanced technologies for the design of new materials for agriculture, focusing on plasma processes and their potential for surface functionalization, highlighting plasma treatments as promising tools to support more efficient and sustainable agricultural practices.

Chapter 2 focuses on the development of plasma coatings encapsulating chemical fungicides or biocontrol agents as a more sustainable approach to crop management. The methodological section describes the AA-APP deposition process used for coatings preparation and the analytical techniques employed (FT-IR, XPS, WCA, profilometry, SEM) for their chemical characterization.

Moreover, this chapter describes the antifungal activity of the developed bilayers. For fungicide-containing coatings, different active ingredient dosages and film thicknesses were tested, demonstrating that plasma deposition preserves or can even enhance antifungal activity. Coatings containing *Bacillus velezensis* spores were also evaluated: the spores remain viable and retain antagonistic activity, although thicker films delay bacterial growth. These results demonstrate that plasma-produced matrices can protect both fungicides and microorganisms without compromising their functionality.

Annex A 2.1 is the applied extension of Chapter 2 and focuses on the development and characterization of fungicide-containing coatings deposited by plasma on maize seeds. The home-made large-scale AAA-PP reactor used in this study is described. Antifungal tests against *Fusarium graminearum* demonstrate the antifungal efficacy of the coated seeds, while the coating itself remains biologically inert. Seed germination assessments reveal only a slight reduction, with no negative impact on seed viability.

Chapter 3 focuses on the preparation and characterization of EO–zeolite composites coated with films deposited by AA-APP. The chemical characterization of the plasma-deposited coatings confirms the formation of an oxygen-containing organic matrix, comparable to that developed in the previous chapter. In vivo tests on tomato plants are described to evaluate the nematicidal activity of EO-containing coatings on zeolite.

The results indicate that all EOs significantly reduce *Meloidogyne incognita* populations,

but EO-containing composites are markedly more effective than both free oils and uncoated loaded zeolites. Although their performance remains lower than that of the synthetic nematicide, the EO-containing coatings show considerable potential as low-impact environmental alternatives.

Chapter 4 is dedicated to the development of zinc-based antimicrobial coatings embedded within a PEG-like organic matrix by plasma deposition using the AA-APP jet technique. These coatings were applied in two ways: deposited onto polyethylene and tested against *Erwinia carotovora*, or applied onto seeds, and their effectiveness was evaluated against three *Fusarium* species. The assessment of antibacterial activity demonstrates that both zinc-containing coatings effectively inhibit the growth of *E. carotovora*, with increasing efficacy at higher zinc contents. In parallel, germination tests, plant-length measurements, and infection assessments against the three *Fusarium* species revealed that the coating process leads to a reduction in infections in all treated seeds and improves seed growth.

Chapter 5 explores the application of cold atmospheric plasma as a practical post-harvest technology for the decontamination of maize kernels from Aspergillus flavus and Fusarium proliferatum, as well as for the degradation of their main mycotoxins, aflatoxin B1 (AFB1) and fumonisin B1 (FB1). Three treatment approaches are described, and conidial germination tests and LC-HRMS analyses were employed to quantify fungal inhibition and to evaluate the degradation of AFB1 and FB1. The results confirm a significant reductio n in fungal germination. In addition, tests carried out on naturally contaminated maize demonstrate the practical applicability of this approach, confirming the effective reduction of FB1 levels. This study highlights the potential for integrating this safe and residue-free technology into food and feed processing chains.

1

Introduction

1.1 Global Dynamics of Food Demand and Implications for Agriculture

A substantial share of global agricultural production is dedicated to meet food demand. Specifically, this refers to the use of agricultural products for direct human consumption, as well as to the use of crops and other plant and animal-based materials to produce animal feed. [1-2] Undoubtedly, the population growth observed over the past century has led to a significant increase in food demand. According to the United Nations, the world population is expected to reach 9.7 billion by 2050, 10.8 billion by 2080, and 11.2 billion by 2100. Compared to approximately 7.3 billion people in 2015, these figures represent population increase of about 32%, 47%, and 53%, respectively, across the three projected periods. [3]

Although these projections suggest a gradual slowdown in overall global population growth, significant increases are expected in Africa and South Asia. [4] Driven by these significant demographic dynamics, global food demand is projected to rise considerably in the coming decades. [5]

Cereals, including maize, wheat, and rice, together reach about one-third of the total agricultural production, and are the primary group of crops cultivated worldwide.

Climate change will be a critical factor in determining the future state of natural resources, as well as the conditions of agricultural production, thereby affecting food availability. One of the most direct impacts of climate change on agriculture is the reduction in crop yields. [6,7]

A meta-analysis of 1,090 studies primarily focused on wheat, maize, rice, and soybeans conducted under various climatic conditions, indicates that climate change could significantly reduce crop yields in the long term. [8] An additional negative effect is the projected increase in atmospheric CO_2 levels by 2050, which is associated with a marked decline in the zinc, iron, and protein content of major staple crops. [9]

Meanwhile, the food systems are becoming increasingly intensive and complex, with longer supply chains, which leads to higher greenhouse gas emissions both during agricultural production (due to fertilizers, machinery, pesticides, etc.) and in the post-production stages (processing, distribution, and retail). [10]

Future emission levels will depend on how much agricultural production is needed to meet demand, how much food is lost or wasted, and the types of technologies adopted for the production. [11]

In recent years, product safety has become an important global issue in agricolture, where problems caused by pathogenic microorganisms are mainly considered.

Plant diseases caused by fungal, bacterial, viral, nematode, and parasitic infections entail significant risks to global agriculture, leading to reductions in crop yield and quality. Moreover, climate change, monoculture, and inadequate farming practices have further intensified the spread of these diseases. [12]

1.2 Plant diseases

Plant health directly influences food security, environmental sustainability, and economic stability. [13] Healthy crops ensure consistent agricultural productivity, which is essential for feeding the world's growing population. However, plant diseases caused by fungi, viruses, bacteria, and nematodes represent a major threat to agricultural systems, as they can rapidly spread through air, water, soil, and vectors such as insects. [12] When these diseases affect crops like wheat, rice, maize, and potatoes, they can lead to food shortages, price volatility, and substantial economic losses. [14]

Given these risks, it is required to develop a comprehensive understanding of plant diseases, including their symptoms and the causal agents, as well as to explore and implement effective management strategies that are both sustainable and environmentally sound. [12,13] Below, **Figure 1** provides a detailed illustration of plant diseases and transmission pathways.

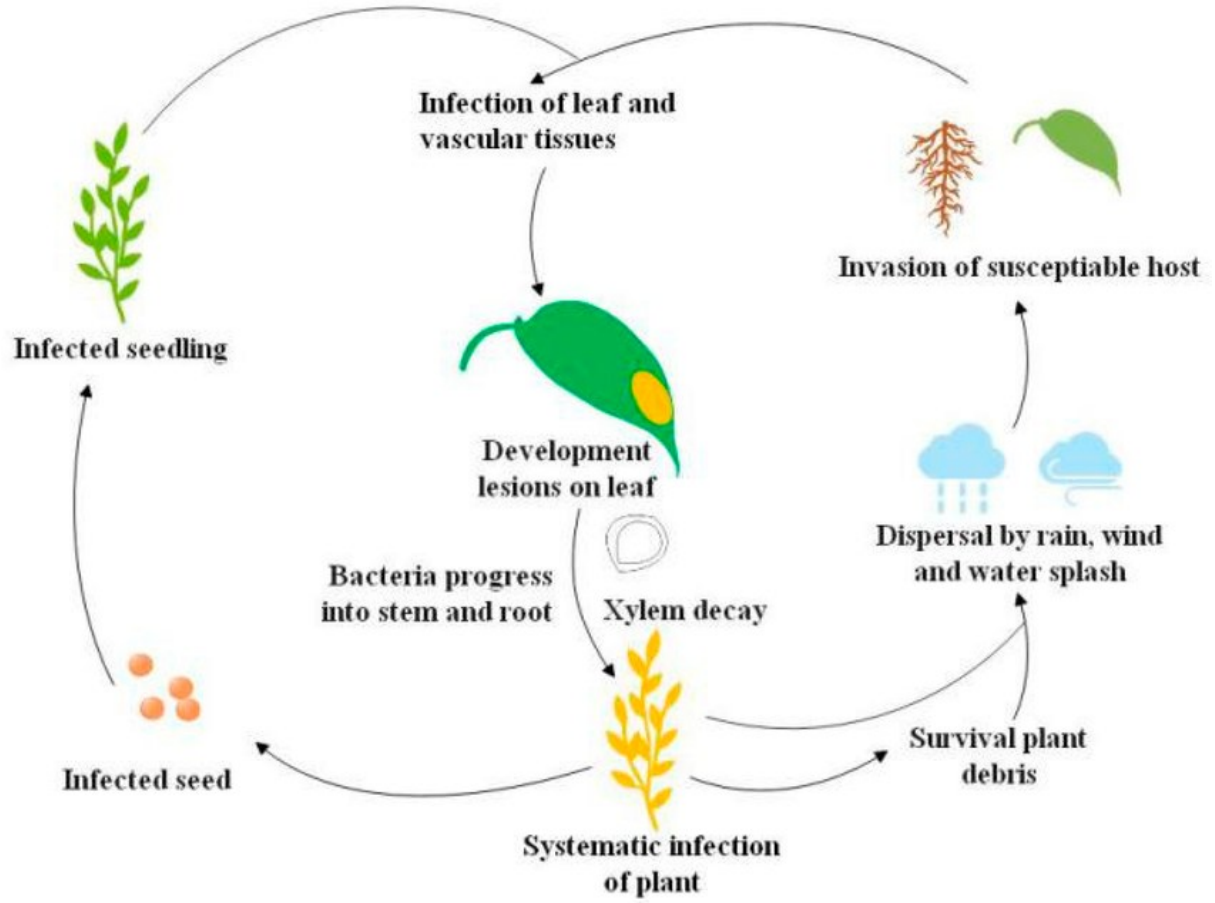

Figure 1. Plant diseases and transmission pathways. [15]

Development and spread of plant diseases are driven by a combination of environmental conditions, farming methods, and adaptive behavior of pathogens. [15-18]

- Environmental Factors

Plant disease dynamics depend strongly on environmental conditions. Warm, humid weather favors many fungal and bacterial pathogens; heavy rains facilitate waterborne spread, and sustain humidity accelerates spore germination. By contrast, drought stress compromises plant defenses, and increases their susceptibility. [15,16]

- Agricultural Practices

Intensive farming techniques can create environments conducive to disease outbreaks. Monocultures deplete soils, erode biodiversity, and allow the buildup of pathogens. Poor irrigation and drainage cause waterlogging that favors root pathogens, while

contaminated seed or planting material introduces diseases, leading to major yield and economic losses. [17,18]

- Pathogen Evolution and Resistance

Plant pathogens evolve rapidly via mutation and recombination, producing more virulent, pesticide- and fungicide-resistant strains. Overuse of chemicals accelerates this process, creating resistant populations and complicating disease control. [19,20]

1.3 Pathogens in agriculture

In addition to environmental factors, agronomic practices, and evolution of resistance, pathogens represent one of the main causes of agricultural losses.

1.3.1 Fungi

Fungal pathogens represent one of the most pressing challenges, particularly in cereal-based agricultural systems. This issue is especially relevant in the Mediterranean basin, where cereals are extensively cultivated and form the basis of the regional diet and economy. It is estimated that average yield losses in cereals due to fungal contamination amount to about 15–20%, with peaks up to 50% under severe epidemic conditions. For instance, in 2019, 22% of wheat yield losses were entirely attributable to fungal diseases. [21]

Pathogenic fungi not only induce a wide range of plant diseases, but also have the ability to synthesize toxic mycotoxins that can accumulate in infected tissues. Mycotoxin formation can begin during the preharvest stage and may persist or even intensify during postharvest handling and storage. [22] The presence of mycotoxins in plant products, as well as in processed food and feed, poses significant risks to food safety and animal health. The fungal genera most frequently associated with mycotoxin contamination are *Fusarium*, *Alternaria*, *Aspergillus*, and *Penicillium*, each of which includes species capable of producing toxic compounds under favorable conditions. [23]

Of particular concern are aflatoxins (AFs), ochratoxin A (OTA), deoxynivalenol (DON), T-2/HT-2 toxins, fumonisins (FBs), and zearalenone (ZEN), which are associated with acute and chronic toxic effects, including carcinogenicity. High levels of AFs and DON contamination in food cereals highlight maize and wheat as particularly vulnerable crops. [24-26]

The genus *Fusarium* is among the most widespread pathogens affecting cereals, including common and durum wheat, barley, oats, rye, and triticale. In these crops, it can cause root rot, leading to severe yield reductions, often estimated between 10 % and 40 %. As previously mentioned, several *Fusarium* strains are also capable of producing mycotoxins, which may be formed either in preharvest plants still standing in the field or in stored grain. In wheat, their presence has become virtually unavoidable in food and feed chains. [27]

Fusarium graminearum is one of the most dangerous *Fusarium* species and the main etiological agent of two distinct diseases affecting different plant tissues. Fusarium Crown Rot (FCR) primarily affects roots and crown tissues, impairing plant development from the earliest growth stages. The second, Fusarium head blight (FHB), is the most destructive form from both agronomic and food safety perspectives, as it directly affects spikes and kernels during flowering, leading to grain contamination with mycotoxins. From a mycotoxicological standpoint, FHB is of particular concern due to the accumulation of stable mycotoxins that pose a serious threat to human food and animal feed safety. By contrast, FCR has a lower mycotoxicological impact, as infections are mainly confined to vegetative tissues and only rarely result in significant kernel contamination. [28]

Maize (*Zea mays L.*) is one of the most important crops worldwide; the American continent accounting for about half of the total production, followed by Asia and Europe. Maize has a nutritional value comparable to wheat but is generally less expensive, making it a key component in both human and animal diets. [29]

Mycotoxins, which mostly affect corn, belong to the genera *Fusarium* and *Aspergillus*. *F. proliferatum* and *F. verticillioides* are associated with severe plant diseases such as ear, stalk, and root rots, while *Aspergillus flavus* is frequently detected on maize kernels at maturity and during storage. These fungi can produce a wide range of mycotoxins that are

chemically stable and can persist even after conventional physical or chemical treatments. [30]

The most relevant mycotoxins in maize are FBs, produced mainly by *F. proliferatum* and *F. verticillioides*, and AFs, produced primarily by *A. flavus*. Due to their impact on food and feed safety, European authorities have established maximum permitted levels of these mycotoxins to protect human and animal health. [31-32]

1.3.2 Bacteria

Although bacteria cause fewer plant diseases than fungi, they are responsible for some of the most severe pathologies affecting cultivated crops. The dissemination of many bacterial pathogens is strongly influenced by environmental factors such as rainfall and wind, insect vectors, and agronomic practices including pruning, grafting, inadequate crop rotation, poor hygiene, and the use of contaminated seeds.

Pectinolytic bacteria belonging to the genus *Pectobacterium* are collectively referred to as Soft Rot Pectobacteriaceae (SRP). Members of the family *Pectobacteriaceae* are able to survive in soil for periods ranging from one week to six months, depending on soil temperature, moisture, and pH. [33] In soils, the presence of these microorganisms has been investigated mainly in association with plant residues, which are thought to act as reservoirs for their survival and dissemination.

Erwinia carotovora is a Gram-negative phytopathogenic bacterium that has become a major global threat to numerous vegetable crops and ornamental species, including onion, garlic, cucumber, potato, carrot, cabbage, and tomato. This pathogen is of particular concern during the pre-harvest phase and post-harvest phas, where it can cause severe losses due to latent infections. It enters plant tissues through wounds or natural openings from the soil and produces a wide array of exoenzymes that degrade cell wall and membrane components, leading to tissue maceration and ultimately plant death [34–37]. Consequently, the effective management of this bacterium is of paramount importance in agricultural systems.

1.3.3 Nematodes

Plant-parasitic nematodes (PPNs) cause severe damage and significant yield losses in a several vegetable crops, with heavy estimated annual global losses. The extent of plant growth impairment caused by PPNs may depend on the nematode species, the physiological race, and the initial nematode population density in the soil at the time of sowing or transplanting. In cases of high soil infestation levels (>64 eggs and juveniles/mL of soil), they can destroy the crop. Moreover, PPNs can cause additional damage through synergistic interactions with the plant pathogens such as *Fusarium spp*., *Verticillium spp*., viruses and bacteria that enter through root lesions induced by nematodes. This phenomenon increases the severity of plant disease symptoms such as yellowing, stunted growth, wilting, and dwarfism. The severity of PPN-induced damage is expected to increase due to global warming and the intensification of agriculture aimed at meeting the needs of a rapidly growing world population.

The PPNs exhibit a wide variety of interactions with their host. They can be classified as ectoparasites or endoparasites depending on the plant tissues they feed on. Some PPNs are migratory, as they can easily move from the soil into plant tissues, whereas others are sedentary. Most PPN species possess a needle-like, protrusible oral structure called stylet, which is used to pierce host plant tissues and release specific enzymes that partially digest plant cells, thereby facilitating their ingestion into the nematode's gut.

Root-knot nematodes are among the most destructive PPN species for nearly all cultivated plant species. Within this group, those belonging to the genus *Meloidogyne* are considered the most damaging pests of horticultural crops, causing severe yield losses. Four species (*Meloidogyne incognita, M. javanica, M. arenaria,* and *M. hapla*) are primarily responsible for reductions of up to 73.3% in tomato production.

The parasitic life cycle of *Meloidogyne incognita* comprises several stages, beginning with egg deposition on the root surface by the adult female. From the eggs, the second-stage juvenile (J2) develops, which represents the infective form capable of penetrating roots and completing development to the adult stage. Under favorable environmental conditions, the entire life cycle can be completed within 4–6 weeks, allowing rapid reinfestations, as shown in **Figure 2**. [39]

Not all nematodes are harmful to plants. In addition to phytoparasitic species, many free-living nematodes play essential roles in soil ecosystems by contributing to nutrient

cycling, regulating microbial communities, and maintaining ecological balance, and they are also considered reliable bioindicators of soil health. [40–42]

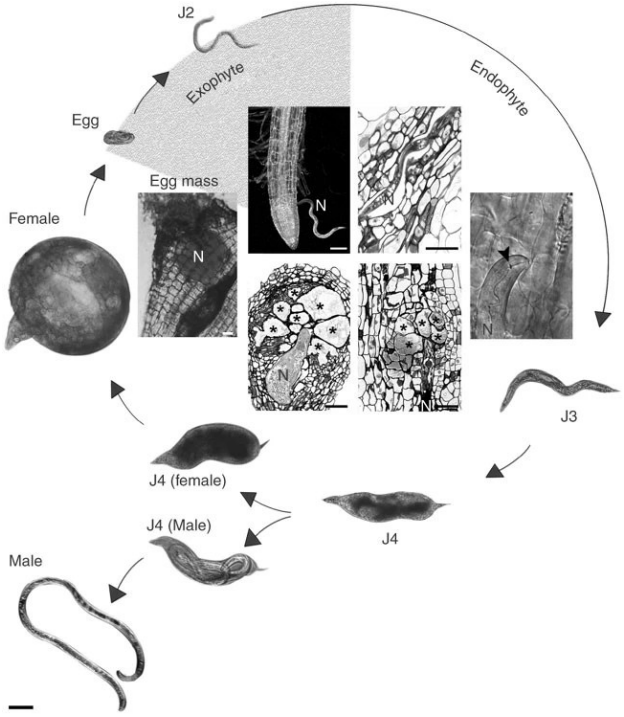

Figure 2. Life cycle of *M. incognita*. [39]

1.4 Chemical plant disease management practices

Plant protection practices have been enriched worldwide, and six main methods have been developed, including agricultural, physical, biological, chemical and plant quarantine methods, and integrated pest management (IPM). Among these, chemical methods, and in particular the use of pesticides are the most widely adopted strategies due to their effectiveness and broad applicability. [43]

In the following sections, each of these categories will be examine, in order to highlight the specific molecules used, their mechanisms of action, and their impact on the environment and human health. Since the materials developed during this PhD course were intended to fight fungi, nematodes and bacteria, the main practice against these pathogens will be described.

1.4.1 Pesticides

Pesticides are synthetic chemical substances that are typically hydrophobic and/or lipophilic. The Food and Agriculture Organization of the United Nations (FAO), together

with the World Health Organization (WHO), defined pesticides in 2016 as “any substance, or mixture of substances, intended for preventing, destroying or controlling any pest, including vectors of human or animal disease, unwanted species of plants or animals, causing harm during the production, processing, storage, transport or marketing of food, agricultural commodities, wood and wood products, or animal feed”.

The classification of pesticides is essential for understanding their diverse applications, as it provides information on how pesticides function, their environmental impact, and the best practices for their application. Pesticides are categorized as insecticides, herbicides, fungicides, rodenticides, molluscicides, nematicides, and plant growth regulators, each targeting specific types of pests or functions, as illustrated in **Figure 3**. [44] However, pesticide can be broadly classified into three categories:

- based on application i.e., to the way pesticides interact with or enter the target organism, described in **Table 1**;[45]
- based on their function, grouped according to their specific roles and the organisms they target;
- Classification based on the chemical composition, on their chemical characteristics and the nature of their active ingredients. Modern pesticides may be either inorganic or organic compounds [44]

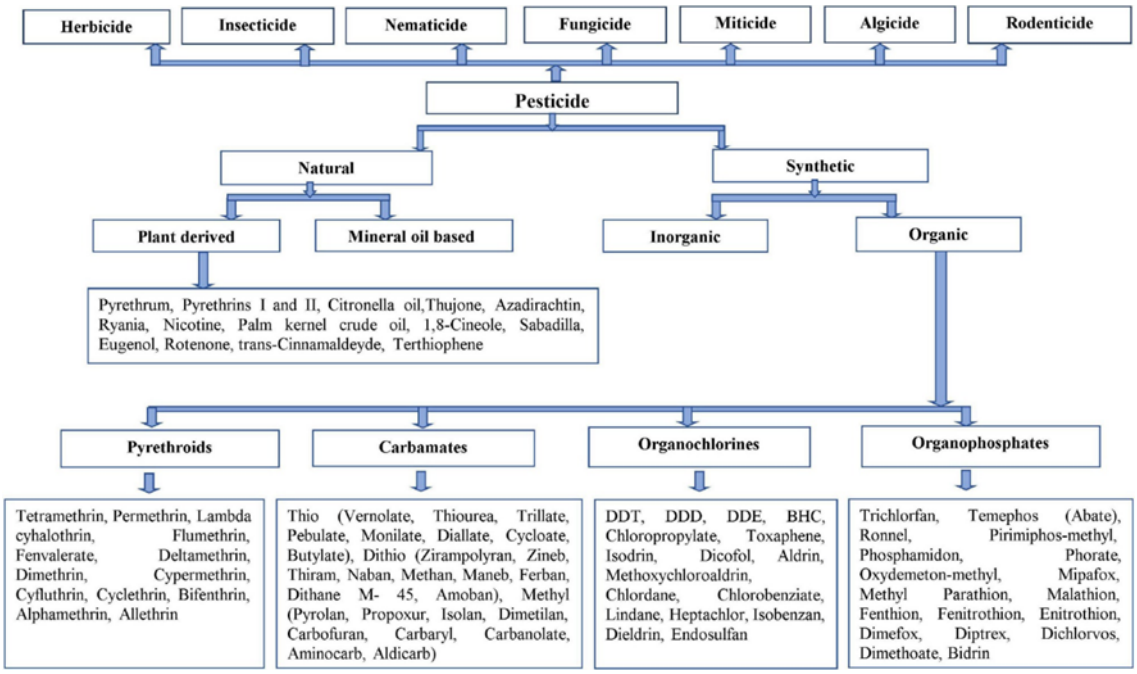

Figure 3. Classification of pesticides.[44]

Table 1. Classification based on application. [45]

Type of Pesticide	Function	Example
Systemic Pesticides	These are pesticides which are absorbed by plants or animals and transfer to untreated tissue	acetamiprid, boscalid or difenoconazole
Contact pesticides	It acts on target pests when they come in contact	Acephate, carbaryl, fipronil, pyrethrins, pyrethroids
Stomach poisons	It enters the pest's body through their mouth and digestive system	Malathion
Fumigants	Pesticides which acts or may kill the target pests by producing vapour and enter pest's body through tracheal system.	Phosphine
Repellents	Repellents do not kill but distasteful enough to keep pests away from treated area. They also interfere with pest's ability to locate crop.	Methiocarb

In agricultural development, pesticides have become a fundamental tool for crop protection and yield enhancement. Worldwide, approximately 2 million tons of pesticides are used annually, of which 47.5% are herbicides, 29.5% insecticides, 17.5% fungicides, and 5.5% other types. [46-47]

In 2019, the five largest consumers of pesticides within the European Union (EU) were Spain, France, Italy, Germany, and Poland. Across the period 2011–2020, fungicides and herbicides consistently represented the dominant pesticide categories, accounting for approximately 40–44% and 30–36% of total sales, respectively. [48] However, over time they tend to accumulate in plant tissues, water, soil, air, and biota.

Pesticides tend to accumulate in soils, where they alter physical, chemical, and biological properties, leading to a decline in microbial populations and harming beneficial organisms such as pollinating insects. Pesticides released into the environment may undergo transformation through photolysis, hydrolysis, oxidation, or microbial metabolism; however, these processes are often slow and incomplete, leading to the long-term persistence of residues. In aquatic systems, they disperse into water through drift, runoff, and leaching, thereby threatening fish populations and compromising the quality of drinking water quality. Furthermore, a correlation has emerged between pesticide use and the development of antibiotic resistance genes. [49] Notably, less than

10% of applied pesticides reach the target pest, while more than 90% are dispersed into the environment through soil deposition, crop uptake, precipitation, leaching, runoff, volatilization, evaporation, and degradation. As a result, pests are exposed to lower pesticide concentrations, which in turn drive the development of resistance mechanisms. [50]These substances then enter the human food chain, where they represent a significant risk to human health. According to a report by the WHO and the United Nations Environment Programme (UNEP), three million people worldwide are poisoned due to pesticide exposure. Continuous exposure to the same pesticide may lead to its accumulation in human adipose tissue, which has been associated with cancers, mutations, reproductive abnormalities, hormonal imbalances, congenital defects, neurodegenerative disorders, pulmonary and hepatic dysfunctions, and hematological diseases. For all these reasons the EU has introduced strict legislation, such as Regulation (EC) No. 1107/2009 on the placing of plant protection products on the market, while the European Food Safety Authority (EFSA) establishes Maximum Residue Limits (MRLs) for pesticides in food.

In 2023, Europe recorded the lowest level of pesticide sales since 2011, with a 9% decrease compared with 2022 and an 18% decrease compared with 2021. This was confirmed by the latest data published by Eurostat and reported in **Figure 4**, the statistical office of the European Union. [51]

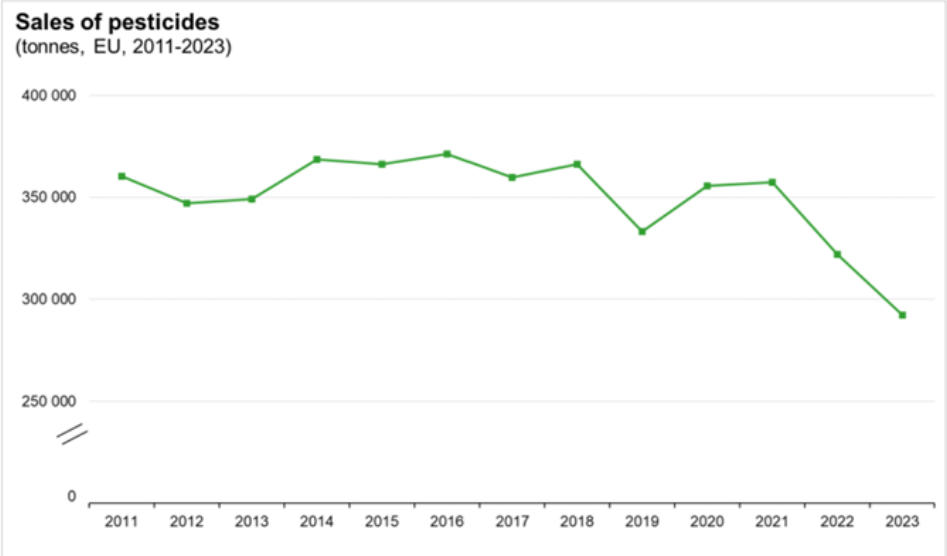

Figure 4. Pesticide sales levels in the EU from 2011 to 2023. [51]

1.4.2 Fungicides

Within the broader category of pesticides, fungicides represent the class specifically designed to target fungal pathogens. As previously described in paragraph **1.3.1**, several *Fusarium* species are associated with Fusarium head blight (FHB), with *F. graminearum* being the predominant pathogen. Since FHB is an economically significant disease, effective management strategies must be implemented to reduce its impact in the field. Chemical control is among the most effective approaches, and fungicides have been reported to lower FHB incidence by up to 77% and mycotoxin levels by 89%. [52]

Fungicides have been classified by the Fungicide Resistance Action Committee (FRAC), which groups them according to their different modes of action, as reported in **Table 2**. [53-54]

Table 2. Classification of pesticide modes of action according to the FRAC. [54]

Fungicide group[a)]	Mode-of-action group
Sterol biosynthesis inhibitors (thereof azoles 28.1%)	G
Multisite Action	M
QoI fungicides	C3
SDHI fungicides	C2
Mitosis and cell division inhibitors	B
Nucleic acid synthesis inhibitors (thereof phenylamides 2.0%)	A
Signal transduction inhibitors	E
Cell wall biosynthesis inhibitors (thereof CAA 1.7%)	H
Amino acids and protein synthesis inhibitors	D
Plant defense modulators	P
Unknown mode of action	U
Others (mainly unclassified, melanin synthesis inhibitors I; electron transport inhibitors (not C2 or C3)	

Among these, sterol biosynthesis inhibitors (SBIs) account for approximately 30% of global fungicide sales and, within this class, demethylation inhibitors (DMIs, FRAC group G) represent the most relevant subgroup, accounting for about 94%. [54] Triazole fungicides as the prothioconazole, which belong to this category, provide highly effective, systemic, and broad-spectrum control of the major plant pathogens. Prothioconazole, developed and commercialized between 2002 and 2004 by Bayer, is a pro-fungicide that

is bioactivated in vivo to prothioconazole-desthio. [55] It ensures long-lasting control of multiple diseases in wheat, barley, and other crops. As reported by Masiello et al. (2020), prothioconazole demonstrated strong activity against *Fusarium graminearum* both in vitro and in vivo. In vitro, assays revealed that prothioconazole was highly effective in completely inhibiting mycelial growth. When evaluated under field conditions on artificially inoculated maize, prothioconazole significantly reduced *F. graminearum* contamination, with decreases of approximately 52% compared to untreated controls. [56]

In addition to DMIs, other fungicide groups are also against FHB. Fludioxonil, classified in FRAC group E, interferes with fungal signal transduction, leading to loss of cell homeostasis and cell death.[57] While its field efficacy against *Fusarium* spp. is generally lower than that of triazoles, it shows strong in vitro activity and is mainly employed in seed treatments.

Pyraclostrobin, a member of FRAC group C and belonging to the quinone outside inhibitor (QoI) group, disrupts mitochondrial respiration by blocking ATP production, which rapidly inhibits fungal growth. According to Chen *et al*. its effectiveness against FHB is particularly high when used in combination with the triazole fungicide epoxiconazole, and this strategy is also important to reduce the risk of resistance development. [58]

Figure 5 reports the chemical structures of prothioconazole, fludioxonil, and pyraclostrobin.

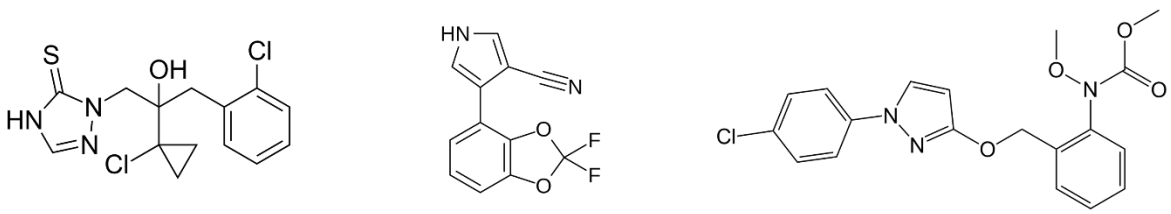

Prothiconazole Fludioxonil Pyraclostrobin

Figure 5. Chemical structure of the fungicides prothioconazole, fludioxonil, and pyraclostrobin.

The effectiveness of fungicide treatments depends on the mode of application, which

determines the degree of contact between the active ingredient and the pathogen. The main approaches are soil treatments, seed treatments, and foliar applications.

Soil treatments include several techniques. Soil drenching involves applying liquids or granules fungicides directly to the soil so that the active compound percolates to a depth of 10–15 cm. Furrow application, in contrast, delivers fungicides directly into planting furrows at sowing. Finally, fumigation employs volatile chemicals that diffuse through the soil as gases.

Seed treatments aim to eliminate pathogens at the surface or inside seeds before sowing. These include physical methods (e.g., hot-water treatment or solarization) and chemical approaches, as well as *seed dressing*, where protective substances are applied directly onto the seed surface. Chemical treatments are divided into wet methods, where seeds are coated with suspensions or solutions, and dry methods, where fungicides are applied directly as powders without additional carriers. These treatments protect the seed itself and help seedlings resist early soil-borne infections. Foliar applications are the most common method and are intended to protect the aerial parts of the plant. They usually involve spraying, which covers the leaves with fungicide. Sprays can be applied in high volumes for full coverage or in lower volumes to reduce product use while maintaining efficiency. In some cases, fungicides are applied as powders (dusting), though this method is less persistent and less commonly used. Overall, soil, seed, and foliar applications represent complementary strategies for disease management. The choice of method depends on the type of crop, the biology of the pathogen, and field conditions.[59]

1.4.3 Nematicides

Chemical control plays an essential role in counteracting PPNs. For this reason, another relevant class of pesticides is represented by nematicides. As a result of the damage caused by PPNs, the synthesis of compounds aimed at controlling nematodes began in the XIX century as a strategy to ensure food security and prevent economic losses. Initially applied directly to the soil, these substances were intended to sterilize it, thereby eliminating pests and phytonematodes. The use of such chemical agents in agriculture

had a major impact on crop production, significantly improving both yield and quality worldwide.

Nematicides applied directly to the soil can be classified into two categories: fumigant and non-fumigant nematicides as reported in **Figure 6**. Fumigants are typically liquid formulations that volatilize upon contact with air. They diffuse deeply into the soil, and upon contact with soil moisture they decompose into products that penetrate the nematode cuticle, where they interact with amino acids, enzymes, and proteins, ultimately leading to metabolic disfunctions and death. Fumigant nematicides are considered biocidal substances because they act on nematodes but also on fungi, bacteria, seeds, and other soil organisms. However, their application may cause significant environmental disturbances and phytotoxicity. These compounds are generally more effective in soils with low organic matter content, as organic compounds and clay minerals tend to absorb and inactivate them. Their dispersion is also temperature-dependent, with optimal performance observed at soil temperatures around 12–15 °C.

From the 1960s, new classes of products were developed, known as non-fumigant nematicides. Among these, organophosphates and carbamates are of particular importance. Compared with fumigants, they exhibit lower environmental persistence and exert systemic activity against plant-parasitic nematodes, being effective at lower concentrations. However, despite their reduced phytotoxicity, they remain highly toxic to non-target organisms such as insects and mammals, thereby posing relevant environmental risks. [60]

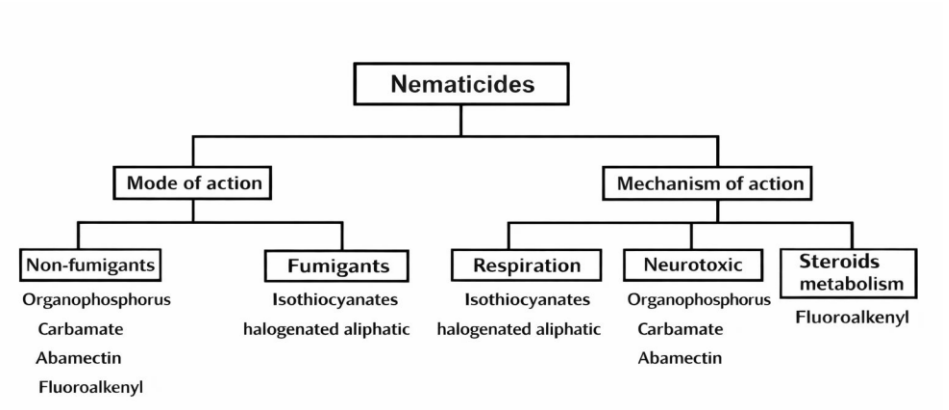

Figure 6. Classification of nematicides based on mode of action and mechanism of action. [60]

The IRAC (Insecticide Resistance Action Committee) has introduced the classification of nematicides based on their mode of action. Nematicides can have a neurotoxic mechanism of action, for example through the inhibition of the acetylcholinesterase enzyme (carbamates and organophosphates) or by causing the continuous opening of sodium channels in cell membranes (abamectin), preventing the transmission of nerve impulses, resulting in paralysis and death. Another mechanism is related to the inhibition of respiration: isothiocyanates interfere with electron transport in the mitochondrial respiratory chain, causing enzymatic inactivation and inducing apoptosis. While, halogenated aliphatic compounds, such as methyl bromide, act as protein alkylating agents and oxidize the Fe^{2+} centers of cytochromes, thus blocking cellular respiration. Methyl bromide has been progressively withdrawn from the market in most countries. Finally, another mechanism of action concerns the dysregulation of steroid metabolism, as in the case of fluensulfone. This nematicide alters the sterol composition of nematodes, interfering with their development. [61]

The most widely used nematicides on the market for the treatment of *M. incognita* in tomato plants are Velum Prime (Bayer) and Nemathorin 10G (Syngenta). The chemical structures are shown in **Figure 7**. The active ingredient of Velum Prime is fluopyram, a nematicidal molecule capable of selectively inhibiting Complex II of the mitochondrial respiratory chain in nematodes, leading to a reduction in ATP production. This results in nematostatic action, causing loss of nematode mobility. Fluopyram is a new-generation chemical nematicide with moderate toxicity towards aquatic organisms, invertebrates, and vertebrates. Moreover, it is not classified as carcinogenic or genotoxic; experimental studies, however, have indicated that such effects may occur only at very high doses, which are not typically used under field conditions. [62]

Nemathorin 10G (Syngenta) contains the active ingredient fosthiazate, an organophosphate that inhibits the enzyme acetylcholinesterase in the nematode nervous system. In a study by Kandil et al., in vitro results showed 94% mortality of *M. incognita* juveniles after 96 hours. When tested in vivo on tomato, the nematicide significantly reduced the number of root galls and juveniles in the soil. Moreover, it also led to an increase in crop yield.

Fosthiazate was developed as an alternative to methyl bromide, a highly toxic fumigant nematicide, to reduce the risks associated with fumigants. However, it has been reported

to affect non-target nematodes and the soil microbial comunity. As an organophosphate, it also carries the risk of inducing neuropathies in humans. [63]

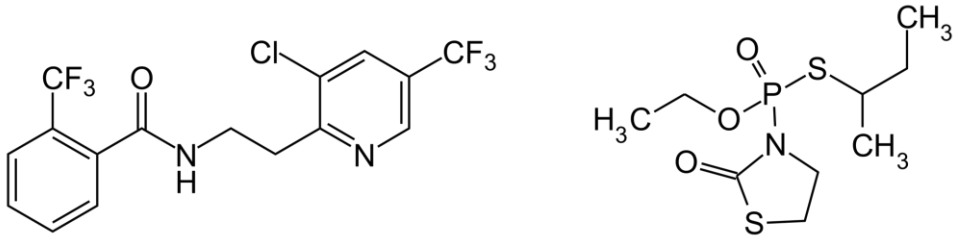

Fluopyram Fosthiazate

Figure 7. Chemical structure of the nematicides Velum Prime (Bayer) and Nemathorin 10G (Syngenta).

1.4.4 Antibiotics

Antibiotics are substances produced by microorganisms that can inhibit or kill other microorganisms. Although their use in plant protection is generally low compared to human and veterinary medicine, plant pathologists soon recognized their potential in managing bacterial plant diseases. Consequently, farmers in different regions of the world have resorted to antibiotics to control these pathogens. However, the actual amounts applied to crops remain difficult to quantify due to the absence of systematic monitoring, raising concerns that their use in plant health may be more widespread than previously assumed. To address these gaps, several international initiatives have recently been launched to collect and harmonize data on antimicrobial use in plants at a global scale. [64-68] Unlike pesticides, which are clearly classified into categories, the antibiotics used in agriculture are not organized within a specific classification, but they are generally grouped under broader categories (e.g., together with fungicides) or referred to according to their pharmacological classes, highlighting the lack of a dedicated regulatory or agronomic framework. [69]

In agriculture, the use of antibiotics is selective and restricted to a limited number of bacterial diseases. Compounds such as streptomycin, oxytetracycline, kasugamycin, oxolinic acid, and gentamicin have been employed primarily for the control of *Erwinia amylovora*, the causal agent of fire blight in pome fruits. Their application, however,

remains highly regulated due to the risks associated with resistance development and public health concerns. [70] Instead, no antibiotics are commercially authorized for the management of soft rot caused by *E. carotovora*. For this disease, conventional strategies have relied mainly on copper-based formulations. These products, represent the most widely adopted chemical approach in practice. Experimental studies have confirmed that copper compounds such as copper sulfate pentahydrate and copper oxychloride are effective in suppressing the growth of *E. carotovora*. Nevertheless, the use of copper-based compounds presents certain limitations: in addition to their restricted efficacy under field conditions, copper formulations may cause phytotoxic effects and negatively influence plant growth when not properly managed. [71]

Copper is an essential micronutrient, but excessive exposure can result in toxic effects. Acute ingestion of high levels of copper may cause gastrointestinal disorders as well as kidney and liver damage, while chronic exposure can lead to tissue accumulation and hepatic dysfunction.

Another potential risk is linked to the presence of copper residues in agricultural products intended for human consumption. Intensive and repeated applications of copper-based formulations can increase their concentration in plant tissues and along the food chain. For these reasons, the EU has introduced restrictions on the use of copper in plant protection products, promoting a more sustainable application.

These constraints highlight the challenges of chemical control of bacterial soft rot and emphasize the need for more sustainable alternatives. [72]

1.5 Green Deal and Farm to Fork

The 2030 Agenda for Sustainable Development adopted in September 2015 by all 193 Member States of the United Nations. It reflects a shared awareness of the urgent global challenges that humanity faces, including poverty, inequality, climate change, and the loss of biodiversity. The framework is built around five guiding principles – People, Planet, Prosperity, Peace, and Partnership – which together define an integrated vision of sustainable progress.

The Agenda establishes 17 Sustainable Development Goals (SDGs) and 169 specific targets to be achieved by 2030, combining economic, social, and environmental

dimensions in a single framework. Among these, SDG 2 plays a crucial role, as it aims to eradicate hunger, ensure food security, improve nutrition, and promote sustainable agriculture. Achieving this objective requires supporting small-scale producers, strengthening agricultural systems, reducing food waste, and safeguarding the biodiversity of crops, seeds, and livestock. These elements are essential to guarantee equitable and reliable access to food resources for present and future generations. [73]

Building on this global vision, the EU has launched the European Green Deal, an ambitious policy framework designed to make Europe the first climate-neutral continent by 2050. The Green Deal mirrors the integration of the United Nations (UN), combining environmental protection with economic transformation and social inclusion. Its measures include the reduction of greenhouse gas emissions, the promotion of renewable energy, the development of sustainable mobility, and the strengthening of the circular economy.

The Farm to Fork Strategy is one of the key pillars of the Green Deal, specifically dedicated to the sustainability of the agricultural and food sectors. Its main objective is to build a safer, healthier, and more environmentally compatible agri-food system by 2030. To this end, it promotes the adoption of innovative technologies, the reduction of pesticide use by 50% and fertilizers by 20%, the halving of nutrient losses in soils, and the expansion of organic farming. In doing so, Farm to Fork directly contributes to the achievement of the 2030 Agenda, particularly SDG 2, while safeguarding biodiversity and enhancing resilience to climate change. [74-76]

Meeting these goals requires of innovative technological solutions. Advances are needed to improve plant protection against emerging pests and diseases, accelerate the transition away from pesticides and antimicrobials, limit excessive dependence on chemical fertilizers, strengthen organic farming, promote higher standards of animal welfare, and reverse the decline of biodiversity. Within this context, the design and application of innovations have been the focus of this doctoral research, aiming to provide tools and approaches that support a more sustainable and resilient agri-food system.

1.6 Innovative Approaches for the Control of Chemicals in Agriculture

In recent years, following the increase in food demand and the need to reduce the environmental impact caused by agrochemicals, the scientific community has been committed to developing a range of practical strategies. In the next sections, the different innovative approaches employed in agriculture for pesticide control are discussed.

1.6.1 Nanotechnologies in Agriculture

In response to the numerous issues associated with the intensive use of pesticides, such as the development of resistance in target pests, adverse effects on non-target organisms, environmental contamination, and toxicity, controlled-release systems have been extensively investigated for environmentally friendly pest management. A major limitation of conventional formulations is that most pesticides are insoluble in water, which compromises their dispersion and stability in the aqueous phase, resulting in a non-uniform distribution on target crops. [77]

The development of nanotechnology has provided a novel approach for the innovation of controlled release pesticide formulations. Since the beginning of the 21st century, when the concept of pesticide nanotechnology was first introduced in the USA, significant progress has been made in the design of nanopesticides. In recent years, a wide range of nanomaterial-based pesticide delivery systems have been developed with improved solubility, enhanced stability, controlled release, and greater efficiency in crop protection, while also reducing the environmental footprint of pesticide applications. [78-79] Furthermore, thanks to Nanotechnology, pesticides management can be driven toward a *local application* in a *controlled manner*, with a resulting reduced and more effcient use of agrochemicals. **Figure 8** provides a classification of the most widely studied nanoformulations for the controlled release of agrochemicals, highlighting the different types of carriers and the active ingredients commonly encapsulated within them.

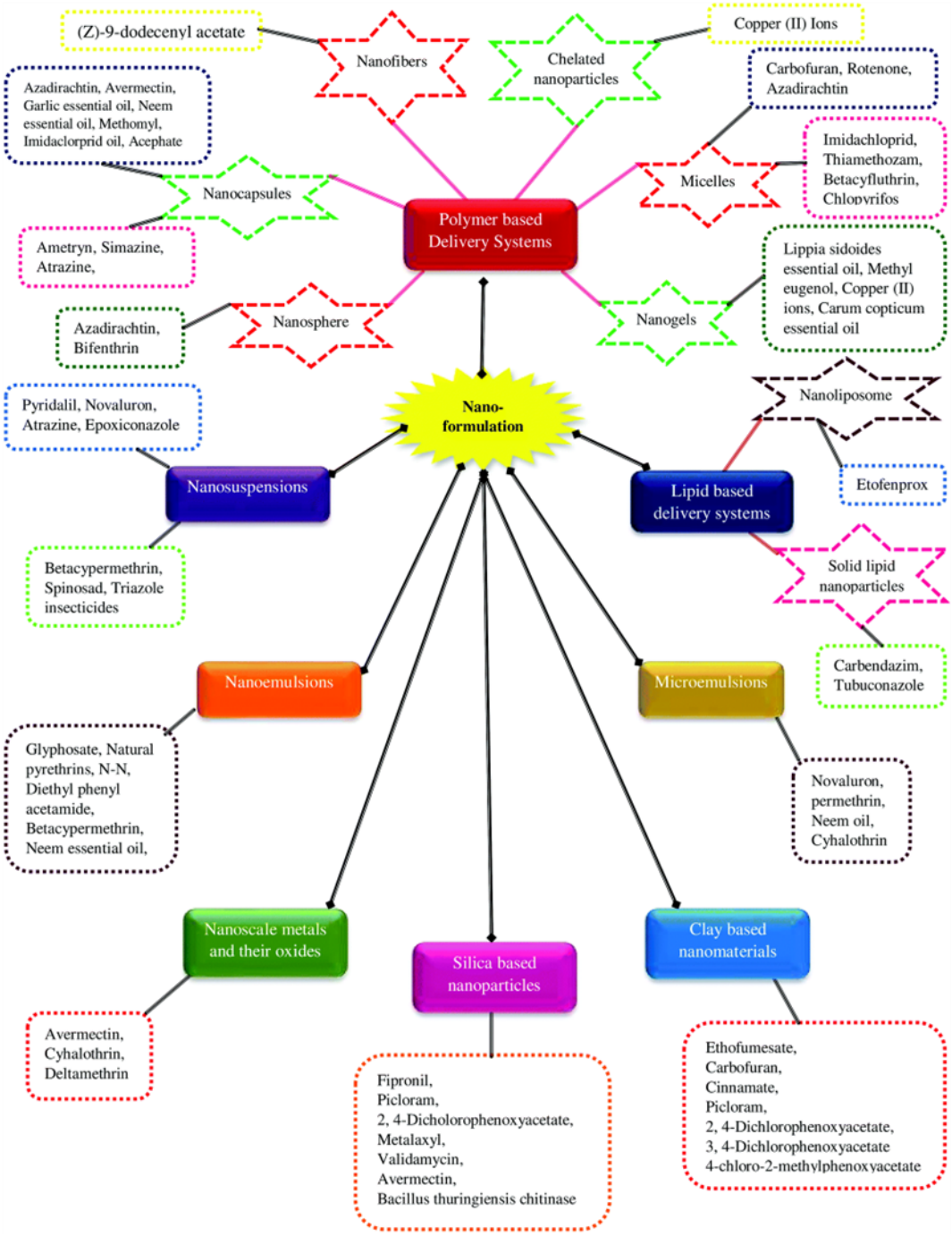

Figure 8. The diagram illustrates different classes of nanocarriers, including polymer-based systems, lipid-based carriers, silica nanoparticles, clay nanomaterials, nanoemulsions, and nanoscale metal oxides along with representative agrochemicals incorporated within each category. [78]

The nanomaterials used for the controlled release of pesticides include nanoparticles, films, capsules, emulsions, layered systems, hydrogels, porous beads, and fibers. These

different configurations influence the release of the active ingredient, its protection from external factors, and its overall efficacy. Among the carrier materials, polymers remain the most widely used, ranging from natural biopolymers (e.g., gelatin, gum arabic) to synthetic ones (e.g., PEG, polyurethane). Recent strategies involve nanocomposites that combine polymers with nanoparticles to improve environmental resistance, adhesion to surfaces, and responsiveness to external stimuli.

A wide range of polymeric and hybrid carriers have been explored for the controlled release of fungicides. Polymeric microcapsules are among the most established systems, providing both protection of the active ingredient and gradual release. [79-80] For instance, Chen et al. developed polyurethane-based microcapsules loaded with prothioconazole and functionalized with chitooligosaccharide (COS). [81] Biodegradable polymers have also attracted attention as sustainable carriers. Polylactic acid (PLA) microspheres, for example, have been used to co-encapsulate prothioconazole and tebuconazole, resulting in a synergistic effect against *F. graminearum*. Compared to the non-encapsulated mixture, the microspheres achieved stronger inhibition of mycelial growth, while offering the additional advantage of biodegradability and reduced environmental persistence. [82]

Another innovative approach is represented by environment sensitive microcapsules, designed to respond to specific environmental stimuli. A prominent example is BASF Seltima®, a commercial pyraclostrobin formulation in which the polymeric capsule wall is humidity sensitive. This enables fungicide to be released directly onto rice leaves after water evaporation, thereby preventing its diffusion into aquatic environments and reducing toxicity toward non-target organisms. [83]

Among the different nanocarriers explored for pesticide delivery, mesoporous silica nanoparticles (MSNs) have attracted particular attention. Several studies have demonstrated the advantages of MSNs in the delivery of triazole and strobilurin fungicides. For instance, Wang et al. developed double hollow-shelled MSNs functionalized with carbon quantum dots for prothioconazole delivery, enabling traceability of plant uptake through foliar and root pathways. [84] In another approach, Mosa et al. reported MSNs coated with quaternized chitosan (HTCC) for the encapsulation of fludioxonil. Similarly, Feng et al. demonstrated the encapsulation of

pyraclostrobin in MSNs, significantly improved resistance to UV degradation and enhanced antifungal activity against *F. graminearum* and reduced toxicity toward non-target organisms. [85]

In addition to polymer carriers and nanoparticles, hydrogels have also proven to be promising systems for the controlled release of pesticides. Hydrogels are 3D, cross-linked polymeric networks with a high-water absorption capacity, which makes them particularly suitable for agricultural applications where water management and the sustained release of active compounds are crucial. Their structure enables the encapsulation of pesticides and their gradual diffusion, while at the same time protecting active ingredients from degradation and leaching.

Several studies have demonstrated the potential of hydrogels in crop protection, many of which exhibit a pH-triggered release behavior. Xu et al. developed hydrogels based on carboxymethyl chitosan cross-linked with Mn^{2+} ions to achieve the controlled release of the fungicide prothioconazole. [86] In another study, Sun et al. described a composite hydrogel of lignin and polyacrylic acid (LBPAA), capable of loading pesticides such as paraquat, β-cyfluthrin, and cyhalofop-butyl. [87] Similarly, Kumar et al. described a biodegradable aloe vera–polyacrylic acid hydrogel with a high swelling capacity, which enabled the controlled release of the insecticide dichlorvos while improving soil water retention for up to 20 days. [88]

In the last decades, protective films have gained increasing attention as innovative carriers for the controlled release of pesticides in agriculture. These films, typically composed of biodegradable polymers, can be applied as coatings on plant surfaces or used as mulching materials, providing both a physical barrier against pathogens and pests and a reservoir for gradual pesticide delivery. [89] Xu et al. developed a biodegradable nanofiber-based seed coating, fabricated through electrospinning of biopolymer blends. This system allows for a tunable release of Cu^{2+}, enhancing germination and seedling biomass of tomato and lettuce under both healthy and *Fusarium* infected soil conditions. [90] Other studies have similarly demonstrated the versatility of biodegradable polymer films in pesticide delivery. For example, poly(vinyl alcohol)–starch (PVA–ST) composite films have been used to encapsulate the herbicide 2,4-dichlorophenoxyacetic acid, showing improved water resistance, mechanical stability, and controlled release

behavior. [91] Chitosan-based coatings loaded with fungicides have been applied to bean and maize seeds, combining the antimicrobial activity of the polymer with the gradual release of the active ingredient during storage.[92] Electrospun cellulose diacetate nanofibers loaded with pesticides (abamectin or fluopyram) have been applied as seed coatings on soybean seeds, showing antifungal activity and a slow, sustained release of active ingredients without impairing germination. [93] The development of nanotechnology-based controlled-release systems represents a promising strategy to use pesticides in a more efficient and sustainable way, paving the road for next-generation solutions in crop protection.

Compared to fungal and nematodes pathogens, the management of bacterial phytopathogens is more complex and limited, mainly because fewer effective compounds are available. The control of bacterial diseases has relied on copper-based formulations. Excessive copper use has led to the emergence of resistant strains, as well as toxic accumulation in soils with harmful effects on non-target organisms, including beneficial microbes and wildlife. [72]

These challenges highlight the urgent need for innovative alternatives. Among the emerging strategies, nanotechnology offers promising perspectives. Metal nanoparticles, including zinc oxide nanoparticles (ZnO-NPs), display strong antibacterial activity due to their high surface-to-volume ratio, which enhances ion release and reactive oxygen species (ROS) production. In addition, ZnO-NPs can physically damage bacterial membranes, interfere with quorum sensing, and act as carriers for bioactive molecules, thereby improving efficacy while reducing chemical inputs. Studies have shown that Zn-based nanomaterials can suppress devastating bacterial pathogens such as *Erwinia carotovora*, opening new possibilities for sustainable crop protection. [94-95]

1.6.2 Seed dressing and mulching

Among the agronomic strategies developed to minimize environmental impact while sustaining productivity, two practices of relevance are *seed dressing* and *mulching*.

Seed dressing, also referred to as seed coating or seed treatment, is the practice of applying external materials at the surface of seeds with the aim of improving handling,

protection, and plant establishment. This technique, which dates back almost a century, has become essential in modern agriculture, particularly in horticultural and crop production systems. Unlike foliar sprays or soil drenches, seed treatments use small quantities of active ingredients, which reduces the overall environmental impact, while ensuring targeted protection during the early stages of plant development.

Seed coating techniques can be broadly divided into dry and wet methods. Dry coating consists in the direct application of powders onto the seed surface and are the simplest but least precise approach; it is mainly used to deliver protective substances in a quick and inexpensive way, but without greatly improving uniformity.

Wet methods, on the other hand, are more versatile and can be adapted to achieve different purposes depending on the thickness of the applied layer and the extent to which the seed shape is modified.

The most common wet method is *seed coating*, which applies to a very thin polymeric layer containing active compounds such as fungicides, insecticides, micronutrients, or bio-stimulants. This technique is used when the goal is to protect the seed or add beneficial substances without altering its natural size or shape, so that sowing behavior remains unchanged. A more elaborate method is seed encrusting, where inert fillers and binders are added to increase the weight and volume of the seed. This does not completely change the seed form but makes it heavier, more uniform, and easier to handle, allowing for greater sowing precision and reduced seed loss in the field. Finally, seed pelleting represents the most intensive form of coating, where seeds are reshaped into spherical or ovoid forms. This manipulation is especially useful for very small or irregularly shaped seeds, because it makes them compatible with mechanical sowing equipment and also allows larger amounts of protective or nutritive substances to be incorporated.

The equipment commonly used for industrial seed coating includes rotating pans, rotary coaters, and fluidized bed systems, shown in **Figure 9,** each designed to deliver a specific type of coating according to the desired level of protection, uniformity, and sowing efficiency. [96]

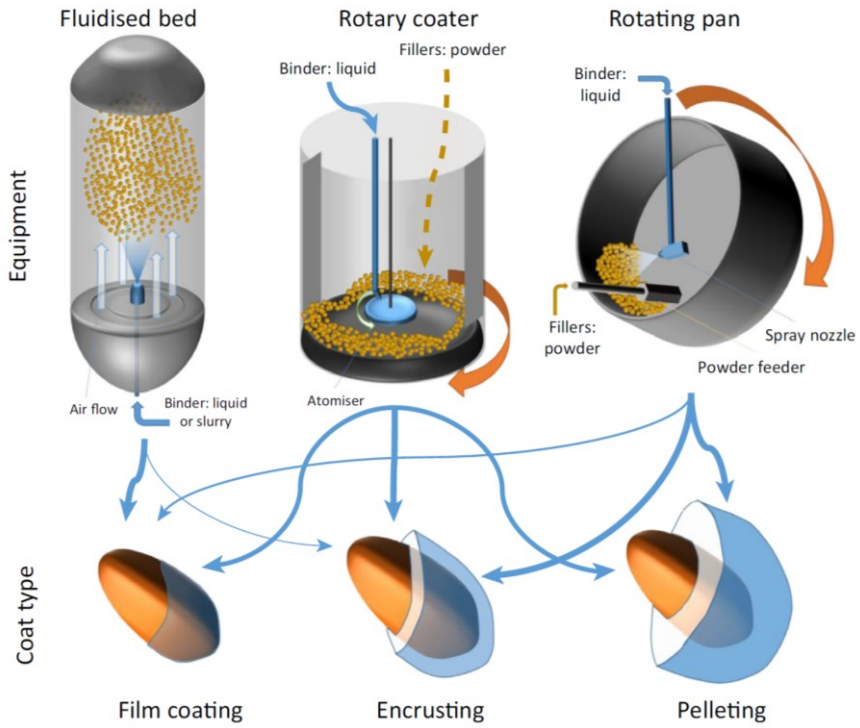

Figure 9. Representation of the main industrial equipment used for seed dressing. Depending on the method and amount of material applied, seeds can be covered by a thin protective film coating, moderately thick encrusting, or reshaped into uniform pellets. [96]

Seed dressing today is not merely a plant protection strategy but a multifunctional technology that supports sustainable agriculture by reducing pesticide use, improving sowing efficiency, and enhancing crop establishment under diverse field conditions.

In addition to interventions on seeds, sustainable agriculture also relies on soil management strategies. Mulching represents one of the most effective of these practices, providing both agronomic and environmental benefits by protecting the soil surface.

Mulching in agriculture is practice of covering the soil with organic or inorganic materials in order to conserve soil moisture, regulate temperature, suppress weeds, and reduce erosion. In the past, natural materials such as straw, compost, or bark were used; however, since the 1950s, synthetic polymers such us polyethylene, have become the most widespread solution due to their low cost. [97] **Figure 10** shows the various materials used in mulching.

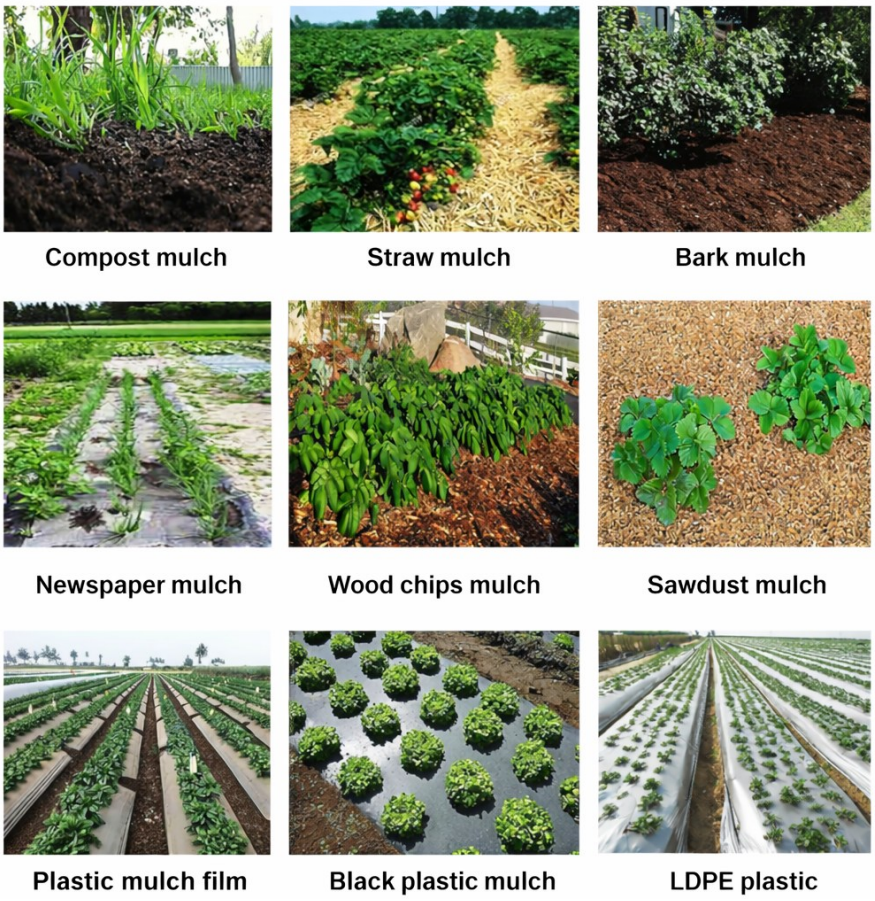

Figure 10. Examples of different types of mulching commonly used in agriculture. Organic (compost, straw, bark, newspaper, wood chips, sawdust) and synthetic materials (plastic film, black plastic, LDPE plastic) are shown. [97]

In recent decades, research has focused on the development of biodegradable mulching materials, capable of maintaining agronomic benefits while ensuring complete degradation in the soil after use. By incorporating pesticides, herbicides, fertilizers, or biostimulants into biodegradable or polymer-based mulch materials, it is possible to create a slow and localized delivery that reduces the frequency of applications, minimizes leaching and volatilization losses, and lowers the environmental impact. In recent years, research has focused not only on the development of biodegradable and bio-based mulch films but also on functional solutions capable of carrying and releasing active substances directly into the soil. An innovative example is that of Xie et al., who developed a biodegradable composite mulch film incorporating temperature-responsive microcapsules containing the fungicide pyraclostrobin, for durable control of

Phytophthora root rot in soybean cultivation. [98] For another example, Liang et al. reported the development of a natural polymer-based mulch film loaded with the fungicide metalaxyl. This film was developed for controlling *Phytophthora sojae*, the causal agent of soybean root rot. [99]

Seed dressing and mulching are key agronomic practices that enhance crop establishment and soil management while serving as a basis for technological innovation. In line with the Farm to Fork Strategy, they demonstrate how traditional techniques can evolve into sustainable solutions with reduced environmental impact.

1.6.3 Natural substances and alternative compounds for pathogen control

In this framework, interest in the use of natural substances and alternative compounds for pathogen management in agriculture has grown considerably, driven by the need to reduce the reliance on synthetic chemical pesticides.

The continuous search for alternatives to pesticides has drawn increasing attention to *biocontrol agents* (BCAs), defined as microorganisms capable of counteracting one or more target plant pathogens by interfering with their life cycles. BCAs protect plants through several complementary mechanisms, illustrated in **Figure 11**. *Mycoparasitism* occurs when the antagonist attacks and parasitizes the pathogen, destroying its structures and reducing its survival. *Competition* takes place when BCAs compete with pathogens for essential resources (e.g., carbohydrates, nitrogen, and micronutrients) and for physical space, for example by colonizing plant surfaces or wounds, thus preventing pathogens from establishing infection sites. *Antibiosis* is based on the production of bioactive compounds that inhibit pathogen growth, including cell wall degrading enzymes and volatile organic compounds (VOCs), which can interfere with pathogen metabolism or damage its structures. Finally, BCAs can act indirectly by triggering the plant's own defenses through induced *systemic resistance*. This mechanism enhances the production of antimicrobial metabolites, strengthens cell walls with lignin and callose, and promotes the synthesis of pathogenesis-related proteins, thereby priming the plant to respond more efficiently to subsequent pathogen attacks. Indeed, most BCAs do not

rely on a single strategy, but combine different mechanisms depending on the crop, the pathogen, and the environmental conditions. [100-101]

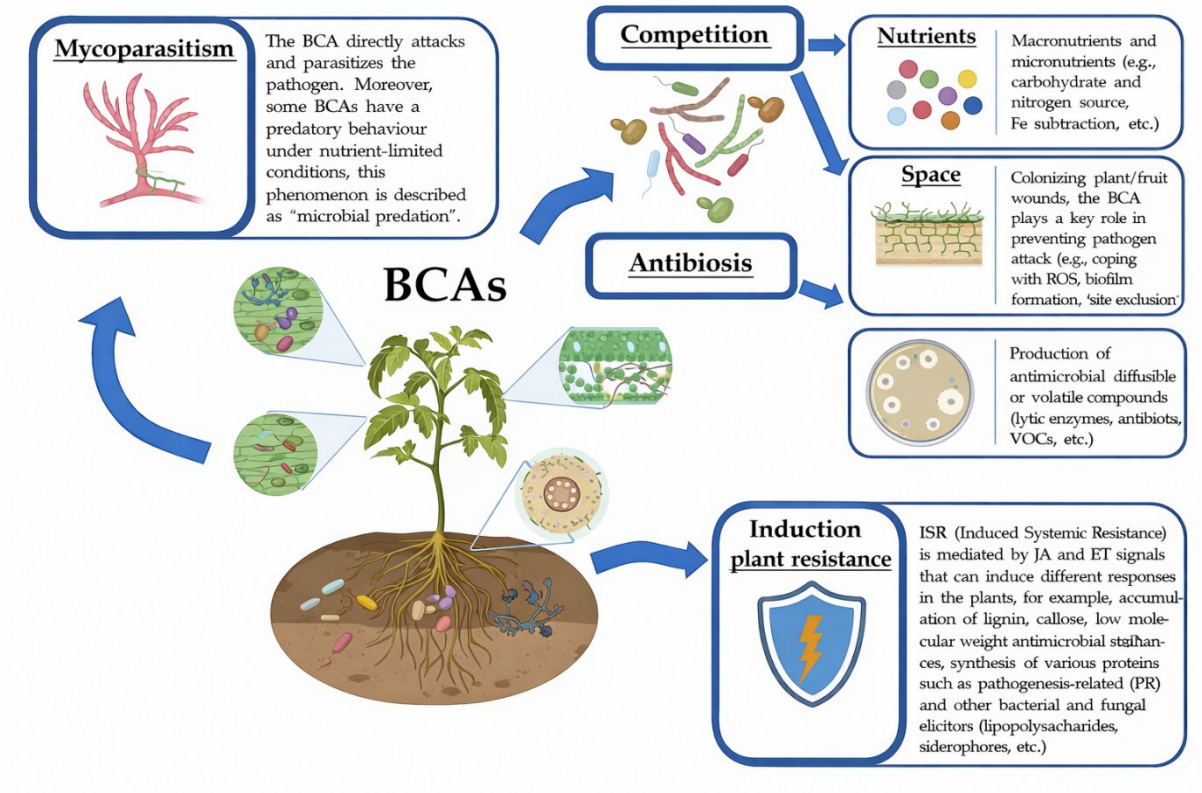

Figure 11. Main mechanisms of action of BCAs. [100]

The application of beneficial microorganisms has proven particularly promising, as it reduces the reliance on chemical pesticides and mitigates the risks associated with human health and the environment.

One group of microorganisms that is attracting increasing interest is represented by lactic acid bacteria (LAB). These microorganisms exert antagonistic activity against phytopathogenic fungi mainly through the production of organic acids such as lactic and acetic acid, which lower the pH and create unfavorable conditions for pathogen proliferation. In addition, LAB are able to synthesize lytic enzymes, including cellulases, proteases, and glucanases, which degrade the cell wall of harmful microorganisms, compromising their vitality and infective capacity. Some strains also exhibit direct competition for nutritional resources, limiting the availability of substrates required for

pathogen growth. These different mechanisms, often acting in combination, make LAB potential candidates for biocontrol applications both in the field and in postharvest management. [102-103]

Bacillus velezensis is of particular relevance, a microorganism widely studied for its effectiveness against *F. graminearum*. [104] *B. velezensis* exerts its antagonistic activity through the production of antifungal lipopeptides (iturins, fengycins, and surfactins) that disrupt fungal cell membranes, the secretion of hydrolytic enzymes (including chitinases and glucanases) capable of degrading the pathogen's cell wall, and the release of siderophores that sequester iron and other essential nutrients from the fungus. Moreover, this bacterium is able to stimulate induced systemic resistance (ISR) in the host plant, thereby enhancing its natural defenses against infections. Its safe use is supported by its inclusion in the Qualified Presumption of Safety (QPS) list of EFSA, and several *B. velezensis* strains are already commercially as biocontrol agents, confirming the practical potential of this bacterium in the sustainable management of cereal crop diseases. [105]

Beyond BCAs, *essential oils* (EOs) have recently gained growing attention as natural alternatives to synthetic pesticides, with particular interest in their potential as nematicides.

EOs are natural volatile substances found in many plants. They are complex mixtures mainly composed of terpenoids, particularly monoterpenes and sesquiterpenes, together with a variety of aromatic phenols, oxides, ethers, alcohols, esters, aldehydes, and ketones that determine the characteristic aroma and fragrance of the plant. Their chemical composition can vary considerably among aromatic plant species and varieties, and even within the same variety, depending on the geographic area. Although aromatic plants and their essential oils have been used since ancient times as antimicrobial and insecticidal agents, interest in them has increased significantly only over the last decade. In recent years, many efforts have therefore been devoted to the study of the nematicidal activity of EOs and their constituents, which are considered potential sources of commercial products for the management of plant-parasitic nematodes. [106]

The nematicidal activity of EOs largely depends on their bioactive components, which belong to the different chemical classes, illustrated in **Figure 12**. Monoterpenes such as

carvone, limonene, thymol, and linalool can penetrate the gelatinous matrix of eggs, alter plasma membrane permeability, and interfere with the nervous system of juveniles and adult nematodes. Sesquiterpenes (e.g., cuminaldehydes, α-bulnesene) and phenylpropanoids such as eugenol, isoeugenol, and (E)-cinnamaldehyde mainly affect cellular processes, including key enzymatic functions like V-ATPase activity, essential for survival and reproduction. In addition, sulfur-containing compounds (e.g., diallyl disulfide and allyl isothiocyanate) act on neurotransmission and chemosensory functions. [107]

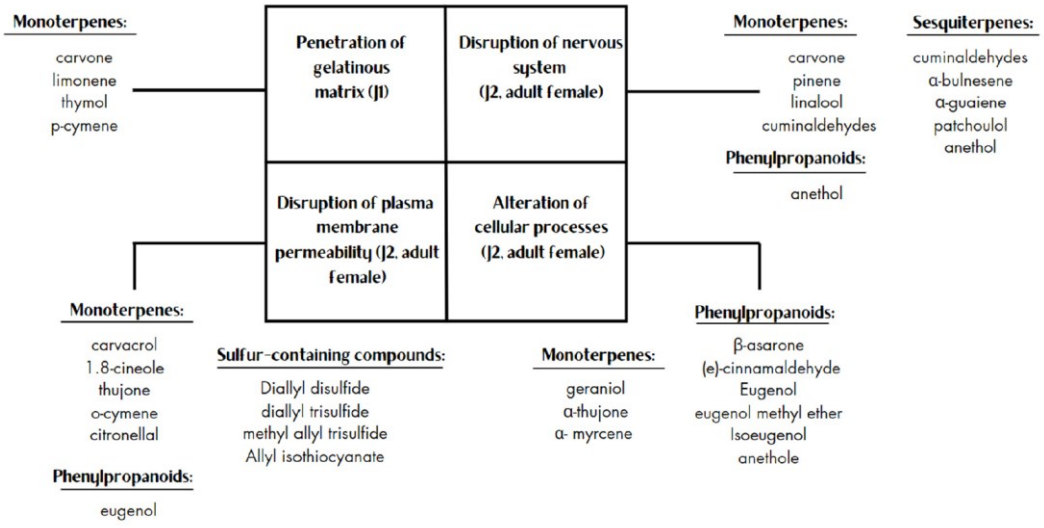

Figure 12. Compounds of EOs and their mode of action against root-knot nematodes. [107]

Among EOs with nematicidal activity, particular attention has been given to *Cinnamomum cassia*, whose activity is mainly attributed to its high content of (*E*)-cinnamaldehyde. This compound represents between 42% and 92% of the EO, depending on environmental and extraction factors.[108-110] Several studies have demonstrated its strong effectiveness against the root-knot nematode *M. incognita*. Both *in vitro* and greenhouse assays showed significant J2 mortality and a reduction in gall formation on host plants. The study also demonstrated that cinnamon essential oil inhibited egg hatching and reduced juvenile survival, thereby interfering with multiple stages of the nematode life cycle. [107,106] Quantitative studies further revealed strong activity at relatively low concentrations, with cassia essential oil proving lethal to J2 at 62 µg/ml of soil. [111]

1.7 Plasma & Agriculture

1.7.1 Plasma processing: Low Pressure and Atmospheric Pressure

Plasma is defined as the fourth state of matter distinct from solids, liquids and gases. It consists of a partially or fully ionized gas in which free electrons, positive ions, and neutral species coexist. Despite the presence of charged particles, plasma remains globally neutral, since the densities of positive and negative charges are approximately balanced. The term "plasma" was introduced in 1928 by Irving Langmuir, Nobel Prize in Chemistry in 1932. He derived it from the Greek *plássein* ("to mold" or "to shape") to emphasize the analogy between the collective behavior of charged particles in an ionized gas and the motion of cells suspended in the liquid plasma of blood.[112-113]

Plasma is formed when enough energy is supplied to a gas in the form of heat, electric or electromagnetic fields, or high-energy radiation to initiate ionization processes. Under these conditions, electrons, being much lighter than ions, rapidly absorb energy from the applied field and transfer it to the system through collisions. These collisions can be classified as elastic and inelastic. Elastic scattering represents the most frequent type of interaction, but it is rather inefficient due to the large mass difference between electrons and neutral particles, thus resulting in minimal energy transfer per collision. In contrast, inelastic scattering is less frequent, but far more significant from an energetic perspective, as it includes rotational, vibrational and electronic excitation as well as ionization. Such processes require overcoming energy thresholds on the order of several tens of electronvolt and can generate excited species such as molecules, atoms, radicals, and ions, through ionization, molecular fragmentation, and both homogeneous and heterogeneous reactions. [113-115]

Plasmas can be broadly categorized into thermal (equilibrium) and non-thermal (non-equilibrium) plasmas, depending on the degree of thermodynamic equilibrium among their constituent species.

In thermal plasmas, all species (electrons, ions, and neutral atoms or molecules) are close to thermodynamic equilibrium, sharing approximately the same temperature. This condition is generally achieved under high pressure and high energy density, where the frequency of collisions ensures efficient energy exchange among species. As a

consequence, the plasma reaches temperatures of several thousand K, often accompanied by a high degree of ionization. Thermal plasmas are commonly encountered in electric arcs, plasma torches, welding processes, metallurgical treatments and analytical techniques. Although thermal plasmas can have various applications, they are not suitable for the treatment of thermodegradable materials. Non-thermal plasmas, also referred to as cold, low-temperature (LTP), or non-equilibrium plasmas, are far from thermal equilibrium. In this case, electrons, being much lighter than the other species, absorb energy far more efficiently from the applied electric field. As a result, the electron temperature (T_e) is significantly higher (10^4- 10^5 K) than the temperature of heavy particles such as ions and neutrals, which remain close to room temperature. A common approach to maintain non-equilibrium conditions is to operate at low pressure (<10 Torr) where the average free path of the electrons increases and collisions become inefficient, thereby reducing the rate of energy transfer between species. As a result, electrons can remain at higher temperatures than ions and neutrals, allowing the plasma to preserve its non-thermal character. [116]

Not only pressure influences the thermal balance of plasma. Indeed, the ignition of an electrical gas discharge between two electrodes requires specific conditions to ensure that the gas becomes partially ionized and thus conductive. The critical parameter is the *breakdown voltage* (V_B), defined as the minimum potential difference necessary to trigger the ionization process. According to Paschen's law ($V_B = f(p \cdot d)$), this voltage depends on the product of the gas pressure (p) and the electrode gap (d). [117] As shown in **Figure 13**, each gas is characterized by a Paschen curve, which describes the trend of V_B as a function of the product $p \times d$. The curve has a minimum that corresponds to the lowest V_B required to ignite plasma. In laboratory environments, both low-pressure (LP) and atmospheric-pressure (AP) plasmas can be ignited, in different plasma reactors.

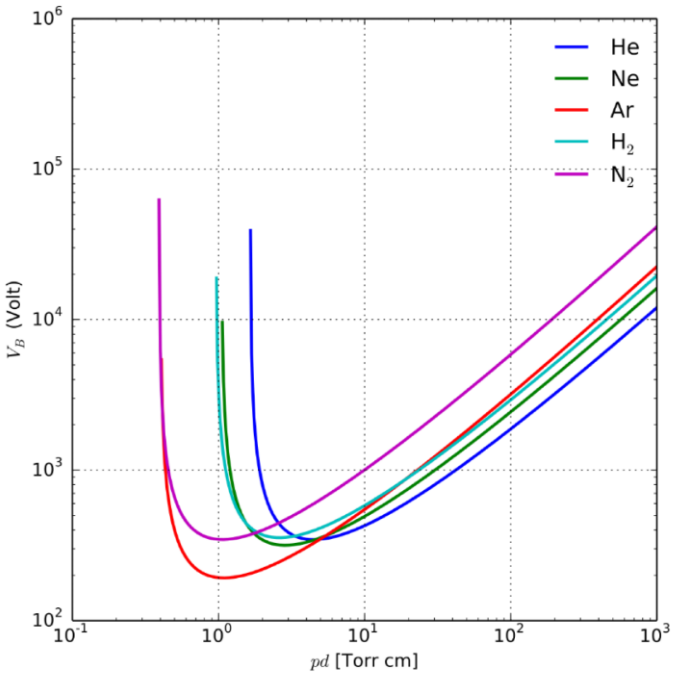

Figure 13. Paschen curves for some commonly used gas.

At LP, plasma can be sustained even with electrode gaps of several centimeters, while maintaining relatively low V_B. However, at AP the distance between electrodes must be reduced to a few millimeters or less to reach the minimum of the Paschen curve and keep the V_B within a few KV. If the gap is larger, the discharge becomes unstable and concentrates into thin arc filaments, or streamers, which produce high temperatures and strong non-uniformities.

The stabilization of cold atmospheric plasmas therefore requires a combination of technical measures. A first strategy is the use of noble gases such as He and Ar. Although helium is expensive, it is widely employed because of its low breakdown voltage (~4 kV/cm) and its ability to sustain diffuse and stable discharges. In addition, AP plasmas are usually operated with high gas flow rates (liters per minute), which reduce the residence time of plasma species, limit the energy deposited per particle, and provide a cooling effect that prevents the transition to arcs.

Another crucial factor is the power supply. With a direct current (DC) source, the discharge typically evolves from a spark into a hot arc, losing its non-thermal character.

To avoid this, alternating current (AC) configurations or ns/μs pulsed power are preferred, as they allow selective excitation of electrons while minimizing gas heating. [118]

The electrode configuration also influences the non-thermal nature of plasma. As shown in **Figure 14** corona discharges (CD) are characterized by highly asymmetric electrode arrangements, with the high voltage (HV) electrode being small and needle or wire shaped. The high voltage applied to such a small-geometry electrode creates an intense field around it, which must be sufficiently high to form a conductive region, but not so high as to allow arc formation, thereby enabling the generation of a non-equilibrium plasma.[119]

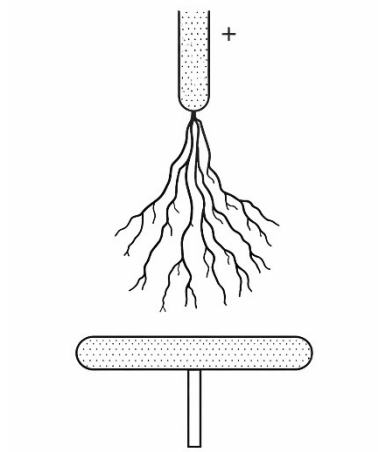

Figure 14. Corona Discharge configuration.

Dielectric barrier discharges (DBDs) are among the most reliable approaches. They are characterized by the presence of at least one dielectric layer in the path between the high-voltage (HV) electrode and the ground one. In DBD systems, the dielectric layer limits charging of the electrode with the consequent formation of a counter-voltage that limits the rise of the current and transition to the arc. Owing to the presence of the dielectric, these discharges can be ignited and sustained by AC electric fields or DC voltages, typically with amplitudes of 10–20 kV and frequencies in the range of 10–100 kHz. The discharge gap usually has a width ranging from less than 0.1 mm to a few mm. Typical dielectric materials include glass, quartz, ceramics (e.g., alumina), as well as thin enamel or polymer coatings. The dielectric constant and the thickness of the insulating layer,

together with the time derivative of the applied voltage (dV/dt), ultimately determine the amount of displacement current that can flow through the electrodes. [116-120]

DBDs can be implemented using different electrode configurations, as reported in **Figure 15**, which allow tailoring of the plasma to specific applications. In parallel plate geometries, a volume discharge is generated that fills the entire inter-electrode gap. The dielectric can be applied to both electrodes (double-sided configuration) or only to one electrode or suspended between them (single-sided configuration). Cylindrical geometries are also widely used, for example in surface treatment processes. In contrast, coplanar and surface electrode geometries do not generate volume discharges but rather produce surface discharges, namely a thin plasma layer confined to the dielectric surface. An important application of coplanar discharges is in plasma display panels, where surface plasma is exploited for light generation. Finally, DBDs can be designed in annular configurations consisting of coaxial electrodes, with the dielectric applied either to both electrodes or to the inner or outer electrode only. For the treatment of 3D objects, jet source configurations can be suitably designed. These arrangements can expose a substrate either to the plasma plume or to the afterglow effluents generated at a certain distance. Such systems are known as atmospheric pressure plasma jets (APPJs). In the setup, the plasma is ignited between two electrodes in a remote position and expands towards the substrate located outside the inter-electrode region. [121-125] This configuration, of which two possible layouts are shown in **Figure 16**, allows integration with a robotic arm for automatic processing, or the treatment of large surfaces by mounting a suitable number of plasma jets in an array.[120]

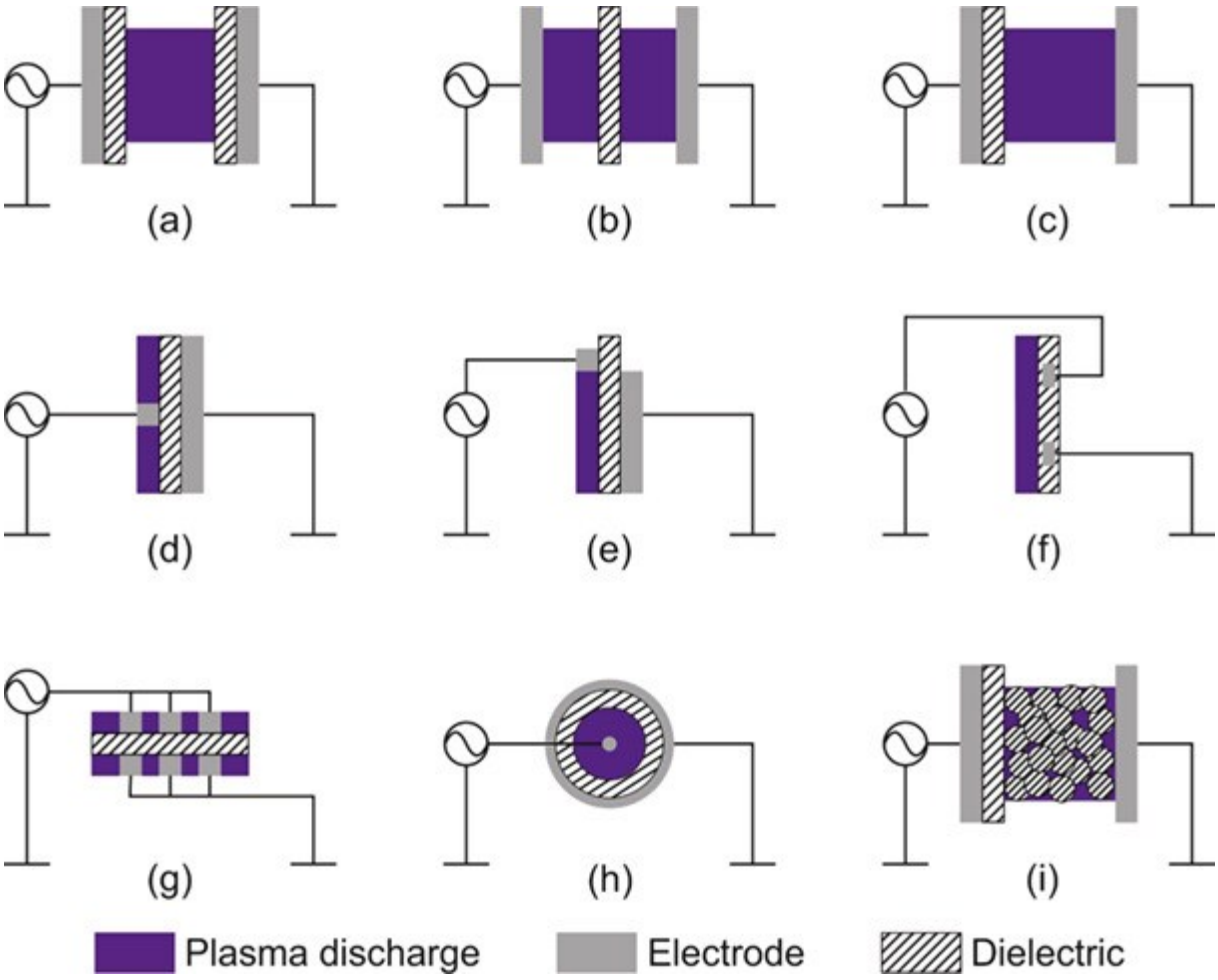

Figure 15. Scheme of possible DBD configurations. [123]

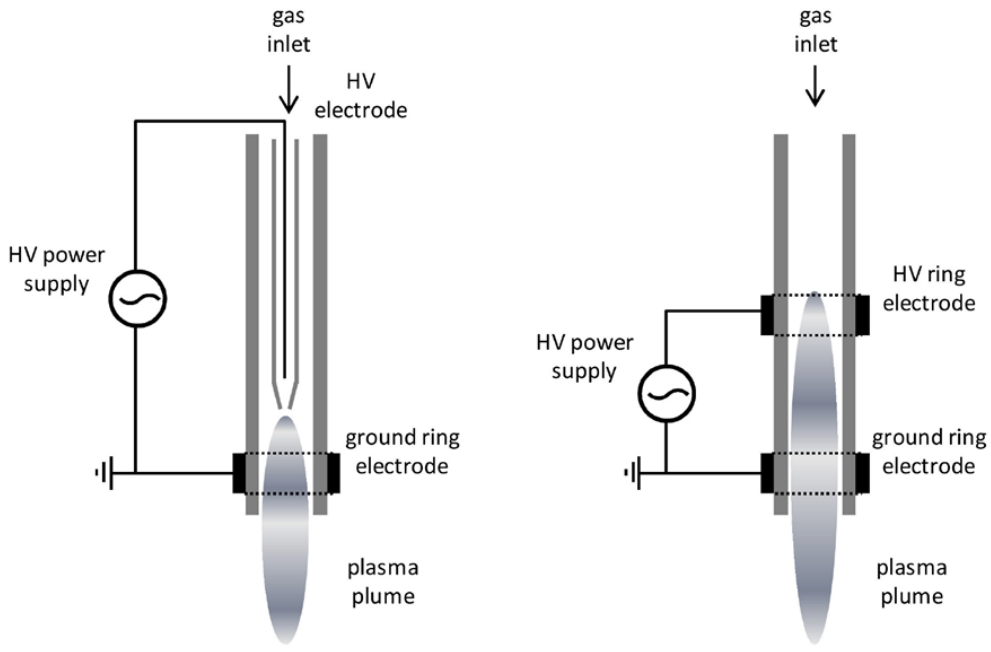

Figure 16. Design of two APPJ sources. [125]

In plasma, gas excitation and ionization generates a large number of reactive species, including highly energetic electrons, metastable states, photons (VUV radiation), ions and radicals produced through the interaction between energetic electrons and additives (e.g., deposition precursors). When these reactive species interact with a solid substrate, in non-equilibrium (cold) conditions they can start several technologically relevant processes, such as: *dry etching*, *surface treatments*, and *plasma-enhanced chemical vapor deposition (PE-CVD)*.

Dry etching is an ablation technique that occurs through reduction/oxidation reactions between a material exposed to the discharge and the active species generated in the plasma. Plasma species react with surface atoms forming volatile species and in turn leading the consumption of the reacting surface. It is an approach used, for example, for cleaning metallic surfaces, capable of removing oxide, chloride, and sulfide layers, or in microchip fabrication. In this technologically relevant process, microlithographic techniques are coupled with etching processes.

Surface treatments are defined as the introduction of different functional groups (amino, carboxyl, hydroxyl, etc.), oxidation, reduction, or crosslinking (for polymers) onto the outermost layers of the substrate subjected to the process, through the use of both reactive gases (O_2, NH_3, CF_4, H_2O, etc.) and inert gases (Ar). This process does not lead to a significant increase in substrate thickness or an appreciable variation in its weight, and it has been widely applied to improve the wettability, printability, and adhesion of polymeric surfaces. [126]

The PE-CVD technique, sometimes also called “plasma polymerization” when an organic monomer used as feed, is employed for the deposition of organic inorganic films, with thicknesses in the nm-μm range. Although LP processes have been widely used for deposition, AP processes can also be applied. A key factor in film formation is the deposition initiated by electron–monomer collisions. Electron impact leads to monomer fragmentation and the formation of deposition precursors, as well as atoms and other radicals. These species can further react in the plasma or diffuse toward the substrate surface, where they can adsorb. Once on the surface, the precursors may react with the substrate or with reactive species, ultimately leading to film growth. Energetic species,

such bombarding positive ions , can also transfer energy to the surface, generating active sites and promoting film growth.

Based on this mechanism, plasma polymerization cannot be understood as the regular chain growth process resulting from the consecutive addition of repeating units (i.e., monomers). Consequently, films produced via plasma typically exhibit a significant degree of crosslinking compared to their counterparts obtained through conventional polymerization processes, as well as a lower retention of the original monomer structure.

In PE-CVD, precursors are introduced into the reaction chamber, where the substrate is located, often together with an inert carrier gas and under LP conditions. One of the main challenges associated with this technique is the handling of solid substances and compounds with low vapor pressure. [127]

1.7.2 Aerosol-Assisted Atmospheric Pressure Plasma Deposition

The deposition of thin films by cold atmospheric pressure plasmas can be carried out either by adding the precursor gas or vapor to the plasma feed, or by injecting a liquid precursor. The *Aerosol-Assisted Atmospheric Pressure Plasma Deposition (AAA-PPD)* technique consists in the introduction of a liquid precursor into the plasma with a nebulization system for aerosol generation. An aerosol is defined as a suspension of liquid droplets or solid particles in a gas medium. Typically, the droplet density is less than 1%, while the particle size is below tens of microns. Three main methods can be used to generate aerosols: ultrasonic generation, pneumatic jet, and electrostatic atomization. The ultrasonic approach relies on a piezoelectric transducer placed under the liquid feed, through which a carrier gas flows; in this case, the resulting droplet size typically ranges between 1-10 μm. In the pneumatic approach a compressed gas is introduced transversely through a nozzle into a liquid stream, fragmenting the fluid into droplets. Although the resulting droplet size is generally larger than in the ultrasonic method, an appropriate nozzle design and generator head geometry can yield droplets with diameters below 1 μm. Finally, in the electrostatic method the liquid can be first atomized by ultrasound and subsequently exposed to a strong electric field, or the electric field can be applied directly at the nozzle, leading to the dispersion of the liquid into charged droplets. Regardless of the electrode assembly and the type of atomizer considered, two

main approaches, shown in **Figure 17** can essentially be identified for injecting a precursor into the plasma when coupled with an aerosol, with the aim of depositing a coating.

In the approach **I**, all the "building blocks" of the coating deposition are introduced through the aerosol, and no auxiliary line is required for the addition of a film precursor. In this case, the monomer (**Ia**) can be supplied either pure or dispersed in a solvent (**Ib**), or the dispersion of an active compound (e.g., a drug) in the feed monomer is atomized into the plasma. [125] This method is particularly effective for the deposition of single-component thin films, such as siloxane coatings from organosilicon monomers like HMDSO or TEOS, acrylic acid–based coatings rich in carboxylic groups, or hydrophobic and PEO-like films. [127-129] Otherwise, it allows the dispersion of nanoparticles within the atomized liquid feed, enabling the one-step synthesis of nanocomposite films (e.g., TiO_2/HMDSO, ZnO/octane, POSS/HMDSO). [130-134]The main limitation, however, is that the relative abundance of the different constituents is fixed by the composition of the starting dispersion, which can only be modified by preparing a new liquid feed.

In the approach **II**, the atomizer is typically used to inject a solution or suspension not directly suitable for film formation, while the main coating precursor is supplied through an auxiliary line (AUX). A significant advantage of this method is the higher degree of tunability: since the relative abundance of the two components in the feed can be continuously adjusted by controlling the respective flow rates, without the need to reformulate the liquid mixture. This flexibility allows precise control over the composition and functionality of the resulting coatings.

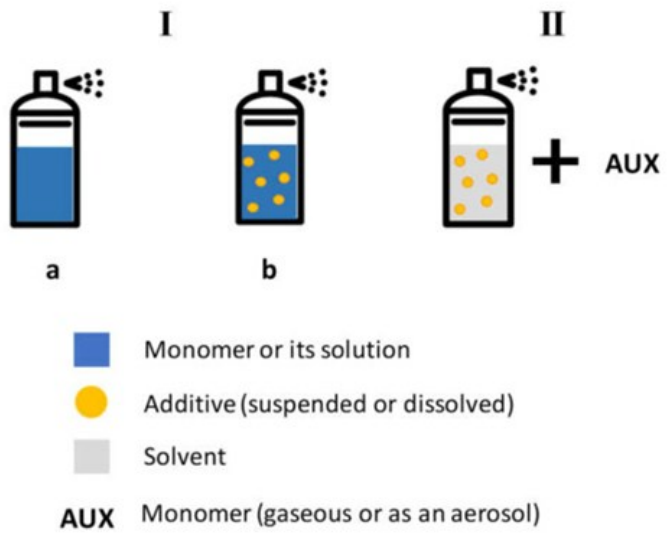

Figure 17. Scheme of possible coupling of atomization sources to atmospheric pressure (AP) plasma: Approach **I** (Ia–Ib), where all components are introduced via aerosol; Approach **II**, where the additive is aerosolized and the monomer is supplied through an auxiliary line (AUX). [122]

When compared to conventional PE-CVD processes, with this latest approach, AAA-PPD offers the ability to deposit nanocomposite (NC) coatings in a single step, as described in **Table 3**. In the framework of Approach II, several studies have demonstrated the successful deposition of bioactive and nanocomposite coatings. [125]For example, Ag NPs dispersed in ethanol were incorporated into an acrylic acid matrix using a plasma jet configuration, [129] yielding uniform antibacterial coatings. Similarly, TiO_2 NPs have been embedded into silica-like matrices formed from organosilicon precursors, producing hybrid coatings with photocatalytic and protective properties.[135]

Particularly relevant results were obtained with biomolecules and drugs. *Palumbo et al*. reported the deposition of lysozyme-containing coatings by nebulizing aqueous lysozyme solutions into an ethylene fed plasma. Spectroscopic analyses confirmed the presence of peptide bonds within the film, while HPLC measurements verified the release of intact lysozyme into aqueous media. Despite minor oxidation of susceptible residues, the enzyme largely retained its native structure and exhibited antibacterial activity comparable to the pristine protein. [136]

The same strategy has been applied to antibiotics such as vancomycin and gentamicin, which were incorporated into plasma-polymerized films. In these cases, the active agents

were encapsulated into spherical nanostructures whose morphology depended on the plasma conditions: continuous plasma favored larger and more uniform spheres, while pulsed regimes produced smaller aggregates. These structures displayed a core–shell architecture, with the drug molecules confined in the core and a polymeric shell derived from the plasma precursor enveloping them. The formation mechanism involves droplet charging, solvent evaporation, and polymer deposition on the resulting aggregates. It is worth noting that both antibiotics maintained their antimicrobial efficacy after encapsulation, while the coatings enabled a gradual and controlled release of the drug. [137-138]

Overall, these findings highlight the potential of AAA-PPD to generate bio-composite coatings in which fragile or complex molecules, including enzymes and pharmaceuticals, are effectively protected by the solvent layer during plasma exposure. This protective effect not only preserves their functionality but also opens the way to coatings for controlled drug delivery, antibacterial and antifungal surfaces, and possibly even the inclusion of more complex biological entities such as spores or cells.

Table 3. Comparison of the different aerosol/plasma couplings. [125]

Type of Coating	Advantages	Disadvantages
Single component	-suitable for deposition of single-phase coatings from one or more monomers -solution of non-volatile or solid monomers feasible	-not suitable for nanocomposite coatings
Nanocomposite	-good for deposition of nanocomposite coatings -one atomizer can feed the two (or more) film components at once -solution of non-volatile or solid monomers feasible	-different aerosol solution necessary to change coating composition
Nanocomposite	-good for deposition of nanocomposite coatings -solution of non-volatile or solid monomers feasible	-two independent feed sources necessary

1.7.3 Plasma in Agriculture

The increase in food demand, caused by the constant growth of the global population, has driven the scientific community to ever greater efforts to develop methods capable of increasing agricultural productivity while, at the same time, ensuring food safety.

Conventional techniques, such as irrigation, fertilization, and the extensive use of pesticides, have long represented the main strategies adopted to achieve this goal. However, these practices often overlook their environmental impact, with serious consequences such as water contamination, loss of biodiversity, soil fertility degradation, and the accumulation of toxic substances. To address this challenge, it is essential to identify innovative solutions that reduce the use of chemical inputs while allowing higher yields and protecting crops from pests and pathogens.

In this scenario, cold atmospheric plasma represents a promising tool capable of combining sustainability and efficiency. Initially, plasma technologies in the agri-food sector were mainly investigated for the treatment of packaging materials, aimed at improving barrier properties, wettability, or surface decontamination. Nowadays, given the non-thermal nature of the plasma, it has proven to be particularly suitable for the treatment of biological substrates such as seeds, soil, plants, and water. [139] As shown in **Figure 18**, atmospheric pressure plasma can be safely applied during the different stages of agricultural production: before sowing, during plant growth, after harvest, throughout storage, and even up to the commercialization of fresh products.

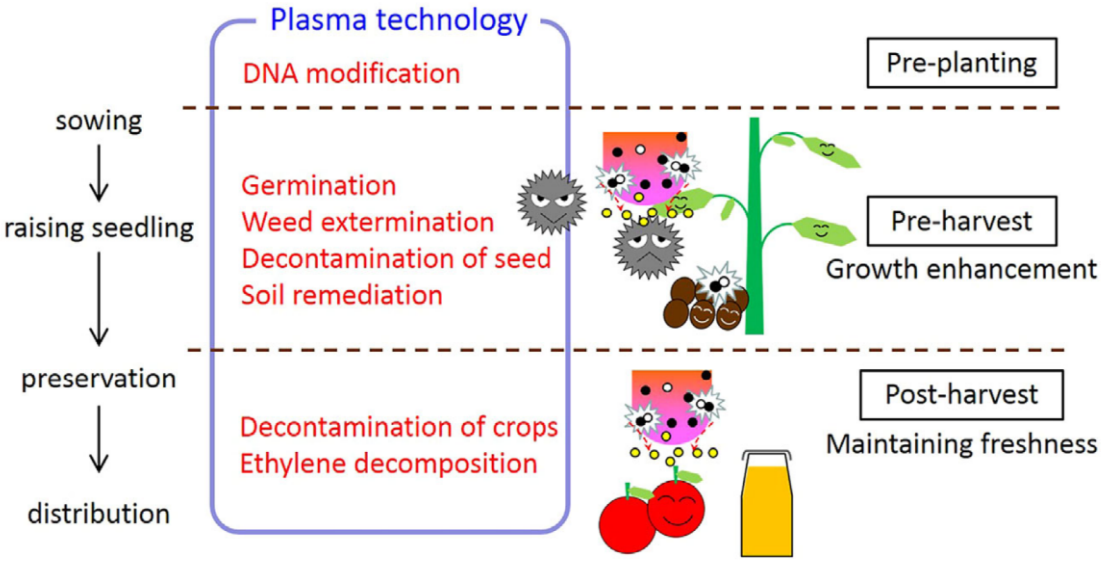

Figure 18. Agricultural applications using non-equilibrium atmospheric-pressure plasma technologies. [140]

In pre-harvest treatments soil, plants or seeds are exposed directly or indirectly to plasma action. In direct treatments, plasma comes into immediate contact with the material to be processed like seeds, soil, plants, or food products, exerting effects such as surface sterilization, seed coat modification, and enhanced water uptake. In indirect treatments, plasma acts on water, generating plasma treated water (PTW), which is later used for irrigation and seed soaking. In this case, the reactive oxygen and nitrogen species (RONS) dissolved in the liquid act gradually, ensuring a more prolonged effect on plant metabolism and growth.[141-142]

Soil is a fundamental component of agricultural productivity, as it hosts both plant root systems and complex microbial communities that include beneficial as well as pathogen organisms. In recent years, the use of non-thermal AP plasma has been investigated as an innovative approach to modulate these interactions, acting simultaneously on soil sanitization and on the enhancement of its fertility. The main mechanism underlying this dual effect lies in the generation of RONS, such as H_2O_2, OH·, O_2^-·, NO·, and NO_2. [141] When produced at controlled concentrations, these molecules can significantly reduce parasites, while at the same time stimulating the activity of nitrogen-fixing bacteria and promoting biochemical processes beneficial to plants. [143]

A representative example is provided by treatments with ozone produced with surface dielectric barrier discharges (SDBD). Experiments conducted with O_3 demonstrated the elimination of approximately 83% of nematodes, without a major impact on beneficial microflora. At the same time, increases in nitrate (NO_3^-) concentration and decreases in ammonium ions (NH_4^+) were observed in the upper soil layers about 5 cm deep. This rebalancing translated into improved growth and yield of radish crops.

The fertilizing effect of plasma manifests itself through three main pathways: the chemical conversion of nitrogen species into forms more readily available to plants, the modulation of microbial communities responsible for mineralization and nitrification, and the regulation of soil pH, which directly influences nutrient availability. Field applications have confirmed this synergy. Diffuse ozone treatments not only reduced the incidence of radish scab caused by *Streptomyces spp*. but also enhanced plant development by accelerating the mineralization of complex organic matter and increasing

the bioavailability of nitrogen compounds. In such cases, plasma does not merely exert a disinfecting action but contributes actively to improving soil fertility.

As previously described, plasma treatment of plants can occur in both direct and indirect ways. One of the direct applications concerns the enhancement of mushroom growth through pulsed high-voltage discharges. An example is the Shiitake mushroom (*Lentinula edodes*), in which, following plasma application during the fruiting body formation phase, the yield increased to 1.9 times. The same technique has also been adopted for other fungal species in specialized agricultural enterprises. In recent years, plasma agriculture has been extended to more than twenty plant species, including corn, wheat, rice, and potato showing beneficial effects such as accelerated growth and increased yields. In the case of strawberry seedlings, plasma irradiation led to a 25% increase in anthocyanin content in the fruits.

In addition to direct treatments, plants can also be exposed to PAW. The RONS species generated through the interaction between plasma and water are present at concentrations that depend on several factors, including the applied voltage, reactor configuration, operating conditions, and the chemical composition of the surrounding environment. Numerous studies have reported the effectiveness of PAW in promoting plant growth. Acting as a source of nitrogen in the form of NO_3^-, PAW can optimize crop yield and reduce the reliance on conventional fertilizers; in hydroponic systems, for instance, it has been shown to double the nitrogen content in leaves, as well as increase leaf area and dry weight. Furthermore, PAW naturally modulates pH, replacing chemical acidifiers commonly used to maintain optimal conditions for nutrient uptake. Thanks to its oxidizing species, it also exerts a strong antimicrobial effect, drastically reducing bacterial loads and offering a sustainable alternative to traditional disinfection methods such as hydrogen peroxide, ozone, or UV radiation. Additional studies have highlighted qualitative improvements associated with PAW treatment: for example, in strawberries, a 27% increase in sugar content was observed, while under drought conditions PAW was able to reduce overall water requirements while still supporting healthy plant growth. These effects are most likely due to a more efficient uptake compared to untreated water, combined with the fertilizing role of plasma-activated nitrogen species. [139]

Seeds can be treated either directly with plasma or indirectly by immersion/irrigation with PAW. Direct treatment is most often performed with DBDs at AP. However, the small volume of this configuration can be a limit to the scalability of this process. During treatment, seeds are exposed to a wide variety of RONS species. One of the most consistent outcomes of direct plasma exposure is an increased germination percentage. This effect is largely attributed to modifications in seed coat chemistry and surface morphology, particularly an increase in hydrophilicity, which enhances water uptake during imbibition. Such changes depend strongly on treatment parameters including duration, applied power, and the gas feed used; indeed, the gas composition can either promote or delay germination depending on the plasma chemistry involved. [140]

Beyond physical surface modification, plasma-generated RONS can also interfere with endogenous hormonal signaling: reactive species contribute to the breakdown of abscisic acid (ABA), which maintains dormancy, while simultaneously stimulating gibberellic acid (GA) biosynthesis, which promotes germination. By altering the redox balance in the seed, plasma thus provides a biochemical stimulus that facilitates dormancy release and initiation of growth. [141]

In addition to germination enhancement, plasma treatment exerts antimicrobial effects on the seed surface. Reactive oxygen species (ROS) in particular are able to inactivate fungal spores and bacterial pathogens, reducing seed-borne diseases during the early stages of germination. This disinfection effect improves the likelihood of establishing healthy seedlings under conditions that are otherwise favorable to pathogen proliferation.

Comparable results have been obtained using PAW as an indirect treatment strategy that contains H_2O_2, NO_2^-, and NO_3^-, which remain stable for days after generation, as well as short-lived radicals when applied immediately after plasma exposure. Irrigation with PAW has been shown to increase germination rates, modify enzymatic activity, and promote seedling growth to a similar extent as direct plasma treatment. In some cases, combining direct plasma exposure with subsequent irrigation using PAW resulted in even more pronounced improvements in both germination and plant development.[139]

An emerging and highly promising application of plasma technology in agriculture is the development of *seed coatings* for controlled release of active compounds. A remarkable

example is the plasma-assisted encapsulation of fungicides, specifically prothioconazole, onto maize seeds.

In the approach reported in **Figure 19**, a multilayer polymeric coating was engineered to act both as a carrier and as barrier system. The process involved three successive steps: first, the deposition of a hydrophilic polymeric film by plasma, designed to increase the wettability of the seed surface and thus improve adhesion of the active compound; second, the application of an aqueous solution containing prothioconazole; and finally, the deposition of a hydrophobic plasma-polymerized layer to encapsulate the fungicide and restore the natural water-repellent character of the seed coat.

This trilayer design proved highly effective: it ensured uniform distribution of the fungicide, minimized leaching into the soil, and allowed for a gradual release of the active ingredient during seed germination. Importantly, the coatings did not interfere with water uptake or germination capacity, while significantly reducing contamination from *Fusarium graminearum*. In fact, infection rates decreased from 94% in untreated controls to negligible levels in coated seeds, confirming both the protective and controlled release functions of the plasma-deposited multilayer.

Figure 19. Schematic representation of the multilayer coating deposited on maize seeds and of the reactor used.

The advantages of this method lie in its ability to maximize fungicidal efficacy with minimal chemical input, thereby reducing environmental impact and improving sustainability in crop protection. Moreover, plasma deposition provides an environmentally friendly and solvent-free platform, fully in line with the increasing demand for greener agricultural technologies.[144]

Part of my doctoral research has been specifically focused on the use of atmospheric-pressure plasma technologies and on the development of reactors capable of transferring this process to a large-scale setting. This advancement has made it possible not only to design coatings incorporating conventional fungicides, but also to successfully embed living materials such as bacterial spores. The atmospheric-pressure approach therefore represents a crucial step toward the industrial implementation of plasma-based seed coatings, broadening both the scope of applications and the potential impact of this technology in sustainable agriculture. In the following chapter plasma processes at atmospheric pressure for the development of films containing fungicides and bacterial spores for the control of fungal pathogens are discussed.

1.8 References

[1] FAO. (2017). The future of food and agriculture – Trends and challenges. Rome: Food and Agriculture Organization.

[2] Alexandratos, N., & Bruinsma, J. (2012). World agriculture towards 2030/2050 (ESA Working Paper No. 12-03). FAO.

[3] United Nations, Department of Economic and Social Affairs, Population Division. (2019). World Population Prospects 2019: Highlights. New York: UN.

[4] FAO. (2021). The State of Food and Agriculture 2021. Rome: FAO.

[5] Food and Agriculture Organization of the United Nations (FAO). “Cereals: Production Quantities.” FAOSTAT, 2023. https://www.fao.org/faostat/en/#data/QC

[6] IPCC. (2022). Climate Change 2022: Impacts, Adaptation and Vulnerability. Contribution of Working Group II to the Sixth Assessment Report. Cambridge University Press.

[7] G.C. Nelson, *et al*. Climate change effects on agriculture: Economic responses to biophysical shocks. *Proceedings of the National Academy of Sciences*, 2014, 111(9), 3274–3279.

[8] J. R. Porter, *et al*. Food security and food production systems. In: Climate Change 2014: Impacts, Adaptation, and Vulnerability. Part A: Global and Sectoral Aspects. IPCC AR5 WGII, Cambridge University Press.

[9] S. Myers, A. Zanobetti, I. Kloog, *et al*. Increasing CO2 threatens human nutrition. *Nature* 2014, 510, 139–142.

[10] F. N. Tubiello *et al*. *Environ. Res. Lett*. 2021, 16 065007.

[11] M. van Dijk, T. Morley, M.L. Rau, *et al*. A meta-analysis of projected global food demand and population at risk of hunger for the period 2010–2050. *Nat Food* 2021, 2, 494–501.

[12] S. Savary, L. Willocquet, S.J. Pethybridge, *et al*. The global burden of pathogens and pests on major food crops. *Nat Ecol*, 2019, 3, 430–439.

[13] R.N. Strange & P.R. Scott, Plant disease: a threat to global food security. *Annual Review of Phytopathology*, 2005, 43, 83–116.

[14] E.C. Oerke. Crop losses to pests. *The Journal of Agricultural Science*, 2006, 144(1), 31–43.

[15] S.Q. An, N. Potnis, M. Dow, F. J. Vorholter, Y.Q. He, A. Becker, D. Teper, Y. Li, N. Wang, L. Bleris, e*t al*. Mechanistic insights into host adaptation, virulence and epidemiology of the phytopathogen Xanthomonas. *FEMS Microbiol. Rev*. 2019, 24.

[16] K. A. Garrett, et al. Climate change effects on plant disease: genomes to ecosystems. *Annual Review of Phytopathology*, 2006 44, 489–509.

[17] D. P. Bebber. Range-expanding pests and pathogens in a warming world. *Annual Review of Phytopathology*, 2015, 53, 335–356.

[18] M. A. Altieri. The ecological role of biodiversity in agroecosystems. *Agriculture, Ecosystems & Environment*, 1999, 74(1–3), 19–31.

[19] B. A. McDonald, E.H. & Stukenbrock. Rapid emergence of pathogens in agro-

ecosystems: global threats to agricultural sustainability and food security. *Philosophical Transactions of the Royal Society B*, 2016, 371(1709), 20160026.

[20] M. C. Fisher, *et al*. Emerging fungal threats to animal, plant and ecosystem health. *Nature*, 2012, 484, 186–194.

[21] F. van den Bosch, et al. The basic reproduction number of fungal plant pathogens. *Annual Review of Phytopathology*, 2014, 52, 427–445.

[22] M. Różewicz, M. Wyzińska, J. Grabiński. The Most Important Fungal Diseases of Cereals-Problems and Possible Solutions. *Agronomy* 2021, 11, 714.

[23] M. Kamle, D.K. Mahato, S. Devi K.E. Lee, S.G. Kang, & P. Kumar, P. Fumonisins: Impact on agriculture, food, and human health and their management strategies. Toxins, 2019, 11(6), 328.

[24] M. Masiello, S. Somma, C. Lo Porto, F. Palumbo, P. Favia, F. Fracassi, A.F. Logrieco, A. Moretti. Plasma technology increases the efficacy of prothioconazole against *Fusarium graminearum* and *Fusarium proliferatum* contamination of maize (Zea mays) seedlings. *International Journal of Molecular Sciences*, 2021, 22, 9301.

[25] IARC. (2002). International agency for research on cancer (IARC), world health organisation (WHO), IARC Monographs on the Evaluation of carcinogenic Risks to humans, some traditional herbal medicines, some mycotoxins, Naphthalene and styrene (Vol. 82, pp. 301–366). Lyon, France: IARC Press

[26] R. L. Latham, J.T. Boyle, A. Barbano, W.G. Loveman, N.A. Brown, N. A. Diverse mycotoxin threats to safe food and feed cereals. *Essays in Biochemistry*, 2023, 67(5), 797–809.

[27] A. Bottalico, G. Perrone. Toxigenic Fusarium species and mycotoxins associated with head blight in small-grain cereals in Europe. *European Journal of Plant Pathology*, 2002, 108, 611–624.

[28] W. Babinska-Wensierska, A. Motyka-Pomagruk, M. Fondi, A. E. Misztak, a. Mengoni, E. Lojkowska, Differences in the constituents of bacterial microbiota of soils collected

from two fields of diverse potato blackleg and soft rot diseases incidences: A case study. *Scientific Reports*, 2024, 14(1), 18802.

[29] S. Lipps, M. Bohn, J. Rutkoski, C. Butts-Wilmsmeyer, S. Mideros, T. Jamann. Comparative Review of Fusarium graminearum Infection in Maize and Wheat: Similarities in Resistance Mechanisms and Future Directions. *Molecular Plant-Microbe Interactions*, 2025, *38*(2), 142-159.

[30] O. Erenstein, M. Jaleta, K. Sonder, *et al*. Global maize production, consumption and trade: trends and R&D implications. *Food Sec*. 2022, 14, 1295–1319.

[31] X. Chen, M.F. Abdallah, S. Landschoot, K. Audenaert, S. De Saeger, X. Chen, A. Rajkovic. *Aspergillus flavus* and *Fusarium verticillioides* and Their Main Mycotoxins: Global Distribution and Scenarios of Interactions in Maize. *Toxins* 2023, 15, 577.

[32] A. K. Pandey, M.K. Samota, A. Kumar, A.S. Silva, N. K. Dubey. Fungal mycotoxins in food commodities: Present status and future concerns. *Frontiers in Sustainable Food Systems*, 2023, 7, 1162595.

[33] M. Dow, S.Q. An, A. O'Connell. Bacterial diseases. In B. Thomas, B. G. Murray, & D. J. Murphy (Eds.), 2017 Encyclopedia of Applied Plant Sciences (2nd ed., Vol. 3: Crop Systems, pp. 59–68). Academic Press.

[34] B. Dupuis, P. Nkuriyingoma, F. Van Gijsegem. Economic Impact of Pectobacterium and Dickeya Species on Potato Crops: A Review and Case Study. In: Van Gijsegem, F., van der Wolf, J.M., Toth, I.K. 2021 (eds) Plant Diseases Caused by Dickeya and Pectobacterium Species. Springer, Cham.

[35] A.O. Charkowski. The changing face of bacterial soft-rot diseases. *Annual Review of Phytopathology*, 2018, 56, 269–288.

[36] R. Parveen, M.A. Pervez, M.A. Hussain, S. Ahmed, M. Hussain, R. Sardar *et. al*. Black rot disease of crucifers: A review of epidemiology and management strategies. *Physiological and Molecular Plant Pathology*, 2021, 115, 101744.

[37] R. Prajapat, A. Marwal, P. N. Jha. I*nternational Journal of Current Microbiology and Applied Sciences*, 2013, 2 (*10*), 83-89.

[38] A. Pulavarty, T. S. Rani, S. Anwar, S. Plant-parasitic nematodes: Agricultural importance, biocontrol strategies and research developments. *Plants*, 2021, 10(11), 2352.

[39] P. Abad, J. Gouzy, JM. Aury et al. *Nat Biotechnol* 2008, *26*, 909–915.

[40] S. Lazarova, D. G. Coyne, M. Rodríguez, B. Peteira, A. Ciancio. Functional Diversity of Soil Nematodes in Relation to the Impact of Agriculture—A Review. *Diversity*, 2021, 13 (2), 64.

[41] D.A. Neher Role of nematodes in soil health and their use as indicators. *Journal of Nematology*, 2001, 33(4), 161-8.

[42] H. Ferris, T. Bongers, R. G. M. de Goede. A framework for soil food web diagnostics: Extension of the nematode faunal analysis concept. *Applied Soil Ecology*, 2001, 18(1), 13–29.

[43] J. Zheng, Y. Xu. A review: Development of plant protection methods and advances in pesticide application technology in agro-forestry production. *Agriculture*, 2023, 13, 2165.

[44] V. M. Pathak, et al. *Frontiers in Microbiology*, 2022, 13, 962619.

[45] S. Ray, S. T. Shaju. Bioaccumulation of pesticides in fish resulting toxicities in humans through food chain and forensic aspects. *Environmental Analysis Health and Toxicology*, 2023, 38(3), e2023017-0.

[46] E. Baigorria, L. F. Fraceto. Biopolymer-nanocomposite hybrid materials as potential strategy to remove pesticides in water: Occurrence and perspectives. *Advanced Sustainable Systems*, 2021.

[47] M. Syafrudin, R. A. Kristanti, A. Yuniarto, T. Hadibarata, J. Rhee, W. A. Al-onazi, T. S. Algarni, A. H. Almarri, A. M. Al-Mohaimeed. Pesticides in drinking water—A review. *International Journal of Environmental Research and Public Health*, 2021, 18, 468.

[48] J. McGinley, M. G. Healy, P. C. Ryan, J. Harmon O'Driscoll, P.-E. Mellander, L. Morrison, A. Siggins. Impact of historical legacy pesticides on achieving legislative goals in Europe. *Science of the Total Environment*, 2023, 873, 162312.

[49] A. Sharma, et al. Worldwide pesticide usage and its impacts on ecosystem. *Environments*, 2019, 6(10), 82.

[50] J. K. Kumar Sathish, et al. Impact of pesticide exposure on environment and biodiversity: A review. *Agricultural Reviews*, 2024, 45(1), 1–12.

[51] Eurostat. Sales of pesticides in the EU down another 9% in 2023. *European Commission*, 2025.

[52] H. Shude, et al. Progress in the management of Fusarium head blight: An overview. *South African Journal of Science*, 2020, 116(7/8).

[53] FRAC. FRAC Code List 2022: Fungal control agents sorted by cross-resistance pattern and mode of action. *Fungicide Resistance Action Committee*, 2022.

[54] D. Hermann, K. Stenzel. FRAC mode-of-action classification and resistance risk of fungicides. *Modern Crop Protection Compounds*, 2019, 3rd ed., 589–596.

[55] G. Chen, L. Cao, C. Cao, P. Zhao, F. Li, B. Xu, Q. Huang. Effective and sustained control of soil-borne plant diseases by biodegradable polyhydroxybutyrate mulch films embedded with fungicide of prothioconazole. *Molecules*, 2021, 26(3), 762.

[56] M. Masiello, S. Somma, V. Ghionna, A. F. Logrieco, A. Moretti. In vitro and in field response of different fungicides against *Aspergillus flavus* and *Fusarium* species causing ear rot disease of maize. *Toxins*, 2019, 11(1), 11.

[57] T. T. Brandhorst, B. S. Klein. Uncertainty surrounding the mechanism and safety of the post-harvest fungicide fludioxonil. *Food and Chemical Toxicology*, 2019, 126, 108–113.

[58] Y. Chen, A. F. Zhang, T. C. Gao, Y. Zhang, W. X. Wang, K. J. Ding, L. Chen, Z. Sun, X. Z. Fang, M. G. Zhou. Integrated use of pyraclostrobin and epoxiconazole for the control of

Fusarium head blight of wheat in Anhui Province of China. *Plant Disease*, 2012, 96(10), 1495–1500.

[59] S. Kumar. Soil application methods of fungicides: Fundamental information. *Just Agriculture*, 2021, 2.

[60] L. A. Ebone, M. Kovaleski, C. C. Deuner. Nematicides: history, mode, and mechanism action. *Plant Science Today*, 2019, 6(2), 91–97.

[61] Insecticide Resistance Action Committee (IRAC). Nematicide mode of action classification scheme (Version 2.1). *IRAC International*, 2022.

[62] J. O. Silva, A. Loffredo, M. R. da Rocha, J. O. Becker. Efficacy of new nematicides for managing *Meloidogyne incognita* in tomato crop. *Journal of Phytopathology*, 2019, 167(5), 295–298.

[63] E. K. Kandil, M. M. Nofel, A. M. Abdelaziz, M. M. Mansour, M. S. Attia. Effectual role of plant growth-promoting fungi and fosthiazate in controlling tomato root-knot nematode infection: In vivo and in vitro studies. *Physiological and Molecular Plant Pathology*, 2024, 134, 102463.

[64] P. S. McManus, V. O. Stockwell. Antibiotic use for plant disease management in the United States. *Plant Health Progress*, 2001.

[65] B. Verhaegen, E. Franz, A. Silva, A. Vingiani, EFSA Plant Health Panel. Data collection on antibiotics for control of plant pathogenic bacteria (EFSA Supporting Publication 2024:EN-8522). *European Food Safety Authority*, 2024.

[66] P. Taylor, R. Reeder. Antibiotic use on crops in low and middle-income countries based on recommendations made by agricultural advisors. *CABI Agriculture and Bioscience*, 2020, 1(1), 1.

[67] World Health Organization. Monitoring global progress on addressing antimicrobial resistance: Analysis report of the second round of results of AMR country self-assessment survey 2018. *WHO*, 2018.

[68] Food and Agriculture Organization of the United Nations. AMU in plant production and protection – InFARM system. *FAO*, 2025.

[69] P. S. McManus, V. O. Stockwell, G. W. Sundin, A. L. Jones. Antibiotic use in plant agriculture. *Annual Review of Phytopathology*, 2002, 40, 443–465.

[70] M. Verhaegen, T. Bergot, E. Liébana, G. Stancanelli, F. Streissl, M. P. Mingeot-Leclercq, J. Mahillon, C. Bragard. On the use of antibiotics to control plant pathogenic bacteria: A genetic and genomic perspective. *Frontiers in Microbiology*, 2023, 14, 1221478.

[71] S. A. Miller, J. P. Ferreira, J. T. LeJeune. Antimicrobial use and resistance in plant agriculture: A One Health perspective. *Agriculture*, 2022, 12, 289.

[72] A. A. Taylor, J. S. Tsuji, M. R. Garry, M. E. McArdle, W. L. Goodfellow Jr., W. J. Adams, C. A. Menzie. Critical review of exposure and effects: Implications for setting regulatory health criteria for ingested copper. *Environmental Management*, 2020, 65(1), 131–159.

[73] United Nations. The 2030 Agenda for Sustainable Development. *United Nations*, 2015.

[74] European Commission. The European Green Deal. *European Commission*, 2019.

[75] European Commission. Farm to Fork Strategy: 50% pesticide reduction target by 2030. *European Commission*, 2020a; 2020b.

[76] Food and Agriculture Organization of the United Nations. Agroecological approaches for biodiversity and resilience. *FAO*, 2018.

[77] K. Schneider, J. Barreiro-Hurle, E. Rodriguez-Cerezo. Pesticide reduction amidst food and feed security concerns in Europe. *Nature Food*, 2023, 4, 746–750.

[78] S. Shekhar, S. Sharma, A. Kumar, A. Taneja, B. Sharma. The framework of nanopesticides: a paradigm in biodiversity. Materials Advances, 2021, 2, 6569-6588.

[79] D. Abdollahdokht, Y. Gao, S. Faramarz, et al. Conventional agrochemicals towards nano-biopesticides: An overview on recent advances. *Chemical and Biological*

Technologies in Agriculture, 2022, 9, 13.

[80] X. Jiang, F. Yang, W. Jia, Y. Jiang, X. Wu, S. Song, H. Shen, J. Shen. Nanomaterials and nanotechnology in agricultural pesticide delivery: A review. *Langmuir*, 2024, 40(36), 18806–18820.

[81] H. Chen, H. Zhi, B. Feng, B. Cui, X. Zhao, C. Sun, Y. Wang, H. Cui, B. Zhang, Z. Zeng. Thermo-responsive quaternary ammonium chitosan nanocapsules with on-demand controlled pesticide release and maximally synergistic biological activity. *Journal of Agricultural and Food Chemistry*, 2022, 70, 7653–7661.

[82] S. Li, X. Yu, X. Wu, X. Song, J. Chen, Y. Hu. Enhanced fungicidal efficacy and improved interfacial properties with the co-delivery of prothioconazole and tebuconazole using polylactic acid microspheres. *Pest Management Science*, 2024, 80(2), 649–660.

[83] M. Kah, T. Hofmann. Nanopesticide research: Current trends and future priorities. *Nanomaterials*, 2018, 8(2), 102.

[84] J. Wang, R. Li, Z. Zhao, M. Zhu, Y. Wang. Bioactivity, uptake, and distribution of prothioconazole loaded on fluorescent double-hollow shelled mesoporous silica in soybean plants. *Journal of Agricultural and Food Chemistry*, 2023, 71(11), 4521–4535.

[85] J. Feng, Z. Chen, W. Chen, L. Sun, J. Yang, K. He, S. Dong, S. Yuan. Facile pathway to construct mesoporous silica nanoparticles loaded with pyraclostrobin: Physicochemical properties, antifungal activity, and biosafety. *Pest Management Science*, 2022, 78(6), 2332–2341.

[86] C. Xu, L. Cao, M. Bilal, C. Cao, P. Zhao, H. Zhang, Q. Huang. Multifunctional manganese-based carboxymethyl chitosan hydrogels for pH-triggered pesticide release and enhanced fungicidal activity. *Carbohydrate Polymers*, 2021, 262, 117933.

[87] Y. Sun, Y. Ma, G. Fang, S. Ren, Y. Fu. Controlled pesticide release from porous composite hydrogels based on lignin and polyacrylic acid. *BioResources*, 2016, 11(1), 2361–2371.

[88] V. Kumar, A. A. Ghfar, et al. Controlled release of harmful pesticide dichlorvos through synthesized biodegradable aloe vera–acrylic acid-based hydrogel and its utilization in soil water management. *Journal of Analytical Science and Technology*, 2023, 14, 12.

[89] S. Di Rago, F. Morandi, F. Pizzetti, F. Rossi. Advances in controlled release systems for sustainable crop production: A review of nano-, micro-, and macro-formulations. *Advanced Agrochem*, 2025.

[90] T. Xu, C. Ma, Z. Aytac, X. Hu, K. W. Ng, J. C. White, P. Demokritou. Enhancing agrichemical delivery and seedling development with biodegradable, tunable, biopolymer-based nanofiber seed coatings. *ACS Sustainable Chemistry & Engineering*, 2020, 8(25), 9537–9548.

[91] S. Wang, Z. Jia, X. Zhou, D. Zhou, M. Chen, D. Xie, Y. Luo, D. Jia. Preparation of a biodegradable poly(vinyl alcohol)–starch composite film and its application in pesticide controlled release. *Journal of Applied Polymer Science*, 2017, 134(28), 45051.

[92] N. A. Godínez-Garrido, D. C. F. Silva, J. B. Carrera, L. M. de Araújo, A. A. de Souza. Chitosan coating on bean and maize seeds: Release of agrochemical fungicide and post-storage condition. *Journal of Seed Science*, 2021, 43, e54286.

[93] S. Farias, T. Pirzada, F. M. Mathew, T. L. Sit, C. H. Opperman, S. A. Khan. Electrospun polymer nanofibers as seed coatings for crop protection. *ACS Sustainable Chemistry & Engineering*, 2019, 7(24), 20032–20040.

[94] M. U. Rashid, S. J. Shah, S. Attacha, et al. Green synthesis and characterization of zinc oxide nanoparticles using *Citrus limetta* peels extract and their antibacterial activity against brown and soft rot pathogens and antioxidant potential. *Waste and Biomass Valorization*, 2024, 15, 3351–3366.

[95] A. Sirelkhatim, S. Mahmud, A. Seeni, N. H. M. Kaus, L. C. Ann, S. K. M. Bakhori, H. Hasan, D. Mohamad. Review on zinc oxide nanoparticles: Antibacterial activity and toxicity mechanism. *Nano-Micro Letters*, 2015, 7(3), 219–242.

[96] S. Pedrini, D. J. Merritt, J. Stevens, K. Dixon. Seed coating: Science or marketing spin? *Trends in Plant Science*, 2017, 22(2), 106–116.

[97] H. S. El-Beltagi, A. Basit, H. I. Mohamed, I. Ali, S. Ullah, E. A. R. Kamel, T. A. Shalaby, K. M. A. Ramadan, A. A. Alkhateeb, H. S. Ghazzawy. Mulching as a sustainable water and soil saving practice in agriculture: A review. *Agronomy*, 2022, 12(8), 1881.

[98] D. Xie, X. Tang, Y. Ma, Y. Liu, C. Sun. Novel biodegradable composite mulch film embedded with temperature-responsive pesticide microcapsules for durable control of *Phytophthora* root rot on soybean. *ACS Sustainable Chemistry & Engineering*, 2023, 11(35), 13061–13072.

[99] W. Liang, Y. Zhao, D. Xiao, J. Cheng, J. Zhao. A biodegradable water-triggered chitosan/hydroxypropyl methylcellulose pesticide mulch film for sustained control of *Phytophthora sojae* in soybean (Glycine max L. Merr.). *Journal of Cleaner Production*, 2020, 245, 118943.

[100] D. Palmieri, G. Ianiri, C. Del Grosso, G. Barone, F. De Curtis, R. Castoria, G. Lima. Advances and perspectives in the use of biocontrol agents against fungal plant diseases. *Horticulturae*, 2022, 8(6), 577.

[101] J. Köhl, R. Kolnaar, W. J. Ravensberg. Mode of action of microbial biological control agents against plant diseases: Relevance beyond efficacy. *Frontiers in Plant Science*, 2019, 10, 845.

[102] Y. Chen, et al. Antifungal activity and mode of action of lactic acid bacteria isolated from kefir against *Penicillium expansum*. *Food Control*, 2021, 130, 108274.

[103] K. Stumbriene, R. Gudiukaite, R. Semaskiene, P. Svegzda, A. Jonaviciene, S. Suproniene. Screening of new bacterial isolates with antifungal activity and application of selected *Bacillus* sp. cultures for biocontrol of *Fusarium graminearum* under field conditions. *Crop Protection*, 2018, 113, 22–28.

[104] A. Keshmirshekan, L. M. de Souza Mesquita, S. P. M. Ventura. Biocontrol manufacturing and agricultural applications of *Bacillus velezensis*. *Trends in Biotechnology*, 2024, 42, 986–1001.

[105] N. Khan, P. Martínez-Hidalgo, T. A. Ice, M. Maymon, E. A. Humm, N. Nejat, E. R. Sanders, D. Kaplan, A. M. Hirsch. Antifungal activity of *Bacillus* species against *Fusarium* and analysis of potential mechanisms used in biocontrol. *Frontiers in Microbiology*, 2018, 9, 2363.

[106] M. Catani, C. C. Toma, F. Fratini. Essential oils as nematicides in plant protection—A review. *Plants*, 2023, 12(7), 1418.

[107] S. Kalaiselvi, P. Kumar, G. Benelli. Essential oils and their bioactive components as nematicides: Modes of action and applications. *Agronomy*, 2024, 14(1), 213.

[108] J. M. S. Faria, P. Barbosa, P. Vieira, C. S. L. Vicente, A. C. Figueiredo, M. Mota. Phytochemicals as biopesticides against the pinewood nematode *Bursaphelenchus xylophilus*: A review on essential oils and their volatiles. *Plants*, 2021, 10, 2614.

[109] T. D'Addabbo, S. Laquale, P. Veronico, et al. Nematicidal activity of the essential oil from *Cinnamomum cassia* and (E)-cinnamaldehyde against phytoparasitic nematodes. *Journal of Pest Science*, 2025, 98, 521–533.

[110] A. Ferreira Barros, V. P. Campos, L. Lopes de Paula, et al. The role of *Cinnamomum zeylanicum* essential oil, (E)-cinnamaldehyde and (E)-cinnamaldehyde oxime in the control of *Meloidogyne incognita*. *Journal of Phytopathology*, 2021, 169, 229–238.

[111] K. Sarri, S. Mourouzidou, N. Ntalli, N. Monokrousos. Recent advances and developments in the nematicidal activity of essential oils and their components against root-knot nematodes. *Agronomy*, 2024, 14, 213.

[112] I. Langmuir. Oscillations in ionized gases. *Proceedings of the National Academy of Sciences*, 1928, 14.

[113] R. D'Agostino, P. Favia, C. Oehr, M. R. Wertheimer. Low-temperature plasma processing of materials: Past, present, and future. *Plasma Processes and Polymers*, 2005, 2.

[114] F. Taccogna, G. Dilecce. *European Physical Journal D*, 2016, 70, 251.

[115] L. Bárdos, H. Baránková. Cold atmospheric plasma: Sources, processes, and applications. *Thin Solid Films*, 2010, 518, 6705–6713.

[116] M. A. Lieberman, A. J. Lichtenberg. *Principles of Plasma Discharges and Materials Processing* (2nd ed.). John Wiley & Sons, 2005.

[117] S. Samal. Thermal plasma technology: The prospective future in material processing. *Journal of Cleaner Production*, 142.

[118] U. Kogelschatz. Dielectric-barrier discharges: Their history, discharge physics, and industrial applications. *Plasma Chemistry and Plasma Processing*, 2003, 23, 1–46.

[119] A. P. Napartovich. *Plasmas and Polymers*, 2001, 6, 1.

[120] U. Kogelschatz, B. Eliasson, W. Egli. *Pure and Applied Chemistry*, 1999, 71.

[121] U. Kogelschatz. *Plasma Physics and Controlled Fusion*, 2004, 46, B63.

[122] H.-E. Wagner, R. Brandenburg, K. V. Kozlov, A. Sonnenfeld, P. Michel, J. F. Behnke. *Vacuum*, 2003, 71, 417.

[123] K. Ollegott, P. Wirth, C. Oberste-Beulmann, P. Awakowicz & M. Muhler. Fundamental properties and applications of dielectric barrier discharges in plasma-catalytic processes at atmospheric pressure. *Chemie Ingenieur Technik*, 2020, 92(10), 1542-1558.

[124] I. Trizio, et al. Plasma processes for life sciences. In *Reference Module in Chemistry, Molecular Sciences and Chemical Engineering*, 2018.

[125] F. Palumbo, C. Lo Porto, F. Fracassi, P. Favia. Recent advancements in the use of aerosol-assisted atmospheric pressure plasma deposition. *Coatings*, 2020, 10.

[126] P. A. F. Herbert, L. O'Neill, J. Jaroszyńska-Wolińska, C. P. Stallard, A. Ramamoorthy, D. P. Dowling. *Plasma Processes and Polymers*, 2011, 8, 230.

[127] A. J. Beck, R. D. Short, A. Matthews. Deposition of functional coatings from acrylic acid and octamethylcyclotetrasiloxane onto steel using an atmospheric pressure dielectric barrier discharge. *Surface and Coatings Technology*, 2008, 203, 822–825.

[128] J. Bour, et al. Different ways to plasma-polymerize HMDSO in DBD configuration at atmospheric pressure for corrosion protection. *Plasma Processes and Polymers*, 2008, 5, 788–796.

[129] G. Da Ponte, et al. Plasma deposition of PEO-like coatings with aerosol-assisted dielectric barrier discharges. *Plasma Processes and Polymers*, 2012, 9, 1176–1183.

[130] A. Dembele, M. Rahman, I. Reid, B. Twomey, J. M. D. MacElroy, D. P. Dowling. Deposition of hybrid organic–inorganic composite coatings using an atmospheric plasma jet system. *Journal of Nanoscience and Nanotechnology*, 2011, 11, 8730–8737.

[131] J. Profili, O. Levasseur, N. Naudé, C. Chaneac, L. Stafford, N. Gherardi. Influence of the voltage waveform during nanocomposite layer deposition by aerosol-assisted atmospheric pressure Townsend discharge. *Journal of Applied Physics*, 2016, 120, 053302.

[132] F. Fanelli, A. M. Mastrangelo, F. Fracassi. Aerosol-assisted atmospheric cold plasma deposition and characterization of superhydrophobic organic–inorganic nanocomposite thin films. *Langmuir*, 2014, 30, 857–865.

[133] I. R. Durán, J. Profili, L. Stafford, G. Laroche. Beyond microelectronics with 1,3,5,7-tetramethylcyclotetrasiloxane: A promising molecule for anti-fogging coatings. *Materials Chemistry and Physics*, 2020, 242, 122508.

[134] A. Liguori, E. Traldi, E. Toccaceli, R. Laurita, A. Pollicino, M. L. Focarete, V. Colombo, M. Gherardi. Co-deposition of plasma-polymerized polyacrylic acid and silver nanoparticles for nanocomposite coatings using a non-equilibrium atmospheric pressure plasma jet. *Plasma Processes and Polymers*, 2016, 13, 623–632.

[135] J. Profili, O. Levasseur, J.-B. Blaisot, A. Koronai, L. Stafford, N. Gherardi. Nebulization of nanocolloidal suspensions for growth of nanocomposite coatings in dielectric barrier discharges. *Plasma Processes and Polymers*, 2016, 13, 981–989.

[136] F. Palumbo, et al. Direct plasma deposition of lysozyme-embedded bio-composite thin films. *Plasma Processes and Polymers*, 2015, 12, 1302–1310.

[137] C. Lo Porto, et al. On the plasma deposition of vancomycin-containing nano-capsules for drug-delivery applications. *Plasma Processes and Polymers*, 2018, 15, 1700232.

[138] F. Palumbo, et al. Plasma-deposited nanocapsules containing coatings for drug-delivery applications. *ACS Applied Materials & Interfaces*, 2018, 10, 35516–35525.

[139] N. Puač, M. Gherardi, M. Shiratani. Plasma agriculture: A rapidly emerging field. *Plasma Processes and Polymers*, 2018, 15(2), e1700174.

[140] M. Ito, J.-S. Oh, T. Ohta, M. Shiratani, M. Hori. Current status and future prospects of agricultural applications using atmospheric-pressure plasma technologies. *Plasma Processes and Polymers*, 2018, 15(1), e1700073.

[141] P. Ranieri, N. Sponsel, J. Kizer, M. Rojas-Pierce, R. Hernández, L. Gatiboni, A. Grunden, K. Stapelmann. Plasma agriculture: Review from the perspective of the plant and its ecosystem. *Plasma Processes and Polymers*, 2020, 17(11), e2000162.

[142] D. Yan, L. Lin, M. Zvansky, L. Kohanzadeh, S. Taban, S. Chriqui, M. Keidar. Improving seed germination by cold atmospheric plasma. *Plasma*, 2022, 5(1), 98–111.

[143] K. Thirumdas, et al. Plasma activated water (PAW): Chemistry, physico-chemical properties, applications in food and agriculture. *Trends in Food Science & Technology*, 2018, 77, 21–31.

[144] C. Lo Porto, F. Palumbo, S. Somma, M. Masiello, A. Moretti, F. Fracassi, P. Favia. Plasma-assisted deposition of fungicide-containing coatings for encapsulation and protection of maize seeds. *Plasma Processes and Polymers*, 2019, 16(7), e1900022.

2

Plasma Deposition of Coatings for Delivery of Bacterial Spores or Fungicides Active Against *Fusarium graminearum*

Part of the results reported in this Chapter concerning the spore-containing coatings are presented in the following paper:

Marianna Roggio, Palmira De Bellis, Fabio Palumbo, Pasquale Trotti, Mario Masiello, Rim Touati, Antonio Moretti, Pietro Favia "Plasma Deposition of Coatings for Delivery of Bacterial Spores Active Against *Fusarium graminearum", Plasma Processes and Polymers,* **2025**, 22, 8, 70055.

2.1 Introduction

Cereals, including maize, wheat, and rice, together reach slightly less than one-third of the total agricultural production, and are the primary group of crops cultivated worldwide. [1-2]

In all cereal cultivated areas, several phytopathogenic microorganisms, including mycotoxigenic fungi, can colonize plants during the whole crop season. The most important mycotoxigenic fungi occurring on wheat and associated to plant diseases belong to the *Fusarium* genus. Several *Fusarium* species have been isolated from wheat

plants and kernels; *F. graminearum*, one of the most dangerous Fusarium species, is the main etiological agent of Fusarium Head Blight (FHB) and involved in Fusarium Crown Rot (FCR), the most destructive diseases of wheat worldwide. For its ability to colonize wheat during the whole crop season, *F. graminearum* represents both a phytopathological problem and a toxicological risk, due to its ability to produce mycotoxins such as trichothecenes and zearalenone. [3-6] These toxic compounds can accumulate in infected plants before harvest and in stored or processed agricultural raw materials such as flours.

According to the new strategies of integrated pest management, several agronomic, genetic, and biological techniques, as well as agricultural practices, are now available to prevent or limit fungal diseases and mycotoxin accumulation. Chemical control, however, is still considered a key tool to limit FHB and FCR of wheat. Indeed, the use of seeds treated with fungicides allows to protect plants in the first growing stage reducing the symptoms of FCR, while fungicide treatments at the flowering time reduce the contamination of grains by *Fusarium* species and their mycotoxins. [7-9]

Several compounds are active against *F. graminearum*, particularly demethylation inhibitor (DMI) fungicides, which are highly effective even at low doses. Among DMIs, prothioconazole (PRO) is a broad-spectrum triazole fungicide with high efficacy, developed by Bayer Crop Science and introduced the market in 2004. [10] Its mode of action is based on the inhibition of the enzyme C-14 demethylase, which is involved in the biosynthesis of fungal sterols, and it is used against a wide range of fungal diseases. [11-12] Other chemical classes of fungicides have also been employed: fludioxonil(FLU), a broad-spectrum, non-systemic phenylpyrrole fungicide, hyperactivates the HOG pathway through Group III hybrid histidine kinases in fungi, [13] and pyraclostrobin (PYR), a strobilurin-class fungicide.[14]

In this context, plant growth-promoting bacteria (PGPB) and biocontrol agents (BCAs), namely microorganisms capable of counteracting one or more target phytopathogens by interfering with their life cycles, [15-16] appear to be the most promising natural tools to ensure plant health, as well as the quality and safety of agricultural products. To reduce the use of chemical compounds against plant diseases, research on BCAs is mainly focused on lactic acid bacteria (LAB), which are able to produce organic acids and consequently create unfavorable conditions for fungal growth in food products. Moreover,

the lytic enzymes produced by LAB are capable of degrading the cell wall of microorganisms and have been demonstrated to play a role in the biocontrol mechanisms of plant diseases. [17] Recent studies have highlighted the antimicrobial capabilities of species belonging to the *Bacillus* genus and their metabolites; their potential biocontrol mechanisms have been investigated. [18-20] In particular, Keshmirshekan et al. focused on *B. velezensis*. [21]

This species is included in Annex E – the list of Qualified Presumption of Safety (QPS) biological agents (https://www.efsa.europa.eu/en/topics/topic/qualified-presumption-safety-qps): certain some strains of *B. velezensis* are already used in agriculture as biocontrol agents.

In recent years, the growing global concerns about environment and food safety associated with residue accumulation in food and feed has forced the researchers to select new crops protection strategies from mycotoxigenic fungi. [22-23]

The practice of coating seeds with external materials is commonly employed to improve handling, protection, and to enhance the germination and rooting of seeds. [24] In traditional coating methods, seeds are wrapped in a thin polymer matrix impregnated with pesticides and other additives. However, during handling, particularly during sowing, coated seeds are subject to mechanical abrasion, which may result in a rapid release of pesticide.

Efforts to reduce the use of agrochemicals have also boosted the use of treatments with BCA and PGPB. It has been reported, for instance, that *Bacillus subtilis* spores have been incorporated into a matrix to coat maize and canola seeds. [25-26] Low-temperature plasma processes are widely applied, thanks to their low thermal impact, to modify the surface of thermodegradable materials without altering their bulk properties.

Plasma deposition has been extensively studied for the incorporation of active compounds, such as drugs, either in sandwich configuration or as composites, for controlled drug-release purposes. [27- 30]

LP and AP plasma techniques can find applications in agri-food practices and, in particular, AP plasma treatments can be used at pre-sowing, pre-harvest, and post-harvest stages, for example, for decontamination. [31] Research into plasma technologies

for agricultural applications is attracting increasing attention, [32] especially for seed treatments; these have been applied for crop decontamination [33] and for enhancing the growth of several plants, including lentils, [34] soybeans, [35] peas, [36] radishes, [37] tomatoes, [38] sweet peppers, [39] oats, wheat, [40] and many other vegetables. However, very few studies have been published on plasma deposition of protective seed coatings, including LP plasma deposition coating. Such an approach produced interesting results in terms of fungal growth inhibition seed germination, and reduced pesticide dispersion in the soil. [7, 41]

In recent years, AP plasma deposition processes have attracted the attention of both academic and industrial researchers, including in agriculture, due to the many potential advantages offered by this technique compared with LP processes, such as simpler operation and easier scalability. [42–45]

The present study focused on the use of composite coatings containing fungicides, with the aim of encapsulating these substances and achieving a controlled release of compounds that can impact the environment and human health. In this way, an antifungal effect against *Fusarium* was achieved using low doses of fungicides. This research also investigated the use of plasma technology for the preparation of composite coatings containing living, though dormant, cells, namely spores. For the first time, the effect of a plasma-deposited coating on the viability and activity of incorporated bacterial spores was investigated.

As a matter of fact, the research described in this thesis represents the first investigation on the deposition of an active biocomposite coating containing a fungicide (synthetic or microbial) onto seeds by means of aerosol-assisted atmospheric pressure plasma (AAA-PP). As illustrated in **Scheme 1**, the coatings were initially deposited onto glass substrates containing either fungicides or bacterial spores, to evaluate their antifungal activity. Subsequently, the deposition process of fungicide-containing coating was scaled up and transferred to a home-made reactor, capable of treating up to 500 seeds, described in **Annex A 2.1**.

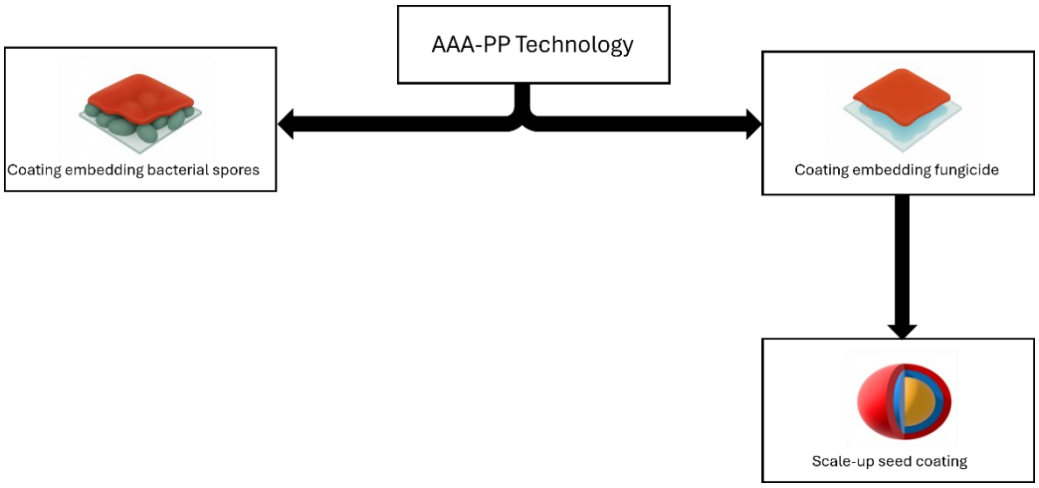

Scheme 1. Workflow of the coating process: from model substrates containing bacterial spores or fungicides to large-scale seed coating using a home-made reactor large scale.

2.2 Materials and Methods

2.2.1 Materials

He 99.999%, C_2H_4 99.95% (Air Liquide) and an aerosol of Milli-Q quality water (Millipore, Bedford, MA) were used as feed in the plasma deposition process. The coatings were deposited on 1 cm^2 shards of double face polished p-doped crystalline silicon (100) wafers (MicroChemicals GmbH, Ulm, Germany) for comprehensive chemical and morphological characterization. On the other hand, biological assessments were conducted on 13 mm diameter microscope cover glasses or filter paper, previously cast with bacterial spores or fungicides, specifically prepared for antifungal tests.

2.2.2 Preparation of the Coatings

To generate the bio-composite layers with the embedded spores or fungicides, the coatings were plasma-deposited on top of the cast bacterial spores or fungicides with the substrates positioned onto the ground electrode of the reactor shown in **Figure 1**. The reactor consists of two parallel plates silver electrodes 5×8 cm^2 wide, 3 mm apart, both covered with 0.63 mm thick alumina. The DBD electrodes set up is sealed in a plexiglas chamber connected to an exhaust pump. A blend of water aerosol, ethylene and helium

was used to feed the plasma. The water aerosol was generated with a pneumatic atomizer (mod. 3076, TSI) activated with 3.5 slm He. In these conditions, the mass flow rate of the atomized water resulted 125 mg/min, as evaluated by weight calibration of the reservoir before and after atomization. Ethylene, precursor of the plasma coating, and additional He were supplied at a flow rate of 50 sccm and 2 slm, respectively. The inlets of C_2H_4 and He were controlled with electronic mass flow meters (MKS). The feed was let from one side of the reactor, passed through the plasma between the electrodes, and has pumped out by a membrane pump from the opposite side. Before and after each process the system was purged for 10 min with 5 slm He.

The discharge was ignited in Continuous Mode (CM) with a power generator system composed of wideband AC power amplifier (Al-1000-HF-A by AMP-LINE Corp., West Nyack, NY, USA) driven by a function generator (Model TG-1000 by TTi). The amplifier was connected to the high-voltage upper electrode with an high voltage transformer (Model AL-T1000, AMP-LINE Corp., West Nyack, NY, USA). Voltage and current delivered to the discharges were measured, respectively, with a high-voltage probe (P6015A, Tektronix, Beaverton, USA) and a resistance-type current probe, both connected to an oscilloscope (TDS 2014C, Tektronix, Beaverton, USA). The applied peak-to-peak voltage was kept at 5 KVpp at a frequency of 20 kHz, resulting in a power density of 1.30 W cm^{-2}.

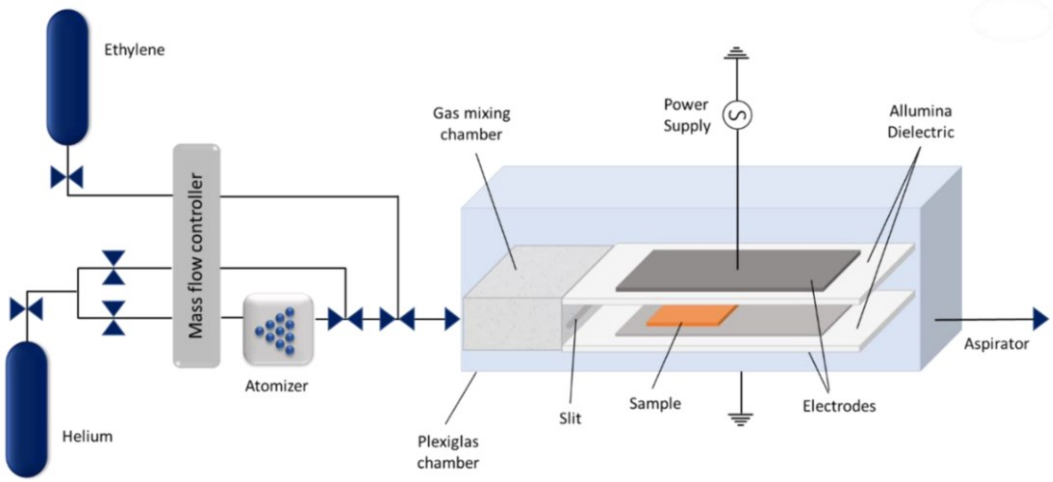

Figure 1. Schematic representation of the AAA-PP reactor used for the deposition of the coatings on bacterial spores.

2.2.3 Preparation of fungicide-Containing Coatings

The fungicide products used for the production of the double-layer coatings were as follows: PROLINE (PRO, Bayer, 250 g/L Prothioconazole), COMET 250 EC (PYR, BASF, 250 g/L Pyraclostrobin), and MCW 5278 (FLU, ADAMA, 48–53 wt% Fludioxonil). Aliquots of 30 µL of aqueous suspensions of the formulations were deposited onto each glass or paper substrate and allowed to dry. Depending on the amount of fungicide to be deposited while maintaining a constant volume on the substrates, different suspension concentrations were used. Samples containing 6, 60, and 100 µg of PRO were prepared. For FLU and PYR, only two quantities were considered: 19.2 µg and 60 µg for the former, and 6 µg and 60 µg for the latter.

To prepare the composite layers containing the different fungicides, the coatings were plasma-deposited on top of the dried fungicide suspensions, with thickness ranging between 90 and 540 nm.

The fungicide containing samples are named in this chapter with the following code:

X_fungicide_Th

Where X = amount of fungicide (µg) deposited on to the sample; *fungicide* = PRO, PYR, or FLU; *Th* = coating thickness, ranging from 0 to 540 nm, *Th=0* corresponds to sample without a plasma-deposited film on top.

2.2.4 Preparation of Spore-Containing Coatings

The strain *Bacillus velezensis* N3.2 (previously named *B. amyloliquefaciens* N3.2) [46] is part of the Culture Collection of the Institute of Sciences of Food Production of the National Research Council (ISPA-CNR), isolated from Italian durum wheat semolina. [47, 48] The strain was stored at −80°C under cryoprotection and cultivated on Plate Count Agar (PCA, Difco, Franklin Lakes, NJ) at 30°C for 5 days before each experiment.

The biological activity of *B. velezensis* N3.2 has been evaluated against the *F. graminearum* ITEM 6415 strain (http://server.ispa.cnr.it/ITEM/Collection/); the fungal strain was grown on Potato Dextrose Agar (PDA, Difco) medium at 25°C for 7 days before each experiment.

A spore suspension of *B. velezensis* N3.2 was obtained in a NaCl 0.85% solution from a culture on PCA. The suspension was heated at 90°C for 20 min to kill bacterial cells; the suspension was then centrifuged (9000 g; 10 min) to collect the spores, which were then resuspended in sterile distilled water at the final density of 10^6 spores/mL, as determined with a Thoma cell counting chamber (Brand, Blaubrand, Germany) and verified by dilution-plating on PCA. Aliquots of 40 µL of suspension were cast on each glass substrate (about 8×10^4 spores/sample) and allowed to dry. To generate the bio-composite layers with the embedded spores, the coatings were plasma-deposited on top of the cast spores.

2.2.5 Chemical and Morphological Characterization of the Coatings

The composition of the coatings deposited on the Si substrates has been probed by means of Fourier-Transform Infrared Spectroscopy (FT-IR, transmission mode) with a Vertex 70 V Bruker spectrometer (32 scans, 4 cm^{-1}). The spectrometer was evacuated to less than 150 Pa for 5 min, to avoid spectral interferences from atmospheric H_2O vapour and CO_2.

The atomic composition of the topmost layer (5–10 nm) of the coating was probed with a X-ray Photoelectron Spectroscopy (XPS) PHI 5000 Versa Probe II spectrometer (Physical Electronics GmbH), using a monochromatic Al Kα X-ray source@1486.6 eV (15 kV, 24.8 W, spot size 200 µm). Wide scan and high-resolution C1s, N1s, and O1s spectra were acquired in Fixed Analyser Transmission mode at a pass energy of 117.40 eV and 29.35 eV, respectively. The surface charge was compensated with a dual beam neutralization system and the C1s photoemission peak at 285.0 eV was used as reference for the Binding Energy (BE) scale. All spectra were collected at 45° with respect to the sample surface. To account for the surface distribution of the O-containing moieties of the coatings, the C1s signals were best-fitted with four peak components at 285.0 eV (C–C, C–H), 286.4 eV (C–OH, C–OC), 287.7 eV (C = O), and 289.0 eV (COOH, COOR), using a 90% gaussian shape and 1.5 eV FWHM [49]. Spectra elaboration was carried out with the MultiPak data processing software (Physical Electronics GmbH).

Static Water Contact Angle (WCA) measurements were carried out with a Ramé-Hart 100-manual goniometer (distilled water, 4 µL drops, room temperature). WCAs were measured on three different points of three replicates.

The thickness of the coatings was measured on three different points of three replicates with a KLA-Tencor instrument (Milpitas, CA, USA) D-120 stylus profiler after scratching part of the coating with a scalpel to form a step. The deposition rate was calculated by dividing the measured film thickness by the corresponding deposition time; the reported deposition rate represents the average of the values obtained at the different deposition times investigated.

Scanning Electron Microscopy (HITACHI TM 3000 Tabletop, Tokyo, Japan) was utilized for the morphological characterization of uncoated and plasma-coated samples in backscattered electron (BSE) mode, at 15 KV acceleration voltage and 6 mm working distance, with no need of prior metallization of the samples.

2.2.6 Biological Characterization of the Fungicide-Containing Coatings

The strain F. *graminearum* ITEM 6415 is known to be a strong DON producer and has already been used in a previous study to evaluate its sensitivity to different fungicides, including prothioconazole.[9] A conidial suspension was prepared by scraping, with a sterilized loop, the mycelium from 7-day-old colonies and suspending it in sterile distilled water containing 0.01% Tween 20. The conidial suspension was then adjusted to a concentration of 1×10^5 conidia/mL wiith a Thoma counting chamber. An aliquot of 100 µL of conidial suspension was spread on the PDA medium of each Petri dish with diameter of 90 mm. Subsequently, a glass slide containing the plasma-coated fungicide was placed at the center of the plate. Plates containing only the *Fusarium* strain and slides with plasma coating and uncoated fungicides were used as negative controls. After 5 days of incubation at 25 °C, the fungicide activity was evaluated considering the inhibition halo (in mm). All experiments were performed in triplicate.

2.2.7 Biological Characterization of the Spore-Containing Coatings

A viability test of the embedded *B. velezensis* N3.2 spores, and a test of their antagonist activity against *F. graminearum* ITEM 6415 strain were performed. Glass slides drop casted with suspended *B. velezensis* N3.2 spores were coated with a plasma-deposited barrier film of different thickness, as described previously, by changing the duration of the plasma deposition process.

The density of the spores on coated and uncoated samples was evaluated after detaching the spores by shaking the samples (110 rpm, 18 h) in 30 mL of sterile NaCl solution (0.85 g/100 mL) and Tween 80 (0.25% v/v). After centrifugation (9000 g, 10 min), the detached spores were resuspended in sterile distilled water, plated on PCA, and incubated (24°C h, 30°C) for counting the germinated bacteria. Colony counts were expressed as log of the Colony-Forming Units per slide (CFU/slide). The viability of the spores on the samples was also assessed on PCA after incubation (24, 30, and 48 h at 25°C). After incubation the spores could germinate, and their viability was determined from the bacterial colony formation expressed as the width (w, mm) of the growth annulus around the slides. Slides with uncoated spores were used as control in both tests.

The antagonistic activity of the bacterial strain against *F. graminearum* ITEM 6415 was evaluated with the dual culture method. In detail, a mycelial plug (4 mm dia) sample was taken from the edge of a 1 week old fungal colony and placed at the center of one of the two halves of a PDA plate; a glass slide with the plasma-coated spores was then placed at the center of the other half of the plate, on the same diameter length of the plug. Plates containing only the *Fusarium* strain and slides with uncoated spores were used as negative controls. After incubation at 25°C for 10 days, the antagonistic activity of *B. velezensis* N3.2 was expressed as the width of the inhibition halo (in mm), measured from the edge of the bacterial growth zone to the edge of the mycelium along the inoculum axis. All experiments were performed in triplicate.

The biological results were presented as mean values ± standard deviations. The statistical analysis was performed with the Statistica 12.0 software (StatSoft Inc., Tulsa, OK, USA). Biological characterization data were compared with a one-way ANOVA test followed by Tukey's test to determine significantly different values ($p < 0.05$).

2.3 Results and Discussion

2.3.1 Chemical Characterization of the Plasma-Deposited Coating

The deposition rate of 82 ± 8 nm/min was measured for the coating used to embed the cast *Bacillus* spores or fungicides in the experimental conditions used; coatings of different thickness could thus be deposited on the spores or fungicides by changing the deposition time.

Transmission FT-IR allowed the identification of the main functional groups present along the thickness of the plasma-deposited layer. In **Figure 2**, the absorption FT-IR spectra of the C_2H_4 precursor film and of the films deposited on Si for 8 min are reported. The spectrum in Figure 2B shows typical bands of organic films characterized by O-containing polar moieties, namely, the broad OH stretching band (3600–3100 cm^{-1}), the C–O stretching (1084 cm^{-1}), and the C=O stretching (1717 cm^{-1}). These polar groups, generated from the interaction of the plasma with the water aerosol, are part of the hydrocarbon network of the coating originated from ethylene fragments. Indeed, the IR bands typical of a hydrocarbon backbone are detected, such as the aliphatic CH_x stretching at 2953–2870 cm^{-1} and the CH_x bending at 1457 cm^{-1}. A similar spectral profile was observed for coatings deposited at different deposition times, confirming that the chemical composition of the film remains consistent as the deposition time changes.

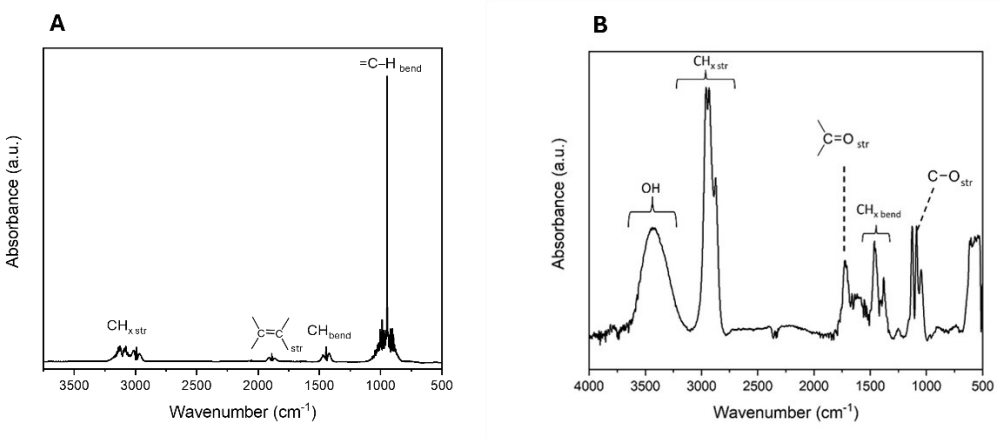

Figure 2. FT-IR transmission spectrum of the precursor and plasma-deposited coating utilized for embedding *B. velezenzis* N 3.2 spores or fungicides. A) FT-IR of C_2H_4 adapted from: https://webbook.nist.gov/chemistry/ , B) FT-IR of film (8 min discharge duration).

XPS analysis has been performed on the plasma deposited coatings. The resulting surface atomic composition of the coatings, whose corresponding IR spectrum is reported in Figure 2, is C = 88.3%, O = 11.0%, and N = 0.7% respectively. Hydrogen cannot be detected by XPS; the presence of nitrogen is likely due to air remaining in the plasma chamber in spite of the purging with He. The presence of oxygen accounts for the polar groups detected by FT-IR. To identify the nature of the O-containing groups in the coating, the C1s spectrum was best-fitted with four components peaked at 285.0 eV (C1, C–C, C–H, reference), 286.4 eV (C2, C–OH, C–OC), 287.7 eV (C3, C = O), and 289.0 eV (C4, COOH, COOR), respectively, as shown in **Figure 3**. The relative area of the peaks was 79.7%, 14%, 4.3%, and 1%, respectively, for the components C1 to C4, in good accordance with the FT-IR analysis, and with the structure of coatings deposited in similar conditions discussed in a previous paper. [49]

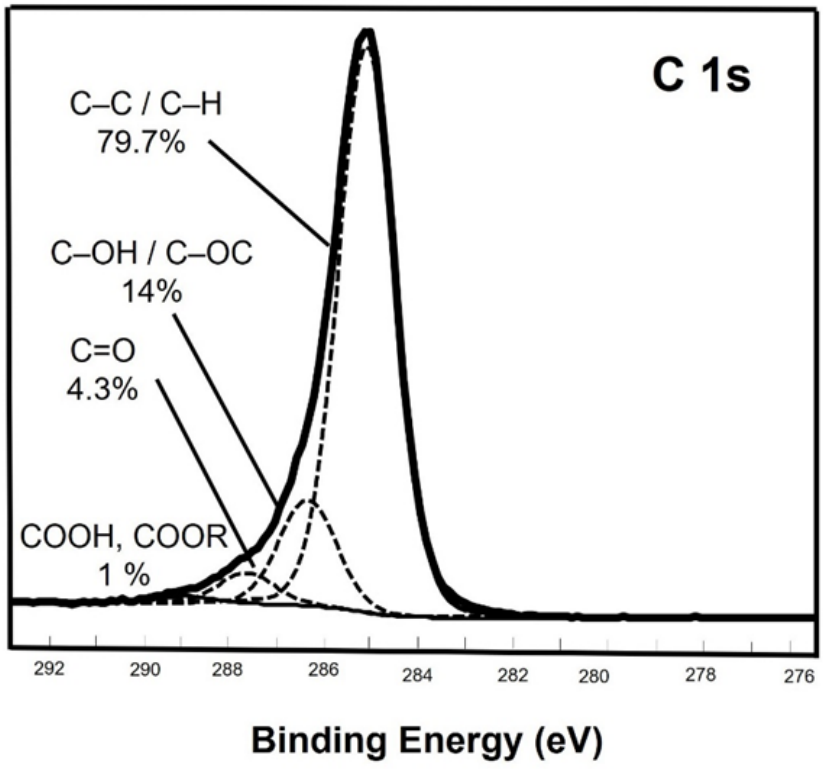

Figure 3. Best fitting of the XPS C1s peak of the plasma-deposited coating utilized for embedding *B. velezenzis* N 3.2 spores or fungicides (8 min discharge duration).

The WCA measurements performed on the plasma-deposited coatings revealed a quite hydrophilic character, with a WCA value of about 52 ± 2°, as measured on the sample deposited with 8 minutes of plasma discharge. The WCA does not change appreciably for coatings of different thickness. This level of hydrophilicity is compatible with the hydrocarbon network grafted with polar O-containing groups, as revealed by XPS and FT-IR analysis.

2.3.2 Biological Characterization of the Fungicide-Containing Coatings

Fungicide activity of coatings containing fungicides.

The activity of the fungicide PRO trapped in the coating against *F. graminearum* ITEM 6415 was evaluated through in *in vitro* tests. **Figure 4** illustrates the results obtained keeping the film thickness at 170 nm, while varying the amount of PRO on the substrates; the uncoated drop casted fungicide is shown for comparison. It can be observed that the sample consisting of a barrier film without fungicide showed no activity against *F. graminearum*, confirming that the antifungal activity is exclusively due to the presence of PRO.

As reported in **Table 1**, samples containing different amounts of PRO without the coating (6-PRO, 60-PRO, 100-PRO) exhibited inhibition zones of 52±3, 46±1, and 45±1 mm, respectively, after 5 days of incubation at 25 °C.

When a 170 nm thick coating is added, varying the amount of PRO between 6 and 100 µg leads to inhibition zones between 59 and 69 mm are obtained, confirming that the presence of the barrier coating does not inhibit the activity of PRO. Looking more in detail to the results reported in table 1, it can be observed that when comparing samples containing the same amount of PRO the inhibition halo appears systematically higher for the coated ones. This result is quite surprising since it should be supposed that the presence of the coating limits the efficient effective diffusion of the fungicide towards the conidia.

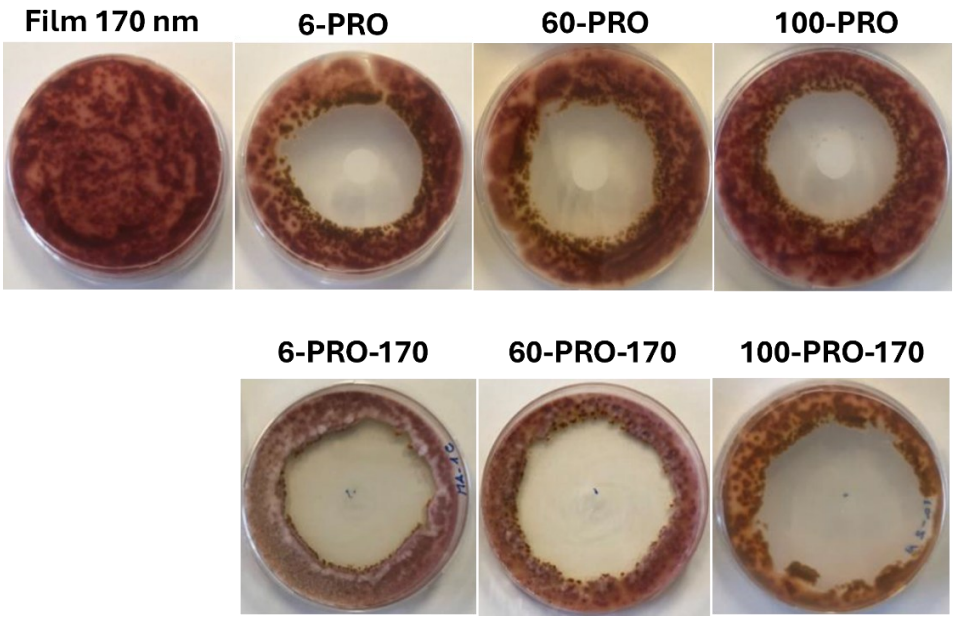

Figure 4. Pictures showing the fungicide activity of PRO at different concentration prepared with and without 170 nm barrier coating. Samples tested versus *F. graminearum* after 5 days of incubation on PDA at 25 °C.

Table 1. Fungicide activity (inhibition halo, mm) of PRO-containing coatings against *Fusarium graminearum* after 5 days of incubation at 25 °C, at different PRO amounts and film thicknesses of the plasma-deposited barrier layer.

Sample	PRO (µg)	Film Thickness (nm)	Activity against *F. graminearum* ITEM 6415 (mm)
Barrier coating	No Fungicide	170 nm	No activity
6-PRO	6	No Film	52^{c} ±3
60-PRO	60	No Film	46^{b} ±1
100-PRO	100	No Film	45^{a} ±1
60-PRO-90	60	90	61^{f} ± 2
60-PRO-170	60	170	69^{i}± 8
60-PRO-270	60	270	62^{g} ± 4
60-PRO-540	60	540	66^{h} ±6
6-PRO-170	6	170	60^{e} ± 2
100-PRO-170	100	170	59^{d}± 4

a–i Values in the same column with different superscript letters are significantly different ($p < 0.05$).

Moreover, as shown in **Figure 5** and **Table 1**, the fungicide activity of the coatings was also evaluated by keeping the PRO amount constant at 60 µg and varying the thickness of the barrier film. The inhibition halos were 61±2 mm (60-PRO-90), 69±8mm (60-PRO-170), 62±4 mm (60-PRO-270), and 66±6 mm (60-PRO-540). Also in this case, it can be observed that the activity of the fungicide is not limited by the presence of the coating in spite of the deposition of a more than 3-fold thicker coating. Furthermore, even if the obtained values are quite similar, the presence of the plasma barrier film seems to lead to higher inhibition with respect to the ones obtained with the 60-PRO barrier-free sample.

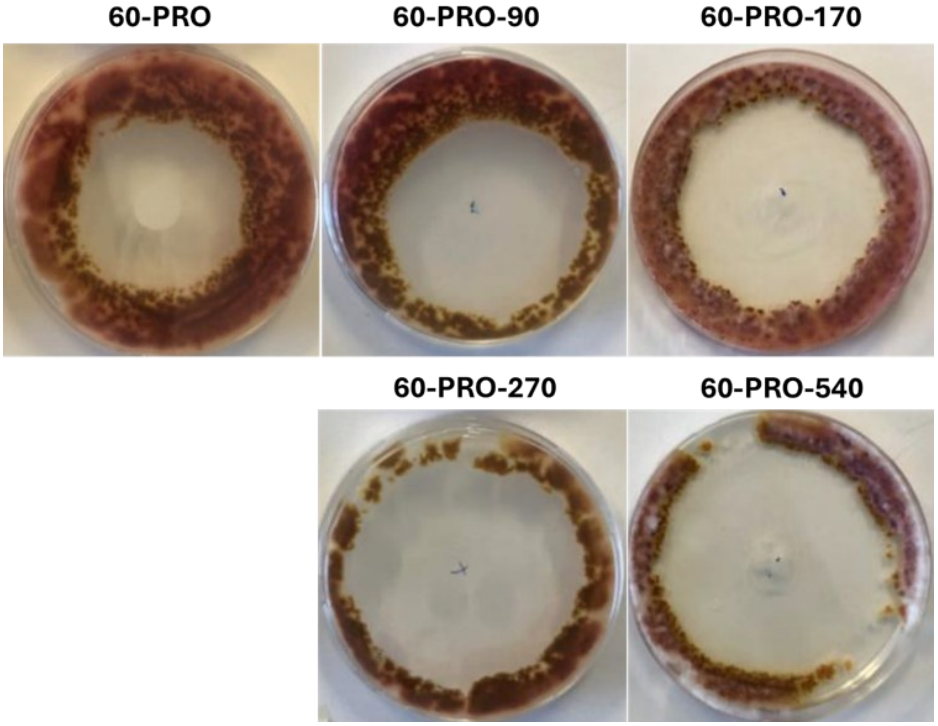

Figure 5. Pictures showing the fungicide activity of PRO (60 µg) coated with different thicknesses against *F. graminearum* ITEM 6415 after 5 days of incubation on PDA at 25 °C.

The effect of the plasma-deposited barrier film with a thickness of 170 nm was evaluated for the fungicides PYR and FLU, the results of the diffusion inhibition tests are reported in **Figure 6**. For samples containing PYR, amounts of 6 and 60 µg were considered for the tests. In contrast, for FLU, 19.2 µg was selected as the lowest amount, since this compound is applied in the field at higher concentrations.

In both cases, the inhibition halo are smaller than those obtained for PRO (**Table 1**), in agreement with the lower intrinsic antifungal activity of PYR and FLU against *F. graminearum*. For the uncoated samples, the inhibition zones were 39.0±2.0 mm and 36.0±0.5 mm for 19.2-FLU and 60-FLU, and 47.0±2.0 mm and 46.0±2.0 mm for 6-PYR and 60-PYR, respectively. (**Table 2**)

When the fungicide was coated with the 170 nm plasma-deposited barrier film, the inhibition halos decreased to 27.0±0.6 mm (19.2-FLU-170), 35.7±0.3 mm (6-PYR-170), and 41.0±3.0 mm (60-PYR-170), while for 60-FLU-170 the value remained similar to the control (60-FLU).

These results show that, unlike for PRO-containing coatings, the presence of the plasma barrier film in the case of PYR and FLU does not enhance antifungal activity but rather tends to reduce it. This behavior can be attributed to the barrier effect of the plasma-deposited film, which limits the diffusion of the active compound from the sample to the agar medium, thereby decreasing the availability of the fungicide in the surrounding area. The results obtained for the bilayer coatings containing PYR and FLU were therefore expected, as they are consistent with the barrier function of the plasma-deposited coating.

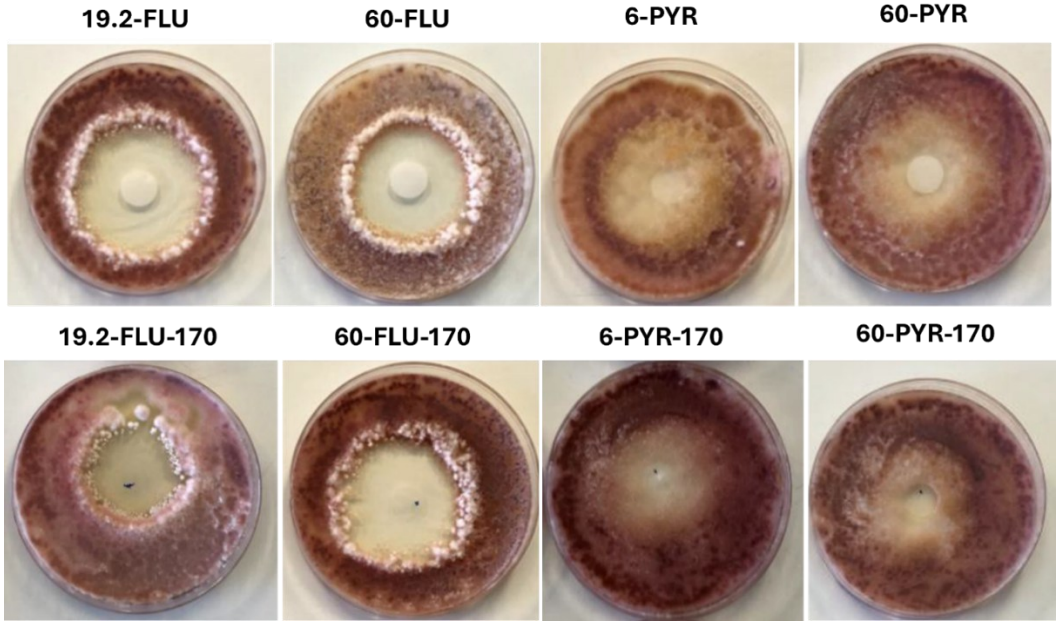

Figure 6. Pictures showing the fungicide activity of FLU and PYR at different doses prepared with and without 170 nm barrier coating. Samples tested versus *F. graminearum* ITEM 6415 after 5 days of incubation on PDA at 25 °C.

Table 2. Fungicide activity (inhibition halo, mm) of FLU- and PYR-containing coatings against *F. graminearum* ITEM 6415 strain after 5 days of incubation at 25 °C, at different fungicide doses (µg) and for a fixed film thickness (170 nm) of the plasma-deposited barrier layer.

Sample	PRO (µg)	Deposition time (min)	Film Thickness (nm)	Antagonistic activity against *F. graminearum* ITEM 6415 (mm)
19.2-FLU	19.2	0	No Film	39.0^{e}± 2.0
60-FLU	60	0	No Film	36.0^{c} ± 0.5
6-PYR	6	0	No Film	47.0^{h} ± 2.0
60-PYR	60	0	No Film	46.0^{g} ±2.0
19.2-FLU -170	19.2	2	170	27.0^{a} ± 0.6
60-FLU -170	60	2	170	37.0^{d} ± 0.6
6-PYR-170	6	2	170	35.7^{b} ± 0.3
60-PYR-170	60	2	170	41.0^{f} ± 3.0

a–h Values in the same column with different superscript letters are significantly different ($p < 0.05$).

Discussion

The plasma-deposited barrier film enabled the coating of 3 different fungicides: PRO, FLU, and PYR. All fungicide-containing composite coatings exhibited inhibition halos, confirming their antifungal activity against *F. graminearum*. The results clearly indicate that the presence of the barrier film does not limit the antifungal activity that in the case of PRO appears even enhanced, with comparison with the uncoated fungicide. This was also observed in a previous similar study where PRO was sandwiched between 2 coatings prepared in a low-pressure plasma reactor. [40]

Such behavior could be attributed to the role of the film as a controlled-release matrix, capable of modulating the diffusion of the active ingredient and maintaining an effective concentration in contact with the fungal mycelium for a longer period.

In the present work, the film was obtained by plasma-assisted deposition fed with C_2H_4 and water, a process that leads to the formation of a $C–O_x$-containing film (–C–O–, –C=O, –OH). The incorporation of oxygen imparts a hydrophilic nature to the coating, enabling

interactions with water and influencing the diffusion of organic molecules through the film. This hydrophilic character may either favor or hinder the release of the active compound depending on its intrinsic polarity.

The increase in antifungal activity observed for PRO in the presence of the plasma film is consistent with its physicochemical properties: PRO exhibits a water solubility of approximately 22 mg L^{-1} and a partition coefficient (Log P) of 2.7, making it more polar and moderately hydrophilic compared to FLU and PYR, which display much lower solubilities (≈ 1.8–1.9 mg L^{-1}) and log P values of 2.6 and 4.1, respectively. The diffusion of more hydrophobic compounds is limited by weak interactions with the polar environment and by the presence of a hydrated surface layer, which hinders the migration of these molecules toward the agar substrate and consequently reduces the inhibition zone.[50-51] It could therefore be hypothesized that a more polar fungicide such as PRO exhibits better compatibility with the hydrophilic environment of the plasma-deposited film, allowing a more gradual yet effective diffusion and consequently benefiting from the controlled-release effect induced by the coating. The increase in antifungal activity observed up to a film thickness of approximately 170 nm suggests that films too thin allow an excessively rapid release, leading to premature depletion of the active compound, whereas films of intermediate thickness ensure a more gradual and prolonged release, maximizing the biological effect. Overall, the results confirm that plasma-deposited coatings containing PRO not only preserve but also enhance the antifungal activity of the active component through their function as hydrophilic, diffusion-regulating barriers. The combination of the film chemical composition (oxygen-containing groups) and its optimal thickness enables controlled fungicide release and a more stable antifungal effect over time, making this technology highly promising for applications in the agronomic field, particularly for direct seed-coating treatments.

On the other hand it is possible that prothioconazole, more than the other two fungicide, can undergo rearrangement during plasma exposure. This could lead to the formation of compounds with a higher activity against *Fusarium*; this hypothesis, however, needs to be confirmed.

2.3.3 Characterization of the Spore-Containing Coatings

Morphological Characterization of the Spore-Containing Coatings

In **Figure 7** the SEM images of *B. velezensis* N3.2 spores uncoated and coated (for 1 and 8 min) with the plasma-deposited barrier film are reported. The typical shape of the *Bacillus* spores can be observed in the cast uncoated sample in Figure 7A and B. As a comparison, the morphology of the coating without spores is reported in Figure 7C. As can be appreciated in Figure 7D, a 1 min coating is not enough to uniformly coat the spores, due to their size and shape. When a coating is deposited for 8 min onto the spores, elongated wrinkles about 2 µm wide can be observed, consistent with the presence of the spores underneath the coating. The formation of wrinkles, evident in Figure 7E and 7F, is most likely induced by the presence of spores, since the coating deposited onto flat sporeless substrates show smooth morphology with no wrinkles (Figure 7C). [49] Additionally, it cannot be ruled out that macromolecular residues from cellular material, possibly present at the substrate surface, may reduce the adhesion of the coating, thus leading to film detachment.

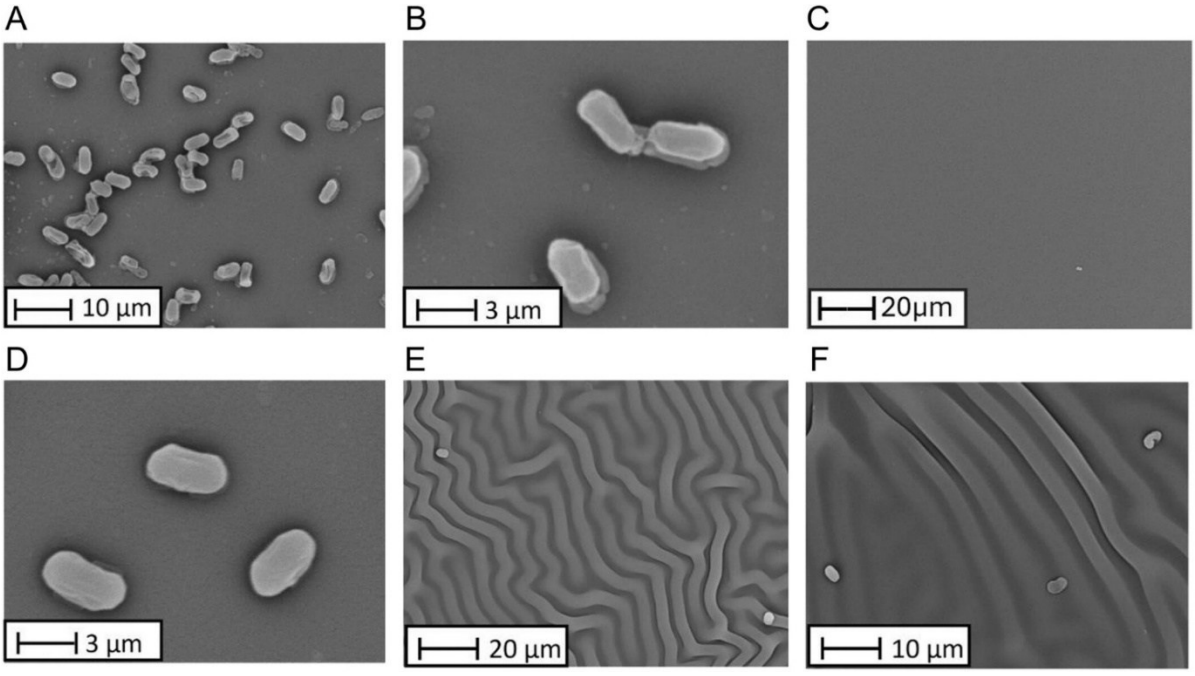

Figure 7. SEM images (BSE mode, 15 kV) at different magnifications of (A, B) *B. velezensis* N3.2 uncoated spores; (C), plasma coating without spores; (D) spores coated with 1 min barrier film, (E, F) spores coated with 8 min barrier film.

Viability Tests

To evaluate the effect of the plasma deposition process and of the thickness of the coating on the viability of the spores, both the germination of the spores on agar and the quantity of viable spores remaining on the slides were evaluated after the deposition. As shown in **Figure 8**, after 2 days of incubation on PCA the bacterial growth became clearly visible around each slide (whitish annulus) for all samples, each with a different width of the bacterial growth annulus, depending on the thickness of the barrier film.

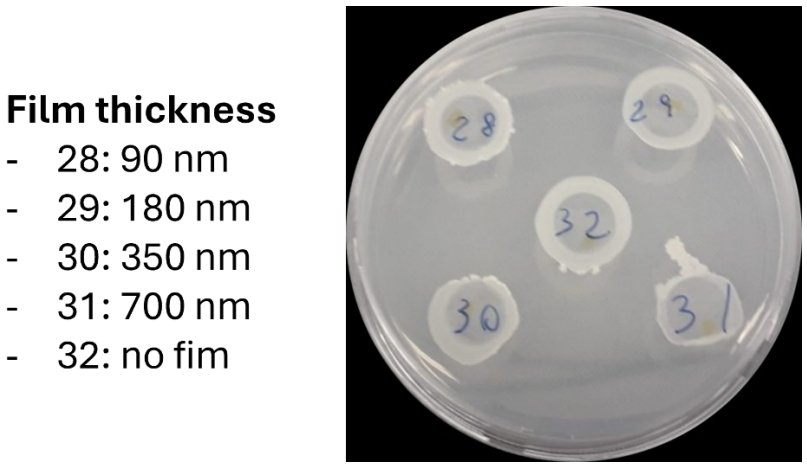

Figure 8 Picture reporting the bacterial growth of *B. velezenzis* N3.2 after 48 h incubation on PCA at 25 °C. The spores were coated on glass samples with the plasma-deposited barrier film at different thickness.

As it can be observed in **Table 3**, the width (w) of the bacterial growth results the same for the uncoated control sample and the one coated with the thinnest (90±10 nm) film, whereas it is found decreasing in the other samples as a function of the increasing thickness of the coating, reaching the lowest value of 0.8 mm for spores coated with the thickest (about 1.4 μm) coating ($p < 0.05$).

Table 3 Bacterial growth (w, mm), quantity of spores recovered from coated and uncoated slides (log CFU/slide), and antagonistic activity of *B. velezenzis* N3.2 against *F. graminearum* ITEM 6415 (mm), at different thickness of the plasma deposited coating.

Film thickness (nm)	Bacterial growth after 48h (w, mm) *	Spore/slide (log CFU/slide)	Antagonistic activity against *F. graminearum* ITEM 6415 strain (mm) **
No Film	4.0±0.1[a]	4.99±0.09[a]	10.0±1.2
90±10	4.0±0.1[a]	4.74±0.01[b]	10±1
180±10	3.0±0.1[b]	3.89±0.01[c]	9.8±0.5
350±20	2.3±0.5[c]	3.08±0.04[c]	9.6±0.5
700±30	1.8±0.2[c]	2.38±0.04[c]	9.5±0.8
1400±50	0.8±0.1[d]	1.14±0.06[c]	8±1

Note: Data are represented as mean ± standard deviation.

* Expressed as the width (w, mm) of the growth annulus after 48 h of incubation at 25°C.

** Expressed as an inhibition halo (mm) after 10 days of incubation at 25°C.

a–d Values in the same column with different superscript letters are significantly different ($p < 0.05$).

To evaluate over time the germination of spore coated with different barrier thickness, and to better identify the role of the coating onto germination and viability of the spores, the bacterial growth has been also observed at different incubation times on spore samples coated with the two thickest barrier films, 700 nm and 1400 nm, respectively, and compared with an uncoated spore sample control. The results reported in **Figure 5** show that the uncoated spores germinate only after 24 h giving rise to a growth annulus around sample 35. After 30 h also the spores on sample 33, corresponding to 700 nm coating, germinate while, at last, after 48 h bacterial growth is observed also around sample 34, the one coated with the thickest film.

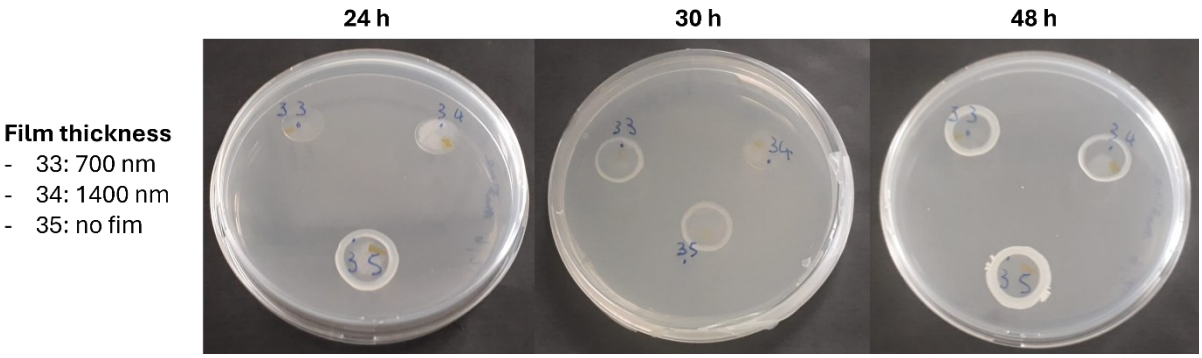

Figure 9 Picture reporting the bacterial growth of *B. velezenzis* N3.2 strain whose spores were coated with the plasma-deposited barrier film at different thickness, after 24 h, 30 h and 48 h of incubation (PCA, 25 °C).

It is evident, based on the data obtained, that the germination of the spores and the subsequent bacterial growth are somewhat delayed by plasma deposited barrier coating. This finding, beneficial for potential applications of plasma deposition approaches on seeds and/or on other substrates of interest in agriculture, can be due to a limitation of the contact of the spores with the culture medium, that is essential to the germination and formation of the bacterial colonies, or/and to the possible reduced viability of the spores after the interaction with the plasma enviroment, in spite of the growing protective coating.

In parallel to the viability test on agar, to obtain information on the adhesion tenacity of the spores to the slides, samples with uncoated spores and coated with the thickest coatings, were subjected to washing, vigorous scraping and subsequent plating to verify the quantity of viable spores remained on the slides. As expected, after washing, 5 log CFU/slide were recovered from the uncoated slides, while the quantity of recovered spores decreased with the increased thickness of the film (**Table 3**). This result could indicate that most spores are more tenaciously protected when the film thickness is higher, making difficult their recovery. In such conditions, however, the inactivation of part of the spores, potentially increasing with the plasma exposure time, cannot be ruled out.

Antagonistic Activity

To evaluate the antagonistic activity of *B. velezenzis* N3.2 strain trapped in the coating against *F. graminearum* ITEM 6415, in vitro antagonism tests were carried out. The results are reported in **Table 3** and **Figure 10**. The efficacy of the coating was assessed by observing the growth of the fungal strain after incubation at 25°C.

After 10 days, no significant difference was observed between treated and untreated samples, attesting that the treatment did not reduce the antifungal activity of the bacterial strain. Furthermore, the activity remained unchanged as the thickness of the barrier film increased ($p > 0.05$). When the samples used in the viability test were also subjected to the antagonism test after washing, the results showed once more the antagonistic activity of *B. velezensis* N3.2 against the *Fusarium* strain, highlighting again the presence of active spores on the slides, since washing was probably not sufficient for removing all the spores. This result leads to the hypothesis that the lower number of spores recovered from treated slides (**Table 3**) could be due to the thickness of the film rather than to a reduction in viability due to the plasma process itself.

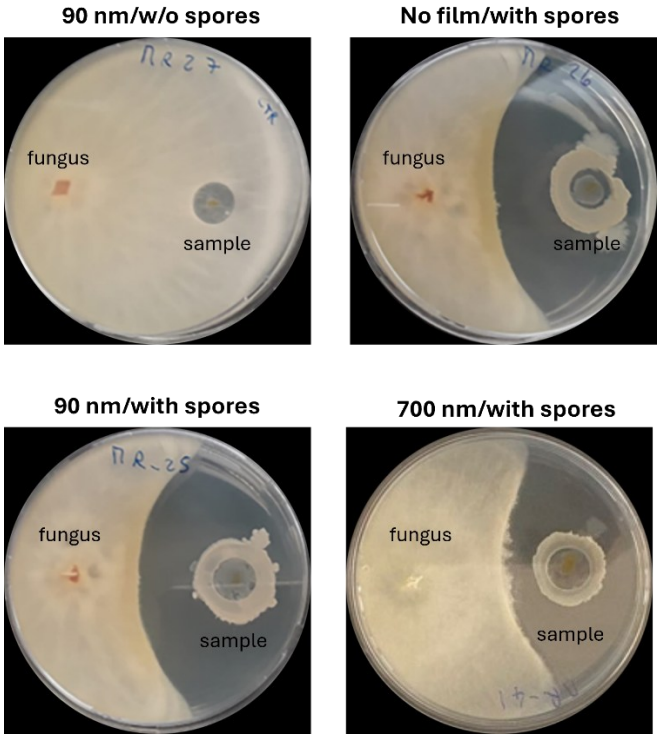

Figure 10 Antagonistic activity of *B. velezensis* N3.2 strain against *F. graminearum* ITEM 6415 strain, whose spores were coated with the plasma-deposited barrier film at different thickness.

Discussion

Fungal plant pathogens, such as many *Fusarium* species, cause huge losses of crops and are dangerous for human health due to the production of mycotoxins. To replace fungicides researchers are focusing attention onto natural products and biocontrol agents. *Bacillus* species are suitable as biocontrol agents, since in addition to producing antimicrobial substances and stimulating plant-induced systemic resistance, they produce spores that increase their resistance to environmental stress conditions. [52] For effective field distribution, it is useful to incorporate beneficial microorganisms into matrices for seed coating. To be effective, a beneficial microorganism should be protected during storage and field application. At the same time, a good film should ensure the integrity of the microorganism and the seeds, allowing their germination. [53]Polyvinyl alcohol (PVA)-based films have recently been proposed to deliver *Bacillus megaterium* as seed coatings. [53] Coatings consisting of *Bacillus* strains and gum arabica have also been developed to manage *Fusarium* wilt disease. [52]

In the present work a plasma deposited coating has been considered for embedding spores with antifungal activity. At the best of the authors' knowledge, this paper explores for the first time the plasma deposition of an organic coating onto bacterial spores. This approach greatly differs from most of the recent studies on plasma processes for agriculture, mostly intended for decontamination and not based on plasma deposition. The results well indicate that the plasma deposition of a coating on top of the spores do not alter their germinability characteristics, as illustrated in **Figures 8** and **9**. Further, the antifungal activity is not reduced with respect to uncoated spores (**Figure 10**). On the other hand, when considering the effect of film thickness, the germination is delayed, and the viability of the spores decreases with increasing deposition time. A possible rationale is the limited contact between the spores and the medium, which is necessary to induce germination. However, it is known that plasma, especially when fed with air or N_2 gas and assisted by the associated UV radiation, can inactivate bacterial spores. [54] On the other hand, it can be hypothesized that the increasing thickness of the coating may at least partially shield the spores from aggressive plasma-generated RONS species. Since it can be hypothesized that UV radiation is in part absorbed by the organic species present in the plasma feed and by the coating itself, the inactivating effect of plasma on spores

might be considered negligible. Further biological tests, indeed, are necessary to support this hypothesis.

2.4 Conclusions

This study demonstrates the potential of plasma-deposited organic coatings as systems for the development of active films with antifungal properties and possible applications in seed protection.

The plasma-deposited barrier film enabled the encapsulation of PRO, FLU and PYR fungicides. All fungicide-containing composite coatings exhibited clear inhibition zones, confirming their antifungal activity against *Fusarium*. The presence of the barrier layer enhanced the antifungal efficacy of PRO compared to the uncoated fungicide, assuming that the organic barrier film matrix act as a controlled-release system capable of maintaining an effective concentration of the active compound in contact with the fungal mycelium over time. The behavior observed for PRO was consistent with its higher polarity and limited water solubility, which favor compatibility with the hydrophilic nature of the plasma-deposited film. In contrast, more hydrophobic fungicides such as FLU and PYR showed reduced activity, likely due to both their intrinsically lower antifungal efficacy compared to PRO and to the decreased bioavailability caused by the physical barrier effect of the plasma-deposited film, which limits their diffusion through the hydrophilic layer of the coating. The barrier film proved to be suitable for the encapsulation of pesticides, effectively controlling their environmental availability, confirming that plasma-assisted processes can be used for seed-coating treatments with tunable release properties.

Furthermore, this study demonstrates, for the first time, the feasibility of incorporating bacterial spores within a plasma-deposited organic coating, introducing a new strategy for the development of active films with antifungal properties and potential applications on seeds with no use of chemical substances with high impact on environment and human health.

The *Bacillus velezensis* N3.2 strain retained both its viability and antifungal activity against *Fusarium* after the plasma deposition process, indicating that the treatment does

not compromise the essential biological functions of the spores. Although an increase in film thickness was associated with a delay in germination, the embedded spores remained effective against fungal pathogens. This innovative offers a promising alternative to conventional seed-coating methods, as it preserves the protection and functionality of beneficial microorganisms capable of acting against pathogens or promoting plant growth. However, further field studies are required to optimize the plasma deposition parameters and to assess their direct impact on seed germination and crop protection.

2.5 References

[1] FAO. The Future of Food and Agriculture—Trends and Challenges. *FAO*, 2017.

[2] FAO. World Food and Agriculture—Statistical Yearbook 2022. *FAO*, 2022.

[3] A. Logrieco, A. Bottalico, G. Mulé, A. Moretti, G. Perrone. Epidemiology of toxigenic fungi and their associated mycotoxins for some Mediterranean crops. *European Journal of Plant Pathology*, 2003, 109, 645–667.

[4] European Food Safety Authority (EFSA). Use of the EFSA Comprehensive European Food Consumption Database in exposure assessment. *EFSA Journal*, 2011, 9, 2097.

[5] E. Balázs, J. S. Schepers. The mycotoxin threat to food safety. *International Journal of Food Microbiology*, 2007, 119, 1–2.

[6] Z. Kang, H. Buchenauer. In: *Mycotoxins in Plant Disease*. Springer, 2002.

[7] M. Masiello, *et al*. Plasma technology increases the efficacy of prothioconazole against *Fusarium graminearum* and *Fusarium proliferatum* contamination of maize (Zea mays) seedlings. *International Journal of Molecular Sciences*, 2021, 22, 9301.

[8] G. P. Munkvold, C. Watrin, M. Scheller, R. Zeun, G. Olaya. In: *Plant Pathology in the 21st Century*. Springer, 2014.

[9] A. Moretti, G. Panzarini, S. Somma, et al. Systemic growth of *Fusarium graminearum* in wheat plants and related accumulation of deoxynivalenol. *Toxins*, 2014, 6, 1308–1324.

[10] X. Wei, X. Guo, J. Jiang, L. Qian, J. Xu, Z. Che, X. Huang, S. Liu. Resistance risk assessment of *Fusarium pseudograminearum* from wheat to prothioconazole. *Pesticide Biochemistry and Physiology*, 2023, 191, 105346.

[11] J. E. Parker, A. G. Warrilow, H. J. Cools, B. A. Fraaije, J. A. Lucas, K. Rigdová, D. E. Kelly, S. L. Kelly. Prothioconazole and prothioconazole-desthio activities against *Candida albicans* sterol 14-α-demethylase (CaCYP51). *Applied and Environmental Microbiology*, 2013, 79, 1639–1645.

[12] F. Zhou, A. Han, Y. Jiao, Y. Cao, L. Wang, H. Hu, R. Liu, C. Li. Exploring the potential mechanism of prothioconazole resistance in *Fusarium graminearum* in China. *Journal of Fungi*, 2023, 9(10), 1001.

[13] K. Bersching, S. Jacob. The molecular mechanism of fludioxonil action is different to osmotic stress sensing. *Journal of Fungi*, 2021, 7(5), 393.

[14] Y. Feng, Y. Huang, H. Zhan, P. Bhatt, S. Chen. An overview of strobilurin fungicide degradation: Current status and future perspective. *Frontiers in Microbiology*, 2020, 11, 389.

[15] D. Palmieri, G. Ianiri, C. Del Grosso, et al. Advances and perspectives in the use of biocontrol agents against fungal plant diseases. *Horticulturae*, 2022, 8(6), 577.

[16] M. Tariq, et al. *Acta Agriculturae Scandinavica Section B – Soil and Plant Science*, 2020, 70, 507.

[17] H. Chen, et al. Antifungal activity and mode of action of lactic acid bacteria isolated from kefir against *Penicillium expansum*. *Food Control*, 2021, 130, 108274.

[18] E. Xu, et al. Evaluation of the biocontrol potential of *Bacillus* sp. WB against *Fusarium oxysporum* f. sp. *niveum*. *Biological Control*, 2020, 147, 104288.

[19] K. Stumbriene, R. Gudiukaite, R. Semaskiene, P. Svegzda, A. Jonaviciene, S. Suproniene. Screening of new bacterial isolates with antifungal activity and application of selected *Bacillus* sp. cultures for biocontrol of *Fusarium graminearum* under field conditions. *Crop Protection*, 2018, 113, 22–28.

[20] N. Khan, et al. Antifungal activity of *Bacillus* species against *Fusarium* and analysis of the potential mechanisms used in biocontrol. *Frontiers in Microbiology*, 2018, 9, 2363.

[21] A. Keshmirshekan, L. M. de Souza Mesquita, S. P. M. Ventura. Biocontrol manufacturing and agricultural applications of *Bacillus velezensis*. *Trends in Biotechnology*, 2024, 42, 986–1001.

[22] European Commission. A European Green Deal: Striving to be the First Climate-Neutral Continent. *European Commission*, 2021.

[23] United Nations. Sustainable Development Goals. *United Nations*, 2015.

[24] S. Pedrini, D. J. Merritt, J. Stevens, K. Dixon. Seed coating: Science or marketing spin? *Trends in Plant Science*, 2017, 22(2), 106–116.

[25] C. Accinelli, H. K. Abbas, N. S. Little, J. K. Kotowicz, M. Mencarelli, W. T. Shier. A liquid bioplastic formulation for film coating of agronomic seeds. *Crop Protection*, 2016, 89, 123–128.

[26] A. G. Taylor, et al. Seed enhancements. *Seed Science Research*, 1998, 8, 245–561.

[27] D. Foqué, J. G. Pieters, D. Nuyttens. Characterization of different pneumatic sowing machines. *Aspects of Applied Biology*, 2014, 122, 77–84.

[28] D. Nuyttens, et al. Pesticide-laden dust emission and drift from treated seeds during seed drilling: A review. *Pest Management Science*, 2013, 69(5), 564–575.

[29] K. D. Weltmann, J. F. Kolb, M. Holub, D. Uhrlandt, M. Simek, K. Ostrikov, S. Hamaguchi, U. Cvelbar, M. Cernak, B. Locke, A. Fridman, P. Favia, K. Becker. The future in plasma science and technology. *Plasma Processes and Polymers*, 2018, 16(1), e1800118.

[30] S. Somma, M. Masiello, M. Haidukowski, B. Ciasca, E. Sardella, P. Favia, F. Palumbo, M. Roggio, A. Moretti. Decontamination of maize kernels and degradation of mycotoxins by means of cold plasmas. *LWT*, 2025, 215, 117205.

[31] P. Favia, et al. Advanced applications of plasmas in life sciences. *Plasma Processes and Polymers*, 2020, 17(10), 2070028.

[32] A. Mitra, Y. F. Li, T. G. Klämpfl, et al. Inactivation of surface-borne microorganisms and increased germination of seed specimen by cold atmospheric plasma. *Food Bioprocess Technology*, 2014, 7, 645–653.

[33] J. Zhang, et al. Growth-inducing effects of argon plasma on soybean sprouts via regulation of demethylation levels of energy metabolism-related genes. *Scientific Reports*, 2017, 7, 41917.

[34] L. Ling, et al. Effects of cold plasma treatment on seed germination and seedling growth of soybean. *Scientific Reports*, 2014, 4, 5859.

[35] T. Stolárik, et al. Effect of low-temperature plasma on the structure of seeds, growth and metabolism of endogenous phytohormones in pea (*Pisum sativum* L.). *Plasma Chemistry and Plasma Processing*, 2015, 35, 659–676.

[36] L. Sivachandiran, A. Khacef. Enhanced seed germination and plant growth by atmospheric pressure cold air plasma: Combined effect of seed and water treatment. *RSC Advances*, 2017, 7, 1822.

[37] B. Sera, P. Spatenka, M. Sery, N. Vrchotova, I. Hruskova. Influence of plasma treatment on wheat and oat germination and early growth. *IEEE Transactions on Plasma Science*, 2010, 38(10), 2963–2968.

[38] J. Jiang, X. He, L. Li, J. Li, H. Shao, Q. Xu, R. Ye, Y. Dong. Effect of cold plasma treatment on seed germination and growth of wheat. *Plasma Science and Technology*, 2014, 16, 54.

[39] D. Dobrin, M. Magureanu, N. B. Mandache, M. D. Ionita. Effect of non-thermal plasma treatment on wheat germination and early growth. *Innovative Food Science & Emerging Technologies*, 2015, 29, 255–260.

[40] C. Lo Porto, et al. Plasma-assisted deposition of fungicide-containing coatings for encapsulation and protection of maize seeds. *Plasma Processes and Polymers*, 2019, 16(6), 1900022.

[41] M. Masiello, et al. Plasma technology increases the efficacy of prothioconazole against *Fusarium graminearum* and *Fusarium proliferatum* contamination of maize seedlings. *International Journal of Molecular Sciences*, 2021, 22(17), 9301.

[42] Y. W. Yang, et al. Fast incorporation of primary amine group into polylactide surface for improving C2C12 cell proliferation using nitrogen-based atmospheric-pressure plasma jets. *Journal of Biomedical Materials Research*, 2013, 102(1), 160–169.

[43] Y. W. Yang, et al. Highly effective large-area inactivation of *Bacillus subtilis* spores using a planar dielectric barrier discharge jet with CF4/air mixture. *IEEE Transactions on Plasma Science*, 2012, 40(11), 3003–3006.

[44] M. H. Chiang, et al. Inactivation of *Escherichia coli* and *Bacillus subtilis* by a parallel-plate dielectric barrier discharge jet. *Surface and Coatings Technology*, 2010, 204(21–22), 3729–3737.

[45] G. Da Ponte, E. Sardella, F. Fanelli, R. d'Agostino, P. Favia. Trends in surface engineering of biomaterials: Atmospheric-pressure plasma deposition of coatings for biomedical applications. *European Physical Journal – Applied Physics*, 2011, 56(2), 24023.

[46] S. Zicca, P. De Bellis, M. Masiello, M. Saponari, P. Saldarelli, D. Boscia, A. Sisto. Antagonistic activity of olive endophytic bacteria and *Bacillus* spp. strains against *Xylella fastidiosa*. *Microbiological Research*, 2020, 236, 126467.

[47] F. Valerio, P. De Bellis, M. Di Biase, S. L. Lonigro, B. Giussani, A. Visconti, P. Lavermicocca, A. Sisto. Diversity of spore-forming bacteria and identification of *Bacillus amyloliquefaciens* associated with ropy spoilage of bread. *International Journal of Food Microbiology*, 2012, 156(3), 278–285.

[48] P. De Bellis, F. Minervini, M. Di Biase, F. Valerio, P. Lavermicocca, A. Sisto. Toxigenic potential and heat survival of spore-forming bacteria isolated from bread and ingredients. *International Journal of Food Microbiology*, 2015, 197, 30–39.

[49] Y. W. Yang, G. Camporeale, E. Sardella, G. Dilecce, J. S. Wu, F. Palumbo, P. Favia. Deposition of hydroxyl-functionalized films by ethylene aerosol-assisted atmospheric pressure plasma. *Plasma Processes and Polymers*, 2014, 11, 1102–1111.

[50] J. Jin, Y. Han, C. Zhang, J. Liu, W. Jiang, J. Yin, H. Liang. Effect of grafted PEG chain conformation on albumin and lysozyme adsorption: A combined QCM-D and DPI study. *Colloids and Surfaces B: Biointerfaces*, 2015, 136, 120–129.

[51] A. Agnusdei, A. M. Maurelli, D. Gerin, D. Monopoli, S. Pollastro, L. Catucci, F. Faretra, V. De Leo. Fungicide-loaded liposomes for the treatment of fungal diseases in agriculture: An assessment on *Botrytis cinerea*. *International Journal of Molecular Sciences*, 2024, 25(15), 8359.

[52] A. Raza, A. Hassan, W. Akram, T. Anjum, Z. H. Aftab, B. Ali. Seed coating with a synthetic consortium of beneficial *Bacillus* microbes improves seedling growth and manages Fusarium wilt disease. *Scientia Horticulturae*, 2024, 325, 112645.

[53] L. A. Lodi, R. Borges, R. Bortoletto-Santos, C. A. de Oliveira-Paiva, C. Ribeiro, C. S. Farinas. Biodegradable PVA-based films for delivery of *Bacillus megaterium* as seed coating. *Journal of Environmental Chemical Engineering*, 2024, 12(6), 114539.

[54] Z. Zhu, et al. The formation, germination, and cold plasma inactivation of bacterial spores. *Food Chemistry Advances*, 2022, 1, 100056.

Annex A 2.1

As outlined in **Chapter 1**, once the AAA-PP deposition process of fungicide-containing films has been developed onto flat substrates, the methodology was transferred to a home-made large-scale reactor designed for coating maize seed. Appendix A 1.2 presents the deposition parameters used, as well as the evaluation of seed germination and the antifungal activity of the PRO-containing coating.

A 2.1.1 Materials and methods

Preparation of fungicide-Containing Coatings onto maize seeds

Maize seeds of the "Marano 0501" variety were plasma-processed and used for testing the antifungal properties of the plasma deposited coating containing fungicides.

PRO was cast onto the 60 maize seeds by spraying 4 g of an aqueous suspension containing 6 µL of the commercial product Proline. Seeds were then allowed to dry for 24 h in a desiccator connected to a membrane pump. Subsequently, a barrier film was deposited using the home-made large-scale AAA-PP reactor schematized in **Figure 1 A**. It consists of a cylindrical stainless-steel chamber, 120 cm long and 50 cm in diameter, connected to a vacuum membrane pump (N 86, KNF), and containing the electrodes assembly shown in **Figure 1B**. This is composed of a support in PVC bearing two horizontal alumina plates (15 cm × 3 cm × 0.63 mm) coated with a silver conductive paste, both acting as High-Voltage (HV) electrodes. Between the electrode a slit (15cmx0.1 cm) is present through which the gas feed is let. In front of the electrode assembly, at a distance of 5 mm, a ground stainless steel stage (60cm x 25 cm) works as counter-electrode. Seeds are placed into a polycarbonate tray (45 cm x 15 cm x 2 mm), located onto the stage connected to a motor allowing forward and backward horizontal, movement. This set up allows for a homogeneous sample processing and treatment of a larger amount of material. The stage movement speed was set at 1 cm/s.

The HV electrodes were connected to a high-voltage power supply (ALMA PULSE) suitable for the ignition of a dielectric barrier discharge. To monitor the electrical parameters of the discharge, an oscilloscope (TDS 2014C, Tektronix, Beaverton, USA) was connected through a high-voltage probe (P6015A, Tektronix, Beaverton, USA) between the electrodes

and the power supply. The gas feed (ethylene and He) was controlled with electronic mass flow controllers (MKS Instruments). The aerosol was generated using a pneumatic atomizer (TSI 3064) operated with He 3.5 slm. Ethylene was fed as precursor for the plasma coating at a flow rate of 60 sccm, with an additional He flow of 3 slm. The discharge duration was 10 min, and the applied peak-to-peak voltage was maintained at 13 kVpp with a frequency of 20 kHz. Before starting the process, the system was purged with 5 slm He for 5 min, and the same procedure was carried out before removing the seeds from the chamber.

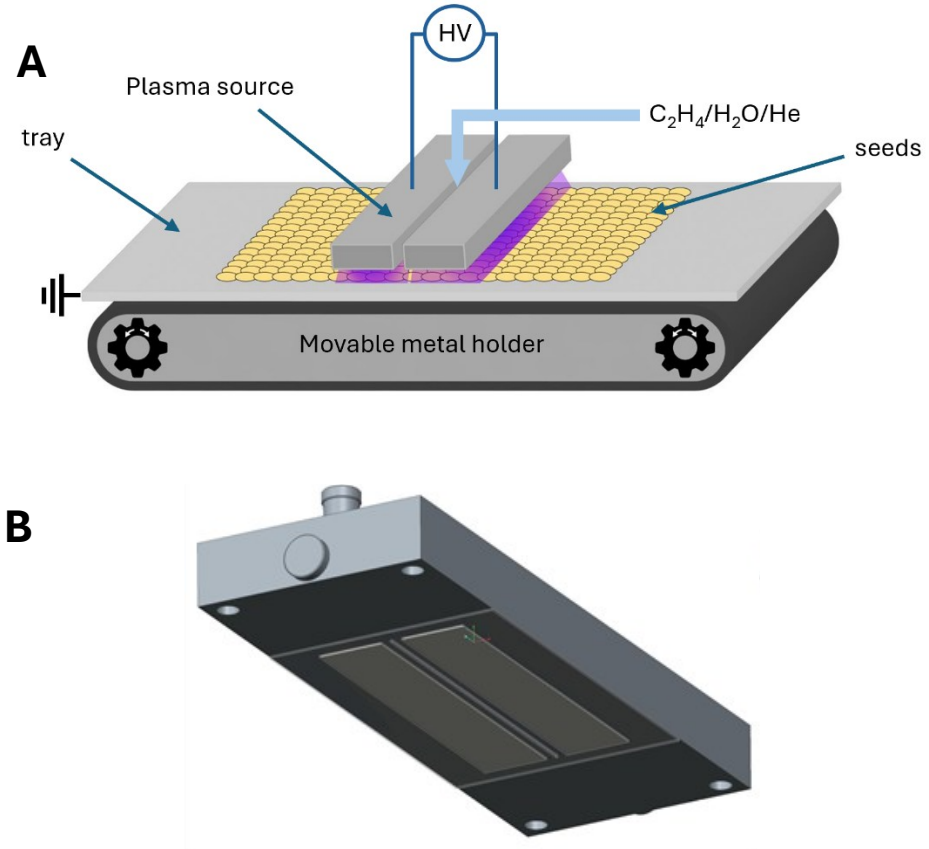

Figure 1 Schematic representation of the AAA-PP reactor (A) and of the electrode assembly (B) used for the deposition of the coatings onto maize seeds.

Chemical Characterization of Fungicide-Containing Coatings onto maize seeds

The composition of the coatings deposited on the Si substrates has been probed by means of FT-IR with a Vertex 70 V Bruker spectrometer (32 scans, 4 cm^{-1}). The spectrometer was evacuated to less than 150 Pa for 5 min, to avoid spectral interferences from atmospheric H_2O vapour and CO_2.

WCA measurements were carried out with a Ramé-Hart 100-manual goniometer (distilled water, 4 µL drops, room temperature). WCAs were measured on three different points of three replicates.

The thickness of the coatings was measured on three different points of three replicates with a KLA-Tencor instrument (Milpitas, CA, USA) D-120 profilometer after scratching part of the coating with a scalpel to form a step.

Activity evaluation of the Fungicide-Containing Coatings onto maize seeds

The *F. graminearum* ITEM 6415 strain was selected from the ITEM Collection of ISPA-CNR (www.ispa.cnr.it/Collection).

To evaluate the fungicidal activity of plasma-deposited coatings containing prothioconazole on maize seeds against *F. graminearum*, five different thesis were prepared and inoculated with the fungal strain, as summarized in **Table 1**: *Thesis NT,* without fungicide treatment or barrier film; *Thesis C*, with barrier film, without fungicide treatment; *Thesis F*, with fungicide treatment, without barrier film; *Thesis FC*, with both fungicide treatment and barrier film; and *Thesis CFC*, with barrier film applied directly to the seed, followed by fungicide treatment and a second barrier layer. In the theses where seeds were coated with a barrier film, the coating thickness was 100 nm.

Table 1 Description of theses used for experimental assay on maize seeds

Thesis	Seed Coating	Fungicide Application
NT	No	No
C	Film	No
F	No	Prothioconazole
FC	Film	Prothioconazole
CFC	double Film	Prothioconazole

For each treatment, five maize seeds were placed on PDA medium supplemented with pentachloronitrobenzene (PCNB). All five treatments were inoculated with a conidial suspension at a concentration of 1×10^5 conidia/mL; a total volume of 100 µL was uniformly spread onto the PDA surface and incubated at 25 °C under fluorescent light with a 12-hour photoperiod.

The effect of each treatment in inhibiting fungal colonization of the seeds was evaluated after 10 days of incubation. At the same time, seed germination was also assessed.

Antifungal activity was expressed as the percent of inhibition area, determined using ImageJ software (version 1.52d; National Institutes of Health, Bethesda, MD, USA). The software was employed to quantify fungal growth by measuring the percent of plate area occupied by fungal mycelium in relation to the total surface area, thus allowing calculation of fungal inhibition. All experiments were performed in triplicate.

A 2.1.2 Results and Discussion

Optimization of the coatings on silicon substrates

The deposition rate of 10 ± 3 nm/min was measured on Si substrates for the coating used to embed the cast of PRO under the experimental conditions employed; a 100 ± 7 nm coating was deposited onto the maize seeds.

FT-IR analysis allowed the identification of the main functional groups present along the thickness of the plasma-deposited layer. Figure 2A of **Chapter 2** (Section 2.3.1, *Chemical Characterization of the Plasma-Deposited Coating*) reports the FT-IR spectrum of the

C_2H_4 monomer. **Figure 2** reports the FT-IR absorption spectrum of films deposited on silicon for 10 minutes. The spectrum shows the typical bands of hydrocarbon films characterized by oxygen-containing polar moieties, as also observed for the coating described in **Chapter 2** (Section 2.3.1, *Chemical Characterization of the Plasma-Deposited Coating*).

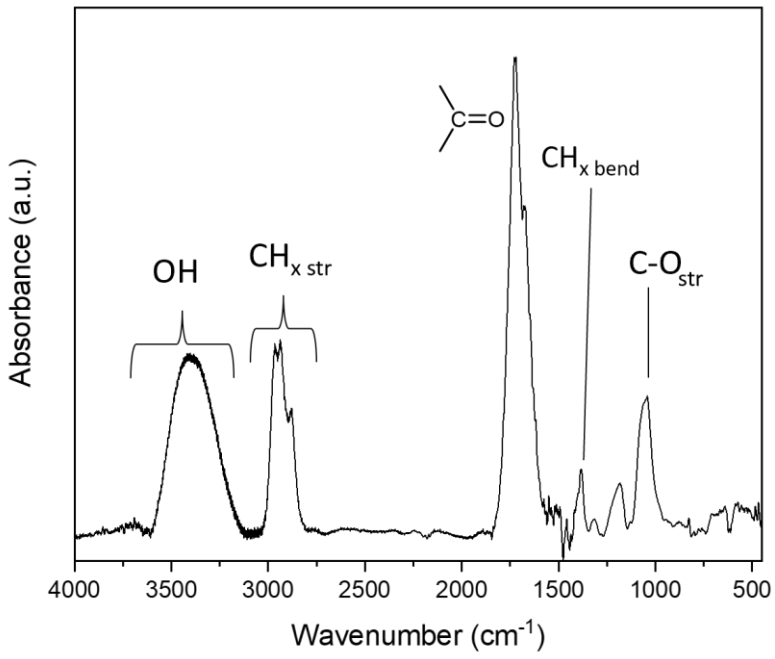

Figure 2 FT-IR transmission spectrum of the plasma-deposited coating utilized for embedding fungicides onto maize (10 min discharge duration).

The WCA measurements performed on the plasma-deposited coatings revealed quite hydrophilic character, with a WCA value of about 50 ± 2°. This level of hydrophilicity is compatible with the hydrocarbon network grafted with polar O-containing groups, as revealed by FT-IR. No further analyses were carried out, as the coating composition was found to be very similar to that of the coating deposited on *Bacillus* spores and fungicides described in **Chapter 2**.

Biological Characterization of Fungicide-Containing Coatings onto maize seeds

The antifungal activity of the fungicide PRO embedded in the coating of 100 nm against *F. graminearum* was evaluated on seeds through agar diffusion tests.

As shown in **Figure 3**, *F. graminearum* colonized the entire surface of the PDA plates for both untreated (NT Thesis) and coated seeds with the barrier film (Thesis C), resulting in complete coverage by the fungal mycelium after 10 days of incubation. In samples containing prothioconazole, the fungicide showed good efficacy in reducing fungal colonization as evidenced by the formation of inhibition zones around the seeds. It is noteworthy that the fungicide embedded coatings (FC and CFC Thesis), are active as demonstrated by reduced mycelium growth, notwithstanding the presence of the barrier layer, confirming the results reported **in Chapter 2.**

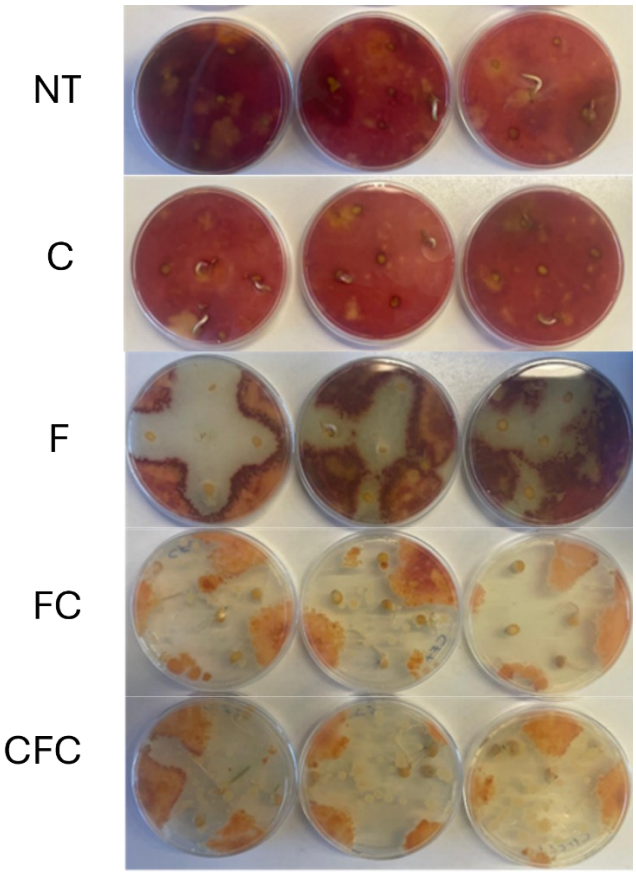

Figure 3 Maize seeds inoculated with *F. graminearum*, coated and not with a barrier film, treated and not with prothioconazole.

In **table 2** the percentage of the inhibition area is reported for each thesis, and as it can be observed it varies significantly among the different treatments. No inhibition zones have been measured for the untreated seeds and those coated only with the barrier film (Thesis C), confirming the complete colonization by *F. graminearum*. Seeds treated only with the fungicide (Thesis F) exhibited an antifungal effect, with an inhibition area of 51%. The highest values were recorded for the bilayer (Thesis FC) and sandwich (Thesis CFC) coatings, showing inhibition areas of 72.8% and 75.0%, respectively. The estimated values of inhibition area percentage indicates that the combination of the fungicide with the coating layers enhanced the protective efficacy against fungal growth. This results confirms the outcomes reported in **Chapter 2**.

Regarding germination, the percentage of germinated seeds ranged between 80% and 100% in all theses. Untreated seeds (Thesis NT) showed the highest germination rate (100%), whereas the coated seeds exhibited a slight reduction in germination efficiency. In particular, seeds coated only with the barrier film (Thesis C) or with combined coatings (Thesis FC and CFC) showed germination values between 80% and 93%, suggesting that exposure to the plasma treatment and the presence of coating layers may slightly interfere with the natural germination process of the seedlings.

Table 2 Percentage of seed germination and fungal contamination on maize seeds.

Sample	Inhibition area (%)	Germination (%)
NT	No Inhibition	100^{d}
C	No Inhibition	$80^{a}\pm5$
F	51 ± 6^{a}	$93^{c}\pm5$
FC	73 ± 3^{b}	$87^{b}\pm6$
CFC	75 ± 5^{c}	$93^{c}\pm7$

a–d Values in the same column with different apex letters are significantly different ($p < 0.05$).

Discussion

Antifungal tests demonstrated that the presence of the fungicide, either alone or incorporated into the coating layers, effectively inhibited the growth of *F. graminearum* on PDA plates. The observation of clear inhibition zones around the treated seeds indicates that the fungicide remained active following plasma coating deposition and was also able to diffuse into the medium, resulting in a reduction of fungal growth. These results confirm

the compatibility between the plasma-deposited barrier films and the efficacy of fungicide, which was preserved after the encapsulation process.

The greater inhibition observed in the bilayer (FC) and trilayer (CFC) coatings compared with the treatment with fungicide alone (F) suggests that the multilayer structure not only protects the active compound but may also promote a controlled release of fungicide from the coating matrix. This delayed and prolonged release could explain the larger inhibition areas observed, as it ensures longer persistence of the fungicidal activity on the seed surface. A similar behaviour has been reported for other plasma-deposited seed coatings containing fungicides. [1-2] On the other hand, the absence of inhibition zones in the treatment with the barrier film alone (C) confirms that the barrier layer itself does not exert antifungal effects. This supports the hypothesis that the reduction in fungal colonization is solely due to the presence of the fungicide and not to any intrinsic antimicrobial property of the coating.

With regard to germination, the slight reduction in germination percentage observed for the coated seeds suggests that plasma exposure and the presence of coating layers may slightly alter the surface properties of the seeds, possibly affecting water uptake or gas exchange. However, since the reduction remained limited (80–93%) and overall germination values were still high, it can be concluded that the plasma deposition and coating processes did not significantly affect seed viability. These results are consistent with previous studies demonstrating that the use of cold atmospheric pressure plasmas in air on maize seeds allows complete devitalization of the native surface microbiota without altering the vital processes of the seed. [3]

Overall, the combination of plasma-deposited barrier films and fungicide proved to be an effective strategy for inhibiting *F. graminearum* growth while maintaining acceptable germination performance. This suggests that the proposed coating technology could represent a promising approach for seed protection, allowing the use of lower amounts of fungicides and providing a more targeted antifungal action directly at the surface of the seeds.

The aim of this study, the first of its kind to our knowledge, was to test whether a coating deposited by atmospheric pressure plasma, capable of encapsulating a fungicidal molecule, could be effectively applied to the surface of seeds using plasma technology

to control fungal infections. The positive results obtained confirmed the potential of this approach and are highly promising, as further technological improvements can certainly be expected for future practical applications.

The data showed that the presence of the plasma-deposited coating did not alter the antifungal activity of prothioconazole. Moreover, seeds containing the fungicide and coated with the barrier film exhibited antifungal activity, as evidenced by the presence of inhibition zones and a higher resistance to *Fusarium graminearum* infections, most likely due to a controlled-release effect enabled by the barrier properties of the film. In addition, the coating did not significantly affect the germination capacity of the seeds.

Overall, this study once again highlights the potential of plasma technology in agriculture, particularly for the control of fungal infections on seeds, offering an innovative and sustainable approach to seed protection.

A 2.1.3 References

[1] C. Lo Porto, et al. Plasma-assisted deposition of fungicide-containing coatings for encapsulation and protection of maize seeds. *Plasma Processes and Polymers*, 2019, 16(6), 1900022.

[2] M. Masiello, et al.Plasma technology increases the efficacy of prothioconazole against *Fusarium graminearum* and *Fusarium proliferatum* contamination of maize (Zea mays) seedlings. *International Journal of Molecular Sciences*, 2021, 22(17), 9301.

[3] A. Zahoranova, et al. Effect of cold atmospheric pressure plasma on maize seeds: Enhancement of seedling growth and surface microorganism inactivation. *Plasma Chemistry and Plasma Processing*, 2018, 38, 969–988.

3

Plasma Deposition of Coatings for Delivery of Essential Oils Active Against Nematodes

3.1 Introduction

Intensive agriculture has led to the over-exploitation of natural resources and the disruption of soil system functionality, primarily due to the excessive use of synthetic products aimed at increasing crop yields. Among the most destructive crop pests are plant-parasitic nematodes (PPNs), which are responsible for approximately 12–15% of global agricultural losses annually. [1] PPNs can also cause additional damage through synergistic interactions with major soilborne pathogens such as *Fusarium spp*., *Verticillium spp*., viruses, and bacteria that penetrate through root lesions induced by nematode infection.[2]

Among PPNs, root-knot nematodes (RKNs) are considered the most destructive group, as they infect the roots of almost all cultivated plant species. Within this group, species belonging to the genus *Meloidogyne* are regarded as the most harmful pests of horticultural crops, causing severe yield reductions. In particular, *Meloidogyne incognita* can lead to yield losses of up to 73.3% in tomato production, representing a major threat to global food security. Its life cycle begins with eggs laid by adult females on the root surface. The first-stage larva (J1) develops within the egg and molts into the second-stage juvenile (J2). When juveniles hatch from the eggs and penetrate root tissues, they establish permanent feeding sites by inducing the formation of multinucleate giant cells. This process alters the roots, causing the characteristic formation of galls and reducing the plant's ability to absorb water and nutrients. [3-6]

Given these challenges, there is an urgent need to replace synthetic pesticides with more sustainable and environmentally friendly alternatives. One promising approach involves the use of biocidal compounds of plant origin such us essential oils (EOs) that show strong nematicidal and antimicrobial activity against both PPNs and soilborne phytopathogens. EOs are bioactive, biodegradable and environmentally safe. However, their practical application is often limited by the high volatility of their active constituents, which leads to evaporation and rapid degradation, thereby reducing their persistence and efficacy. Consequently, the development of new formulations capable of stabilizing and prolonging the biocidal activity of EOs is important. [7-8]

Among the bioactive compounds present in plant-derived essential oils, cinnamaldehyde, the major constituent of *Cinnamomum zeylanicum* EO, is known to have a central role in nematode suppression. It was demonstrated that pure (*E*)-cinnamaldehyde caused over 68% mortality of *M. incognita* J2, whereas the whole *C. zeylanicum* EO induced only 12–13% mortality under the same concentrations, confirming the cinnamaldehyde as the main nematotoxic agent of cinnamon oil. [9] Morover, Fanelli et al. reported that *C. zeylanicum* EO induced nematode mortality through the disruption of the nervous system and cuticle integrity, and by altering the expression of genes related to stress response and motility.[10]

Nematicidal activity has been investigated for the essential oils of *Allium sativum* and *Ruta graveolens*. The EO of A. *sativum* and its sulfur-containing compounds shown strong nematicidal effects against *M. incognita* by interfering with enzymatic systems and oxidative metabolism. [11] Likewise, the EO of *R. graveolens*, rich in alkaloids and furanocoumarins such as chalepensin and graveolin, has been documented to inhibit egg hatching and J2 motility through neurotoxic and cuticle-disrupting mechanisms. [12]

These findings highlight the potential of EOs and their key constituents as natural sources of bioactive compounds for sustainable nematode management strategies.

In this context, LTP processes have attracted increasing interest due to their minimal thermal impact, allowing surface modification of thermally sensitive materials without altering their bulk properties. LP and AP plasma deposition techniques are considered environmentally friendly, as they use minimal reactants and no solvents. [13-16] Recent studies have demonstrated the effectiveness of plasma-based methods for depositing

nanocomposite coatings containing fungicides on seeds, providing protection against *Fusarium* infections, as shown in the previous chapter. [17-18]

Therefore, exploring plasma-assisted deposition methods for the development of active coatings against soilborne pathogens and pests represents a particularly promising alternative to traditional agriculture practices.

The aim of this study was to encapsulate *Allium sativum, Cinnamomum zeylanicum* and *Ruta graveolens* EOs into composite films plasma deposited on zeolites, a widely used inert material in agriculture, by means of the Aerosol-Assisted Atmospheric Pressure Plasma Deposition (AA-APPD) technique, in order to evaluate their nematicidal activity against *M. incognita* through in vivo studies.

3.2 Materials and Methods

3.2.1 Materials

He 99.999%, C_2H_4 99.95% (Air Liquide) and an aerosol of Milli-Q quality water (Millipore, Bedford, MA) were used as feed in the plasma deposition process. The coatings were deposited on 1 × 1 cm^2 shards of double face polished p-doped crystalline silicon (100) wafers (MicroChemicals GmbH, Ulm, Germany) for comprehensive chemical characterization. On the other hand, biological assessments were conducted using zeolites (Molecular Sieve 0.4 nm, Beads 1.6–2.5 mm) purchased from Sigma-Aldrich. The essential oils used to load the zeolites were: *Allium sativum* (AS, garlic essential oil, Aroma-Zone, France), *Cinnamomum zeylanicum* (CZ, cinnamon bark essential oil, Flora srl, Italy), and *Ruta graveolens* (RG, rue essential oil, Mystic Moments, United Kingdom). The extraction solvent used to recover CZ from the zeolites was cyclopentyl methyl ether (CPME, VWR Chemicals, purity ≥ 99.9%). Absolute ethanol (Honeywell, ACS reagent, ≥ 99.8%) was used to inject the extracts into the GC–MS; *Trans*-cinnamaldehyde (≥ 99%, Sigma-Aldrich) was used as the standard for the calibration curve.

3.2.2 Preparation of EOs-Containing Coatings onto zeolite

EOs were cast onto zeolite before the plasma deposition process. Zeolite (80 g) was placed in a 150 mm diameter Petri dish and kept under agitation on a rocking shaker. Subsequently, 20 mL of ethanol containing 1 g of the respective EOs (*A. sativum, C. zeylanicum, and R. graveolens*) were slowly dropped onto the zeolite under continuous agitation and left for 2 h until complete solvent evaporation.

The amount of each EO used to load the zeolite was selected based on experimental tests, which demonstrated that the effective dose required to achieve nematocidal activity of these EOs was 200 mg per kg of soil. The EO-loaded zeolites were then coated with barrier films using the large-scale DBD reactor described in **Chapter 1**, **Appendix A 2.1**. Briefly, the film deposition process on the zeolite granules was carried out in a DBD discharge fed with 60 sccm ethylene as matrix precursor and an aerosol of water generated with 3.5 slm He, and an additional 3 slm He buffer. The discharge durations used to produce coatings with thicknesses of 100 and 200 nm were 10 and 20 min, respectively. The applied peak-to-peak voltage was maintained at 13 kV_{pp} with a frequency at 20 kHz. The distance between the plasma source and the zeolite was maintained at 2 mm. The EO loaded zeolites in the amount of 80 g were laid onto a tray and placed onto the movable ground stage integrated into the reactor, which was moved back and forth during the process. Before starting the process, the system was purged with 5 slm He for 5 min, and the same procedure was repeated before removing the zeolites from the chamber.

3.2.3 Chemical Characterization of Coatings Deposited onto Si Substrates

For all the analyses Si substrates were placed on top of the zeolite during the plasma deposition process to obtain the same coating conditions. The composition of the coatings was analyzed by means of Fourier Transform Infrared Spectroscopy (FT-IR, transmission mode) with a Vertex 70 V Bruker spectrometer (32 scans, 4 cm^{-1} resolution). The spectrometer was evacuated to less than 150 Pa for 5 min to avoid spectral interferences of atmospheric H_2O vapor and CO_2.

Static Water Contact Angle (WCA) measurements were carried out with a Ramé-Hart 100-manual goniometer (distilled water, 4 µL drops, room temperature). WCAs were measured on three different points of three replicates.

The thickness of the coatings was measured on three different points of three replicates with a KLA-Tencor instrument (Milpitas, CA, USA) D-120 profilometer after scratching part of the coating with a scalpel to form a step.

To prepare the composite layers containing the different EOs, 100 and 200 nm thick coatings were plasma-deposited on the surface of the zeolites loaded with the three different essential oils.

The EO-containing samples are referred to in this chapter using the following code:

EO_ZEO_Th

where: *EO* = essential oil (AS, CZ, RG); *ZEO* = indicates that the essential oil is loaded onto the zeolite; and *Th* = coating thickness, ranging from 0 to 200 nm (*Th* = 0 corresponds to the absence of a plasma-deposited film).

GC-MS characterization of Cinnamomum zeylanicum EO embedded onto Zeolite

The extraction of *C. zeylanicum* essential oil and the quantification of its main constituent, *trans*-cinnamaldehyde, were carried out with the following samples: CZ, 20 g of zeolite loaded with 260 mg of EO; CZ-100, 20 g of zeolite loaded with 260 mg of EO and coated with a 100 nm barrier film; CZ-200, 20 g of zeolite loaded with 260 mg of EO and coated with a 200 nm barrier film. The EO was extracted from the zeolite with 20 mL of CPME in a thermostatic ultrasonic bath at 20 °C for 30 min. Subsequently, the zeolite was separated from the extraction solvent using a separatory funnel equipped with a filter. The solvent was removed by evaporation under reduced pressure up to 200 mBar, the EO was then recovered with ethanol, and the *trans*-cinnamaldehyde quantified by gas chromatography (GC–MS) with a Shimadzu GCMS-QP2010 SE instrument equipped with a BP-5MS capillary column (SGE, length 30 m, internal diameter 0.25 mm, stationary phase thickness 0.25 µm). Identification of *trans*-cinnamaldehyde in the samples was performed by GC- MS analysis under the following conditions: injector and column

temperatures 250 °C and 100 °C, respectively (GC), split injection mode, ion source and interface temperatures 200 °C and 230 °C, respectively (MS). He was used as the carrier gas at an initial pressure of 62.7 kPa (total flow: 54 mL/min; column flow: 0.89 mL/min). A four-point calibration curve was constructed for the quantification of trans-cinnamaldehyde content. Each calibration point was injected in triplicate, as was each extract.

3.2.4 Assessment of nematicidal activity

These nematicidal experiments were carried out in collaboration with Dr. Pasqua Veronico and Dr. Trifone D'Addabbo (IPSP-CNR). An Italian population of *M. incognita* was previously reared for two months on the tomato cultivar Regina di Fasano in a greenhouse at 25 ± 2 °C. The infested tomato roots were finely chopped and thoroughly mixed before taking four random 10 g samples, on which the density of *M. incognita* eggs and second-stage juveniles (J2s) per gram of root was determined. Nematode eggs and J2s were extracted by shaking the root samples for 3 min in a 1% aqueous sodium hypochlorite solution. Extracted eggs and J2s were recovered on a 20 µm sieve and counted under a microscope. Appropriate amounts of this inoculum were added to the non-sterilized experimental soil to reach an initial nematode population density of approximately 16 eggs and J2s per mL of soil. The homogeneous distribution of the inoculum in the soil was ensured by mixing for 10 min in a concrete mixer.

The soil was then amended with zeolites loaded with essential oils (EOs) of *A. sativum, C. zeylanicum, and R. graveolens*, both uncoated and coated with a barrier film of 100 nm or 200 nm, and distributed into 1 L pots (14 cm diameter), which were maintained for two weeks in a greenhouse at 26 °C.Five replicates were prepared for each condition. The controls consisted of untreated soil, free EOs and soil treated with a commercial formulation of the nematicide Fluopyram (Velum Prime®, Bayer Crop Science, Milan, Italy). The synthetic nematicide was applied at a dose of 0.625 L ha^{-1}.

Subsequently, one-month-old tomato seedlings (cv. Regina di Fasano) were transplanted into treated and untreated soils and allowed to grow for 50 days. The pots were arranged

on greenhouse benches in a randomized block design, maintaining a constant temperature of 26 °C.

Root gall formation caused by *M. incognita* infestation was evaluated on each root system using a 0–5 scale, where: 0 = no galls; 1–2 = galls only on secondary roots; 3 = galls on main lateral roots; 4 = 50% of roots galled; and 5 = maximum possible nematode infestation. Nematode multiplication on tomato roots was determined by extracting and microscopically counting the eggs and J2s present in the roots and in the soil of each replicate.

At the end of the experiment, the tomato plants were uprooted, and the fresh weight of shoots and roots of each plant was recorded. Leaf chlorophyll content was also measured using a SPAD meter (Konica Minolta, Japan,). The SPAD (Soil Plant Analysis Development) value is a dimensionless index based on light transmittance at 650 and 940 nm and provides a relative estimate of leaf chlorophyll concentration, which is closely related to the nitrogen status and photosynthetic activity of the plant. Measurements were taken from the middle portion of healthy leaves from two different branches (SPAD1 and SPAD2) located in the upper part of each plant.

3.3 Results and Discussion

3.3.1 Optimization of coatings on silicon substrates

The deposition rate of 10 ± 3 nm/min was measured on Si substrates for the coating used to embed the EOs under the experimental conditions employed; processes lasting 10 and 20 min produced coatings of 100±7 nm and 200±15 nm, deposited on zeolites to entrap the EOs. Transmission FT-IR analysis allowed the identification of the main functional groups present along the thickness of the plasma-deposited layer. For reference, the FT-IR spectrum of the C_2H_4 monomer is reported in Figure 2A of **Chapter 2** (Section *2.3.1 Chemical Characterization of the Plasma-Deposited Coating*). **Figure 1** reports the FT-IR absorption spectrum of films deposited on silicon for 10 min. The spectrum shows the typical bands of hydrocarbon organic films characterized by oxygen-containing polar moieties, as also observed for the coating described in Figure 2B of **Chapter 2** (Section 2.3.1).

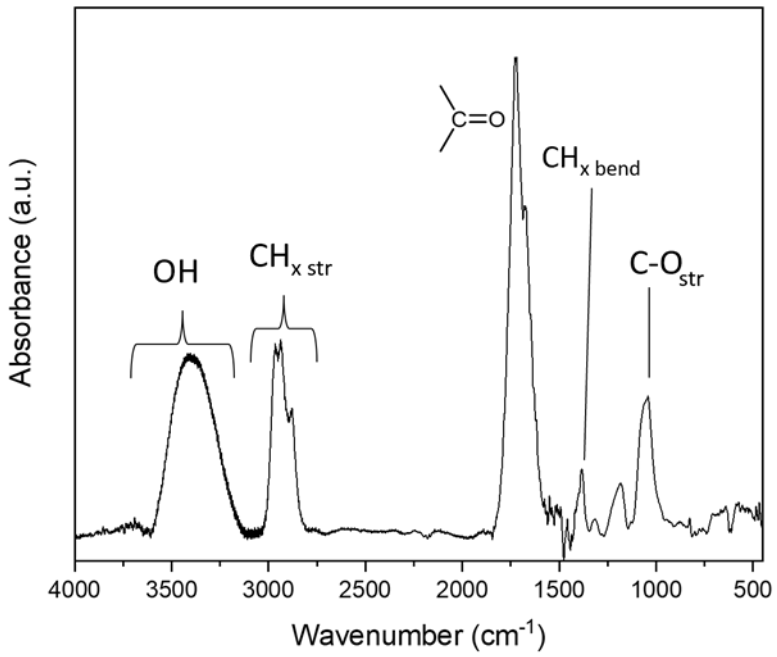

Figure 1 FT-IR transmission spectrum of the plasma-deposited coating utilized for embedding EOs onto zeolite (10 min discharge duration).

The WCA measurements performed on the plasma-deposited coatings revealed quite hydrophilic character, with a WCA value of about 54 ± 3°. This level of hydrophilicity is compatible with the hydrocarbon network grafted with polar O-containing groups, as revealed by FT-IR analysis. No further analyses were carried out, as the chemical composition was found to be very similar to that of the coating deposited on *Bacillus* spores and fungicides described in **Chapter 2**.

3.3.2 Chemical Characterization of Cinnamomum zeylanicum EO Entrapped onto Zeolite by GC–MS

Cinnamaldehyde, quantified as the main constituent (93%$_{w/w}$) of *C. zeylanicum* essential oil and responsible for its nematicidal activity, was analyzed in the different zeolite samples loaded with EO and coated with barrier films of different thickness. As reported in **Table 1**, cinnamaldehyde was recovered in similar amounts from all the analyzed

samples, indicating that no substantial loss of the compound occurs during the preparation steps on zeolite (CZ) or in the presence of coatings of 100 (CZ-100) and 200 nm (CZ-200).

Although slight variations among the samples are observed, most of the cinnamaldehyde content is retained by the zeolite. In particular, the samples with barrier coatings show a comparable or slightly higher retention capacity, suggesting that the coating may help stabilize the active compound without reducing its availability.

Table 1 Amount of cinnamaldehyde contained in the zeolite loaded with EO and coated with barrier films of different thicknesses.

Sample	*trans*-cinnamaldehyde (mg)
CZ-ZEO	239.6 ± 6
CZ-ZEO-100	207.2 ± 5
CZ-ZEO-200	240.0 ± 7

Values are reported as mean ± standard deviation (n=3).

3.3.3 Nematicidal activity of Coatings Containing EOs

All soil treatments with the three essential oils, either applied in their free form or carried by zeolites, significantly reduced the multiplication of *Meloidogyne incognita,* measured as the number of eggs per gram of root and per milliliter of soil, as well as the formation of galls on tomato roots, as reported in **Table 2**.

Among the treatments, the EO-loaded zeolites coated with plasma-deposited barrier films showed the highest nematicidal efficacy. Samples coated with the thinner 100 nm film (AS-ZEO-100, CZ-ZEO-100, and RG-ZEO-100) were already more effective in reducing nematode reproduction compared with both the free essential oils and the uncoated EO-loaded zeolites. When the coating thickness increased to 200 nm (AS-ZEO-200, CZ-ZEO-200, and RG-ZEO-200), the inhibitory effect became even more pronounced.

Specifically samples with the 100 nm coatings reduced the number of eggs per gram of root by 54%, 47%, and 59% for garlic, cinnamon and rue essential oils, respectively, whereas the 200 nm coatings achieved reductions of 77%, 72%, and 69%, respectively,

as reported in **Table 3**. In comparison, treatments with the free essential oils resulted in lower reductions (51%, 22%, and 51%).

A similar trend was observed for the number of eggs and J2 per milliliter of soil. Samples with the 100 nm coatings induced reductions of about 44%, while the 200 nm coatings resulted in greater decreases of 64%, 60%, and 52% for garlic, cinnamon, and rue, respectively. These reductions were consistently higher than those obtained with the free essential oils (44%, 20%, and 48%).

Overall, the results clearly demonstrate that increasing of the thickness coating enhances the nematicidal efficacy of the EO-loaded zeolites, likely by limiting EO volatilization and prolonging its activity in soil. Nevertheless, the nematicidal effect of all EO-based treatments remained significantly lower than that achieved with the synthetic nematicide Fluopyram, which almost completely suppressed nematode multiplication.

Table 2 Effect of soil treatments with the zeolite-carried EOs of *A. sativum, C. zeylanicum, and R. graveolens* on the infestation of *M. incognita* on tomato.

Treatment	Nematode population		Root gall index
	Eggs/g roots	EGGs and J2/mL soil	
AS-ZEO-100	23159 ± 3429^{cd}	8.8 ± 0.8^{cde}	2.8 ± 0.4^{c}
AS-ZEO-200	11605 ± 1255^{f}	4.6 ± 1.3^{f}	1.8 ± 0.4^{f}
AS-ZEO	20079 ± 4511de	7.8 ± 2.0^{de}	2.2 ± 0.4^{def}
AS	24906 ± 1960^{cd}	9.4 ± 1.5^{cd}	2.8 ± 0.4^{c}
CZ-ZEO-100	26583 ± 3901^{c}	10.0 ± 1.2^{c}	2.8 ± 0.4^{c}
CZ-ZEO-200	13805 ± 1154^{f}	5.0 ± 1.0^{f}	2.0 ± 0.0^{ef}
CZ-ZEO	24466 ± 2529^{cd}	9.2 ± 0.8^{cde}	2.6 ± 0.5^{cd}
CZ	38855 ± 1624^{b}	14.6 ± 0.9^{b}	4.0 ± 0.0^{b}
RG-ZEO-100	20531 ± 2568^{d}	7.6 ± 1.5^{e}	2.8 ± 0.4^{c}
RG-ZEO-200	15408 ± 2764^{ef}	5.8 ± 1.5^{f}	2.4 ± 0.5^{cde}
RG-ZEO	15213 ± 2374^{f}	5.6 ± 1.1^{f}	2.0 ± 0.0^{ed}
RG	24545 ± 2015^{cd}	9.2 ± 1.9^{cde}	2.6 ± 0.5^{cd}
Fluopyram	491 ± 135^{g}	0.8 ± 0.4^{g}	1.0 ± 0.0^{g}
Non-treated	50003 ± 10820^{a}	18.8 ± 1.5^{a}	5.0 ± 0.0^{a}
Non-infested	-	-	-

a-g Values in the same column with different apex letters are significantly different ($p < 0.05$).

Table 3 Percentage reduction of *M. incognita* multiplication after the different soil treatments.

Treatment	Eggs/g roots			Eggs and J2/ml soil		
	garlic	cinnamon	rue	garlic	cinnamon	rue
EO liquid	-51%	-22%	-51%	-44%	-20%	-48%
EO loaded zeolite	-60%	-51%	-70%	-56%	-48%	-60%
EO loaded zeolite + 100 nm	-54%	-47%	-59%	-44%	-44%	-44%
EO loaded zeolite + 200 nm	-77%	-72%	-69%	-64%	-60%	-52%
Fluopyram	-99%			-80%		
Non-treated	-			-		

The results of tests relative to the health status of the tomato plants investigated in this trial are reported in **Table 4**. As it can be observed, overall the health status of the plants was not negatively affected by the different soil treatments. However, the growth parameters were differently influenced depending on the essential oil and coatings applied.

Plants treated with *A. sativum* EO-loaded zeolites, either uncoated or coated with the thicker 200 nm film (AS-ZEO and AS-ZEO-200), as well as those treated with *C. zeylanicum* EO-loaded zeolites coated with the 200 nm film (CZ-ZEO-200), showed significantly greater height and aerial biomass compared with the non-treated control.

Conversely, plants grown in soils treated with free *C. zeylanicum* and *R. graveolens*, or with uncoated cinnamon EO-loaded zeolites (CZ-ZEO), show a significant reduction in both plant height and aerial biomass, suggesting a possible phytotoxic effect related to the higher volatility or concentration of the unprotected oils. SPAD1 and SPAD2 values did not differ significantly among treatments and were comparable to non-treated and non-infested controls, indicating that none of the treatments adversely affected the chlorophyll content or photosynthetic performance of tomato leaves. In contrast, all soil treatments with the three essential oils, as well as the chemical nematocide Fluopyram, led to a marked reduction in root biomass compared with plants grown in non-treated

soils, either infested or non-infested by *M. incognita*. However, among EO-based treatments, AS-ZEO-200 and CZ-ZEO-200 maintained relatively higher root weights, suggesting that the thicker coating layer may mitigate the negative impact of EO release on root development and plant vigor.

Table 4 Effect of soil treatments with the zeolite-carried EOs *A. sativum, C. zeylanicum, and R. graveolens* on the growth of tomato plants.

Treatment	Plant height (cm)	Plant weight (g)		SPAD values	
		Aerial part	Roots	SPAD1	SPAD2
AS-ZEO-100	27.2 ±1.9^{cde}	35.6 ±3.4^{fg}	16.2 ±1.6^{efg}	38.4 ±5.2^{bcd}	41.0±4.2^{cde}
AS-ZEO-200	27.6 ±1.9^{de}	38.4 ±3.6^{gh}	17.8 ±2.5^{gh}	36.4 ±6.8^{abcd}	38.4±3.9^{abcd}
AS-ZEO	33.6 ±3.6^{gh}	47.4 ±3.2^{j}	13.6 ±1.3^{bcd}	45.6 ±1.8^{e}	43.2 ±4.4^{de}
AS	27.6 ±2.3^{de}	31.4 ±1.8^{de}	19.0 ±1.6^{h}	38.6 ±2.9^{bcd}	38.4 ±4.3^{abcd}
CZ-ZEO-100	25.8 ±2.8^{bcd}	31.8 ±4.1^{de}	12.2 ±1.6^{ab}	32.4 ±4.4^{ab}	33.8 ±5.1^{ab}
CZ-ZEO-200	26.6 ±2.1^{cd}	37.6 ±1.8^{gh}	17.2 ±0.8^{fgh}	37.8 ±7.9^{abcd}	37.8 ±8.7^{abcd}
CZ-ZEO	23.4 ±2.1^{b}	22.6 ±1.3^{b}	10.6 ±1.7^{a}	31.8 ±5.1^{a}	32.8 ±4.9^{a}
CZ	24.2 ±2.5^{bc}	27.0 ±1.6^{c}	17.4 ±0.9^{gh}	40.8 ±4.1^{de}	38.8 ±2.6^{bcd}
RG-ZEO-100	25.8 ±3.2^{bcd}	32.2 ±1.6^{de}	13.8 ±1.8^{bcd}	33.6 ±3.4^{abc}	35.4 ±0.5^{abc}
RG-ZEO-200	27.6 ±2.3^{de}	33.4 ±1.1^{ef}	14.8 ±1.5^{cde}	36.8 ±3.6^{abcd}	37.8 ±3.3^{abcd}
RG-ZEO	32.2 ±2.2^{fg}	36.0 ±1.9^{fg}	15.2 ±2.2^{def}	36.8 ±5.4^{abcd}	36.2 ±2.6^{abc}
RG	19.4 ±2.1^{a}	16.0 ±1.7^{a}	13.0 ±1.4^{bc}	33.6 ±8.3^{abc}	32.8 ±6.9^{a}
Fluopyram	39.8 ±3.1^{i}	30.4 ±1.7^{d}	12.6 ±1.1^{ab}	38.2 ±3.5^{bcd}	40.4 ±3.2^{cd}
Non-treated	29.8 ±1.5^{ef}	33.4 ±1.8^{ef}	24.2 ±1.3^{i}	39.2 ±3.8^{cd}	38.6 ±4.6^{abcd}
Non-infested	28.0 ±2.0^{de}	40.2 ±1.8^{hi}	28.2 ±1.5^{j}	47.0 ±2.8^{e}	46.4 ±4.0^{e}

a-i Values in the same column with different apex letters are significantly different ($p < 0.05$).

Discussion

The ZEO-samples loaded with three EOs coated with barrier films of different thicknesses were all effective in reducing *M. incognita* infestation on tomato plants. The degree of nematocidal efficacy was strongly influenced by the presence and the thickness of the

plasma-deposited barrier coating applied to the zeolite carriers loaded with essential oils.

Among the treatments tested, the results reported in **Tables 2** and **3** indicate that zeolites loaded with cinnamon and garlic oils and coated with a thicker plasma layer exhibit consistently higher nematicidal activity. This enhanced efficacy may be attributed to the thicker coating, which likely plays a role in controlling the release of the active compounds into the soil. In contrast, treatments based on rue oil yielded less consistent results, and in this case the effect of the plasma coating does not appear to be significant.

The beneficial effect of the plasma-deposited coating was also evident in plant growth performance (**Table 4**). The coated zeolites loaded with EOs led to significantly greater plant height and shoot biomass compared with the EO-loaded but uncoated zeolites, suggesting that the indirect exposure of plants to the essential oils improved vegetative vigor while maintaining effective nematode control. Conversely, plants directly exposed to free cinnamon EO or to CZ-ZEO showed reduced height and aerial biomass, likely due to localized phytotoxic effects caused by excessive exposure. The systems coated with the 200 nm film, however, appeared to mitigate these effects, as indicated by the better vegetative growth and higher root biomass observed for the AS-ZEO-200 and CZ-ZEO-200 samples. SPAD1 and SPAD2 values did not show significant differences among treatments and were comparable to those of the non-treated and non-infested controls. This indicates that the chlorophyll content and photosynthetic efficiency of tomato plants were not negatively affected by any of the treatments, confirming that they did not cause harmful effects on the general physiological status of the plants.

Although the efficacy of the EO-based treatments was lower than that of the synthetic nematicide Fluopyram, their lower toxicity and well known nematicidal activity make these coated zeolite systems a promising and environment safer alternative for the sustainable management of root-knot nematodes in tomato cultivations.

3.4 Conclusions

The results of this study demonstrate that barrier coatings plasma-deposited on EOs-loaded zeolite supports offer an effective strategy to enhance the nematocidal performance of EOs the potential phytotoxic effects of *M. incognita*. The coating acts as a barrier improving the stability of the volatile compounds and allowing their gradual diffusion into the soil, resulting in a prolonged nematode suppression compared with uncoated EOs-loaded zeolite or pure mixed with the soil

In addition to their nematocidal efficacy, the coated formulations contributed to maintaining or even improving plant growth and vigor, confirming that controlled release of EOs is compatible with plant health. The absence of significant differences in SPAD values across treatments further indicated that the photosynthetic efficiency and chlorophyll content of tomato plants were not adversely affected.

Although the performance of these natural formulations did not reach that of the synthetic nematicide Fluopyram, the combination of moderate efficacy, low toxicity, and environmental safety highlights their potential as a sustainable and eco-friendly alternative for root-knot nematode management in tomato cultivation.

3.5 References

[1] J. M. Nicol, S. J. Turner, D. L. Coyne, L. Nijs, S. Hockland, Z. T. Maafi. Current nematode threats to world agriculture. In: *Genomics and Molecular Genetics of Plant-Nematode Interactions*. Springer, Dordrecht, 2011, pp. 21–43.

[2] A. Pulavarty, T. S. Rani, S. Anwar. Plant-parasitic nematodes: Agricultural importance, biocontrol strategies and research developments. *Plants*, 2021, 10(11), 2352.

[3] P. Abad, J. Gouzy, J.-M. Aury, et al. Genome sequence of the metazoan plant-parasitic nematode *Meloidogyne incognita*. *Nature Biotechnology*, 2008, 26, 909–915.

[4] S. Lazarova, D. Coyne, M. G. Rodríguez, B. Peteira, A. Ciancio. Functional diversity of soil nematodes in relation to the impact of agriculture—A review. *Diversity*, 2021, 13, 64.

[5] D. A. Neher. Role of nematodes in soil health and their use as indicators. *Journal of Nematology*, 2001, 33(4), 161–168.

[6] H. Ferris, T. Bongers, R. G. M. de Goede. A framework for soil food web diagnostics: Extension of the nematode faunal analysis concept. *Applied Soil Ecology*, 2001, 18(1), 13–29.

[7] P. Farina, F. Venturi, R. Ascrizzi, G. Flamini, O. Chiriboga, M. C. Rodrigo Echeverría, S. Ortega, A. Zinnai, S. Bedini, B. Conti. Andean plants essential oils: A scented alternative to synthetic insecticides for the control of blowflies. *Insects*, 2021, 12, 894.

[8] S. Bedini, F. Cosci, C. Tani, E. C. Pierattini, F. Venturi, A. Lucchi, C. Ioriatti, R. Ascrizzi, G. Flamini, G. Ferroni, I. Taglieri, B. Conti. Essential oils as post-harvest crop protectants against the fruit fly *Drosophila suzukii*: Bioactivity and organoleptic profile. *Insects*, 2020, 11, 1–17.

[9] T. D'Addabbo, S. Laquale, P. Veronico, et al. Nematicidal activity of the essential oil from *Cinnamomum cassia* and (E)-cinnamaldehyde against phytoparasitic nematodes. *Journal of Pest Science*, 2025, 98, 521–533.

[10] E. Fanelli, A. Vovlas, T. D'Addabbo, et al. Molecular mechanism of *Cinnamomum zeylanicum* and *Citrus aurantium* essential oils against the root-knot nematode *Meloidogyne incognita*. *Scientific Reports*, 2025, 15, 6077.

[11] L. Catani, B. Manachini, E. Grassi, L. Guidi, F. Semprucci. Essential oils as nematicides in plant protection—A review. *Plants*, 2023, 12, 1418.

[12] L. Nahar, H. R. El-Seedi, S. A. M. Khalifa, M. Mohammadhosseini, S. D. Sarker. *Ruta* essential oils: Composition and bioactivities. *Molecules*, 2021, 26, 4766.

[13] I. Trizio, et al. Plasma processes for life sciences. In: *Reference Module in Chemistry, Molecular Sciences and Chemical Engineering*. Elsevier, 2018.

[14] K.-D. Weltmann, J. F. Kolb, M. Holub, D. Uhrlandt, M. Simek, K. Ostrikov, S. Hamaguchi, U. Cvelbar, M. Cernak, B. Locke, A. Fridman, P. Favia, K. Becker. The future

in plasma science and technology. *Plasma Processes and Polymers*, 2019, 16, e1800118.

[15] N. Puac, M. Gherardi, M. Shiratani. Plasma agriculture: A rapidly emerging field. *Plasma Processes and Polymers*, 2018, 15, 1700174.

[16] D. B. Graves. The emerging role of RONS in redox biology and implications for plasma applications to medicine and biology. *Journal of Physics D: Applied Physics*, 2012, 45, 263001.

[17] C. Lo Porto, F. Palumbo, S. Somma, M. Masiello, A. Moretti, F. Fracassi, P. Favia. Plasma-assisted deposition of fungicide-containing coatings for encapsulation and protection of maize seeds. *Plasma Processes and Polymers*, 2019, 16(6), 1900022.

[18] M. Masiello, S. Somma, C. Lo Porto, M. Haidukowski, B. Ciasca, E. Sardella, P. Favia, F. Palumbo, A. Moretti. Plasma technology increases the efficacy of prothioconazole against *Fusarium graminearum* and *Fusarium proliferatum* contamination of maize seedlings. *International Journal of Molecular Sciences*, 2021, 22(17), 9301.

4

Plasma Jet Deposition of Antimicrobic Zinc-Based Nanocomposite Thin Films

4.1 Introduction

A substantial portion of global agricultural production is destined to meet the food demand resulting from current population growth. Crops with high nutritional and productive value, such as potatoes (Solanum tuberosum L.), play a strategic role because they are characterized by a high carbohydrate content, considerable versatility, and relatively affordable cost. The quality, yield, and shelf life of potato tubers can be significantly reduced by pectinolytic bacteria belonging to the genus *Pectobacterium*. [1] *Pectobacterium carotovorum* subsp. *carotovora*, commonly known as *Erwinia carotovora*, is a gram-negative, facultative anaerobic bacterium. Its virulence is mainly attributable to enzymes that cause the maceration of plant tissues, leading to the onset of a disease known as potato soft rot. [2] Tuber rot can occur immediately in the soil, shortly after harvest, or during storage. In particular, in growing plants, the bacteria attack the base of the stems, which become black, slimy, and soft under moist conditions. [3] *Erwinia carotovora* is particularly known for its ability to survive in the soil in contaminated tubers, crop residues, and weed root systems. [4]

Among the major fungal phytopathogens affecting wheat are *Fusarium graminearum*, *Fusarium culmorum*, and *Fusarium moniliforme*, which cause Fusarium head blight (FHB) and foot rot diseases, leading to significant reductions in both yield and wheat quality. In recent years, the use of nanomaterials has gained increasing attention in agriculture for pathogen control. [5]

It is evident that the efficacy of disease control methodologies, which include practices such as crop rotation, soil sanitation, and the use of chemical substances, including copper-based compounds, often does not reach the expected levels. Moreover, these methodologies are not without their own well-documented deleterious effects on living organisms. [6] Such limitations have led to growing interest in mulching, one of the oldest agricultural practices, which today has assumed an innovative role in the agricultural sector thanks to the advent of nanotechnologies.

Mulching, defined as the application of a protective layer on the soil, is an agronomic method aimed at promoting crop growth. Plastic mulching represents the most widespread form of mulching worldwide among fruit and vegetable producers, primarily because of its ease of management and simple installation in the field. [7] The material employed is mainly polyethylene (PE), chosen for its advantageous economic characteristics, malleability, impermeability, chemical inertness, and ability to incorporate additives and/or pigments. [8] Recent studies have demonstrated that PE mulch films can be transformed into “active mulches” through surface modifications, enabling the controlled release of nutrients or agrochemicals. For example, films modified with mineral particles (such as talc, zeolite, calcium carbonate) can serve as carriers for micronutrient salts such as iron, copper, and manganese sulfates, which are gradually released under natural field evaporation–condensation cycles. This approach ensures a sustained supply of nutrients without altering the structural properties of polyethylene and represents a step toward more functional mulching systems.[9]

Modifying mulching materials with antimicrobic but environmentally friendly compounds, appears as an intriguing way to fight pathogens like *Erwinia carotovora* which can survive in soils.

Currently, the use of nanomaterials in agriculture is attracting increasing attention, particularly for the control of pathogens that threaten crops. Metallic nanomaterials (such as silver, zinc, and iron) and those based on metal oxides (such as titanium dioxide and iron oxides) have demonstrated significant antibacterial activity. [9] Among these, zinc oxide nanoparticles (ZnO NPs) stand out as a promising alternative due to their broad-spectrum antimicrobial effectiveness and favorable physicochemical properties, such as high thermal and chemical stability, UV protection, controlled release of Zn^{2+} ions, and

low toxicity.[10-11] These characteristics have led to their approval by the FDA for safe applications. [12] Other compounds widely used in agriculture for pathogen control are zinc salts. In particular, zinc acetate dihydrate (ZAD) is recognized as a reliable source of zinc. The EFSA has confirmed the safety of using this substance in materials and applications intended to come into contact with food. [13] However, both forms of zinc present certain limitations. ZnO NPs tend to aggregate and bioaccumulate; their antimicrobial efficacy strongly depends on particle size distribution, and their production costs are relatively high. Zinc salts, although more economical and readily available, release Zn^{2+} ions rapidly in solution, leading to higher toxicity. [14-16] For these reasons, the encapsulation of ZnO NPs and zinc salts, such as ZAD, in an organic matrix can represent a promising strategy capable of reducing toxicity, improving stability, and optimizing the controlled release of Zn^{2+} ions, making their use more efficient and sustainable.

In light of these challenges, among the various polymers used to produce material coatings, polyethylene glycol (PEG) has attracted particular attention as an ideal candidate for the incorporation of antimicrobial agents, thanks to its non-toxicity and biodegradability, which have enabled its use in the pharmaceutical, biomedical, and food packaging sectors, as well as its approval by the FDA. [17] Recent studies report that PEG can be used to prepare a coating matrix containing ZnO NPs and alginate as antibacterial agents on the surfaces of PE food packaging materials. [18-20] Unfortunately, the development of such coatings on PE is extremely difficult, as PEG forms a viscous liquid or wax at room temperature. [21-22] To overcome these limitations, various techniques have been employed for the production of PEG coatings, including grafting [23] and self-assembled monolayers (SAMs). [24] In this framework, plasma polymerization has emerged as an innovative alternative for the deposition of PEG-like films through the use of low-pressure plasma techniques, such as capacitively coupled plasma chemical vapor deposition (CCP-CVD). [25,26] However, these techniques present practical limitations, including the need for complex and expensive vacuum equipment, as well as the difficulty of vaporizing liquid monomers such as PEG due to its low vapor pressure, which hinders their direct use in the vapor phase. Recently, research has shown a growing interest in the development of polymer films deposited by aerosol-assisted atmospheric pressure plasma (AA-APP) processes, which allow liquid precursors to be introduced into the plasma in the form of microdroplets, thereby facilitating their polymerization and

deposition on different substrates, while overcoming the disadvantages of low-pressure systems. [27-31] Notably, the use of aerosol-assisted atmospheric plasma jet (AA-APPJ) techniques has enabled not only the deposition of degradable PEG-like films using liquid precursors such as tri(ethylene glycol) divinyl ether (DVE-3), [20] but also the simultaneous incorporation, during polymerization, of antimicrobials such as ZnO NPs,[30] Ag NPs, and $AgNO_3$,[32] which are of great relevance for biomedical and food-packaging applications.

So far, plasma processes in the agricultural field have been mainly employed for decontamination purposes and to promote the germination of seeds and plants. [33-42] However, to date, no studies have reported the use of plasma for the deposition of films on materials of agricultural interest.

Taking these factors into account, the present study aimed to develop zinc-based antimicrobial nanocomposite coatings on polyethylene substrates, a material widely used for agricultural mulching, by means of the AA-APPJ technique. Specifically, the research focused on comparing the effectiveness of plasma deposition of two different zinc forms, ZnO NPs and ZAD, evaluating their antimicrobial activity within plasma-polymerized PEG-like films. To the best of our knowledge, this work represents the first study in which a plasma-deposited atmospheric pressure film exhibits antibacterial activity against an agriculturally relevant phytopathogenic bacterium, such as *E. carotovora*. Moreover, the antifungal activity was assessed against *Fusarium graminearum*, *Fusarium culmorum*, and *Fusarium moniliforme*, to explore the potential of plasma-deposited zinc-based nanocomposites as multifunctional and environmentally sustainable coatings for crop protection. These nanocomposite coatings were transferred onto wheat seeds to assess their effectiveness directly on the plant material.

4.2 Materials and Methods

4.2.1 Materials

Argon and helium with a purity of ≥ 99.999 %, used as plasma gases, were obtained from Air Liquide (Belgium). DVE-3 and ZAD were purchased from Sigma-Aldrich (Belgium). ZnO nanoparticles were acquired from US Research Nanomaterials, Inc. (USA), with a

diameter range of 10–30 nm and a purity of 99 %. Milli-Q water was produced by filtering deionized water through a Millipore system. All culture media, including brain heart infusion broth (BHI, CM1135), tryptone soy agar (TSA, CM0131), nutrient broth (NB, CM0001), and plate count agar (PCA, CM1012), were obtained from Oxoid (Belgium). Phosphate-buffered saline (PBS) was purchased from VWR (Belgium). The formulation of soybean casein digest broth with lecithin and polyoxyethylene sorbitan monooleate (SCDLP), per liter, contained: 17 g casein peptone, 3 g soybean peptone, 2.5 g dipotassium hydrogen phosphate, 1 g L-α-phosphatidylcholine, 7 g TWEEN® 80, 5 g sodium chloride, and 2.5 g D (+) anhydrous glucose. All components were supplied by Sigma-Aldrich (Belgium), except for sodium chloride (CHEM-LAB CL00.1429) and glucose (CHEM-LAB CL00.0710). Ultrahigh-molecular-weight polyethylene (UHMWPE) film, purchased from Goodfellow (England), was used as the coating substrate, cut into 5 × 5 cm^2 squares, and subsequently cleaned with 2-propanol and ethanol (≥ 99.5 %, Carl Roth , Germany). Prime-grade silicon wafers with a diameter of 100 mm were supplied by Siegert Wafer GmbH (Germany).

4.2.2 Plasma deposition

The AA-APPJ reactor, based on a dielectric barrier discharge (DBD) system, was employed for the deposition of zinc-based nanocomposites and it is illustrated in **Figure 1**. The plasma configuration consists of two coaxial electrodes coated with Al_2O_3: the internal one made as a hollow cylinder (12 mm in diameter) is connected to an RF supply, while the external electrode (14 mm in diameter) is grounded. The body of the plasma source includes conical reductions to facilitate installation and mechanical fixation of the system. The reactor is powered by a CESAR 136 RF generator (Advanced Energy Industries), operating at 13.56 MHz and connected to an L-type matching network, with an output power of 40 W. [43] The working gases are introduced into the 2 mm inter-electrode gap through two symmetrical inlets positioned 10 cm above the discharge region, ensuring a laminar gas flow at the outlet of the source. A helium (3 slm) and argon (1 slm) gas mixture is used to generate the annular plasma. Two different liquid dispersions were used as precursors: (i) a DVE-3 monomer-based dispersion containing 0.5, 1, and 2 wt% ZnO nanoparticles, and (ii) a DVE-3-based dispersion containing 1.5, 2,

3, and 6 wt% ZAD. Before using the dispersions in the aerosol atomizer, it was sonicated for 10 min. The dispersions were introduced inside the inner electrode in the form of an aerosol, generated by a pneumatic atomizer and carried by argon gas. The argon flow rate for aerosol generation was 0.50 slm, while a dilution flow rate of 4 slm was used to adjust the precursor concentration. The deposition process was carried out by moving the plasma head over the substrate using a movable stage controlled by software ST 43.2, BZT-CNC, with a scan speed of 500 mm/min and a track width of 2 mm. The distance between the plasma head and the substrate was maintained at 2 mm, and to obtain coating thickness above 100 nm, a total of three passes were performed.

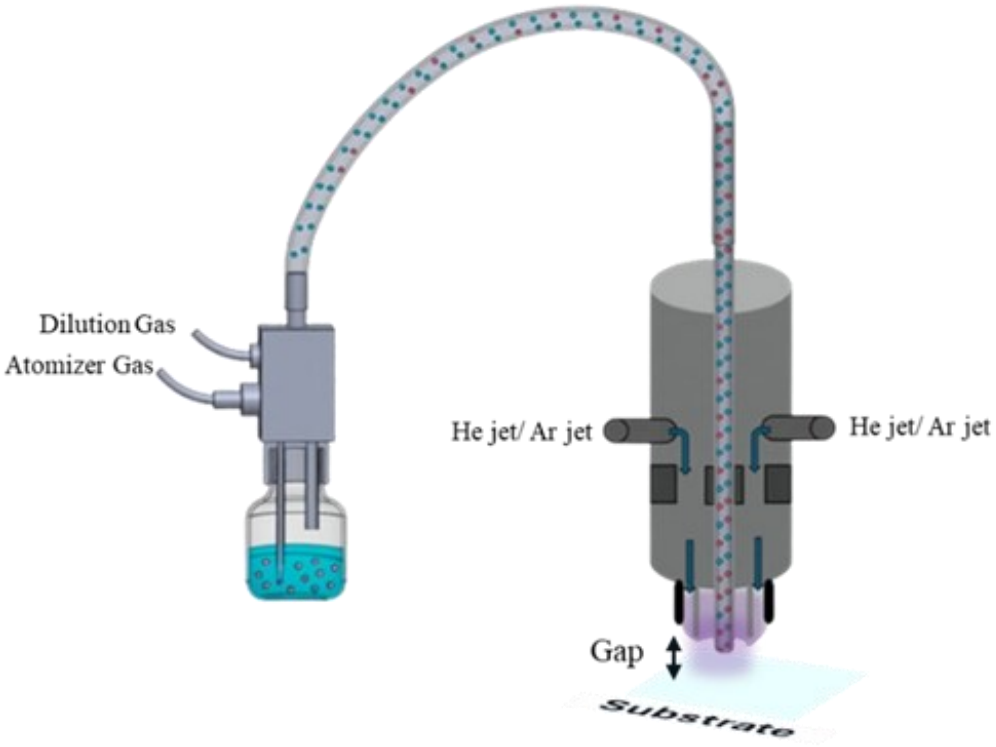

Figure 1. Schematic representation of the aerosol assisted atmospheric pressure jet used for nanocomposite deposition.

4.2.3 Assessment of antibacterial activity

The antimicrobial properties of plasma-polymerized PEG-ZnO and PEG-ZAD nanocomposite coatings were tested against *Erwinia carotovora* CNPB 2046 following the ISO 22196 guidelines, with appropriate modifications. The *E. carotovora* strain was obtained from the culture collection of the Research Unit Food Microbiology and Food Preservation (FMFP) at Ghent University. The strain was suspended in a cryovial containing cryobeads, BHI broth, and 15% glycerol. After thorough mixing, the BHI solution was removed, and the cryovial containing the cryobeads with the strain was stored at –75 °C. Two beads of each strain were then cultured in fresh BHI broth and incubated for 48 h at 30 °C. Pure cultures were obtained using the four-quadrant streak method on TSA, incubated at 30 °C for 48 h. The pure cultures thus obtained were subsequently transferred to TSA slants and stored for up to six weeks at 4 °C. For the preparation of the test inoculum, a small aliquot from each subculture was transferred into fresh BHI broth and incubated at 30 °C for 24 h. After incubation, 100 µL of the homogenized cell suspension were transferred into fresh BHI and incubated again at 30 °C for 24 h. Subsequently, the cultures were centrifuged at 9500 rpm for 15 minutes at 4 °C, and the BHI supernatant was removed. The bacterial pellets were resuspended and diluted to obtain a final concentration of approximately $4.5 \times 10^5 – 4.5 \times 10^6$ colony forming units (CFU)/mL, using a 1:500 dilution of NB in sterile distilled water. Uncoated (control) and plasma-coated UHMWPE samples, each measuring 50 mm × 50 mm, were placed in sterilized Petri dishes. Then, 0.5 mL of the prepared test inoculum was added to each sample. The inoculum was covered with a piece of sterile stomacher bag (polyethylene, Nerbe Plus) measuring 40 mm × 40 mm. Gentle pressure was applied to ensure uniform distribution of the inoculum, after which the Petri dishes were sealed. The prepared Petri dishes were placed inside a sealed chamber, the bottom of which contained a saturated aqueous solution of potassium sulfate to maintain an internal relative humidity above 90%. After sealing, the chamber was incubated at 30 °C for 24 h. Following incubation, the bacteria were recovered from Petri dishes with 10 mL of SCDLP. The number of viable bacteria present in the SCDLP medium was determined using the standard pour plate technique on PCA. The plates were incubated at 30 °C for 48 h, after which CFUs were enumerated.

To calculate the antimicrobial activity of each tested condition, the following formula was used:

$$R = \text{Log}(B/C)$$

R = antibacterial activity; B = average number of viable bacteria on the control sample (UHMWPE) after 24 h; C = average number of viable bacteria on the antibacterial sample after 24 h.

Each sample was analyzed in three biological replicates, and each replicate was plated in triplicate. The calculated CFU/mL values are expressed as mean ± standard deviation.

4.2.4 Assessment of Antifungal Activity

The PEG-ZnO and PEG-ZAD nanocomposite coatings were deposited onto seeds durum wheat variety *Senatore Cappelli and* tested against *F. graminearum*, *F. culmorum*, *F. moniliforme*.

F. graminearum F206, *F. culmorum* F7, and *F. moniliforme* F232, stored in a 15% water–glycerol solution in the isolate collection of the Department of Soil, Plant and Food Sciences (DISSPA) – University of Bari, were reactivated by culturing on MEA medium (Malt Extract Agar; 20 g/L malt extract, 20 g/L agar). Conidial suspensions were obtained by adding sterile water and gently scraping the colonies with a sterile spatula. The suspensions were subsequently quantified and adjusted to a final concentration of 5×10^4 conidia/mL.

30 seeds were used for each pathogen and each treatment. Seeds were sown individually in cell trays containing 15 mL of sterile potting soil, and 500 µL of the corresponding conidial suspension were applied to each pot. As a control, an additional 30 untreated seeds were sown under the same conditions.

Plants were grown in a greenhouse at 25 °C, with supplemental lighting and constant humidity, for a period of 15 days. After 7 days, germination percentage was assessed, whereas after 15 days the plants were collected to perform the following measurements: collar browning (cm), apical necrosis (cm), and total plant length (cm). The infection

severity index was calculated by normalizing the data to the germination of the control group as follow:

$$Infection\ (\%) = \frac{\text{basal browning} + \text{apical necrosis}}{plant\ lenght} \times 100$$

All collected data were analyzed using Costat Cohort software, applying a completely randomized Two-way ANOVA with a significance level of p >0.05, followed by Duncan's post hoc test.

4.2.5 Chemical and Morphological Characterization of the nanocomposite coating

The physicochemical properties of the PEG-ZnO and PEG-ZAD nanocomposites were investigated using various surface characterization techniques.

The surface chemical composition was analyzed using Fourier-Transform Infrared Spectroscopy (FT-IR), performed in both transmission and ATR (attenuated total reflectance) modes, and X-ray photoelectron spectroscopy (XPS). The surface morphology was examined by Atomic Force Microscopy (AFM) and field emission scanning electron microscopy coupled with energy-dispersive X-ray analysis (SEM-EDX). Water contact angle (WCA) measurements were conducted to evaluate the surface wettability of the nanocomposites, and profilometry analysis was carried out to determine the coating thickness.

FT-IR analysis

The composition of the coatings deposited on the silicon substrates was analyzed by FTIR spectroscopy using a Bruker Tensor 27 spectrometer (64 scans, 4 cm^{-1} resolution) equipped with a single-reflection Attenuated Total Reflectance (ATR) accessory (MIRacle, Pike Technology) and a mercury cadmium telluride (MCT) detector. The OPUS 6 software was used for spectral analysis and for correcting the absorption of atmospheric H_2O vapor and CO_2 present in the environment.

The precursor materials used for the plasma deposition process were analyzed by FTIR in transmission mode using a Bruker Vertex 70 V spectrometer (32 scans, 4 cm^{-1} resolution). In this case, the spectrometer was evacuated to a pressure below 150 Pa for 5 minutes to avoid spectral interferences from atmospheric H_2O vapor and CO_2.

XPS analysis

The atomic composition of the topmost layer (5–10 nm) of the plasma-polymerized coatings was analyzed by XPS using a PHI 5000 Versa Probe II spectrometer (Physical Electronics GmbH), equipped with a monochromatic Al Kα X-ray source with a photon energy of 1486.6 eV and operating at a power of 24 W. During the analysis, both wide-scan spectra and high-resolution C1s and O1s spectra were acquired in Fixed Analyser Transmission mode, with a pass energy of 187.0 eV for survey scans and 23.50 eV for high-resolution scans. The surface charge was compensated using a dual-beam charge neutralization system, and the C1s photoemission peak at 285.0 eV was used as the binding energy (BE) reference.

All spectra were collected at a 45° angle relative to the sample surface. To account for the surface distribution of oxygen-containing functional groups in the coatings, the C1s signals were fitted with four peak components at 285.0 eV (C–C, C–H), 286.4 eV (C–OH, C–OC), 287.7 eV (C=O), and 289.2 eV (COOH, COOR), using a 95% Gaussian peak shape and a full width at half maximum (FWHM) of 1.2 eV.

The spectra processing was carried out using the MultiPak data analysis software.

AFM analysis

Surface morphology and roughness of both the UHMWPE substrate and the PEG-ZnO nanocomposites were characterized using an XE-70 atomic force microscope (Park Systems, Korea) operating in non-contact mode. The surface roughness parameter (Rq), describing the average deviation of height values from the mean surface profile, was evaluated through XEI software. Measurements were carried out over a 10 × 10 μm^2 scan area. For each experimental condition, three areas were randomly selected across three independent samples, and the results are expressed as the mean Rq ± standard deviation.

FE-SEM analysis

The FE-SEM analyses were carried out on silicon substrates and used for the morphological characterization of the films containing either ZnO NPs or ZAD, by a Zeiss Sigma microscope (Carl Zeiss Co., Oberkochen, Germany) equipped with an in-lens secondary electron detector and an INCA Energy energy-dispersive spectroscopy (EDS) detector. The analyses were performed at an accelerating voltage of 5 kV and a working distance of 1.1 mm, without the need for prior metallization of the samples.

Furthermore, the samples with the highest zinc content, namely PEG-ZnO 2% and PEG-ZAD 6%, were analyzed using an EDX spectrometer coupled to the FE-SEM at an accelerating voltage of 15 kV, acquiring elemental analyses over three different areas.

WCA analysis

The surface wettability of the samples was evaluated through static water contact angle (WCA) measurements using an OCA115EC digital goniometer (DataPhysics Instruments) on silicon substrates. Drops of distilled water, each with a volume of 2 µL, were deposited on the sample surface at room temperature. The drop angle was determined using the dpiMAX software.

Profilometry analysis

The thickness of the coatings was measured on three different points of three replicates with a KLA-Tencor instrument (Milpitas, CA, USA) D-120 profilometer after scratching part of the coating with a scalpel to form a step.

4.3 Results and discussion

4.3.1 Antimicrobial efficacy of PEG-ZnO and PEG-ZAD nanocomposites

The antibacterial activity of the deposited coatings has been evaluated against *E. carotovora*, and the results are reported in **Figure 2** and **Table 1**, for different content of ZnO NPs and ZAD. The plates shown the bacterial growth obtained after 48 h of incubation on PCA from the E. carotovora cells recovered following the ISO 22196-based assay. A

clear reduction in the number of recovered colonies is observed as the Zn concentration in the PEG-like nanocomposite coatings increases.

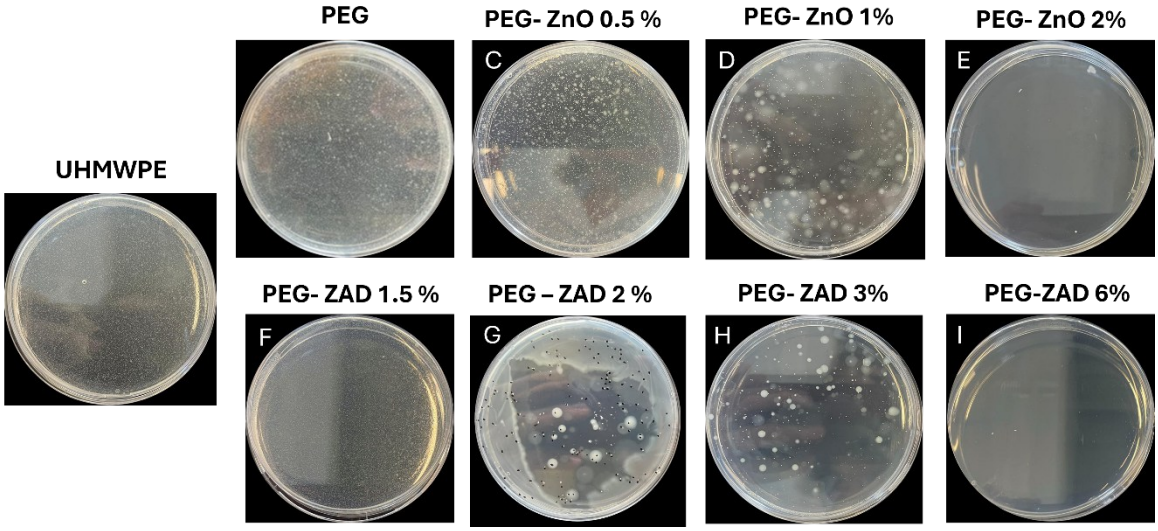

Figure 2. Antibacterial activity of PEG-ZnO and PEG-ZAD nanocomposite coatings against *E. carotovora,* evaluated after recovery following the ISO 22196 protocol and 48 h of incubation on PCA.

The antimicrobial effects of the PEG-ZnO and PEG-ZAD nanocomposite coatings depend onto the composition of the aerosol used for the plasma deposition. In particular, the PEG-ZnO coatings exhibited an increase in antibacterial activity as the ZnO NPs content in the aerosol is increased from 0.5 to 2 wt%. It is evident that, at the same concentration, the PEG-ZnO 2% coatings showed higher antibacterial efficiency compared to the corresponding PEG-ZAD 2% coatings. For this reason, further plasma deposition conditions were investigated using higher ZAD concentrations in the DVE-3 precursor (3 and 6%). The results indicated that, as the ZAD content increased, the antibacterial activity of the films progressively improved, reaching values comparable to those of PEG-ZnO 2% in the case of PEG-ZAD 6%. The antibacterial activity was found to be dependent on the zinc dose contained in the coatings, as reported in previous studies. [44-45]

Table 1. Results of the antibacterial activity of PEG-ZnO and PEG-ZAD nanocomposite coatings against *E. Carotovora*.

Sample	Number of viable bacteria log (CFU/ml), 24h incubation	Antibacterial activity (R)
UHMWPE	$5.2^{a} \pm 0.4$	-
PEG	$4.8^{a} \pm 0.2$	$0.4^{d} \pm 0.2$
PEG-ZnO 0.5%	$4.0^{ab} \pm 0.2$	$1.2^{c} \pm 0.2$
PEG-ZnO 1 %	$2.7^{cd} \pm 0.7$	$2.5^{b} \pm 0.7$
PEG -ZnO 2%	$1.0^{d} \pm 0.7$	$4.2^{a} \pm 0.7$
PEG-ZAD 1.5%	$4.3^{ab} \pm 0.6$	$0.9^{cd} \pm 0.6$
PEG-ZAD 2%	$3.5b^{c} \pm 0.1$	$1.3^{c} \pm 0.1$
PEG-ZAD 3%	$3.0b^{cd} \pm 0.7$	$1.7^{bc} \pm 0.7$
PEG-ZAD 6%	$0.8^{d} \pm 0.2$	$4.4^{a} \pm 0.2$

[a-e] Values in the same column with different superscript letters are significantly different ($p < 0.05$).

The PEG-ZAD coatings therefore required higher Zn^{2+} concentrations to achieve antibacterial effectiveness similar to that of PEG-ZnO coatings. Indeed, previous studies have reported that the antibacterial activity of ZnO NPs has been investigated both against phytopathogenic bacteria such as *E. carotovora* [13] and against other bacterial species including *Staphylococcus aureus*, *Pseudomonas aeruginosa* and *Escherichia Coli* [46] showing higher efficiency due to their distinct mechanisms of action. ZnO NPs operate through a dual antibacterial mechanism: (i) upon exposure to visible light, they can generate high concentrations of reactive oxygen species (ROS), mainly hydroxyl radicals, hydrogen peroxide (H_2O_2), and singlet oxygen; and (ii) ZnO NPs, or the Zn^{2+} ions possibly released from them, can accumulate on the bacterial surface, in the cytoplasm, or within the periplasmic region, thereby interfering with cellular functions and/or damaging the membranes. [47-50] Furthermore, the antibacterial activity of ZnO NPs also depends on their size distribution. Smaller nanoparticles exhibit higher solubility, leading to an increased concentration in the medium. At the same time, the reduced size of the NPs facilitates the penetration and accumulation of ZnO NPs within bacterial cells. [50]

These factors collectively enhance the overall antibacterial effectiveness of the nanoparticles. Conversely, zinc salts owe their antibacterial activity exclusively to the presence of Zn^{2+} ions dissolved in solution. At sufficiently high concentrations, these ions interact with microbial membranes, altering their permeability, and with intracellular structures, particularly enzymes and nucleic acids, thereby interfering with metabolic and respiratory processes and ultimately leading to cell death.[49] However, this effect is strongly dependent on the available ionic concentration: in neutral or slightly basic media, such as bacterial culture conditions, the amount of free zinc tends to decrease, thus limiting the activity of the salts. We hypothesize that, due to the multiple mechanisms of action exhibited by ZnO NPs as described above, their incorporation into a plasma-polymerized matrix makes them more active even at lower concentrations compared to traditional zinc salts such as ZAD.

4.3.2 Assessment of Antifungal Activity: Germination, Plant Height, and Browning Degree

The influence of Zn-containing coatings on seed germination was evaluated against *F. graminearum*, *F. culmorum*, and *F. moniliforme*. As shown in **Figure 3**, after 7 days all treatments exhibited high germination rates, ranging between approximately 86% and 91%. The highest germination was observed in PEG-ZAD 6% and PEG-ZAD 3%, with values of 91% and 94%, respectively. Coatings containing ZnO NPs deposited on the seed surface also maintained high germination rates, above 89%, while PEG and the untreated control showed slightly lower values (86% and 84%, respectively). However there is not a statistic difference between the different coatings. But it is interesting that the increase in germination due to the presence of Zn compounds onto the seeds is statistically significant with respect to the control.

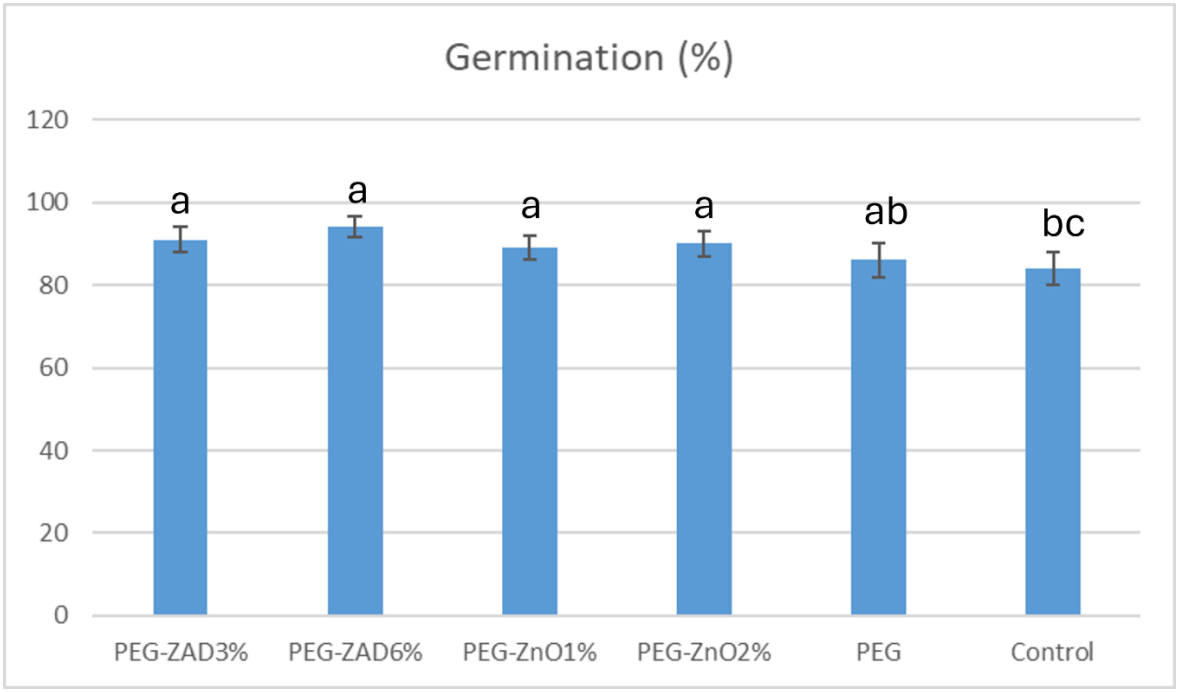

a-c Values letters are significantly different ($p < 0.05$).

Figure 3. Germination percentage of wheat seeds coated with PEG-ZAD and PEG-ZnO after 7 days of incubation in soil contaminated with *F. graminearum*, *F. culmorum*, and *F. moniliforme*.

The assessment of plant height after 15 days is reported in **Figure 4** revealed that seeds coated with PEG-ZnO1% and PEG-ZnO2% reached the greatest heights, measuring 21 cm and 20 cm, respectively. This suggests a potential growth-promoting effect or reduced stress during early development. PEG-ZAD3% and PEG-ZAD6% showed intermediate plant heights, whereas PEG and the control produced shorter plants, measuring 18 cm and 15 cm, respectively. These results indicate that nanocomposite coatings containing ZnO may contribute to improved seedling vigor.

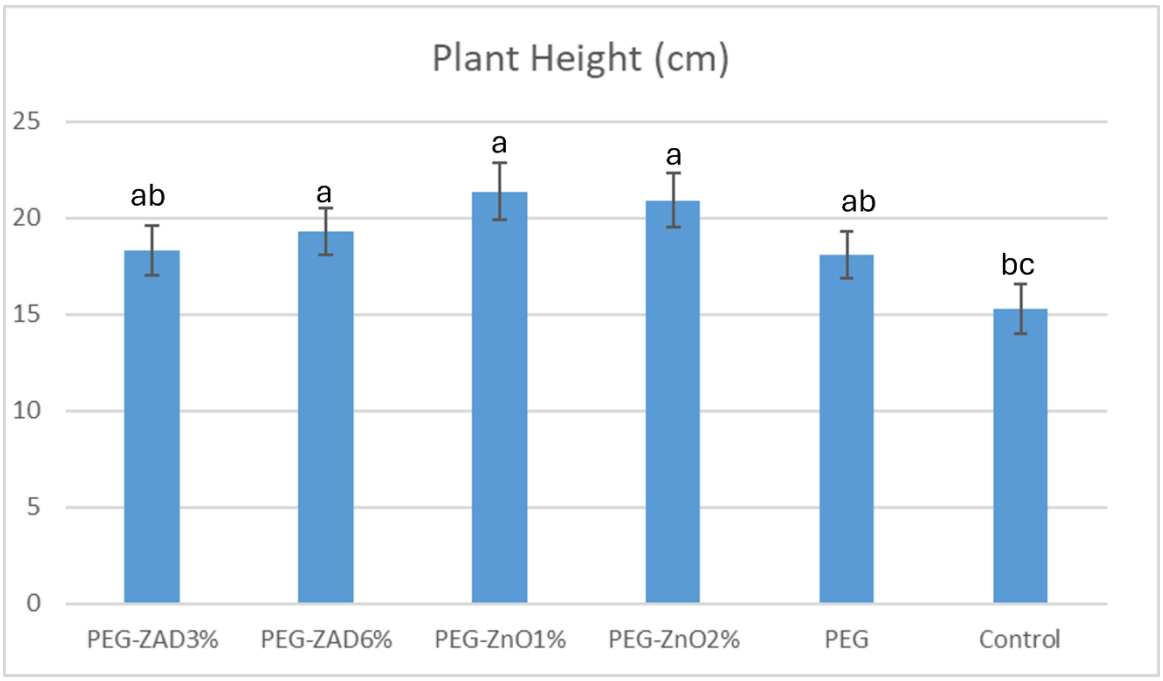

a-c Values letters are significantly different ($p < 0.05$).

Figure 4. Plant Height of wheat seeds coated with PEG-ZAD and PEG-ZnO after 15 days of incubation in soil contaminated with *F. graminearum*, *F. culmorum*, and *F. moniliforme*.

Figure 5 shows the browning degree evaluated after 15 days of incubation with the *Fusarium* species. PEG-ZAD6% and PEG-ZnO2% showed the lowest browning levels (18% and 17%, respectively), indicating a reduction of infection. PEG-ZAD3% and PEG-ZnO1% displayed moderate browning values (20% and 22%, respectively), while PEG and the control exhibited the highest levels (23% and 25%), consistent with greater susceptibility to pathogen damage. These findings demonstrate that PEG-ZnO and PEG-ZAD coatings can reduce browning symptoms compared to the untreated control.

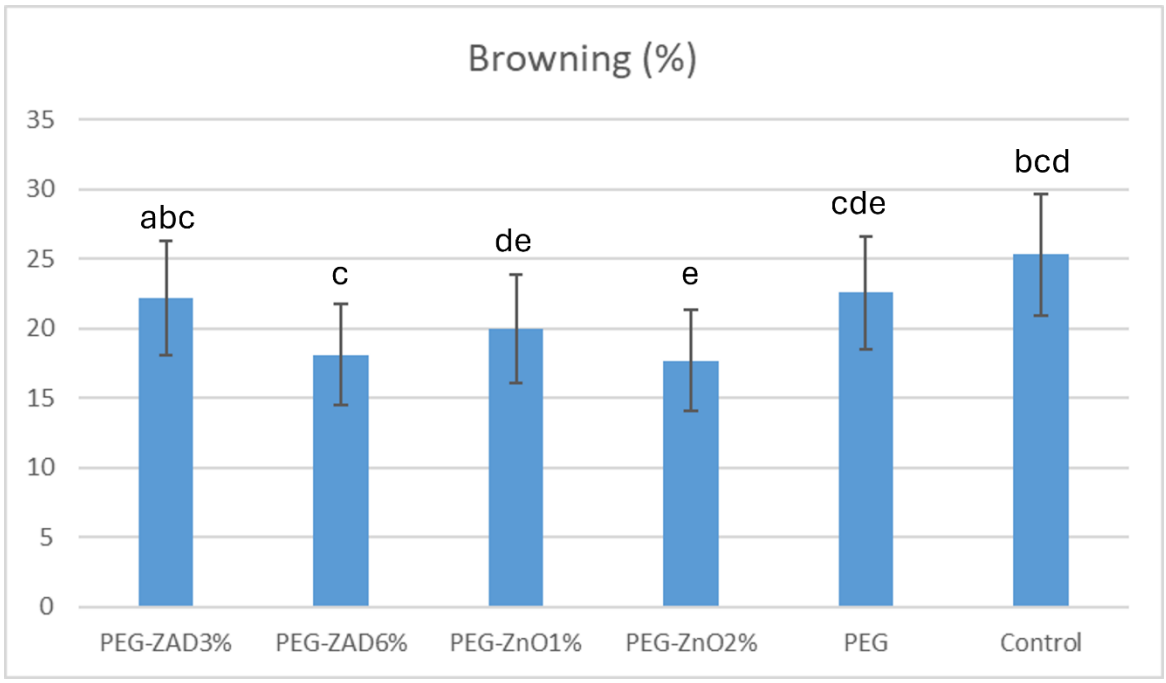

a-e Values letters are significantly different ($p < 0.05$).

Figure 5. Browning wheat seeds coated with with PEG-ZAD and PEG-ZnO after 15 days of incubation in soil contaminated with *F. graminearum*, *F. culmorum*, and *F. moniliforme*.

Seed coatings based on Zn showed a slightly protective antifungal effect against the tested *Fusarium* species. Germination remained high in all treatments, and the slightly higher values observed in PEG-ZAD 3% and PEG-ZAD 6% may suggest a positive contribution of Zn supplied through zinc salts such as ZAD. This trend is consistent with previous findings showing that Zn compounds can enhance seed metabolic activation and early enzymatic processes, improving germination performance. [51]

PEG-ZnO1% and PEG-ZnO2% produced the tallest seedlings, since Zn is able to promote root–shoot elongation and early plant vigor, as reported for ZnO-based treatments that slightly stimulated wheat seedling growth and did not impair germination. [52] In addition, nanoscale ZnO has been shown to improve plant biomass and reduce stress-related biochemical responses in wheat, which could partially align with the growth-promoting trend observed in these cases.[53]

The browning degree indicated a reduction in infection symptoms in PEG-ZAD6% and PEG-ZnO2%. Zn-based antifungal action has been associated with membrane destabilization, ROS generation, and structural damage to *Fusarium* hyphae. These

mechanisms may contribute to the reduction in browning observed, although further investigation would be necessary to confirm the specific processes occurring in this system.[54]

4.3.3 Chemical and Morphological Characterization of PEG-ZnO and PEG-ZAD nanocomposites coatings

Considering the antimicrobial activity observed for the PEG-like nanocomposites containing ZnO NPs or ZAD, the surface chemistry of these coatings was investigated. FT-IR analyses were performed for the characterization of the coatings and of the precursors, and the results are presented in **Figure 6**. In particular Figure 6 A-C reports the FTIR spectra of the DVE-3 precursors, of the ZnO NPs and of ZAD.

The FTIR spectrum of the DVE-3 monomer was found to exhibit the characteristic absorption bands of an aliphatic divinyl ether. Specifically, the C–H stretching vibrations of methyl and methylene groups were observed at 2950–2850 cm^{-1}, the C=C stretching vibration at 1616–1634 cm^{-1}, and the C–O–C ether stretching vibration at 1100–1120 cm^{-1}.

The molecular structure of DVE-3, featuring both ether linkages and reactive vinyl terminal groups, is considered chemically relevant to plasma-induced polymerization and crosslinking processes.

The FT-IR spectrum of ZnO NPs 10–30 nm was recorded in the wavenumber range of 4000–400 cm^{-1}. The main absorption peaks, located between 522 and 422 cm^{-1}, were assigned to the stretching vibrations of the Zn–O bond. In contrast, the FT-IR spectrum of the ZAD compound showed two distinct bands corresponding to the COO^- anion at 1564 cm^{-1} and 1445 cm^{-1}, which are typical of zinc carboxylate salts.

In Figure 6D the spectrum of the plasma-polymerized PEG-like coating (Zn-free) is reported for the wavenumber range of 4000–600 cm^{-1}. As it can be observed, the characteristic peaks of the pristine DVE-3 were preserved, along with the appearance of a broad O–H stretching band at 3500–3100 cm^{-1} and a C=O stretching vibration at 1730–1700 cm^{-1}.

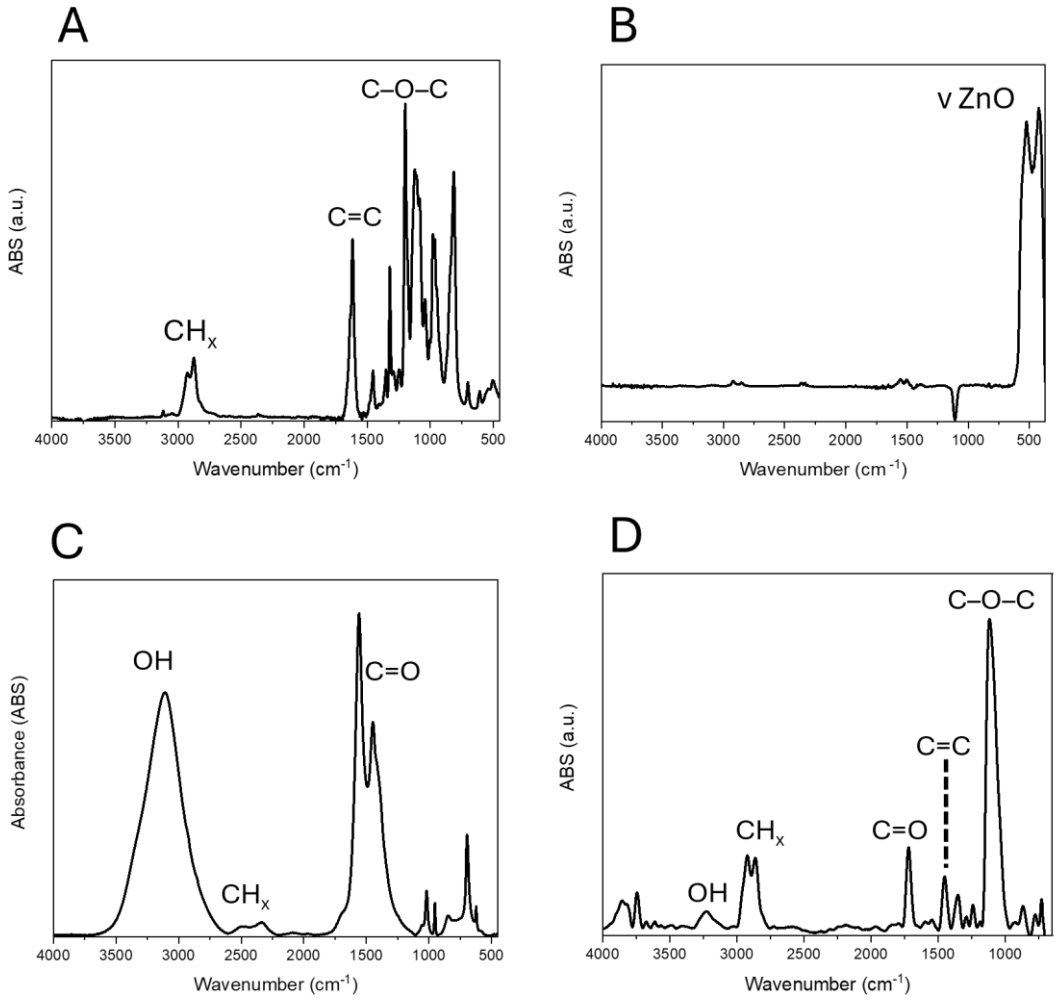

Figure 6. FTIR spectra (ATR and transmission) of the precursors and the PEG-like coating. A) ATR of DVE-3, B) FT-IR of ZnO NPs, C) FT-IR of ZAD, D) ATR of PEG-like coating.

The absorption spectra of the PEG–ZnO and PEG–ZAD nanocomposites (not reported) did not show any distinctive characteristic peaks and were similar to that of the PEG-like coating, likely due to the very low concentration of the additives.

The surface elemental composition of the developed PEG coatings, whose corresponding IR spectrum is shown in Figure 6D, as well as that of the PEG–ZnO and PEG–ZAD nanocomposites, was investigated by means of XPS measurements. The results are summarized in **Table 2**. As expected, the plasma-polymerized PEG-like coatings primarily consist of carbon and oxygen, originating from the DVE-3 monomer. The relative ratio of these elements is consistent with that previously reported for PEG polymers obtained

using other plasma polymerization methods and resembles the O/C ratio of conventional PEG polymers. [19]

Similarly, for the PEG–ZnO and PEG–ZAD coatings, the XPS analysis revealed the presence of carbon and oxygen on the surface, while zinc was not detected. This absence is most likely due to the incorporation of zinc within the deeper layers of the polymeric matrix, below the typical sampling depth of the XPS technique. It is noteworthy that, with increasing concentrations of ZnO NPs and ZAD within the coatings, the overall oxygen content slightly increases. This behavior can be attributed to the higher amount of incorporated ZnO NPs and zinc-based carboxylate salt, both of which also contain oxygen.

Table 2 Surface elemental composition of the plasma-polymerized PEG, PEG-ZnO and PEG-ZAD nanocomposite coatings.

Sample	C (at.%)	O (at.%)
PEG	65.7 ± 0.7	34.5 ± 0.7
PEG-ZnO 0.5%	63.9 ± 0.5	36.1 ± 0.5
PEG-ZnO 1%	63.9 ± 0.4	36.1 ± 0.5
PEG-ZnO 2%	64.1± 0.5	35.9 ± 0.4
PEG-ZAD 1.5%	64.0± 0.6	36.0 ± 0.6
PEG-ZAD 3%	63.0± 0.5	37 ± 0.5
PEG-ZAD 6%	63.0 ± 0.3	37 ± 0.4

To identify the nature of the oxygen-containing groups present in the coatings, the C1s spectrum of the PEG-like film was best-fitted with four components, showing peaks at 285.0 eV (C1, C–C, C–H, reference), 286.4 eV (C2, C–OH, C–OC), 287.7 eV (C3, C=O), and 289.2 eV (C4, COOH, COOR), respectively, as shown in **Figure 7**. The relative areas of the peaks were 27%, 55.1%, 11.4%, and 6.5% for the C1–C4 components, respectively, in good agreement with the FT-IR analysis and with the structure of coatings deposited under similar conditions, as discussed in a previous study.

Moreover, the dominant peak is associated with the functional C–O–C groups, which exist in the initial monomer structure, indicating a high retention of the monomer functionality. Other oxygen-containing groups, including C=O and O–C=O, were also identified in the C1s spectra. These groups are not inherently part of the DVE-3 structure. It is likely that the C–O–C groups of the monomer are partially destroyed during the plasma polymerization process, leading to the formation of small monomer fragments. These fragments can reassemble to form a coating with increased relative amounts of C=O and O–C=O groups. These findings are consistent with previous studies, which also report the incorporation of oxygen-containing functional groups, such as carboxylic (O–C=O) and carbonyl (C=O) groups, on the surface of developing coatings through atmospheric-pressure plasma polymerization.

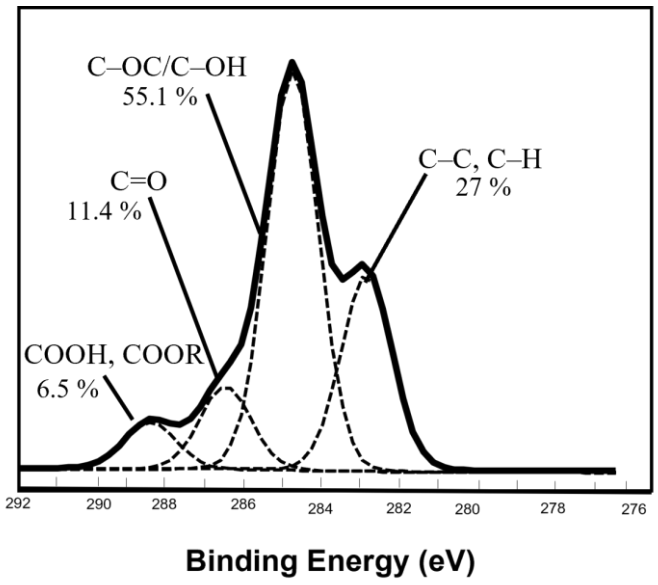

Figure 7. XPS high-resolution C1s peak fitting for plasma-polymerized PEG.

To gain a deeper understanding of the coating morphology, AFM analysis was performed on the film surface, and the obtained images are illustrated in **Figure 8**. As it can be observed, the plasma-polymerized PEG-like coating exhibits a notably smooth surface. In contrast, the PEG–ZnO nanocomposite coatings display rougher surfaces, and an increase in the ZnO nanoparticle content results in a progressive rise in surface roughness. From these images, the root mean square roughness (Rq) values were calculated and are summarized in **Table 3**.

A pronounced decrease in UHMWPE roughness is observed upon deposition of the PEG-like layer, suggesting that the plasma-polymerized coating levels the substrate by occupying surface irregularities.

The PEG-like coating shows a low Rq value (15.0 ± 0.2 nm), indicative of a smooth surface, whereas the PEG–ZnO coatings exhibit significantly higher roughness, particularly for the sample containing 2 wt% of ZnO NPs, where the Rq value reaches 28.2 ± 1.4 nm. The observed trend likely arises from a more pronounced aggregation of ZnO nanoparticle clusters on the surface, which is responsible for the increased roughness.

To obtain a comprehensive understanding of the dispersion degree of ZnO nanoparticles within the PEG matrix, SEM images were also acquired and are reported in **Figure 8**. With increasing NP concentration in the DVE-3 monomer, the nanoparticles begin to aggregate within the monomeric dispersion, and these aggregates, once introduced into the plasma, lead to the formation of non-uniform clusters on the surface. Furthermore, due to their high surface energy and frequent Brownian collisions, small-sized nanoparticles, such as those used in this study, tend to agglomerate more readily.

It is worth noting that the formation of similar NP agglomerates has been widely reported and discussed in the literature for aerosol-assisted plasma processes involving the atomization of NP dispersions. [31]

The maximum antimicrobial activity observed for the PEG–ZnO 2 wt% coatings against *E. carotovora* may be attributed to locally high ZnO concentrations on the surface, which continue to release ROS and Zn^{2+} ions, thus providing a strong antibacterial effect. These agglomerates could act as “hot spots” that enhance microbial inhibition, despite the non-uniform NPs dispersion. Given the nanoparticle size, even in the form of clusters, they remain small enough to penetrate bacterial membrane and induce oxidative stress. [51]

The SEM images clearly highlight the densely packed structure of NPs agglomerates, covered by a thin organic layer. The presence of this organic layer may explain why the surface atomic composition of the nanocomposite coatings, as determined by XPS (with a maximum sampling depth of ~10 nm), is dominated by the hydrocarbon polymer.

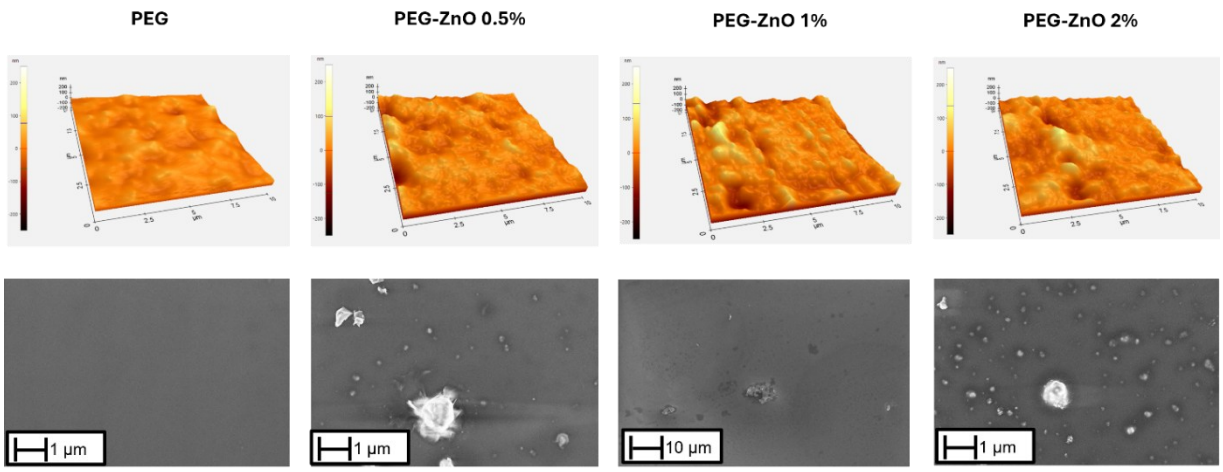

Figure 8. SEM and AFM images of plasma-polymerized PEG and PEG–ZnO nanocomposite coatings (0.5%, 1%, and 2%).

The plasma-deposited PEG–ZAD coatings, as showed in **Figure 9**, exhibited an increase in surface roughness with the rising percentage of ZAD dispersed in the starting monomer. As reported in **Table 3**, the Rq value of these coatings increases compared to the PEG reference, reaching a maximum of 20.6 ± 1.2 nm for the PEG–ZAD 6% sample, indicating a modest topographical variation with increasing zinc acetate concentration. During deposition, part of the salt may accumulate in the uppermost regions of the film, leading to microscopic discontinuities or higher-contrast areas, which result in a slight increase in the roughness measured by AFM.

However, these irregularities are less pronounced than the surface asperities generated by the presence of ZnO clusters in the PEG–ZnO coatings, confirming that the PEG–ZAD film maintains a more continuous and compact surface morphology. Nevertheless, in both PEG–ZnO and PEG–ZAD coatings, the surface morphology observed by AFM may also be influenced by the deposition conditions. In particular, the absence of continuous agitation during deposition may favor particle sedimentation and aggregate formation already within the precursor suspensions, which is subsequently reflected in the coating morphology.

As observed in the SEM images, small aggregates and residual salt fragments are irregularly distributed within the polymer matrix, and their density and dimensions tend

to increase with increasing ZAD concentration in the PEG-like coating. Moreover, it is evident that in some areas of the coating, these agglomerates are covered by a thin layer of the organic polymer matrix. Accordingly, the following mechanism was hypothesized. ZAD although highly soluble in polar solvents such as water, is insoluble in the organic monomer DVE-3, where it remains as a finely dispersed solid phase.

The low volatility of DVE-3 (*K*) combined with the very limited diffusive mobility of the solid particles in the viscous monomer (*D*) results in a high Péclet number (*Pe* = *K/D*). Under these conditions, the salt forms aggregates irregularly distributed throughout the monomer phase. [55]

The rapid plasma-induced polymerization then consolidates this microstructure, leading to PEG-like coatings containing salt-rich spots partially covered by the organic matrix, in agreement with the morphological and surface observations.

The antimicrobial activity of PEG-ZAD coatings could also be attributed, similarly to what was observed for the PEG–ZnO coatings, to the high local concentration of salt agglomerates and to the continuous release of Zn^{2+} ions.

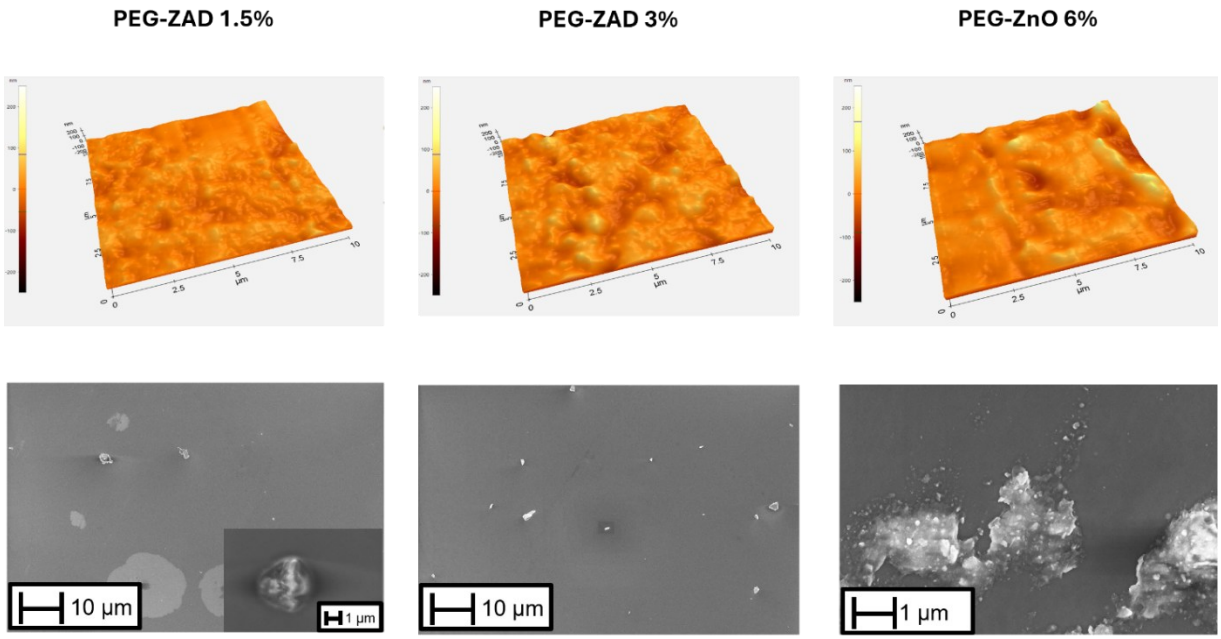

Figure.9 SEM and AFM images of PEG-ZAD nanocomposite coatings (1.5%, 3%, and 6%).

Table 3 Surface roughness value (Rq) for the plasma-polymerized PEG, PEG-ZnO and PEG-ZAD nanocomposite coatings.

Sample	Rq (nm)
UHMWPE	23.2 ± 0.2
PEG	15.0 ± 0.2
PEG-ZnO 0.5%	25.0 ± 0.6
PEG-ZnO 1 %	27.0 ± 1.3
PEG -ZnO 2%	28.2 ± 1.4
PEG-ZAD 1.5%	17.1 ± 1.4
PEG-ZAD 3%	18.4 ± 3
PEG-ZAD 6%	20.6 ± 1.2

Furthermore, EDX analysis performed on the same area as the SEM surface images revealed zinc atomic content of 2.9±0.5 % at. for the PEG–ZnO 2% coating and 1.5±0.3 % at. for the PEG–ZAD 6% sample. The detection of Zn with EDX and not with XPS confirm that Zn is mostly inside the matrix. In fact the maximum analyzed depth with XPS is few nanometers whereas the one of EDX is hundreds of nm. Hence for EDX the detection of Zn is straightforward.

The study also investigated how the incorporation of ZnO NPs and ZAD influences the surface wettability of the PEG–ZnO and PEG–ZAD nanocomposite coatings. **Table 4** reports the measured WCA values for PEG and for the zinc-based nanocomposites. As expected, PEG exhibits hydrophilic properties, with a WCA value of 42 ± 1°. Similarly, the PEG–ZnO coatings also show hydrophilic behavior; however, in the presence of ZnO nanoparticles or ZAD, the WCA value slightly increases, ranging from 45–48° for PEG–ZnO and 45–46° for PEG–ZAD. A low increment in WCA is observed for the coatings containing ZnO or ZAD, likely due to the change in the morphology, that is know to have a role in WCA evaluation.

Table 4 WCA values for plasma-polymerized PEG, PEG-ZnO, PEG-ZAD.

Sample	WCA (°)
PEG	42 ± 1
PEG-ZnO 0.5%	48 ± 1
PEG-ZnO 1 %	45 ± 3
PEG -ZnO 2%	47 ± 1
PEG-ZAD 1.5%	46 ± 1
PEG-ZAD 2%	45 ± 1
PEG-ZAD 3%	46 ± 1

In **Table 5** the thicknesses values of the plasma deposited coatings are reported. Variations in film thickness are observed as a function of the ZnO NPs and ZAD aerosol content. In particular, an increase in coating thickness is detected when higher concentrations of ZnO NPs and ZAD are used in the monomer suspension. When the lowest concentrations of ZnO NPs (2 wt%) and ZAD (1.5 wt%) are considered for the plasma deposition, thin films are obtained, with thicknesses of 92 ± 10 nm and 98 ± 10 nm, respectively. However, increasing the concentrations to 2 wt% in ZnO NPs and 6 wt% in ZAD the thickness is considerably affected, reaching 164 ± 40 nm and 120 ± 20 nm, respectively. It is also important to note that coatings with a higher zinc content exhibit a lower degree of thickness uniformity, as indicated by the higher standard deviation values compared to nanocomposite coatings with lower Zn content. The observed increase in film thickness can be attributed to the presence of nanoparticles whose size is larger than that of the polymer precursors and as such have an important impact in determining the film growth. Furthermore, as also evidenced by SEM and AFM analyses, the limited solubility of these components in the monomer may lead to the formation of aggregates within the solution. As a result, clusters of nanoparticles and zinc salt can be introduced into the plasma, acting as nucleation centers. This process may promote the growth of plasma-polymerized PEG chains around the agglomerations in the gas phase, which subsequently deposited onto the substrate in the form of larger clusters, leading to the formation of a non-uniform and rough coating.

Table 5 Thickness values for plasma-polymerized PEG, PEG-ZnO, PEG-ZAD.

Sample	Thickness (nm)
PEG	90 ± 10
PEG-ZnO 0.5%	92 ± 10
PEG-ZnO 1 %	100 ± 10
PEG -ZnO 2%	164 ± 40
PEG-ZAD 1.5%	98 ± 10
PEG-ZAD 2%	112 ± 10
PEG-ZAD 3%	120 ± 20

4.4 Conclusions

This study demonstrates, for the first time, the development of antimicrobial nanocomposites produced by AA-APPJ deposition, aimed at controlling microbic phytopathogens. The antibacterial activity of the coatings proved to be effective when using different concentrations of ZnO and ZAD (zinc acetylacetonate dihydrate) dispersed in the monomer. The results showed a strong ability of coatings to inhibit the growth of *E. carotovora*, the bacterium responsible for soft rot in potatoes, one of the most significant bacterial diseases causing tissue maceration and considerable post-harvest losses. This innovative approach represents a promising alternative to conventional polyethylene coating methods used in agriculture, as it enables a controlled release of zinc and provides a prolonged and targeted antimicrobial action against agricultural pathogens, thereby contributing to improved crop health and the sustainability of farming practices.

The application of the same Zn-based nanocomposites as seed coatings further extends their potential within plant protection strategies. Once deposited onto wheat seeds, these coatings demonstrated the ability to not alter seed germination, support the initial development of seedlings, and mitigate infection symptoms caused by *Fusarium* species. The presence of zinc entrapped within the films may have determined physiological activation during germination and a reduction of browning symptoms in wheat plants.

4.5 References

[1] R. Czajkowski, M. C. M. Pérombelon, S. Jafra, E. Lojkowska, M. Potrykus, J. M. van der Wolf, W. Sledz. Detection, identification and differentiation of *Pectobacterium* and *Dickeya* species causing potato blackleg and tuber soft rot: A review. *Annals of Applied Biology*, 2015, 166(1), 18–38.

[2] V. Duarte, S. H. De Boer, L. J. Ward, A. M. R. De Oliveira. The bacterial soft rot pathogens, *Pectobacterium carotovorum* and *Dickeya* spp. *Horticulturae*, 2022, 6(1), 13.

[3] M. C. M. Pérombelon. Potato diseases caused by soft rot erwinias: An overview of pathogenesis. *Plant Pathology*, 2002, 51(1), 1–12.

[4] M. C. M. Pérombelon, L. J. Hyman. Survival of soft rot coliforms, *Erwinia carotovora* subsp. *carotovora* and *E. carotovora* subsp. *atroseptica* in soil in Scotland. *Journal of Applied Bacteriology*, 1989, 66(2), 95–106.

[5] Z. Mansoor, F. Tchuenbou-Magaia, M. Kowalczuk, G. Adamus, G. Manning, M. Parati, I. Radecka, H. Khan. Polymers used as mulch films in agriculture—A review of history, problems and current trends. *Polymers*, 2022, 14(23), 5062.

[6] Q. C. Burandt, H. B. Deising, A. von Tiedemann. Further limitations of synthetic fungicide use and expansion of organic agriculture in Europe will increase the environmental and health risks of chemical crop protection caused by copper-containing fungicides. *Environmental Toxicology and Chemistry*, 2024, 43(1), 19–30.

[7] Z. Mansoor, F. Tchuenbou-Magaia, M. Kowalczuk, G. Adamus, G. Manning, M. Parati, I. Radecka, H. Khan. Polymers used as mulch films in agriculture—A review of history, problems and current trends. *Polymers*, 2022, 14(23), 5062.

[8] C. Scopetani, S. Selonen, A. Cincinelli, J. Pellinen. Chemical leaching from polyethylene mulching films to soil in strawberry farming. *Frontiers in Environmental Science*, 2023, 11, 1129336.

[9] P. B. Linares, L. A. Castillo, S. E. Barbosa. Micronutrients release from active polyethylene films under mulched conditions. *Results in Surfaces and Interfaces*, 2025, 18, 100419.

[10] Y. Li, P. Zhang, M. Li, N. Shakoor, M. Adeel, P. Zhou, M. Guo, Y. Jiang, W. Zhao, B. Lou, Y. Rui. Application and mechanisms of metal-based nanoparticles in the control of bacterial and fungal crop diseases. *Pest Management Science*, 2022, 79(1), 21–36.

[11] Z. Wang, Y. He, S. Liu, X. Xu, Y. Song, L. Zhang, X. An. Toxic effects of zinc oxide nanoparticles as a food additive in goat mammary epithelial cells. *Food Research International*, 2023, 167, 112682.

[12] J. A. Lemire, J. J. Harrison, R. J. Turner. Antimicrobial activity of metals: Mechanisms, molecular targets and applications. *Nature Reviews Microbiology*, 2013, 11(6), 371–384.

[13] F. Suárez, A. P. F. Monteiro, D. C. Ferreira, F. D. Brandão, K. Krambrock, L. V. Modolo, M. E. Cortés, R. D. Sinisterra. Efficient antibacterial nanosponges based on ZnO nanoparticles and doxycycline. *Journal of Photochemistry and Photobiology B: Biology*, 2017, 170, 85–94.

[14] EFSA FEEDAP Panel. Scientific opinion on the safety and efficacy of zinc compounds (E6) as feed additives for all animal species. *EFSA Journal*, 2015, 13(4), 4058.

[15] M. R. Yazdanshenas, M. R. Rezaei, J. Kharkan. Comparative toxicity of zinc oxide nanoparticles and zinc salts in male mice: Hematological, biochemical, and histopathological impacts. *Toxicology Reports*, 2025, 14, 102003.

[16] S. H. Kim, S. Bae, Y. W. Sung, Y. S. Hwang. Effects of particle size on toxicity, bioaccumulation, and translocation of zinc oxide nanoparticles to bok choy in garden soil. *Ecotoxicology and Environmental Safety*, 2024, 280, 116519.

[17] Australian Government, Department of Health, NICNAS. Soluble zinc salts: Human health tier II assessment. *IMAP Group Assessment Report*, 2014.

[18] A. A. D'souza, R. Shegokar. Polyethylene glycol (PEG): A versatile polymer for pharmaceutical applications. *Expert Opinion on Drug Delivery*, 2016.

[19] M. Zabihzadeh Khajavi, A. Nikiforov, G. Tomei, R. Morent, F. Devlieghere, P. Ragaert, E. Marotta, N. De Geyter. Hydrolysis of plasma-polymerized poly(ethylene glycol)/ZnO nanocomposites in food simulants: Identification of components and potential toxicity. *Food Chemistry*, 2025, 464.

[20] M. Zabihzadeh Khajavi, A. Nikiforov, M. Nilkar, F. Devlieghere, P. Ragaert, N. De Geyter. Degradable plasma-polymerized poly(ethylene glycol)-like coating as a matrix for food-packaging applications. *Nanomaterials*, 2023, 13.

[21] M. Zabihzadeh Khajavi, A. Nikiforov, R. Morent, I. Fraeye, F. Devlieghere, P. Ragaert, N. De Geyter. Engineering antibacterial plasma-polymerized polyethylene glycol–ZnO nanocomposite coatings for extending pork sausage shelf life. *Food Research International*, 2025, 201, 115568.

[22] A. A. D'souza, R. Shegokar. Polyethylene glycol (PEG): A versatile polymer for pharmaceutical applications. *Expert Opinion on Drug Delivery*, 2016, 13(9), 1257–1275.

[23] L. Denis, P. Marsal, Y. Olivier, T. Godfroid, R. Lazzaroni, M. Hecq, J. Cornil, R. Snyders. Deposition of functional organic thin films by pulsed plasma polymerization: A joint theoretical and experimental study. *Plasma Processes and Polymers*, 2010, 7(2), 172–181.

[24] J. Groll, Z. Ademovic, T. Ameringer, D. Klee, M. Moeller. Comparison of coatings from reactive star-shaped PEG-s Tat-PPG prepolymers and grafted linear PEG for biological and medical applications. *Biomacromolecules*, 2005, 6, 956–962.

[25] M. Veiseh, M. H. Zareie, M. Zhang. Highly selective protein patterning on gold–silicon substrates for biosensor applications. *Langmuir*, 2002, 18, 6671–6678.

[26] C. Choi, I. Hwang, Y.-L. Cho, S. Y. Han, D. H. Jo, D. Jung, D. W. Moon, E. J. Kim, C. S. Jeon, J. H. Kim, et al. Fabrication and characterization of plasma-polymerized poly(ethylene glycol) film with superior biocompatibility. *ACS Applied Materials & Interfaces*, 2013, 5, 697–702.

[27] D. Sakthi Kumar, M. Fujioka, K. Asano, A. Shoji, A. Jayakrishnan, Y. Yoshida. Surface modification of poly(ethylene terephthalate) by plasma polymerization of poly(ethylene glycol). *Journal of Materials Science: Materials in Medicine*, 2007, 18, 1831–1835.

[28] J.-P. Booth, M. Mozetič, A. Nikiforov, C. Oehr. Foundations of plasma surface functionalisation of polymers for industrial and biological applications. *Plasma Sources Science and Technology*, 2022, 31, 103001.
[29] A. Nikiforov, Z. Chen. *Atmospheric Pressure Plasma: From Diagnostics to Applications*. IntechOpen, London, 2019.

[30] M. C. Ramkumar, K. Navaneetha Pandiyaraj, A. Arun Kumar, P. V. A. Padmanabhan, P. Cools, N. De Geyter, R. Morent, S. Uday Kumar, V. Kumar, P. Gopinath, et al. Atmospheric-pressure non-thermal plasma-assisted polymerization of PEGMA on LDPE films for enhancement of biocompatibility. *Surface and Coatings Technology*, 2017, 329, 55–67.

[31] F. Fanelli, F. Fracassi. Aerosol-assisted atmospheric pressure cold plasma deposition of organic–inorganic nanocomposite coatings. *Plasma Chemistry and Plasma Processing*, 2014, 34, 473–487.

[32] G. Laghi, D. Franco, G. G. Condorelli, R. Gallerani, S. Guglielmino, R. Laurita, D. Morganti, F. Traina, S. Conoci, M. Gherardi. Control strategies for atmospheric pressure plasma polymerization of fluorinated silane thin films. *Plasma Processes and Polymers*, 2023, 20, 2200194.

[33] A. Liguori, E. Traldi, E. Toccaceli, R. Laurita, A. Pollicino, M. L. Focarete, V. Colombo, M. Gherardi. Co-deposition of plasma-polymerized polyacrylic acid and silver nanoparticles using an atmospheric pressure plasma jet. *Plasma Processes and Polymers*, 2016, 13(6), 623–632.

[34] P. Favia, E. Sardella, H. Tanaka. Special issue: Advanced applications of plasmas in life sciences. *Plasma Processes and Polymers*, 2020, 17, 2070028.

[35] A. Mitra, Y.-F. Li, T. G. Klämpfl, et al. Inactivation of surface-borne microorganisms and increased germination of seed specimen by cold atmospheric plasma. *Food and Bioprocess Technology*, 2014, 7, 645–653.

[36] J. J. Zhang, J. O. Jo, D. L. Huynh, et al. Growth-inducing effects of argon plasma on soybean sprouts. *Scientific Reports*, 2017, 7, 41917.

[37] L. Li, J. Jiafeng, J. Li, et al. Effects of cold plasma treatment on seed germination and seedling growth of soybean. *Scientific Reports*, 2014, 4, 5859.

[38] T. Stolárik, M. Henselová, M. Martinka, O. Novák, A. Zahoranová, M. Černák. Effect of low-temperature plasma on seed structure, growth and phytohormones in pea. *Plasma Chemistry and Plasma Processing*, 2015, 35, 659–676.

[39] L. Sivachandiran, A. Khacef. Enhanced seed germination and plant growth by atmospheric-pressure cold air plasma. *RSC Advances*, 2017, 7, 1822–1832.

[40] B. Sera, P. Spatenka, M. Sery, N. Vrchotova. Influence of plasma treatment on wheat and oat germination and early growth. *IEEE Transactions on Plasma Science*, 2010, 38, 2963.

[41] J. Jiang, X. He, L. Li, et al. Effect of cold plasma treatment on seed germination and growth of wheat. *Plasma Science and Technology*, 2014, 16, 54–58.

[42] D. Dobrin, M. Magureanu, N. B. Mandache, M. D. Ionita. The effect of non-thermal plasma on wheat germination and early growth. *Innovative Food Science & Emerging Technologies*, 2015, 29, 255–260.

[43] I. Sremački, A. Jurov, M. Modic, U. Cvelbar, L. Wang, C. Leys, A. Nikiforov. On diagnostics of annular-shape RF plasma jet in argon under atmospheric conditions. *Plasma Sources Science and Technology*, 2020, 29(3), 035027.

[44] A. A. Alswat, M. B. Ahmad, T. A. Saleh, M. Hussein, Z. Bin, N. A. Ibrahim. Effect of zinc oxide amounts on the properties and antibacterial activity of zeolite/ZnO nanocomposites. *Materials Science and Engineering C*, 2016, 68, 505–511.

[45] Y. Liu, L. He, A. Mustapha, H. Li, Z. Q. Hu, M. Lin. Antibacterial activities of zinc oxide nanoparticles against *E. coli* O157:H7. *Journal of Applied Microbiology*, 2009, 107(4), 1193–1201.

[46] C. R. Mendes, G. Dilarri, C. F. Forsan, et al. Antibacterial action and target mechanisms of zinc oxide nanoparticles against bacterial pathogens. *Scientific Reports*, 2022, 12, 2658.

[47] B. Lallo da Silva, M. P. Abuçafy, E. Berbel Manaia, J. A. Oshiro Junior, B. G. Chiari-Andréo, R. C. L. R. Pietro, L. A. Chiavacci. Relationship between structure and antimicrobial activity of zinc oxide nanoparticles. *International Journal of Nanomedicine*, 2019, 9395–9410.

[48] Y. Liu, M. Zheng, Z. Xie. Chiral organic nanoparticles–based photodynamic antibacterial films for food preservation. *Chemical Engineering Journal*, 2024, 486, 150361.

[49] J. Pasquet, Y. Chevalier, J. Pelletier, E. Couval, D. Bouvier, M.-A. Bolzinger. Contribution of zinc ions to antimicrobial activity of ZnO. *Colloids and Surfaces A*, 2014, 457, 263–274.

[50] N. Padmavathy, R. Vijayaraghavan. Enhanced bioactivity of ZnO nanoparticles—An antimicrobial study. *Science and Technology of Advanced Materials*, 2008.

[51] M. A. Islam, M. S. Kabir, M. T. Rahman, T. Ferdous, A. S. M. Kamal. Zinc oxide nanoparticles improve seed germination and seedling performance in rice (*Oryza sativa* L.). *Journal of Plant Growth Regulation*, 2022, 41, 1235–1247.

[52] A. Rehman, M. Farooq, R. Ahmad, S.M.A. Basra. Seed priming with zinc improves the germination and early seedling growth of wheat. *Seed Science and Technology*, 2015, 43(2), 262–268.

[53] G. D. Savi, K. C. Piacentini, S. R. de Souza, M. E. B. Costa, C. M. R. Santos, V. M. Scussel,
Efficacy of zinc compounds in controlling *Fusarium head blight* and deoxynivalenol formation in wheat (*Triticum aestivum* L.). *International Journal of Food Microbiology*, 2015, 205, 98–104.

[54] E. Ibrahim, L. Xu, R. Nasser, A.-S. M. Adel, R. Hafeez, S. O. Ogunyemi, Y. Abdallah, Z. Zhang, L. Shou, D. Wang, B. Li. Utilizing zinc oxide nanoparticles as an environmentally safe biosystem to mitigate mycotoxicity and suppress *Fusarium graminearum* colonization in wheat. *Sustainable Materials and Technologies*, 2024, 41, e01028.

[55] A. Moncho-Jordá, A. A. Louis, J. T. Padding. How Péclet number affects microstructure and transient cluster aggregation in sedimenting colloidal suspensions. *Journal of Chemical Physics*, 2012, 136(6), 064517

.

5

Decontamination of maize kernels and degradation of mycotoxins by means cold plasmas

This Chapter is based on the following publication of the PhD candidate:

Stefania Somma, Mario Masiello, Miriam Haidukowski, Biancamaria Ciasca, Eloisa Sardella*, Pietro Favia, Fabio Palumbo, Marianna Roggio, Antonio Moretti* "Decontamination of maize kernels and degradation of mycotoxins by means of cold plasmas" *LWT*, **2025**, 215, 117205.

At the basis of this chapter, my contribution consisted in the design and execution of decontamination experiments using plasma technologies. I carried out treatments on artificially contaminated maize kernels and on filter paper, applying the different plasma configurations (CP, PTG, and PTW) and the corresponding operating conditions.

5.1 Introduction

Maize, among the most cultivated crops worldwide, plays a key and increasing role in global agri-food systems including direct food consumption and indirect feed pathways for animal-sourced foods. [1] In all maize-cultivated areas, specific pedoclimatic conditions can lead to both abiotic and biotic stresses, resulting in significant economic losses and threatened food safety for both unprocessed maize and its derived products.

Among biotic stresses, mycotoxigenic fungi are of particular concern, as they can colonize maize during the entire crop cycle and the post-harvest storage.

The most frequently occurring mycotoxigenic fungal species belong to the genera *Fusarium* and *Aspergillus*. *Fusarium proliferatum*, along with *F. verticillioides*, is associated to some of the most devastating fungal diseases of maize, including *Fusarium* ear and stalk rots, and *Fusarium* stem and root rots. *Aspergillus flavus* is also commonly detected on maize kernels in maturity and during storage. Although primarily found in tropical regions, this species has increasingly been reported in various areas of Europe due to recent climatic changes. [2] Contamination by *Fusarium* and *Aspergillus* species poses phytopathological issues and toxicological risks for humans and animals. Many of these species produce a wide range of mycotoxins, harmful secondary metabolites, that accumulate in maize kernels and often remain stable even after physical and chemical treatments, including high temperature used in food processing. The mycotoxins most frequently found worldwide on maize are fumonisins (FBs), particularly FB_1, FB_2, and FB_3 types, produced mainly by *F. verticillioides* and *F. proliferatum*, and aflatoxins (AFs), produced by *A. flavus* and, to a lesser extent, by other *Aspergillus* species. [3] Moreover, *F. proliferatum* is ubiquitous, capable of colonizing a wide range of important agricultural crops besides maize and other cereals, including vegetables and fruit trees. [4] This species produces not only FBs, but also other mycotoxins such as moniliformin,[5] beauvericin,[6] fusaproliferin,[7] and fusarins, [8] thus increasing the risk of multiple mycotoxin occurrence in foodstuff. Among FBs, FB_1 is classified by the International Agency for Research on Cancer (IARC) as possible carcinogen compound for humans (Group 2B; IARC, 2002). [9] Additionally, FBs can induce several significant health effects in livestock and other animals. [10] In contrast AFs, known for their acute toxicity, carcinogenicity, mutagenicity, teratogenicity, and immunosuppressive properties, are classified as Group 1 carcinogens for humans. [11] To address the toxic effects of FBs and AFs on humans and animals, European authorities have established maximum levels for these mycotoxins in food and feed to ensure safety (EC, 2006, 2007; EFSA, 2018). [12-13]

In line with Integrated Pest Management strategies, various agronomic, genetic and biological techniques, as well as agricultural practices, are now available to prevent or limit fungal diseases and associated mycotoxin accumulation. Different chemical and physical strategies are used globally to combat crop contamination and reduce fungal

species responsible for mycotoxin production. However, currently used decontamination procedures often have drawbacks, such as loss of nutritional properties and high environmental impact, which limit their application in the food industry.[14] Moreover, since the biological and chemical detoxification of mycotoxins is not permitted for human food within the European Union, physical methods are the only approved approaches in food industry. [15] This opens the way to the research of newer physical detoxification methods

When an atmospheric pressure plasma is fed with O_2, N_2 or mixtures of them, including air, reactive oxygen and nitrogen species (RONS) are produced. The most commonly found reactive species in atmospheric air plasma are O, OH, O_2^*, O_3, O_2^-, HO_2, H_2O_2, N, N_2^-, NO, NO_2, NO_3, and N_2O. When AP interacts with moisture, H_2O_2, NO_2^-, NO_3^- and $ONOO^-$ species are generated; these are considered long-lived reactive species with extended stability in aqueous phases. [16-20] It is widely believed that plasma-assisted food decontamination processes are initiated by RONS, creating a highly reactive environment that induces various changes in exposed targets. The decontamination efficiency is influenced by multiple factors, including feed gas, process parameters and plasma exposure mode (e.g., direct vs. indirect). [21]

Most literature focuses on the direct exposure of contaminated samples to plasmas, [22-23]where the target is completely immersed in the ionized gas and becomes part of the electric circuit, influencing the electrical properties of the discharge. This allows the target to benefit from the synergistic effects of direct UV radiation and short- and long-lived reactive species against fungi and/or mycotoxins, resulting in highly efficient processes. [24-27]The primary mechanisms of microbial destruction involve the breakdown of cell walls through reactions of RONS with peptiglycan layers, deterioration of cell membranes due to hyperoxidation of unsaturated fatty acids and proteins primarily attributed to OH radicals, and DNA oxidation.

In direct exposure modes, UV light and temperature are thought to have minimal effects on decontamination. [25,28-29] Indeed, increased UV light and heat can compromise product quality and organoleptic properties, potentially altering the genetics of kernels. [30-31]Furthermore, kernels germination time may be affected, posing ecological and safety risks to the final product. [32]Thus, it is crucial to develop milder approaches that maximize the beneficial decontaminating effects of plasma and minimize possible damage.

The referenced studies highlight growing interest in CAPs for food decontamination. Although several papers have reported the effects of direct CAPs on fungal species responsible for food spoilage and their metabolites, including mycotoxins,[33-34] most of these studies deal with *in vitro* experiments. However, recent advances on the application of CAPs vs mycotoxin degradation are available, providing discussion on possible working mechanisms and their effect on food quality, and on the toxicity of degradation products. [24,35-36]

The present paper shows that, besides the effects of UV radiation and electrical field, the RONS produced in N_2 and/or O_2 gas feeds play a pivotal role in mycotoxin degradation, as stated also by Liu et al. [21]To evaluate the effectiveness of RONS in kernel decontamination, we decided to test plasma processes fed with either pure O_2 or synthetic dry air. To enhance versatility and efficiency of these processes and minimize the risk of altering food quality, we opted to test the effect of a remote configuration, switching on the plasma far from the target, as well as evaluating the decontamination effects induced by plasma-treated water. [37-38]

The aim of this study is to explore alternative decontamination approaches for maize kernels and methods for mycotoxins degradation aided by soft plasma technologies. Additional aims are the investigation of the pattern of the degradation products of mycotoxins derived from plasma treatments, and the application of plasma technologies on naturally contaminated maize kernels.

5.2 Materials and Methods

5.2.1 Chemicals

Analytical-grade methanol (MeOH) was purchased from Mallinckrodt Baker (Milan, Italy). UPLC grade Acetonitrile was obtained from Merck (Merck KGaA, Germany). Ultrapure water was produced in house with a Millipore Milli-Q system (Millipore, Bedford, MA, USA). The (3*S*,7*R*)-11-methoxy-6,8,19-trioxapentacyclo[10.7.0.0^{2,9}.0^{3,7}.0^{13,17}]nonadeca-1,4,9,11,13(17)-pentaene-16,18-dione ($C_{17}H_{12}O_6$; AFB1 purity >99 %), the (2*R*)-2-[2-[(5*S*,6*S*,7*R*,9*R*,11*S*,16*S*,18*R*,19*R*)-19-amino-6-[(3*S*)-3,4-dicarboxybutanoyl]oxy-11,16,18-trihydroxy-5,9-dimethylicosan-7-yl]oxy-2-oxoethyl]butanedioic acid ($C_{34}H_{59}NO_{15}$, FB_1,

purity >99 %) and NaCl were purchased from Sigma (Milan, Italy). Filter paper grade 4 (20-25 µm particle retention) and glass microfiber filters (GF/A) were purchased from Whatman International Ltd. 132 (Maidstone, UK). AOF MS-PREP® immunoaffinity columns were obtained by Romer Lab (Romer Labs Inc., Tulln, Austria). The Phosphate Buffered Solution (PBS) at pH 7.4 was prepared by dissolving commercial PBS tablets (Sigma–Aldrich, Milan, Italy) in distilled water. Regenerated cellulose membrane filters (RC 0.2 µm) were obtained from Phenomenex (Bologna, Italy)

5.2.2 Plasma Processing

Three different treatment approaches were utilized on conidial suspensions of *A. flavus* and *F. proliferatum* plated on potato dextrose agar (PDA) medium or directly applied to maize seeds, namely: 1) remote plasma processing, where samples were positioned a few millimeters away from the plasma phase (Close Plasma treatment, CP); 2) introducing a stream of plasma-treated gas (Plasma Treated Gas, PTG) into a container with the contaminated samples; 3) processing the samples with plasma-treated tap water (Plasma Treated Water, PTW). All experiments and conditions, while part of a fundamental study, were selected with consideration of potential industrial scale-up, aiming to make the proposed processes competitive with current market decontamination protocols. For example, shorter treatment times, or, in the case of the PTW approach, using tap water instead of distilled water, could facilitate progress toward practical and industrial applications.

CAPs were generated with a modified Dielectric Barrier Discharge (DBD) PetriPlas+ plasma source, shown in **Figure 1** and described in detail elsewhere. [20, 39-40] The source consists of a Plexiglas flow unit equipped with gas connections and a discharge unit. A dry diaphragm pump (Pfeiffer Vacuum, Aßlar, GER) is connected directly to the flow unit for the CP approach and during the production of PTW, or through the sample holder containing the Petri dish with maize kernels in the case of PTG as shown in **Figure 1b**. The pump is used to evacuate exhaust gases and maintain the constant pressure of about 760 Torr, as measured with a MKS baratron.

An electric field of 6 kHz frequency and 13.8 kV peak-to-peak voltage was generated using a power supply connected to a programmable 10 MHz DDS function generator (TG1010A, Aim-TTi, Huntingdon, UK) to ignite a volume discharge of the size of the high voltage (HV) electrode (3 cm dia). The DBD discharges were ignited for 5 min, pulsed with a 50% duty cycle (D.C.), 50 ms of plasma on (t_{on}) over a period ($t = t_{on} + t_{off}$) of 100 ms. In the CP and PTW modes the discharge unit was adapted for treating maize kernels and tap water, respectively, contained in a Petri dish (6 cm dia) fastened under the DBD source, in a slot of the same diameter of the flow unit (Figure 1a-b). In both cases, the distance between the plasma and the surface of the sample to be treated was set at 2 mm.

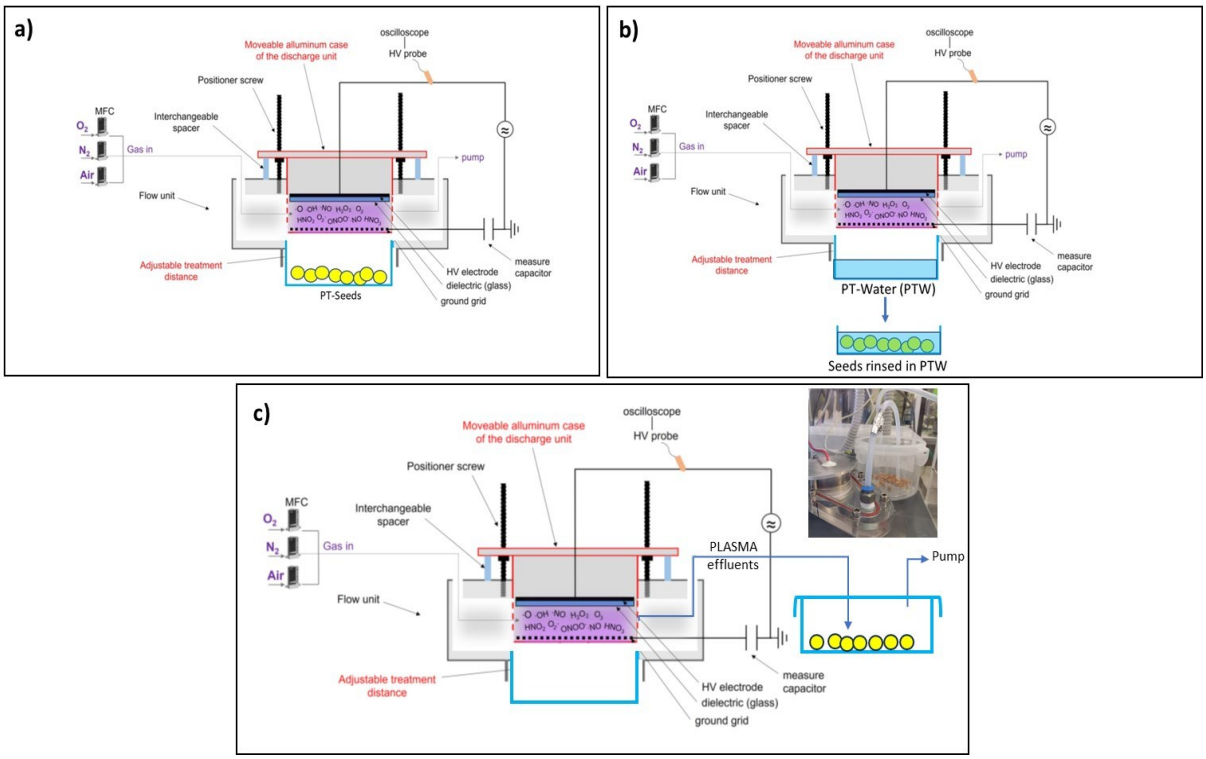

Figure 1. Schematic representations of cold atmospheric plasma treatment of maize kernels with a volume Dielectric Barrier Discharge (DBD) used in three different remote approaches: (a) CP treatment, with the sample underneath the plasma source; (b) PTW treatment, with the samples rinsed in tap water previously exposed to plasma; c) PTG process, with the samples exposed downstream to plasma gas effluents.

For the PTG treatments, a glass petri dish was positioned beneath the DBD, allowing the exhaust gas, along with its long-lived species, to flow through an external holder

containing a Petri dish filled with agar or maize kernels as shown in **Figure 1c**. All processes for the three approaches were carried out in a closed system, not exposed to the surrounding atmosphere; the reaction chamber was purged with the designed gas feed for 1 or 2 min before plasma ignition, depending on the approach used.

PTG and CP treatments of maize kernels were facilitated by diffusing RONS from the CAP to the samples through the grid, grounded, of the DBD (Figure 1b). Pure O_2 (air liquid, 99.999%) and synthetic air (air liquid, 99.999%) were used for the treatments. Gas flow rates were measured with MKS mass flow controllers. Concerning the PTW treatment, the H_2O_2 and NO_2^- concentration were previously determined, and the water pH as well.

The H_2O_2 concentration was quantified by a colorimetric copper–2,9-dimethyl-1,10-phenanthroline assay, while NO_2^- was determined using the Griess reaction; samples were appropriately diluted (1:4) with ultrapure water to ensure measurements within the linear range of the assays. The quantification of Reactive Oxygen and Nitrogen Species in PTW revealed that PTW-O_2 contain 218±9 μM of H_2O_2 and 1.4 ± 0,9 μM of NO_2^-, while PTW-Air contain 91± 9 μM H_2O_2 and 100 ± 7 μM of NO_2^-. The PTW-O_2 and PTW-Air have a pH respectively of around 6.1 and 5.8 starting from tap water at a pH of 6.2.

Table 1 summarizes the experimental conditions utilized in the plasma treatments, where each condition is denoted with a name that combines the treatment approach (CP, PTG or PTW) with the gas feed and treatment duration (es. CP-O_2 3 min).

Table 1. Experimental conditions used for plasma treatments of fungal conidia (agar medium-PDA, maize kernels) and AFB_1 and FB_1 mycotoxins (paper, maize kernels)

Treatment	Typology of sample	Duty Cycle (%)	Peak to peak voltage (kV)	Frequency (kHz)	Gas feed and flow (SLM)	Purging time (min)	Treatment time (min)
CP	Maize kernels (n°40 or 5 grams*), PDA, paper	50	13	6	O_2 or Air (0.5 SLM)	1	3, 20
PTG	Maize kernels (n°40 or 5 grams*), PDA, paper	50	13	6	O_2 or Air (1 SLM)	2	3, 20
PTW	Maize kernels (n°40), PDA sprayed with 2ml of tap water	50	13	6	O_2 or Air (0.5 SLM)	1	5

* for investigating the degradation of mycotoxins; SLM: standard liter per minute

5.2.3 Determination of the effects of plasma and reactive species on Aspergillus flavus and Fusarium proliferatum

Artificial contamination of Potato Dextrose Agar (PDA) medium and maize kernels and evaluation of conidial germination

Two aflatoxigenic *Aspergillus flavus* strains, ITEM 8095 and ITEM 8111, along with a single *Fusarium proliferatum* strain, ITEM 12072, were used to assess the effects of different plasma treatments on conidial germination. These strains, isolated from Italian maize, were selected within the ITEM microbial collection of the Institute of Sciences of Food Production (CNR-ISPA), for their ability to produce high levels of aflatoxins and fumonisins under both field conditions and *in vitro*.

For each strain, 100 µL aliquots of conidial suspension, along with three decimal dilutions were spread on PDA plates and subsequently exposed to CAPs in triplicate. Three untreated inoculated plates served as control. The conidial germination rates of control and plasma treated samples were analysed after 48 h of incubation at 25 °C.

To evaluate the effects of CAP treatments on maize kernel surface-contaminated with conidia, the kernels were first sterilized in autoclave. They were then inoculated after 1

min immersion in 100 µL conidial suspension (10^7 conidia/mL) and allowed to dry in microbiological hood at room temperature. For the CP and PTG treatments, maize samples artificially contaminated with fungal spores were placed in Petri dishes (40 kernels per dish). After the treatment, each sample was rinsed with 10 mL sterile distilled water to obtain conidial suspensions, which were then properly diluted and spread (100 µL) onto PDA plates.

For testing the activity of PTW, tap water instead of sterile distilled water was plasma treated to prepare conidial suspensions. This strategy was adopted to prevent a situation in which the initial contamination of samples with the conidial suspension, followed by either spraying or, more critically, immersion in PTW, might result in mechanical removal (wash-off) of the conidia, rather than achieving the intended inhibitory effect. After 48 h of incubation at 25 °C the germinated conidia capable of forming fungal colonies on the PDA plates were counted. A conidial suspension in sterile distilled water was used as control.

Evaluation of the effects of plasma treatments on conidial germination

After 48 h of incubation at 25 °C the germinated conidia capable of forming fungal colonies on the PDA plates were counted. The effect of plasma treatments on the germination was assessed by comparing the number of colonies in each treated group with the number of colonies in the controls (untreated theses). Each reported value represents the mean of three replicates. The inhibition of germination, expressed as a percentage, was calculated using the following formula:

$$\text{Inhibition (\%)} = [(C - T)/C] \times 100)$$

where C is the number of colonies grown in the control sample and T represents the number of colonies grown in the treated sample.

5.2.4 Evaluation of the effect of plasma on AFB_1 and FB_1 mycotoxins

Preparation of mycotoxins standard solutions

Stock 1 mg/mL solutions of AFB_1 and FB_1 were prepared by dissolving solid commercial toxins in acetonitrile and a 50:50 (v/v) acetonitrile/water solution, respectively. The AFB_1 solution was then diluted to 1 µg/mL in acetonitrile, while the FB_1 solution was diluted to

100 µg/mL in the acetonitrile/water mixture. These solutions were utilized for spiking experiments on maize kernels and paper filter to evaluate the degradation efficiency of the various treatments. Quantification of mycotoxins was performed using a matrix-matched calibration curve for the detection on maize kernels (20 - 100 µg/kg for AFB_1 and 100 - 1000 µg/kg for FB_1) and a standard calibration curve for the detection on paper (0.02-0.10 µg/mL for AFB_1 and 0.1-1.0 µg/mL for FB_1).

Contamination of filter paper and maize kernels with AFB_1 and FB_1 standard solutions

The effect of plasma exposure on AFB_1 and FB_1 was evaluated independently using distinct samples on both filter paper and maize kernels. For each mycotoxin, a set of 18 samples was prepared and analyzed: 3 contaminated samples for each plasma treatment (CP-O_2, CP-Air, PTG-O_2, PTG-Air); 3 contaminated untreated samples (positive control); 3 uncontaminated plasma treated samples of maize kernels (negative control).

Filter paper and maize kernels (5 g) were artificially contaminated with 0.25 mL of AFB_1 solution (1 µg/mL) and 0.05 mL of FB_1 solution (100 µg/mL). This resulted in final concentrations of 0.05 µg/mL on paper and 50 µg/kg on maize kernels for AFB_1, as well as 1 µg/mL on paper and 1000 µg/kg on maize kernels for FB_1. To detect potential AFB_1 degradation products, which are likely to be present in much smaller amounts than the original compounds, and considering the instrumental sensitivity, it was necessary to select a level of AFB_1 contamination in maize kernels that was one order of magnitude above the maximum limit in food and feed. The samples were allowed to rest at room temperature for approximately two hours to facilitate the evaporation of the solvent.

Mycotoxin analysis by LC-HRMS

The quantification of mycotoxins in filter paper samples was performed after extraction with 3 mL of methanol/water (70:30, v/v). The samples were filtered through a 0.22-µm RC syringe filter before injection into the LC-HRMS apparatus.

For quantifying the mycotoxins in kernel samples, AOF MS-PREP® immunoaffinity column cleanup was run according to the manufacturer instructions. Briefly, 5 g of kernel samples and 1 g of NaCl were extracted with 20 mL of methanol/water (60:40, v/v), blended at high speed for 2 min. After centrifugation (4000 rpm, 10 min), 10 mL of the filtrate were diluted

with 15 mL of PBS. Following filtration through glass microfiber filter paper, 5 mL of the filtrate (equivalent to 0.5 g of sample) were injected in the column. The column was rinsed with 20 mL of water before elution. The toxins were eluted from the column with 1 ml of methanol followed by 1 mL of water. The final sample (10 µL) was then injected in the UHPLC-HRMS/MS equipment.

For analysing degradation products, additional sample of treated and control maize kernels were prepared and extracted with 20 mL of methanol/ultrapure water (80:20, v/v) in orbital shaker for 1 h. The extracts were then diluted tenfold with water, centrifuged (15000 rpm, 4 °C, 20 min) and injected in the UHPLC/HRMS equipment.

Liquid chromatography–HRMS analysis was performed with a Q-ExactiveTM Plus mass spectrometer, equipped with a heated electrospray ion source (HESI II) coupled to an Ultimate 3000 UHPLC system (all from Thermo Fisher Scientific, San Jose, CA, United States). A Gemini UHPLC C18 column (150 × 2 mm, 5-µm particles, Phenomenex, Torrance, CA, United States) was used, preceded by a Gemini C18 guard column (4 × 2 mm). The column oven was set at 40 °C. The injection volume was 20 µL. The flow rate of the mobile phase was set at 200 µL/min, with eluent A water and eluent B methanol, both containing 0.5% acetic acid and 1 mM ammonium acetate. For creating the gradient, the proportion of eluent B was kept constant at 10% for 5 min and then linearly increased to 80% in 36 min. Finally, it was raised to 100% and kept constant for 5 min. The column was re-equilibrated with 10% eluent B for 9 min. The HESI II ion source was operated both in positive and in negative ion modes, with parameter settings reported in Ciasca *et al*. [38]
AFB_1 and FB_1 degradation ratio and degradation standard deviation (SD) were evaluated using the following formulas:

$$(AFB_1/FB_1)\ degradation\ ratio\ \% = \frac{(AFB_1/FB_1)\ peak\ area\ in\ control\ -\ (AFB_1/FB_1)\ peak\ area\ in\ treatment}{(AFB_1/FB_1)\ peak\ area\ in\ control} \times 100$$

$$\text{Degradation SD} = \frac{\text{Treatment peak area}}{\text{Control peak area}} * \sqrt{\left(\frac{\text{treatment SD}}{\text{treatment peak area}}\right)^2 + \left(\frac{\text{control SD}}{\text{control peak area}}\right)^2}$$

Statistical analyses

The standard deviation values for all theses were calculated, based on three replicates. The one-way analysis of variance (ANOVA) was used to determine whether there are any statistically significant differences between the treatments. The means were then compared using the Tukey's multiple comparisons method as post-hoc test. If the p-value for the 95% confidence interval was below 0.05, differences were considered significant. Statistical analyses were performed using GraphPad version 10.0.0 software.

5.3 Results

5.3.1 Activity of the plasma treatments on Aspergillus flavus

The quantification of the fungal colonies developed on PDA after each treatment compared to the untreated controls was used to calculate the inhibition of germination induced by the plasma treatments. The results shown in **Figure 2** and **Figure 3** are derived from at least six different experiments in all treatment conditions. The data for *A. flavus* result from experiments run on two different strains showing a high level of reproducibility.

Figure 2 shows the results of conidia spread on PDA before the treatments. All treatments were found to effectively reduce conidial germination, with inhibition values ranging from 35% (PTW) to 100% (PTG). Specifically, PTW exhibited a notable but lower and significant ($P<0.0001$) efficacy compared to the other treatments, with about 44% inhibition. In contrast, both CP and PTG treatments resulted in 100% inhibition of germination for *A. flavus*, regardless of gas feed and treatment times used.

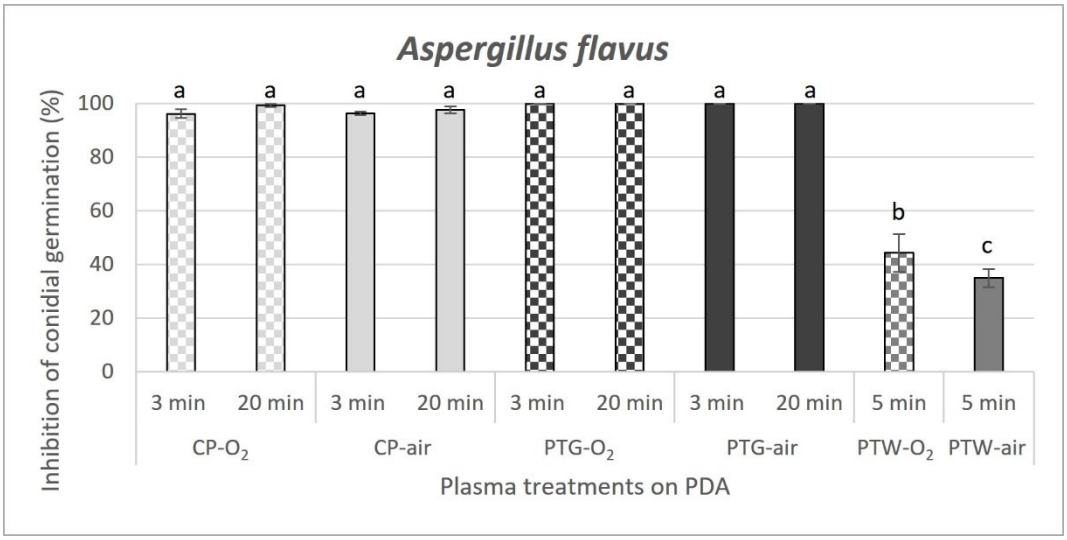

Figure 2. Inhibition of conidial germination of *Aspergillus flavus* grown on potato dextrose agar (PDA) after plasma treated tap water (PTW), direct plasma treatment (CP) and plasma treated gas (PTG), with air or O_2. Inhibition values were calculated by comparing the germinated conidia of each treatment thesis with the relative control. Standard deviations are also reported. Means with a different letter indicate significant differences between treatments at 0.05 level of significance.

The second set of experiments, with results shown in **Figure 3**, focused on maize kernels contaminated in the lab with *A. flavus* spores to simulate natural contamination. These experiments dealt only with the CP and PTG approaches, which were identified as the most effective in the previous set of data, as illustrated in Figure 2.

A comparison of **Figure 2** and **Figure 3** clearly shows that treatments on maize kernels result generally less effective than those on PDA. Additionally, the standard deviations in **Figure 3** suggest that the results for kernels are less reproducible, likely due to the irregular shape of the kernels. Among the treatments tested, the PTG-O_2 20 min appeared to be the least effective, although any significant difference ($P<0.1$) was detected from statistical analysis. In contrast,

for the CP approach, particularly at 3 min treatment time, the CP-O_2 treatment exhibits greater efficacy compared to CP-Air. At 20 min treatment time, the CP processes display similar effectiveness independently on the feed used.

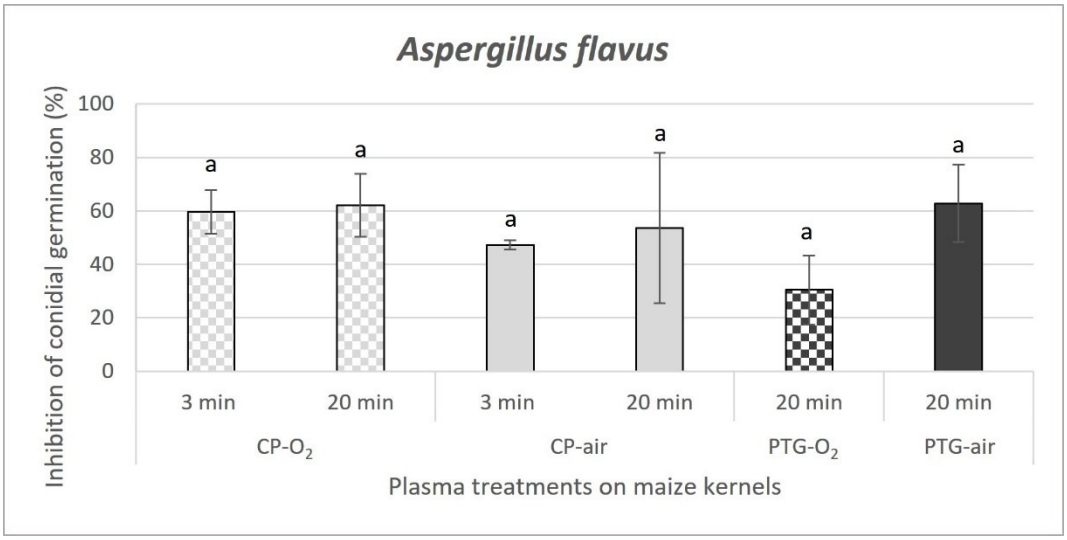

Figure 3. Inhibition of conidial germination of *Aspergillus flavus* contaminating maize kernels surface, after direct plasma treatment (CP) and plasma treated gas (PTG), with air or O_2. Inhibition values were calculated by comparing the germinated conidia of each treatment thesis with the relative control. Standard deviations are also reported. Means with a different letter indicate significant differences between treatments at 0.05 level of significance.

5.3.2 Activity of the plasma treatments on F. proliferatum

Similarly to *A. flavus*, the conidial suspensions of *F. proliferatum* spread on PDA also showed complete inhibition of conidial germination under all conditions tested in both CP and PTG experiments, as shown in **Figure 4**.

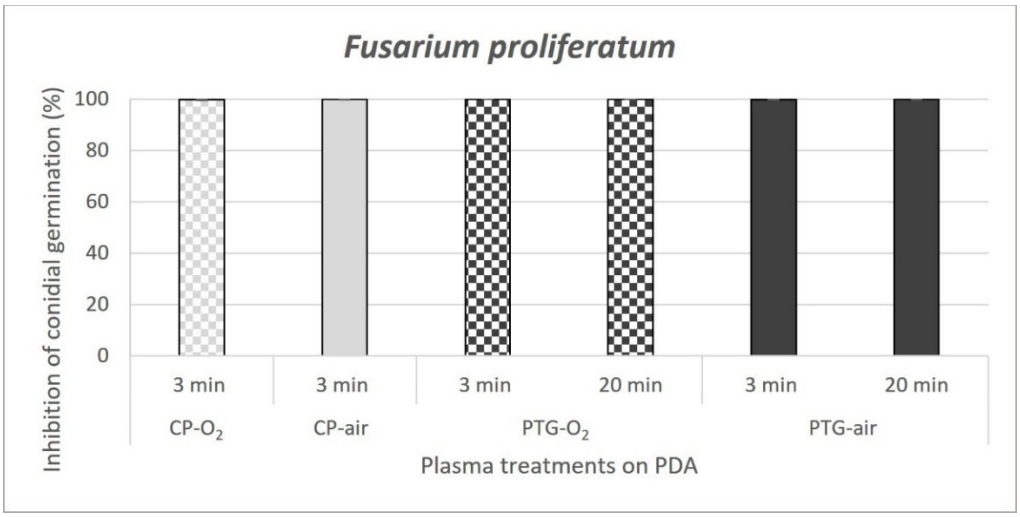

Figure 4. Inhibition of conidial germination of *Fusarium proliferatum* grown on potato dextrose agar (PDA), after plasma treated tap water (PTW), direct plasma treatment (CP) and plasma treated gas (PTG), with air or O_2. Inhibition values were calculated by comparing the germinated conidia of each treatment thesis with the relative control. Standard deviations are also reported.

Maize kernels contaminated with *F. proliferatum* were exposed to CP and PTG treatments using either O_2 or air-feeds; the resulting inhibition growth data are presented in **Figure 5**. As for *A. flavus*, on maize kernels contaminated with *F. proliferatum* the PTW approach proved less effective than the other methods, with significant differences ($P<0.0001$) in inhibiting the conidial germination, regardless the gas feed. Indeed, the two other approaches yielded approximately 60% inhibition across all treatment times and feeds used, except for the PTG-air 20 min treatment, which gives about 90% inhibition. Similarly to what is found for *A. flavus*, the PTG-air 20 min treatment appears to be the most effective, significantly different ($P<0.0001$) from the other treatments. Overall, under the experimental conditions investigated, regardless of the gas feed used, the PTW approach results less effective than the two approaches in dry conditions.

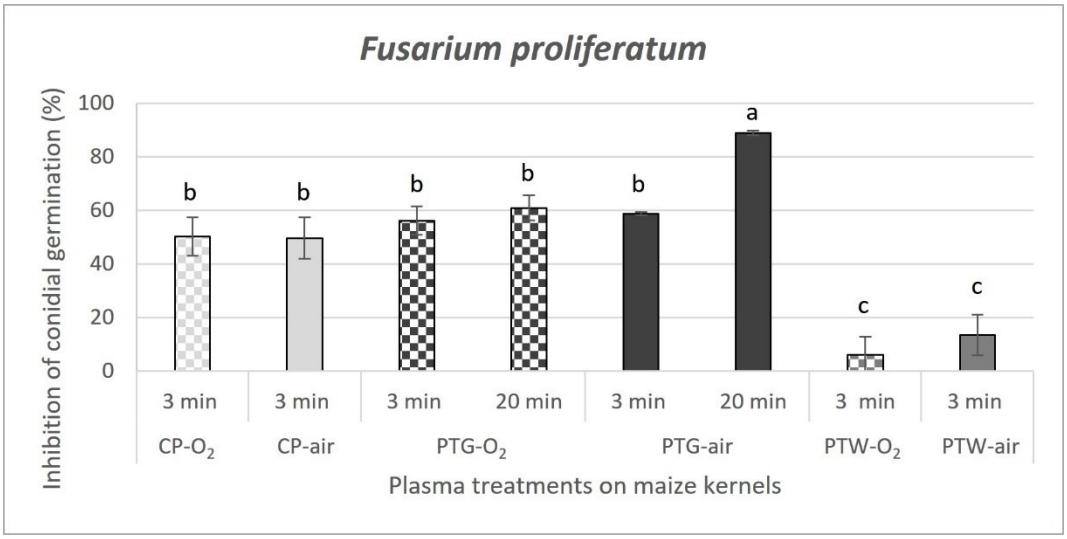

Figure 5. Inhibition of conidial germination of *Fusarium proliferatum* contaminating maize kernels surface, after plasma treated tap water (PTW), direct plasma treatment (CP) and plasma treated gas (PTG), with air or O_2. Inhibition values were calculated by comparing the germinated conidia of each treatment thesis with the relative control (C). Standard deviations are also reported. Means with a different letter indicate significant differences between treatments at 0.05 level of significance.

We can conclude that for maize kernels artificially contaminated with *F. proliferatum* or *A. flavus*, an inhibition percentage of conidial germination of at least 50% was obtained with the CP and PTG treatments investigated.

5.3.3 Activity of plasma treatments on mycotoxin contamination

After having established the various efficacy of CP and PTG treatments on conidial germination of *F. proliferatum* and *A. flavus*, we have investigated the ability of the plasma processes to degrade AFB_1 and FB_1 mycotoxins produced by these fungi on filter papers and on maize kernels artificially contaminated (50 µg/kg AFB_1; 1000 µg/kg FB_1). Indeed, as shown in **Figure 6**, all treatments exhibit satisfactory degradation rates for AFB_1 on filter paper, higher than 52%, with the exception of the CP-O_2 3 min treatment. In contrast, for FB1 on paper a slightly lower degradation efficacy is measured, higher than 40%, compared to AFB_1. A significant difference between the CP-O_2 20 min treatment and the other treatments is observed for the degradation of FB_1 on paper. Most of the treatments lead to higher degradation efficiency when applied to a standard mycotoxin solution, except for the CP-O_2 20 min treatment which shows a higher efficiency of FB1 degradation

on maize kernels. Overall, only minor differences in degradation rate are observed based across all treatment approaches and feed used.

The degradation percentage of FB_1 after the CP-O_2 20 min treatment was also assessed for maize samples naturally contaminated with 650±56 µg/kg of FB_1, resulting in a 68% contamination reduction, consistent with the detoxification results obtained on paper for the same process.

In summary, for artificially FB_1 contaminated maize kernels, treatments with O_2 were found significantly more effective than those with air, with the CP-O_2 approach showing the highest mycotoxin degradation rate at both treatment times used. Conversely, for AFB_1 contaminated maize kernels, the two indirect PTG processes at the longest treatment time of 20 min gave the best results for AFB_1 degradation.

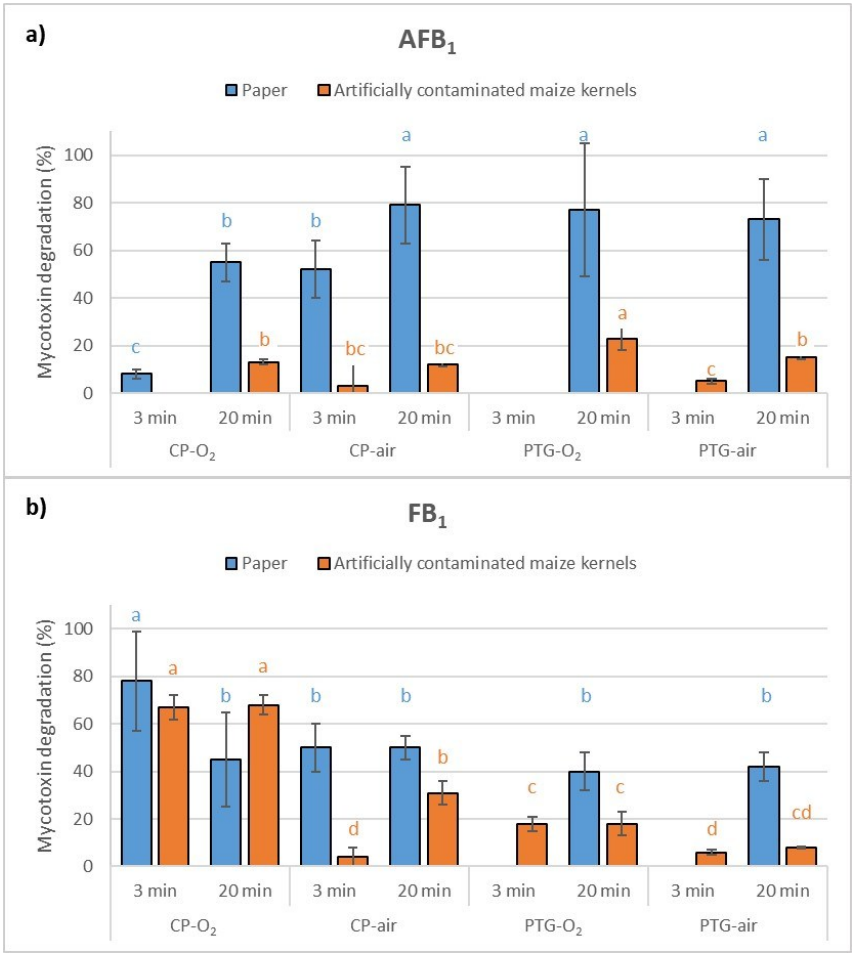

Figure 6. Degradation percentage (%) of **a)** aflatoxin B_1 (AFB_1) and **b)** fumonisin B_1 (FB_1) on paper and kernel maize after CP or PTG treatments with different feed (O_2 or air) and process time (3 or 20 min). Standard deviations are also reported. Means with a different letter indicate significant differences between treatments at 0.05 level of significance.

5.3.4 Investigation of the degradation products in maize kernels contaminated with AFB$_1$

Given the effectiveness of the PTG-O_2 20 min treatment against AFB_1 and considering that the conditions of such treatment are particularly gentle, very interesting for practical applications, we decided to investigate the by-products formed after treating AFB1 in such way. The presence of AFB_1 degradation by-products was assessed on maize kernels artificially contaminated and treated using the PTG-O_2 20 min mode as shown in **Figure 7**.

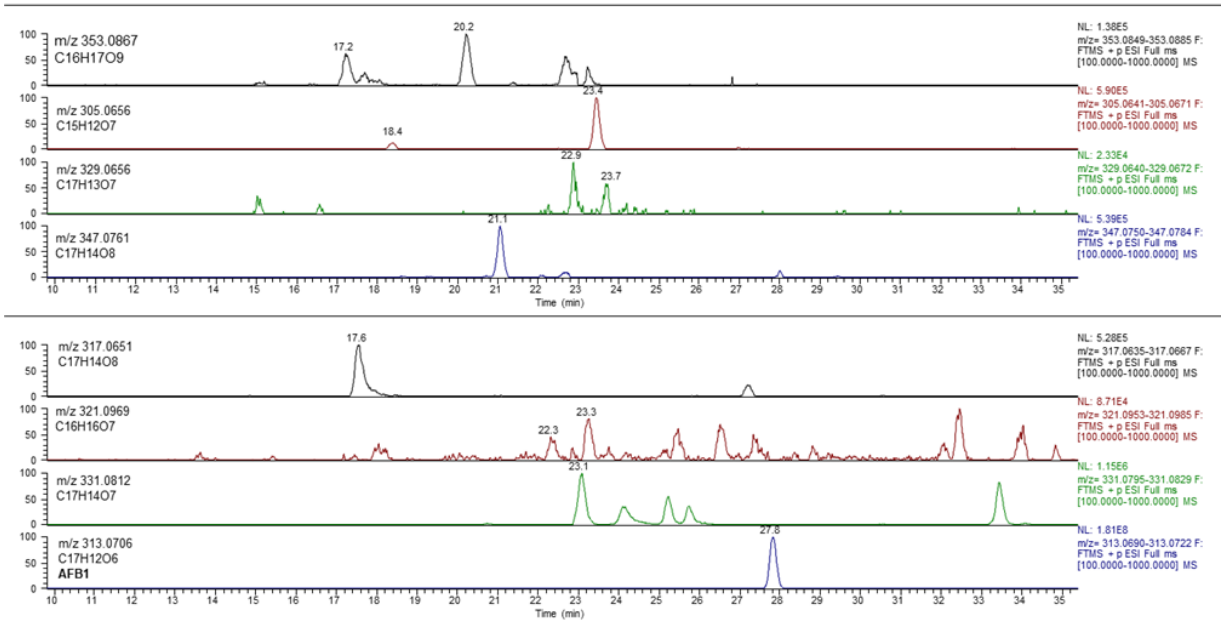

Figure 7. UHPLC-HRMS chromatogram of maize contaminated with 1 µg/g of AFB_1, treated with the PTG-O_2 20 min process. Peaks attributable to AFB_1 and degradation products (m/z 353.0867, 305.0656, 329.0656, 347.0761, 317.0651, 321.0969, 331.0812 and 313.0706) are shown. Resolution: 70,000 FWHM; extraction window tolerance 5 ppm.

In **Table 2** the proposed degradation products of AFB_1 are listed, with their molecular formula, structures, and n-octanol-water partition coefficient (log P).

Table 2. Proposed degradation products with relative molecular formula, exact mass ([M+H]+), retention time (RT) and n-octanol-water partition coefficient (LogP).

AFB_1 $C_{17}H_{12}O_6$ 313.0706/335.0526 logP:0.45	2,3,6a, 9a – tetrahydro-4-methoxycyclopenta [c]furo[2,3:4,5[furo[2,3-h] chromene-1,11-dione 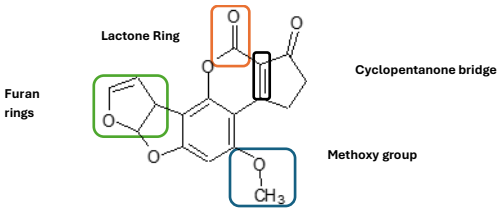
Product 1 $C_{16}H_{16}O_9$ 353.0867/375.0686 logP: -2.68 RT: 17.2 min, 20.2 min	2-oxo-5-(2,4,6,7-tetrahydroxy-2,3,3a,8a-tetrahydrofuro[2,3-b]benzofuran-5-yl)cyclopentanecarboxylic acid 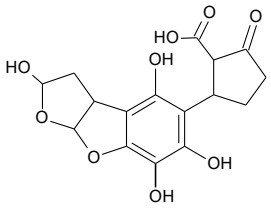
Product 2 $C_{15}H_{12}O_7$ 305.0656 logP: -0.91 RT: 18.4 min	2,3-dihydroxy-9-methoxy-2,3,7,8-tetrahydrocyclopenta[c]furo[2,3-h]chromene-5,6-dione 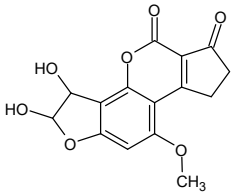
Product 3: AFQ1/ epi AFQ1 $C_{17}H_{12}O_7$ 329.0656 logP: -0.5 RT: 22.9 min, 23.7 min	3(R) -3 -hydroxy-4-methoxy-2,3,6a, 9a-tetrahydrocyclopenta[c]furo[3', 2':4,5]furo[2,3-h]chromene-1,11-dione 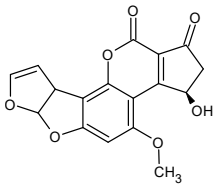
Product 4 $C_{17}H_{14}O_8$ 347.0761/369.0581 logP: -0.39 RT: 21.05 min	(A) AFB_1 8,9 dihydrodiol 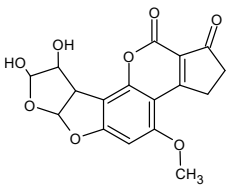 (B) AFB_1 8,9 dihaldeide 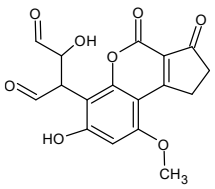

Product 5 $C_{16}H_{12}O_7$ 317.0656/339.0475 logP: 0.07 RT: 17.6 min, 23.4 min	4,8 - dihydroxy-2,3,6a,8, 9, 9a-hexahydrocyclopenta*[c]*furo[3',2':4,5]furo[2,3-h]chromene-1,11-dione 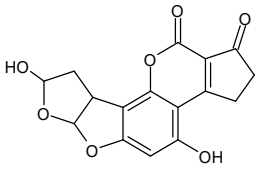
Product 6 $C_{16}H_{16}O_7$ 321.0969 logP: 0.6 RT: 22.3 min, 23.6 min	2-(2,4-dihydroxy-2,3,3a,8a-tetrahydrofuro[2,3-b]benzofuran-5-yl)-5-hydroxycyclopent-1-ene-1-carboxylic acid 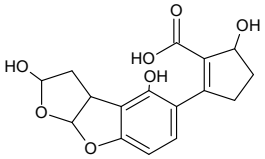
Product 7 $C_{17}H_{14}O_7$ 331.0812/ 353.0632 logP: 1.37 RT: 23.1 min	2-(6-methoxy-4-methyl-3a,8a-dihydrofuro[2,3-b]benzofuran-5-yl)-5 oxocyclopent-1-ene-1-carboxyl acid 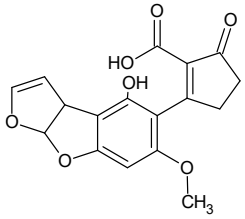

To elucidate the structure relative to all detected peaks, MS/MS spectra were analysed (**Table 3**), and the detected fragments were compared with MS/MS spectra reported in the literature.

Table 3. Retention time, molecular formula, and exact mass of the investigated products.

		Parent Ion		Product Ions	
	Retention Time (min)	Molecular Formula	Exact Mass $[M+H]^+$	Exact mass $[M+H]^+$	Molecular formula
Product 1	17.2	$C_{16}H_{16}O_9$	353.0867	No detected	
Product 2	18.4	$C_{15}H_{12}O_7$	305.0656	259.0601	$C_{14}H_{10}O_5$
Product 3 (AFQ1 – epi AFQ1)	22.9/23.7	$C_{17}H_{12}O_7$	329.0656	311.0542 283.0588 259.0594	$C_{17}H_{11}O_6$ $C_{16}H_{11}O_8$ $C_{14}H_{11}O_5$
Product 4	21.1	$C_{17}H_{14}O_8$	347.0761	329.0656 319.0811 311.0538 301.0697 273.0747	$C_{17}H_{13}O_7$ $C_{16}H_{15}O_7$ $C_{17}H_{11}O_6$ $C_{16}H_{13}O_6$ $C_{15}H_{13}O_8$
Product 5	17.6/23.4	$C_{16}H_{12}O_7$	317.0651	289.0707	$C_{15}H_{12}O_6$
Product 6	22.3/23.6	$C_{16}H_{16}O_7$	321.0969	301.0697 273.0747	$C_{16}H_{13}O_6$ $C_{15}H_{13}O_8$
Product 7	23.1	$C_{17}H_{14}O_7$	331.0812	313.0707 285.0757	$C_{17}H_{12}O_6$ $C_{16}H_{12}O_5$
AFB_1	27.8	$C_{17}H_{12}O_6$	313.0706	285.0757 241.0495	$C_{16}H_{12}O_5$ $C_{14}H_9O_3$

5.4 Discussion

Food contamination by toxigenic fungi like *Aspergillus*, *Fusarium*, *Alternaria*, and *Penicillium,* as well as by their mycotoxins, is a current health issue arising significant political and economic implications. The CAP technology offers a promising alternative to conventional decontamination methods, demonstrating effectiveness in fungi inactivation, in interfering with mycotoxins biosynthesis, and in mycotoxins degradation. [39-41]

In this study we compared different plasma assisted approaches, both in dry (CP and PTG) and in wet conditions (PTW) to assess their efficacy against two toxigenic fungal

species and their AFB_1 and FB_1 mycotoxins commonly found in maize. The PTW approach indeed has been soon excluded after preliminary tests due to its low effectiveness on fungal inactivation in the experimental conditions used in this research.

The limited efficacy of PTW was attributed to the low concentrations of stable reactive species (i.e., H_2O_2 and NO_2^-) generated, as well as to a pH that was not sufficiently low, as reported in the literature for plasma-treated water approaches to achieve effective inhibition of fungal proliferation.

Our findings indicate that CAP treatments significantly inhibit conidial germination and subsequent colony development of *A. flavus* and *F. proliferatum*. Previous studies have reported similar efficacy of cold plasma processe against mycotoxigenic fungi. [27,33,42] Although studies exist on *A. flavus* and aflatoxins reduction after plasma treatments,[43-44] we believe that our research is the first to examine the effects of CAP processes on *F. proliferatum*, since most of the reports found deal with other *Fusarium* species.[45-46]

Plasma processes, indeed, were found more effective versus conidia grown in vitro in PDA compared to conidia contaminating maize kernels. This discrepancy may be attributed to the complexity of the maize kernels tridimensional shape, which limits the complete exposure of their surface to plasma components (i.e. UV-vis, electromagnetic field etc.) and, mainly, to plasma-generated RONS. Indeed, to improve the reproducibility and the homogeneity of the treatment, the holder of the kernels was shaken during the plasma processes. This could be considered a limitation of the treatments on plant materials but can be easily overcome in the industrial applications.

This study, however, shows clearly that fungal development could be inhibited by at least 50% and up to 90% with just few minutes of dry CAP treatments using air or O_2 (**Figure 3** and **5**). Notably, in the case of PTG, air plasma appeared more effective than O_2. Working in a closed system we are sure that no contamination from atmospheric N_2 occurs in O_2 plasma processes; this allows to exclude any effect of reactive nitrogen species (RNS) on the targets with respect to reactive oxygen species (ROS). Using O_2 as gas feed of CAPs enhances the production of ROS such as ozone (O_3), which is beneficial for reducing microbial load .[47] Higher levels of O_3 in O_2-fed CAPs have been linked to reduced microbial counts on surfaces like hazelnuts.[48] N_2 is also used as feed in CAPs for generating reactive nitrogen species that can further interact with O_2 to form gaseous

compounds such as NO, NO_2, and NO_3^- ions in water media, all of known antimicrobial activity. [49]

The application of various approaches to decontaminate maize kernels indicates that, in the case of CP treatments, changing treatment time and gas feed among our parameters has minimal impact. The slight effects of the electric field, UV radiation, and both long- and short-lived species may be more influential, instead. Although the CP process is carried out in remote, the potential influence of other plasma components with RONS, cannot be entirely disregarded. [39] In contrast, for the plasma treatments with the gas effluents from CAPs, PTG, where only chemical effects can be active obviously due to the presence of stable ROS, a clear difference is seen depending on the feed used on maize kernels contaminated with *A. flavus* and *F. proliferatum*. Specifically, the PTG-air process results significantly more effective than the PTG-O_2, highlighting the more active role of RONS (e.g.,NO, NO_2,) with respect to ROS (e.g. O_3) in the decontamination process. NO_3^- ions can also be formed in presence of moisture or liquid water.

In contrast, among the approaches tested in our research, PTW treatments cannot be recommended for further investigation, as this approach proved to be the least effective against both *A. flavus* and *F. proliferatum*. The reduced efficacy of PTW compared to CP and PTG tretaments may stem from the absence of RONS insoluble in the PTW, such as O_3, which indeed play a crucial role in dry decontamination processes. [50]Another disadvantage of PTW processes is that their implemention for industrial kernel processing may be more complex, more costly and less versatile than dry decontamination methods.

In terms of mycotoxin abatement, similalyr as it is found for conidia contaminated substrates, CAP approaches proved more effective on flat (paper) substrates than on to maize kernels. The reduced degradation of mycotoxins observed in the presence of a food matrix is documented; a recent review, [21] in fact, highlights that in CAP-based degradation approaches, mycotoxins may not be directly exposed to plasma and its components because hidden in the grooves of the food. Additionally, food features such as surface area, roughness and composition can influence degradation rates. Specifically, roughness and smoothness of the food surface affect the contact area between mycotoxins and reactive species, thereby impacting the degradation efficiency.

Our processes revealed different effects for FB_1 and AFB_1. For FB_1, treatment time did not

significantly influence the degradation efficiency. Among the tested approaches, a 20 min CP-O_2 treatment resulted in the highest FB_1 degradation (68%) for artificially contaminated maize, a finding that was also confirmed for naturally contaminated kernels.

In contrast, treatment time was particularly relevant for degrading AFB_1, as the maximum degradation (23±5% on kernels and 77±28% on paper) was only achieved after 20 min of the PTG-O_2 process. These results were consistent for both paper and artificially contaminated kernels. The impact of exposure time on AFB_1 degradation was also studied by Siciliano *et al.*,[51] who assessed the efficiency of DBD plasma for degrading AFs in standard solutions under different conditions. They found that at low plasma power (400 W) 12 min exposure time was needed to be effective, while in more aggressive conditions, 1000 W power with 100% N_2 feed, 100% degradation of AFB_1 was achieved even at the short exposure time of 1 min. When comparing our data (from dry food) with those reported by Siciliano *et al.*, [52] which were conducted on liquid solutions of mycotoxins, it is important to consider that the liquid matrix can actively contribute to the formation of additional RONS, further aiding in mycotoxin degradation.

In artificially contaminated maize kernels, the PTG-O_2 treatments achieved a higher degradation of AFB_1, comparable with that reported by Iqdiam *et al*. [53] for aflatoxin degradation in peanuts after CAP jet treatments. However, our approach is clearly less invasive and quicker, as it can process several seeds simultaneously. It is important to mention that the AFB_1 concentration used in our research on artificially contaminated kernels was ten times higher than the allowed limit.

We have also investigated the degradation products of AFB_1 after a 20 min PTG-O_2. treatment. So far, only a limited number of studies have explored the degradation pathways and products of mycotoxins plasma treated in remote. Most papers on AFB_1 degradation products focus on modifications of the terminal furan rings,[53] indeed, alterations to the lactone ring and the methoxy group have also been reported .[54]

AFB_1 can be metabolized and bioactivated by CYP450 enzymes, leading to the formation of the highly toxic epoxy compound aflatoxin B1-8, 9-epoxide, which can bind to intracellular biomacromolecules like DNA, RNA, and proteins, causing gene mutations, thus potentially resulting in cytotoxicity and carcinogenesis. [33] The difuran ring in AFB_1 is

considered primarily responsible for its toxicity and carcinogenicity, particularly the double C=C bond on the terminal furan ring . [54]

Our study identified the most abundant degradation product in the PTG-O_2 treated maize samples at m/z 305.0656, resulting from the cleavage and hydroxylation of the remaining furan ring. This finding is in agreement with those of Wielogorska *et al.* [53] We identified seven AFB_1 degradation products after accurate mass measurements, with an error of less than 2 ppm, and fragmentation pattern analysis, as detailed in **Table 3**.

Product 3 (m/z: 329.0656) is related to AFQ1 or epi-AFQ1, a metabolic AFB_1 product produced by cytochrome P450 enzymes, which is readily excreted in urine. Product 1 (m/z: 353.0867) results from the addition of a hydroxyl group to the benzene ring. Product 4 (m/z: 347.0761) differs by 34 mass units from AFB_1, suggesting the presence of two hydroxyl groups; it is attributed to AFB_1 8,9-dihydrodiol or AFB_1 dialdehyde, as noted by Loi *et al.* (2023). Product 5 (m/z: 321.0969) is believed to form through an addition reaction at the C(8)–C(9) bond, accompanied by lactone ring opening and O-cleavage of the methoxy group at C(4) of the benzene ring, a product also reported by Wang *et al.* [54] Finally, product 7 (m/z: 331.0812) was detected by Shi *et al.* [53] after a high-power CAP treatment of pure AFB_1 powder on a glass slide. The double C=C bond on the terminal furan ring is the main functional group responsible for toxic effects, and our results demonstrate that plasma-generated ROS can react with this moiety of the molecule.

Based on the considerations presented, the plasma-chemical treatments discussed in this paper offer a valid and significantly more versatile alternative to the technologies currently employed and tested in the field of food and seed decontamination. Among the promising low-temperature decontamination methods, high-pressure carbon dioxide (HPCD) could be a potential alternative to plasma-based approaches, particularly due to its ability to operate at lower temperatures than thermal pasteurization. [54] However, HPCD has limitations, notably requiring the sample to be moist for optimal efficacy, which makes it less suitable for dehydrated seeds like maize.[53] While HPCD is effective against microorganisms, it has minimal effect on biomolecules such as mycotoxins, as CO_2 exhibits little reactivity with these toxins. In contrast, plasma-assisted technologies offer similar low-temperature benefits but are also effective in degrading mycotoxins, as shown in our study. Moreover, plasma-based methods can be easily integrated into existing production lines and applied after packaging, enhancing their potential for

industrial use.

5.5 Conclusions

This study investigates the feasibility of fungal decontamination and mycotoxins degradation through plasma assisted processes run in three different approaches. The results indicate that both *A. flavus* and *F. proliferatum* are significantly impacted by plasma treatments, both *in vitro* and on maize kernels. A notable advantage of the indirect use of CAPs has been registered, with no contact on the kernels, which minimizes possible heating of the target. Our results demonstrate that the chemical effects of plasma on fungi arise from a combination of RONS. Specifically, air-fed plasmas in the PTG configuration result more effective than those fed with O_2. The investigation on mycotoxins shows that both air and O_2-fed CAPs possess high degradation potential for AFB_1, while CP-O_2 treatment proves most effective to degrade FB_1, probably due to the structural differences between the molecules.

In summary, this paper highlights the significant impact and efficacy of remote plasma-assisted approaches in promoting the decontamination of food from fungi and mycotoxins. It emphasizes the versatility of these soft physical decontamination methods, as they can be consistently applied regardless of the target of interest.

5.6 References

[1] O. Erenstein, M. Jaleta, K. Sonder, K. Mottaleb, B. M. Prasanna. Global maize production, consumption and trade: trends and R&D implications. *Food Security*, 2022, 14, 1295–1319.

[2] M. Camardo Leggieri, P. Toscano, P. Battilani. Predicted aflatoxin B1 increase in Europe due to climate change: actions and reactions at global level. *Toxins*, 2021, 13(4), 292.

[3] R. H. Proctor, A. E. Desjardins, A. Moretti. The role of plant pathology in food safety and food security: Biological and chemical complexity of *Fusarium proliferatum*. Springer, Dordrecht, 2009, pp. 97–111.

[4] W. F. O. Marasas, P. G. Thiel, C. J. Rabie, P. E. Nelson, T. A. Toussoun. Moniliformin production in *Fusarium* section *Liseola*. *Mycologia*, 1986, 78, 242–247.

[5] A. Moretti, A. Logrieco, A. Bottalico, A. Ritieni, G. Randazzo. Production of beauvericin by *Fusarium proliferatum* from maize in Italy. *Mycotoxin Research*, 1994, 10, 73–78.

[6] A. Ritieni, V. Fogliano, G. Randazzo, A. Scarallo, A. Logrieco, A. Moretti, L. Mannina, A. Bottalico. Isolation and characterization of fusaproliferin. *Natural Toxins*, 1995, 3, 17–20.

[7] J. D. Miller, M. E. Savard, A. W. Schaafsma, K. A. Seifert, L. M. Reid. Mycotoxin production by *Fusarium moniliforme* and *Fusarium proliferatum*. *Canadian Journal of Plant Pathology*, 1995, 17, 233–239.

[8] T. Damiani, L. Righetti, M. Suman, G. Galaverna, C. Dall'Asta. Analytical issues related to fumonisins. *Food Control*, 2019, 95, 1–5.

[9] EFSA (European Food Safety Authority) (2018). Risks for animal health related to the presence of fumonisins, their modified forms and hidden forms in feed. EFSA Journal, 16(5), e05242.

[10] EC – European Commission (2006). Commission Regulation (EC) No 1881/2006 of 19 December 2006 setting maximum levels for certain contaminants in foodstuffs. Official Journal of European Union, L364, 5-24.

[11] EC – European Commission (2007). Commission Regulation (EC) No 1126/2007 of 28 September 2007 amending Regulation (EC) No 1881/2006 setting maximum levels for certain contaminants in foodstuffs as regards Fusarium toxins in maize and maize products. Official Journal of European Union, L255.

[12] V. Ostry, F. Malir, J. Toman, Y. Grosse. Mycotoxins as human carcinogens. *Mycotoxin Research*, 2017, 33, 65–73.

[13] P. Karlovsky, M. Suman, F. Berthiller, et al. Impact of food processing and detoxification treatments on mycotoxins. *Mycotoxin Research*, 2016, 32(4), 179–205.

[14] M. Liu, J. Feng, X. Yang, et al. Degradation mechanisms of mycotoxins by cold plasma. *Ecotoxicology and Environmental Safety*, 2024, 270, 115944.

[15] K.-D. Weltmann, J. F. Kolb, M. Holub, et al. The future for plasma science and technology. *Plasma Processes and Polymers*, 2019, 16, e1800118.

[16] N. N. Misra, B. Yadav, M. S. Roopesh, C. Jo. Cold plasma for fungal and mycotoxin control. *Comprehensive Reviews in Food Science and Food Safety*, 2019, 18(1), 106–120.

[17] A. S. Katsigiannis, D. L. Bayliss, J. L. Walsh. Cold plasma decontamination of stainless steel surfaces. *Food Control*, 2021, 121, 107543.

[18] Y. Gorbanev, A. Privat-Maldonado, A. Bogaerts. Short-lived reactive species in plasma–air–water systems. *Analytical Chemistry*, 2018, 90(22), 13151–13158.

[19] V. Veronico, P. Favia, F. Fracassi, R. Gristina, E. Sardella. Long-lived RONS formation in plasma-treated water. *Plasma Processes and Polymers*, 2022, 19, e2100158.

[20] A. Sakudo, Y. Yagyu, T. Onodera. Disinfection and sterilization using plasma technology. *International Journal of Molecular Sciences*, 2019, 20(20), 5216.

[21] A. R. Ganesan, U. Tiwari, P. N. Ezhilarasi, G. Rajauria. Cold plasma on food matrices. *Journal of Food Processing and Preservation*, 2021, 45, e15070.

[22] J. Mravljé, M. Regvar, K. Vogel-Mikuš. Development of cold plasma technologies for seed decontamination. *Journal of Fungi*, 2021, 7(8), 650.

[23] R. Ma, G. Wang, Y. Tian, et al. Plasma-activated water inactivation of pathogens. *Journal of Hazardous Materials*, 2015, 300, 643–651.

[24] L. Ten Bosch, K. Pfohl, G. Avramidis, et al. Plasma-based degradation of mycotoxins. *Toxins*, 2017, 9, 97.

[25] N. Wannicke, R. Wagner, J. Stachowiak, et al. Biological decontamination of seeds using plasma-processed air. *Plasma Processes and Polymers*, 2021, 18, e2000207.

[26] M. Peťková, R. Švubová, S. Kyzek, et al. Cold plasma effects on barley germination. *International Journal of Molecular Sciences*, 2021, 22, 2833.

[27] A. S. Katsigiannis, D. L. Bayliss, J. L. Walsh. Cold plasma for disinfection of food-contact surfaces. *Comprehensive Reviews in Food Science and Food Safety*, 2022, 21, 1086–1124.

[28] R. A. Priatama, A. N. Pervitasari, S. Park, et al. Molecular mechanism of plasma treatment in seeds. *International Journal of Molecular Sciences*, 2022, 23(9), 4609.

[29] L. Hoppanová, S. Kryštofová. Nonthermal plasma effects on fungi. *International Journal of Molecular Sciences*, 2022, 23(19), 11592.

[30] M. Veerana, N. Yu, W. Ketya, G. Park. Application of non-thermal plasma to fungal resources. *Journal of Fungi*, 2022, 8(2), 102.

[31] R. Ranjan, A. K. Gupta, R. Pandiselvam, et al. Plasma treatment for mycotoxin decontamination. *Journal of Agriculture and Food Research*, 2023, 14, 100867.

[32] Q. Xiang, L. Huangfu, S. Dong, et al. Atmospheric cold plasma for food safety. *Critical Reviews in Food Science and Nutrition*, 2021, 63(20), 4431–4449.

[33] Y. Wang, X. Wang, Q. Li. Aflatoxin B1 in poultry liver. *Toxicon*, 2023, 233, 107262.

[34] M. M. Cherif, I. Assadi, L. Khezami, et al. Cold plasma for sustainable food production. *Applied Sciences*, 2023, 13, 2381.

[35] H. N. McQuaid, D. Rutherford, D. Mariotti, P. D. Maguire. Free hydroxyl radicals via remote plasma. *Plasma Sources Science and Technology*, 2023, 32(1), 1–13.

[36] E. F. Ricciardi, M. A. Del Nobile, A. Conte, F. Fracassi, E. Sardella. Plasma treatments on ricotta cheese. *Innovative Food Science & Emerging Technologies*, 2022, 76, 102935.

[37] B. Ciasca, A. Lanubile, A. Marocco, et al. LC-HRMS metabolomics of maize infected by *F. verticillioides*. *Frontiers in Plant Science*, 2020, 11, 664.

[38] G. M. Hamad, T. Mehany, J. Simal-Gandara, et al. Strategies for controlling mycotoxins. *Food Control*, 2023, 144, 109350.

[40] Y. Devi, R. Thirumdas, C. Sarangapani, et al. Cold plasma effects on aflatoxin in groundnuts. *Food Control*, 2017, 77, 187–191.

[41] C. Lo Porto, F. Palumbo, S. Somma, et al. Plasma-assisted deposition on maize seeds. *Plasma Processes and Polymers*, 2019, 16, e1900022.

[42] J. Guo, J. Wang, H. Xie, et al. Plasma-activated water inactivates *Fusarium graminearum*. *Food Control*, 2022, 134, 108683.

[43] Y. Q. Wang, B. Li, H. H. Shang, et al. Inhibition of *Fusarium* by cold plasma. *Chemical Engineering Journal*, 2022, 437, 135307.

[44] Z. Zhongping, Z. Zhang, M. Geng, M. Ding. Method of degrading polysaccharide using ozone. *U.S. Patent Application*, 2019, 16/474,350.

[45] Y. Sen, B. Onal-Ulusoy, M. Mutlu. Aspergillus decontamination in hazelnuts. *Innovative Food Science & Emerging Technologies*, 2019, 54, 235–242.

[46] M. Dharini, S. Jaspin, R. Mahendran. Cold plasma reactive species and biomolecules. *Food Chemistry*, 2023, 405, 134746.

[47] A. Bogaerts, E. Neyts, R. Gijbels, J. van der Mullen. Gas discharge plasmas. *Spectrochimica Acta Part B*, 2002, 57, 609–658.

[48] I. Siciliano, D. Spadaro, A. Prelle, et al. Detoxification of aflatoxins in hazelnuts by cold plasma. *Toxins*, 2016, 8, 125.

[49] B. M. Iqdiam, M. O. Abuagela, Z. Boz, et al. Plasma jet treatment of peanuts. *Journal of Food Processing and Preservation*, 2020, 44(1), e14305.

[50] E. Wielogorska, Y. Ahmed, J. Meneely, et al. Plasma detoxification of mycotoxins in maize. *Food Chemistry*, 2019, 301, 112528.

[51] S. Q. Wang, G. Q. Huang, Y. P. Li, et al. Aflatoxin B1 degradation by RF plasma. *European Food Research and Technology*, 2015, 241, 103–113.

[52] H. Shi, B. Cooper, R. L. Stroshine, K. E. Ileleji, K. M. Keener. Degradation pathways of AFB1 by HVACP. *Journal of Agricultural and Food Chemistry*, 2017, 65(30), 6222–6230.

[53] R. Zulli, C. Dittadi, F. Santi, et al. High-pressure CO_2 microbial inactivation. *Innovative Food Science & Emerging Technologies*, 2024, 96, 103765.

[54] L. Garcia-Gonzalez, A. H. Geeraerd, S. Spilimbergo, et al. High pressure CO_2 inactivation of microorganisms in foods. *International Journal of Food Microbiology*, 2007, 117(1), 1–28.

Conclusions and Perspectives

The research carried out in this thesis has demonstrated how plasma technologies represent highly versatile and adaptable tools for agricultural systems. The entire work has been developed through a series of complementary research lines, which have made it possible to coherently and experimentally address issues related to crop protection, the sustainable use of plant protection products, the management of fungal and bacterial pathogens, and post-harvest food safety. The results obtained highlight how plasma, thanks to its non-thermal nature, its ability to generate reactive species, and its operation without solvents, can offer innovative solutions across the agricultural chain from seed coating to the treatment of agricultural materials.

The first research area focused on the encapsulation of fungicides using plasma-deposited films. The coatings obtained through plasma processing proved capable of effectively incorporating molecules such as prothioconazole, fludioxonil, and pyraclostrobin while preserving their antifungal properties. The studies conducted showed that the deposited films exhibit a hydrocarbon-based, carbon-rich structure containing oxygenated groups, which ensured the protection of the active compound. In vitro antifungal tests confirmed that the activity of the plant protection product persists even when it is incorporated into films of variable thickness, demonstrating that the plasma-deposited matrix does not hinder diffusion. Moreover, when prothioconazole was coated with a plasma-deposited film, larger inhibition halos against fungal growth were obtained. This approach not only reduces the direct and massive use of fungicide since the doses employed were lower than those used in the field, but also minimizes dispersion in soil, thereby contributing to reduced environmental impact and improved operator safety.

From encapsulation on model substrates, the process was then validated on maize seeds. The transfer was carried out inside an atmospheric-pressure DBD reactor designed to treat hundreds of seeds uniformly. Tests on seeds coated with prothioconazole encapsulated within the plasma-deposited film confirmed the compatibility of the process with seed viability, showing that plasma treatment does not compromise germination. At the same time, agar tests conducted in the presence of

Fusarium graminearum demonstrated that the fungicide trapped beneath the film continues to exert significant protective activity, reducing fungal colonization compared to untreated seeds or seeds coated only with the barrier film. The coating acts as a protective barrier for the plant protection product, limiting losses due to abrasion or leaching—factors particularly relevant during transport, sowing, and storage. This technology could represent a starting point for application within industrial seed-coating processes, offering a safer and more environmentally friendly alternative to conventional treatments.

Another experimental approach explored in this thesis involved the development of coatings containing *Bacillus* spores. This aspect of the research is particularly innovative, as no previous studies in the literature have demonstrated the possibility of embedding living cells—in this case, bacterial spores—within plasma-generated films while maintaining their viability. This result represents a paradigm reversal compared to what is commonly reported in the literature in this field. In fact, plasma is often proposed as a means to decontaminate surfaces from spores and bacteria. In the case examined in this thesis, however, plasma is employed with the aim of protecting the spores and enabling their subsequent germination. This is made possible by the use of a plasma capable of depositing a thin film that shields the spores from any germicidal species present in the plasma.

The treated spores remained viable and capable of inhibiting *Fusarium graminearum* once released from the plasma-deposited film, producing inhibition halos comparable to control samples. This result opens new perspectives for seed treatments: the possibility of combining, within a single coating, both chemical molecules or biocontrol agents while modulating their release. Such an approach meets the growing need for sustainable, environmentally friendly, and biologically based crop protection strategies, offering a concrete alternative to synthetic pesticides or to chemical processes that are less environmentally respectful.

In parallel with seed applications, the research extended the use of plasma technologies to granular agricultural materials, particularly zeolites loaded with essential oils known for their nematocidal activity, such as those from *Allium sativum*, *Cinnamomum zeylanicum*, and *Ruta graveolens*. Despite their efficacy, these compounds are

characterized by high volatility and poor long-term stability, properties that limit their direct use in the field. Plasma coating enabled the protection of essential oils from immediate evaporation, stabilizing them on the zeolite surface. Tests conducted on *Meloidogyne incognita* showed that coated zeolites maintained strong nematicidal activity and that film thickness likely influenced release kinetics, allowing their use in soil environments.

Another major contribution was the development of zinc-based nanocomposite films through aerosol-assisted atmospheric pressure plasma jet deposition at Ghent University. Incorporating ZnO or zinc acetate into PEG-like matrices resulted on polyethylene coatings with strong antibacterial activity against *Erwinia carotovora*, a pathogen of great importance for horticultural crops such as potato. The same process was transferred onto wheat seeds, and its effectiveness was evaluated in terms of germination, plant length, and infection severity caused by three *Fusarium* species: F. *graminearum*, *F. culmorum*, and *F. moniliforme*. The results showed a reduction in infection levels across all coated seeds. The effectiveness demonstrated by these nanocomposites confirms that plasma-deposited films can become active tools not only for seed protection but also for the development of functionalized agricultural materials, such as mulching films or packaging surfaces. The possibility of modulating zinc content by adjusting deposition conditions gives the process substantial flexibility. Additionally, the fact that these materials were successfully tested on real substrates, such as wheat seeds, highlights both the robustness and the transferability of the method.

The final chapter of the thesis addressed a critical issue for food safety: the decontamination of maize kernels from toxigenic fungi and mycotoxins using cold plasma for post-harvest applications. Tests conducted on *Aspergillus flavus* and *Fusarium proliferatum* capable of producing aflatoxins (AFB1) and fumonisins (FB1) showed that remote treatments, plasma-treated gas, or plasma-treated water can significantly reduce conidial germination, with reductions ranging from 50% to 90%. Even more relevant is the demonstration that plasma can degrade mycotoxins such as AFB1 and FB1 directly on the food matrix, generating degradation metabolites that are structurally different and less toxic, thus confirming the effectiveness of oxygen- and nitrogen-reactive species-mediated processes. The use of indirect exposure configurations also minimized potential side effects on kernel quality, preserving nutritional characteristics and

structural integrity. This is particularly important within the European regulatory framework, which prohibits chemical detoxification of food and allows only physical methods for treating contaminated raw materials.

Taken together, the various research lines explored in this thesis demonstrate that plasma can serve as a transversal technology for agronomic innovation. Owing to its adaptability to different substrates, its ability to incorporate chemical and biological agents, its capacity to modulate the release of active compounds, and its role as a post-harvest decontamination tool, plasma technology shows enormous potential for future sustainable agriculture. It enables the reduction of pesticide use, the stabilization of natural molecules, the exploitation of biological agents, the functionalization of agricultural materials, and the improvement of food safety—all through solvent-free, energy-efficient processes that are compatible with living matter.

Overall, this thesis confirms that plasma represents an innovative tool capable of responding to the emerging needs of modern agriculture: greater sustainability, reduced chemical inputs, enhanced use of biocontrol agents, crop protection, and improved food safety. Future perspectives involve the integration of these technologies into industrial processes, the optimization of operating parameters according to specific agricultural matrices, and the development of hybrid chemical–biological formulations that fully exploit the flexibility and non-thermal nature of plasma.

List of Publications

- M. Roggio, P. De Bellis, F. Palumbo, P. Trotti, M. Masiello, R. Touati, A. Moretti, P. Favia. Plasma Deposition of Coatings for Delivery of Bacterial Spores Active Against *Fusarium graminearum*. Plasma Processes and Polymers, 2025, 22(8), 70055.

- S. Somma, M. Masiello, M. Haidukowski, B. Ciasca, E. Sardella, P. Favia, F. Palumbo, M. Roggio, A. Moretti. Decontamination of maize kernels and degradation of mycotoxins by means of cold plasmas. LWT - Food Science and Technology, 2025, 215, 117205.

List of Oral and Poster Communications

- M. Roggio, M. Zabihzadeh Khajavi, A. Nikiforov, F. Palumbo, P. Favia, D. Cornacchia S. Pollastro, N. De Geyter, “Plasma Jet Deposition of Antimicrobic Zinc-Based Nanocomposite Thin Films” Oral Contribution in: CHIMICA SOTTO L’ALBERO 2025-EDIZIONE, Bari (Italy), 18-19 December 2025.
- M. Roggio, M. Zabihzadeh Khajavi, A. Nikiforov, F. Palumbo, P. Favia, N. De Geyter, “Atmospheric Pressure Plasma Assisted Deposition of Zinc-Based Coatings for Agriculture Applications” Oral Contribution in: PLATHINIUM 2025, Antibes (France), 22-26 September 2025.
- M. Roggio, P. De Bellis, F. Palumbo, M. Masiello, R. Touati, A. Moretti, P. Favia, “On the use of Atmospheric Pressure for the deposition of coatings embedding bacterial spores in agriculture application” Oral Contribution in: EMRS European Materials Research Society, Strasburg (France), 25-30 May 2025.
- M. Roggio, F. Palumbo, A.M. Lanza, A. Moretti, S. Somma, M. Masiello, P. De Bellis, P. Favia “Aerosol Assisted Atmospheric Pressure Plasma deposition of fungicide and bacterial spores containing coatings” Oral Contribution in: PSE, 19th Conference on Plasma Surface Engineering, Erfurt (Germany), 2-5 September 2024.

- M. Roggio, F. Palumbo, A.M. Lanza, A. Moretti, S. Somma, M. Masiello, P. De Bellis, P. Favia “Aerosol Assisted Atmospheric Pressure Plasma deposition of fungicide and bacterial spores containing coatings” Oral Contribution in: 4th workshop Plasma applications for smart and sustainable agriculture, Belgrade (Serbia), 20-22 May 2024.
- M. Roggio, F. Palumbo, A. M. Lanza, A. Moretti, S. Somma, M. Masiello, P. De Bellis, and P. Favia, “Cold Plasma Processes and Technologies for Sustainable Agriculture and Food Processing” Poster Contribution in: AIV XXVI Conference, Roma, (Italy), 7-10 November 2023.
- M. Roggio, A.M. Lanza, P. Favia, F. Fracassi, E. Sardella, S. Cosmai, D. Benedetti, F. Palumbo, “Cold Plasma Processes and Technologies for Sustainable Agriculture and Food Processing” Poster Contribution in: 3rd Workshop on Plasma Applications for Smart and Sustainable Agriculture, Gozd Martuljek, (Slovenia), 16-18 May 2023.
- M. Roggio, A.M. Lanza, P. Favia, F. Fracassi, E. Sardella, S. Cosmai, D. Benedetti, F. Palumbo, “Cold Plasma Processes and Technologies for Sustainable Agriculture and Food Processing” Poster contribution in: 2nd Training School “Cold plasmas to fight microorganisms, viruses & toxins for medical and agricultural applications”, Bari (Italy), 13-16 February 2023.